Title

In vitro generation of large-scale CAR-iNKT cells from engineered human stem cells for off-the-shelf cancer immunotherapy

Author

Zhou, Yang

Publication Date

2022

Peer reviewed|Thesis/dissertation

UNIVERSITY OF CALIFORNIA

Los Angeles

In vitro generation of large-scale CAR-iNKT cells from engineered human stem cells for off-the-shelf cancer immunotherapy

A dissertation submitted in partial satisfaction of the

requirements for the degree Doctor of Philosophy

in Molecular Biology

by

Yang Zhou

2022

ABSTRACT OF THE DISSERTATION

In vitro generation of large-scale CAR-iNKT cells from engineered human stem cells for off-the-shelf cancer immunotherapy

by

Yang Zhou

Doctor of Philosophy in Molecular Biology

University of California, Los Angeles, 2022

Professor Lili Yang, Chair

Adoptive cell therapy, especially chimeric antigen receptor (CAR) therapy, has revolutionized cancer immunotherapy, showing remarkable results in the treatment of chronic viral infections and malignancies. Currently, there are six US Food and Drug Administration (FDA) approved adoptive CAR-engineered T (CAR-T) cell products for treating B cell lymphoma (BCL) or multiple myeloma (MM) patients: Yescarta (Kite Pharma, 2017), Kymriah (Novartis, 2017), Tecartus (Kite Pharma, 2020), Breyanzi (Bristol Myers Squibb, 2021), Abecma (Bristol Myers Squibb, 2021), and Carvykti (Legend, 2022).

Despite the impressive outcomes, the current FDA-approved cell therapies fall into the autologous category: T cells obtained from the patient via leukapheresis and reinjected back into the same patient. This approach is high-cost, time-consuming, and patient-selective. Some patients may not have enough time waiting for the manufacturing to be completed. Therefore, new approaches that allow rapid production of large-scale and ready-to-use therapeutic cells are in great demand. The work presented in this thesis aims to provide alternative platforms for off-the-shelf cancer immunotherapy. By differentiating genetically engineered stem cells (i.e.,

hematopoietic stem cells and pluripotent stem cells), we developed multiple *in vitro* culture systems to robustly generate large-scale CAR-armed invariant nature killer T (NKT) cells suitable for allogeneic cell therapy.

Chapter 1 introduces the background of iNKT cells, the-state-of-the-arts of stem cell engineering, and the previous study of engineering stem cell into iNKT cells.

Chapter 2 reports a successful platform that utilizing artificial thymic organoid (ATO) culture methods to generate large-scale CAR-armed iNKT (CAR-iNKT) cells for cancer immunotherapy. The HSC-engineered iNKT cells closely resembled endogenous iNKT cells and exhibited potent antitumor efficacy and high safety in the xenograft multiple myeloma mouse model.

Chapter 3 reports a feeder-free *in vitro* culture system to differentiate engineered stem cells into CAR-eNKT cells. The novel platform is robust and compatible for delivering different CAR cargos and additional molecules. The independence of murine derived feeder cells eliminates the potential risk of cross-species contamination during manufacturing.

Chapter 4 switch the focus from previous chapters and starts to develop pluripotent stem cells (PSCs) derived CAR-iNKT cells for cancer immunotherapy. The unlimited expansion capability, capacity for clonal selection and ease of genetic engineering of PSCs allow them to be an ideal candidate providing unlimited source for off-the-shelf allogeneic cell therapies.

Chapter 5 summarizes the thesis, discusses the challenge, and provides future perspectives for developing stem cell and iNKT-based off-the-shelf cancer immunotherapy. It is believed that more fundamental studies will be critical to further develop the next generation immunotherapy.

The dissertation of Yang Zhou is approved.

Donald Barry Kohn

Dinesh Subba Rao

Arnold I. Chin

Maureen An-Ping Su

Lili Yang, Committee Chair

University of California, Los Angeles

2022

DEDICATION

This dissertation is dedicated to:

Cuiping Zhang (Mom)

Guojun Zhou (Dad)

and

Xiang Gao (Husband)

who love and shaped me.

TABLE OF CONTENTS

LIST OF FIGURES AND TABLES

Chapter 1

Chapter 2

Chapter 3

Chapter 4

ACKNOWLEDGEMENTS

As it approaches to the graduation, I strongly realize that I have been so lucky to explore my Ph.D journey with so much of love, support and help from all the people I have interacted with. Words can barely express my gratitude to my mentor, professors in my committee, my collaborators, lab members, my students, as well as my friends and my family members. I could not have undertaken this journey without any of you.

First and foremost, I would like to thank UCLA where I got the opportunity pursuing my Ph.D degree and learning from the greatest people. Thank UCLA graduate division for awarding me the Summer Mentored Research Fellowship and Dissertation Year Fellowship to support my research. A special thank you to my mentor, Dr. Lili Yang for the great opportunity joining in the lab and I am very grateful for the invaluable patience and feedbacks. I joined Lili's lab as a lab manager six years ago. By then, I just quit my Ph.D from anther university and was very hesitating whether to continue my education or not. My first experience of graduate life was not as delightful as I expected, so that I used up all my courage to terminate my struggling, which turned out to be the most correct decision I had made during my current life. My first two years working as a lab manager, Lili showed me her patience in mentoring and teaching. She taught me how to write professional emails, how to lead negotiations, and most importantly, how to collaborate with people. With her encourage, I picked up my confidence, my enthusiasm toward research, and made my decision to apply for graduate school. At this moment, I am very proud to say that I made it. And this endeavor would not have been possible without the generous support from Dr. Lili Yang.

I am also grateful to my defense committee, Professor Donald Kohn, Dinesh Rao, Arnold Chin and Maureen Su, who generously provided knowledge and expertise on my projects. I

really appreciate the time and effort they spent serving on my committee board. To Dr. Kohn and Dr. Su, I still remember the kind words they told me during my qualifying exam. They mentioned that it was not easy to transit from a technician to a student as the mindset between the two was completely different. However, they greatly endorsed my previous efforts, encouraged me, and emphasized that they would be my backs if there were any challenges. And Dr. Kohn, I really appreciated all the reference letters for my fellowship application. If Lili is the light that guides me moving forward, the professors, are my strong backings.

Then, I would like to thank my lab supervisors, Dr. Yanni Zhu, Dr. Drake Smith, Dr. Xi Wang, and Dr. Zhe Li. Thank you for the generously sharing your knowledge and experimental skills. A special thank you to Xi Wang, a super mom with two cute daughters, for being the most supportive person inside and outside the lab. Thank lab members, Dr. Stefono, Dr. Yujeong Kim, Dr. Inyoung Choi, Dr. Yucheng Wang, Dr. Xiaoya Ma, and Dr. Bo Li, for the supportive and collaborative lab environment, and also the great lab gathering times. I would like to thank my fellow graduate student labmates Dr. Jiaji Yu, Dr. Yanruide Li, Derek Lee, and Dr. Sam Zeng for supporting each other and sharing the journey of Ph.D. study. And thank you, our lab manager Jie Huang, for the great support on maintaining lab. I would also like to thank the new lab members, Dr. Yanqi Yu, Dr. Miao Li, Kuangyi Zhou, James Brown and Zach Dunn, especially to Miao and Kuangyi who helped me a lot for closing my manuscripts. They are the next generation of the lab. I cherish all the mentorship and friendship that I gained in the lab.

Next, I would like to thank all the undergraduates that I worked with in the lab, Levina Lin, Christian Hardoy, Josh Ku, Tasha Tsao, Emily Peng, Tiffany Husman, Xinjian Cen and Aarushi Bajpai. I need to specially acknowledge Tasha, Tiffany, Xinjian and Aarushi, who I directly supervised. Thank you for being core members of the Yang (Alice) Zhou stem cell

engineering team. My research work would not be possible without your hardworking and you are my keys to survival in those days of intense lab work. I am very proud to see that some of you gradated with honors and some of you already were the co-first authors.

I would like to thank my wonderful collaborators, Dr. Feiyang Ma, Dr. Shuo Li, Yonggang, and Dr. Jasmine Zhou, who were super supportive with their bioinformatic expertise. The BSCRC FACS core, Jessica, Jeff and Felicia who helped with flow sorting. I would like to thank UCLA core services: the UCLA Virology Core, Pathology Core, and Technology Center for Genomics & Bioinformatics.

I also would like to thank Dr. Zoran Galić, Dr. Jerry Zack, and Dr. Timothy O'Sullivan, whom I had the pleasure to TA the Immunology class with during the pandemic. In particular Zoran, he showed us his enthusiasm for teaching, responsibility and caring for students. I would also like to thank all the students that I have taught, and the kind words they put on my evaluation form. You gave me the confidence, made my experience, and I really enjoyed learning together with them.

I am also grateful to my friends, Ting fu and her two cute cats, Min Chai, Chi Zhang, Weijie Yin, Ruya Zhang, Jiuchao Yin, Yi Lei, Xinlei Gao, Yajing Gao, Han Li, for their moral support. I enjoyed all the time we spent together.

Lastly but the most importantly, my eternal gratefulness goes to my family members, my mom, dad and my husband, for their unconditional support throughout all these years. Thanks to my parents, for supporting me pursuing my degree in a foreign country. We haven't seen each other for the last five years. I really miss you at home and I cannot make this journey without your encouragement and absolute love. Thanks to my husband. I am so lucky and grateful to have you in my life. Thank you for being my best friend and for being a caring and trustworthy

partner. Thank you so much for all the little things you do for me. I appreciate your care and support all the time.

With all of you in my life, I count myself as lucky and blessed.

VITA

EDUCATION

Ph.D candidate
Molecular Biology, Immunology from University of California, Los Angeles
M.S. in Nutrition Sciences from University of Georgia 2016
B.S. in Biology from University of Science and Technology of China 2013

RESEARCH & WORKING EXPERIENCE

University of California, Los Angeles **Graduate Researcher** 2018-2022

- Managed 4 projects with the team size up to 8 members to develop the next generation of cancer immunotherapy with hematopoietic stem cell engineered cells (iNKT, γδT, T cells).
- Led publications of 2 US patents and 8 research papers reported in high-profile news media.
- Provided mentorship to undergraduates with impartment of PhD-level research experience.

University of California, Los Angeles **Teaching Assistant**
2020/2021

- Immunology, MIMG 185A, Department of MIMG

University of California, Los Angeles **Lab Manager** 2016-2018

- Organized research activities for several prestigious cell therapy grants such as California Institute for Regenerative Medicine (CIRM) with a total budget of $ 6.9 million.
- Involved in the conduction, development, and preparation of the preclinical studies, clinical trial protocols, and an IND package submission.

University of Georgia **Research Associate** 2013-2016

- Researched the genetic regulation of age-associated disease which led to 4 publications.
- Set up a new lab from scratch with the establishment of full chemical inventory and SOPs.

PUBLICATIONS

A. Patents

1) UC-2020-913-2 US (UCLA: 30435.0410USU1), Engineered gamma delta T cells and methods of making and using thereof. Inventor.
2) UCLA: 30435.430-US-P1, Pluripotent stem cell-engineered immune cell for off-the-shelf cell therapy. Inventor.

B. Academic publications

1) **Y. Zhou**, et al., Lili Yang. Methods for studying mouse and human invariant Natural Killer T cells. *Methods in Molecular Biology*. 2021. (**Book chapter**)
2) X. Cen, A. Bajpai, **Y. Zhou** and Lili Yang. Happiness therapy. *Nature Portfolio, Science in Shorts* 2022. (**Video**)
3) Zhu Y.*, Smith DJ*, **Y. Zhou**, et al., Lili Yang. Development of hematopoietic stem cell-engineered invariant natural killer T cell therapy for cancer. *Cell Stem Cell.* 2019, 25(4):542-557.
4) Y Li*, **Y. Zhou***, et al., Lili Yang**.** Development of allogeneic HSC-engineered iNKT cells for off-the-shelf cancer immunotherapy. *Cell Reports Medicine.* 2021. (*co-first author)
5) **Y. Zhou** et al. Engineering induced pluripotent stem cells for cancer immunotherapy. *Cancers*. 2022.
6) **Y. Zhou**, et al., Lili Yang. Cytokine IL-15 in cell-based cancer immunotherapy. *IJMS.* 2022.
7) Y Li, Z Dunn, **Y. Zhou**, et al., Lili Yang. Development of Off-The-Shelf Hematopoietic Stem Cell-Engineered Invariant Natural Killer T Cells for COVID-19 Therapeutic Intervention. *Stem Cell Research & Therapy*. 2021
8) S. De*, X. Ma*, **Y. Zhou** et al., Lili Yang. Creatine uptake regulates CD8 T cell antitumor immunity. *J Exp Med*. 2019, 216(12): 2869-2882. Epub 2019 Oct 18.
9) Y. Wang, X. Wang, J. Yu, **Y. Zhou**, et al., Lili Yang. Target monoamine oxidase A-regulated TAM polarization for cancer immunotherapy. *Nature Communications*. 2020.
10) X. Wang, B. Li, **Y. Zhou**, et al., Lili Yang. Targeting monoamine oxidase A for cancer immunotherapy. *Science* Immunology. 2021.
11) **Y. Zhou**, et al., R. Pazdro. Genetic Analysis of Tissue Glutathione Concentrations and Redox

Balance. *Free Radical Biology and Medicine*. 2014. 71:157-164.

12) **Y. Zhou**, et al., R. Pazdro. Circulating Concentrations of Growth Differentiation Factor 11 Are Heritable and Correlate with Life Span. *J Gerontol A Biol Sci Med Sci*. 2016.
13) Bumgardner SA, **Y. Zho**u, et al., R. Pazdro. Genetic influence on splenic natural killer cells frequencies and maturation among aged mice. *Exp Gerontol*. 2018. Apr;104:9-16.
14) Gould RL, **Y. Zhou**, et al., R. Pazdro. Heritability of the aged glutathione phenotype is dependent on tissue of origin. *Mamm Genome*. 2018 Jul 14.
15) Y Li*, **Y. Zhou***, et al., Lili Yang. Engineering stem cells for cancer immunotherapy. *Trends in Cancer*. 2021
16) Y Li, Z Dunn, **Y. Zhou** et al.. Development of stem cell-derived immune cells for off-the-shelf cancer immunotherapies. *Cells*. 2021.
17) ZS Dunn, **Y. Zhou** et al.. Minimally invasive preclinical monitoring of the peritoneal cavity tunor microenvironment. *Cancers*. 2022.
18) D. Lee, et al., **Y. Zhou**, Lili Yang. Human γδ T Cell Subsets and Their Clinical Applications for Cancer Immunotherapy. *Cancers.* 2022.
19) Y. Li, **Y. Zhou**, et al. Tumor-localized administration of a-GalCer to recruit invariant natural killer T cells and enhance their antitumor activity against solid tumors. *IJMS*. 2022.
20) Y. Li, S. Zeng, Z. Dunn, **Y. Zhou**, et al. Off-the-shelf third-party HSC-engineered iNKT cells for ameliorating GvHD while preserving GvL effect in the treatment of blood cancers. *iScience*. 2022.
21) **Y. Zhou**, et al., Lili Yang. Hematopoietic stem cell-engineered IL-15 enhanced off-the-shelf CAR-iNKT cells for treating multiple myeloma. *In preparation*.
22) **Y. Zhou**, et al., Lili Yang. HLA gene-edited hypoimmunogenic HSC-engineered CAR-iNKT cells for treating multiple myeloma. *In preparation*.

HONORS & AWARDS

- UCLA Graduate division Dissertation Year Fellowship (DYF) (awarded) 2022
- Nucleate 1st place prize in Los Angeles, Team Gammunity 2022
- Nucleate Petri Funding Award ($200k) for Team Gammunity 2022
- UCLA Jonsson Comprehensive Cancer Center retreat, 1st prize of poster presentation 2022
- UCLA Summer Mentored Research Fellowship (SMRF) 2020
- UGA June & Bill Flatt Nutrition Excellence Graduate Scholarship 2016
- UGA Eleonora M. Costa Graduate Scholarship 2016
- UGA Scholars of Excellence Assistantship 2013
- UGA Excellence in Graduate Recruitment Fund 2013
- UGA Eleonora Costa Graduate Support Fund 2013
- USTC Outstanding Undergraduate Research Project 2013
- USTC Outstanding Student Scholarship 2012
- USTC Prize of Outstanding Student Leader 2012
- USTC Gold Medal, Asia Regional Jamboree of International Genetically Engineered Machine Competition (iGEM) 2010

CHAPTER 1

Developing stem cell-derived iNKT cells for cancer immunotherapy

In this chapter, we introduce the background of iNKT cells, including the biology, the development, the function and the current status of iNKT cell-based therapies. Then we discuss the overall landscape of cell therapy, in particular the importance and remaining challenging of stem cell-based immunotherapy. Lastly, we present the previous evidence showing the feasibility of developing stem-cell-derived iNKT cells for cancer immunotherapy.

1.1 Introduction of iNKT cells

1.1.1 The biology of iNKT cells

Natural killer T (NKT) cells are a unique subpopulation of αβT cells that are characterized with certain NK properties[1]. Unlike conventional T cells that recognize protein peptides presented by MHC I or MHC II molecules, NKT cells recognize both endogenous and exogenous glycolipids in the context of a MHC I-like monomorphic molecule CD1d. There are two major subpopulations of NKT cells: type I and type II NKT cells, based on their TCR and glycolipid reactivity. Invariant NKT (iNKT) cells, or type I NKT cells, are defined with a semi-invariant T cell receptor (TCR): TCR α chain (Vα24-Jα18 in human and Vα14-Jα18 in the mouse) paired with a limited Vβ chains (Vβ 11 in human and Vβ 2, 7, or 8 in mouse), that can respond to a marine sponge-derived α-galactosylceramide (αGalcer)[1,2]. Upon activation, iNKT cells can rapidly produce copious amounts of cytokines and chemokines, such as IFN-γ, IL-4, IL-13, IL-17, IL-22 and IL-10, as well as cytotoxic molecules, such as perforin and granzyme B. In human, there are $CD4^+$, $CD8^+$, and $CD4^-CD8^-$ three subsets of iNKT cells, while in mice, there are only $CD4^+$ and DN iNKT cells[2]. Furthermore, iNKT cells can be divided into NKT1, NKT2, and NKT17 subsets based on their cytokine expression and functionality. Type II NKT cells have

more diverse Vα rearrangement allowing them to recognize self-lipids, including lysophosphatidylcholine and sulfatide. Studies have shown that sulfatides activated type II NKT cells promoted tumor growth, indicating a pro-tumor role, whereas iNKT cells exhibit potent anti-tumor activity. Since the type II NKT cells are not well-studied as iNKT cells, all the following research will be focused on type I NKT cells.

1.1.2 Development of iNKT cells

iNKT cells are originated from the same lymphoid precursors as conventional αβT cells and gdT cells, while the iNKT TCR expression instructs the iNKT lineage differentiation. During thymocyte development, hematopoietic stem cells (HSCs) migrate into thymus and differentiate into lymphoid progenitors. Lymphoid progenitors rearrange the TCRβ chain and develop from $CD4^-CD8^-$ double-negative (DN) stage into $CD4^+CD8^+$ double-positive (DP) stage[1,2]. iNKT cell precursors diverge from the mainstream αβ T cells at the DP stage where convectional αβ T cells are selected by the epithelial cells while iNKTs are not. The cortical DP thymocytes temporarily upregulate monomorphic class I major histocompatibility complex (MHC-I) like molecule CD1d and present endogenous agonist ligand providing differentiation signal to iNKT cells. Unlike conventional αβ T cells recognizing peptide antigens, iNKT cells recognize lipid antigens, such as isoglobotrihexosylceramide (iGb3). The interaction of iNKT TCR and glycolipid-CD1d, along with other signal through the signaling lymphocytic activated molecules (SLAM) receptor family, drives the further differentiation of iNKT cells[1,2]. Mature iNKT cells exit the thymus with a memory phenotype and further gain NK properties in the periphery.

1.1.3 iNKT cells in immunotherapy

Although iNKT cells have been characterized by their extremely low numbers (~0.1%–1% in mouse blood, ~0.001%–1% in human blood), mature iNKT cells are reported to play an

important role in anti-tumor responses[2]. TRAMP mice deficient in iNKT cells had progressive tumor development and metastasis, resulting reduced survival compared to the wild-type TRAMP mice. In human, cancer patients frequently have low iNKT cell counts and/or impaired iNKT cell function. The iNKT infiltration into tumors is also found to be associated with a good prognosis in neuroblastomas, pancreatic adenocarcinoma, and colorectal carcinoma. iNKT cells are also recognized as a bridge between innate and adaptive immunity, as many cytokines released by iNKT cells can induce dendritic cell maturation and αβT cell differentiation.

iNKT cells can exert cytotoxicity both directly and indirectly. Through iNKT TCR-glycoplid-CD1d interaction, iNKT cells have the capacity to mediate killing against $CD1d^+$ tumor cells, immunosuppressive tumor-associated macrophages (TAMs) and myeloid-derived suppressor cells (MDSCs), via peforin, granzyme B, and TNF-related apoptosis-inducing ligand (TRAIL) pathways[1,2]. High expression of CD1d on tumor cells leads to enhanced tumor cell elimination, while downregulation of CD1d is usually related to reduced iNKT cell performance. However, the expression of NK activating receptors, such as NKG2D and DNAM-1, can allow iNKT cells directly kill tumor in the absence of TCR-CD1d recognition, providing alternative tumor targeting mechanism on CD1d negative cells. Meanwhile, iNKT cells can also potentiate antitumor activities through activating NK cells and cytotoxic T lymphocytes (CTLs).

Because of the importance of iNKT cells in immunosurveillance and anti-tumor activity, iNKT cell-based immunotherapy has garnered a lot of attention. The overall efficacy of iNKT cell therapies is greatly restricted by the extremely low frequency of iNKT cells as well as the level of CD1d expression on tumor cells. It is proved in both preclinical and clinical studies that iNKT cells in immunotherapy are safe, while not all clinical trials are effective. The classic approach to activate iNKT cells is using a-Galcer loaded DCs, which can provide strong co-

signaling of CD40 and IL-12[2,3]. This approach was tested to prolong median survival in clinical trials of myeloma and head and neck cancer, without any serious adverse events. Treatment with aGalcer-loaded APCs was also well tolerated in a phase I/II trial of non-small cell lung cancer. Patients responded to the treatment had increased IFN production as well as iNKT cell expansion. For cancer patients who have insufficient number of iNKT cells, the efficacy of aGalcer treatment is limited. To overcome this limitation, directly adoptively transferring *ex vivo* expanded iNKT cells into patients were tested. Patients received *ex vivo* activated iNKT cells exhibited increased circulating iNKT cell numbers as well as IFN-γ production.

1.1.4 CAR-iNKT cells in cancer immunotherapy

Chimeric antigen receptor engineered T (CAR-T) cell therapies have yielded significant clinical success especially in treating B cell malignancies[5]. T cells engineered with CAR that can specifically target a specific antigen, maximize their killing capacity. Given the potent antitumor responses of iNKT cells with direct tumor lysis, enhanced tumor infiltration, and modulating other immune effector cells via cytokine production, they are recognized as an ideal candidate for CAR-engineering. Especially that allogeneic iNKT cells do not cause GvHD, iNKT cells represent a promising option for developing next-generation off-the-shelf CAR cell products[3,4]. Furthermore, CAR-NKT cells that co-express the invariant iNKT TCR and NK receptors in addition to the CAR, provide multiple killing mechanism against tumor cells. It is also worth noting that CAR-iNKT cell with 4-1BB costimulatory domain did not produce elevated level of IL-6, which is the key cytokine that associates with cytokine release syndrome (CRS).

Heczey et al. demonstrated that CAR-iNKT cells susccessfully localized to the soild tumor site and illustrated dual antitumor activity against CD1d-positive tumor associated macrophages (TAM) and GD2-positive neuroblastoma site[6]. Both B cell maturation antigen (BCMA)-

targeting CAR-iNKT and CD19-targeting CAR-iNKT cells have also shown good efficacy on CD1d-expressing multiple myeloma (MM) and lymphoma cells. These encouraging results demonstrate the feasibility of CAR-engineered iNKT cells and their potential advantages over conventional CAR-T cells in treating cancers.

Unfortunately, due to their insufficient numbers and short-term persistence, iNKT cell-based immunotherapy has not yet been fully developed. Our lab has working on utilizing stem cell engineering approach to overcome such limitation[7,8]. We have successfully developed serval platforms that allow us to generate large-scale, multifunctional, and hypoimmunogenic CAR-NKT cells for cancer immunotherapy.

References

1. Bendelac, A., Savage, P.B. & Teyton, L. The biology of NKT cells. *Annu Rev Immunol* **25**, 297-336 (2007).
2. Van Kaer, L. alpha-Galactosylceramide therapy for autoimmune diseases: prospects and obstacles. *Nat Rev Immunol* **5**, 31-42 (2005).
3. Liu, Y. et al. iNKT: A new avenue for CAR-based cancer immunotherapy. *Transl Oncol* **17**, 101342 (2022).
4. Lee, P.T., Benlagha, K., Teyton, L. & Bendelac, A. Distinct functional lineages of human V(alpha)24 natural killer T cells. *J Exp Med* **195**, 637-641 (2002).
5. June, C.H., O'Connor, R.S., Kawalekar, O.U., Ghassemi, S. & Milone, M.C. CAR T cell immunotherapy for human cancer. *Science* **359**, 1361-1365 (2018).
6. Heczey, A. et al. Anti-GD2 CAR-NKT cells in patients with relapsed or refractory neuroblastoma: an interim analysis. *Nat Med* **26**, 1686-1690 (2020).
7. Li, Y.R. et al. Development of allogeneic HSC-engineered iNKT cells for off-the-shelf cancer immunotherapy. *Cell Rep Med* **2**, 100449 (2021).
8. Zhu, Y. et al. Development of Hematopoietic Stem Cell-Engineered Invariant Natural Killer T Cell Therapy for Cancer. *Cell Stem Cell* **25**, 542-557 e549 (2019).

1.2 Stem cell engineering in cancer immunotherapy

Trends in Cancer

CellPress

Opinion

Engineering stem cells for cancer immunotherapy

Yan-Ruide Li,[1,5] Yang Zhou,[1,5] Adam Kramer,[1] and Lili Yang[1,2,3,4,*]

Engineering stem cells presents an attractive paradigm for cancer immunotherapy. Stem cells engineered to stably express various chimeric antigen receptors (CARs) or T-cell receptors (TCRs) against tumor-associated antigens are showing increasing promise in the treatment of solid tumors and hematologic malignancies. Stem cells engraft for long-term immune cell generation and serve as a sustained source of tumor-specific effector cells to maintain remissions. Furthermore, engineering stem cells provides 'off-the-shelf' cellular products, obviating the need for a personalized and patient-specific product that plagues current autologous cell therapies. Herein, we summarize recent progress of stem cell-engineered cancer therapies, and discuss the utility, impact, opportunities, and challenges of cellular engineering that may facilitate the translational and clinical research.

Highlights

Gene engineering of stem cells provide a persistent and stable source for long-term *in vivo* generation of immune cells with specific tumor targeting.

Gene engineering of stem cell provide an 'off-the-shelf' allogeneic cellular product for cancer immunotherapy.

Stem cells can be engineered and differentiated into a variety of cell types, such as conventional αβ T, natural killer (NK) cells, invariant NK T (iNKT) cells, γδ T, mucosal associated invariant T (MAIT), and myeloid cells.

Chimeric antigen receptors (CARs) can be engineered on stem cells to generate potent effector cells with enhanced anti-tumor efficacy.

Gene knock-out on stem cells provides a stable and efficient gene ablation in stem cell-derived immune cells.

Introduction

Over the past decade, cell-based immunotherapy has shown great promise as the new-generation cancer medicine [1]. Genetic engineering of T cells, natural killer (NK) cells, invariant NK T (iNKT) cells, and other immune cells, have yielded encouraging results for cancer immunotherapy [2,3]. A series of clinical trials using engineered immune cells with CARs or TCRs have been conducted to treat various forms of cancer, ranging from solid tumors to hematologic malignancies [4–9]. Despite remarkable successes in the clinic, most of the current FDA-approved CAR T-cell products are manufactured using autologous T cells obtained from the intended recipient patient. Such an approach is costly, labor intensive, and difficult to broadly deliver to all patients in need. Allogeneic immune cellular products that can circumvent the manufacturing issues of inadequate cell numbers, suboptimal T cell states, and delays in treatment therefore are in great demand [10].

'Off-the-shelf' or allogeneic cell products, such as CAR-engineered T cells or NK cells, can potentially overcome the issues of autologous cell products, and allow for multiplex genetic modifications and CAR construct combinations to target various tumor antigens and avoid tumor escape [11–15]. By virtue of the powerful genome editing tools, especially CRISPR/Cas9, the allogeneic cell products could conquer the two current limitations of 'off-the-shelf' therapy: graft-versus-host disease (GvHD) and host cell-induced allorejection [11–14,16]. Recent clinical studies have reported the feasibility, antileukemic activity, and manageable safety of the two allogeneic cell products (i.e., CAR19-engineered T cells and NK cells), revealing an encouraging step forward for the field of allogeneic cell therapy [16,17].

Engineered stem cells provide another attractive approach for cell-based cancer immunotherapy. For hematopoietic stem cell transplantation (HSCT), genetically engineered stem cells provide a persistent and stable source for long-term generation of immune cells with specific tumor targeting. In addition, CAR-engineered stem cells have the capability to generate CAR-NK or CAR-myeloid cells in addition to CAR-T cells, resulting in broader antitumor activity that arises quickly post-transplantation and does not solely require *de novo* thymopoiesis [18,19].

[1]Department of Microbiology, Immunology and Molecular Genetics, University of California, Los Angeles, Los Angeles, CA 90095, USA
[2]Eli and Edythe Broad Center of Regenerative Medicine and Stem Cell Research, University of California, Los Angeles, Los Angeles, CA 90095, USA
[3]Jonsson Comprehensive Cancer Center, David Geffen School of Medicine, University of California, Los Angeles, Los Angeles, CA 90095, USA
[4]Molecular Biology Institute, University of California, Los Angeles, CA 90095, USA
[5]These authors contributed equally to this work

*Correspondence: liliyang@ucla.edu (L. Yang).

Engineered stem cells could also provide an 'off-the-shelf' cellular product, obviating the need for a personalized and patient-specific product. Performing gene engineering or gene editing on a small starting number of stem cells could reduce the amount of gene-engineering/editing materials (e.g., lentivector and CRISPR/Cas9/gRNA), which can be cost-limiting, and enable the maximal efficiency of gene engineering/editing, which can be inherited by the subsequent divisions and the final cell products. Furthermore, the development of stem cell-engineered cellular therapy will provide opportunities for upscaling the manufacturing and banking of products (Figure 1). In this review, we will discuss the potential of engineering stem cells for cancer immunotherapy.

Stem cell sources and engineering approaches

Multiple stem cell resources could be utilized for effector cell production, including PSCs, hematopoietic stem cells (HSCs), and iPSCs. PSCs including ESCs and iPSCs have the capacity for self-renewal while maintaining pluripotency, and could potentially provide unlimited supplies for target cells [20]. Established ESC and iPSC lines have been utilized to generate hematopoietic

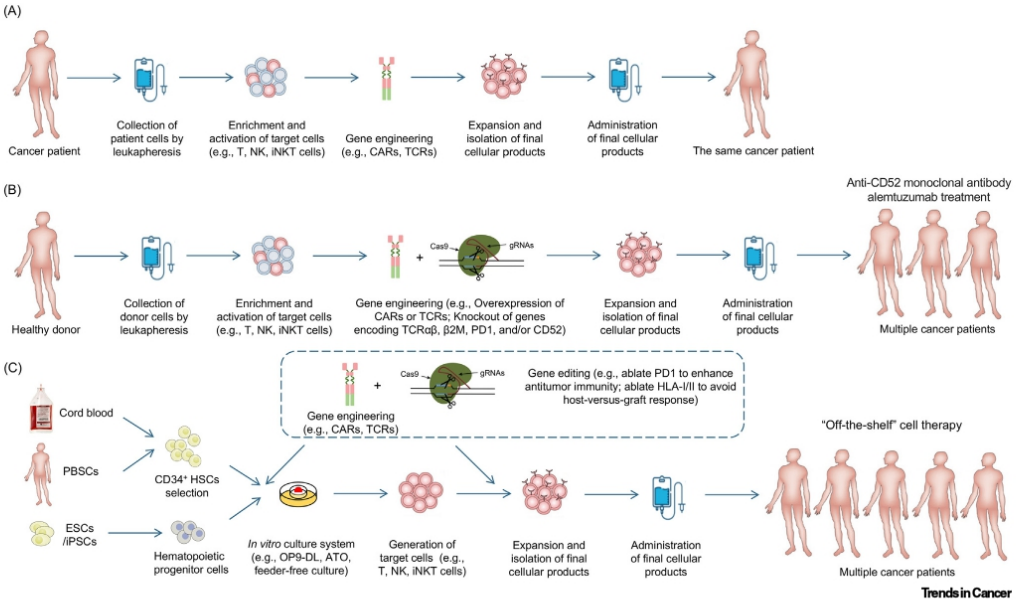

Figure 1. Schematics of current autologous and allogeneic cell-based cancer immunotherapies. (A) Schematics of autologous cellular product manufacturing. Target cells (e.g., T, NK, or iNKT cells) are collected from patients by leukapheresis and are then genetically engineered. The engineered cells are expanded *ex vivo* while the patient undergoes bridging and/or lymphodepleting chemotherapy. The engineered cellular products are then infused into the same patient. (B) Schematics of healthy donor PBMC-derived allogeneic cellular product manufacturing. Healthy donors for banking are selected and their PBMCs are used to generate genetically engineered immune cells. Notably, because conventional αβ T cells risk inducing GvHD in allogeneic hosts due to HLA incompatibility, these T cells need to be gene-edited to ablate endogenous TCR expression, usually through disrupting the *TRAC* or/and *TRBC* gene loci, to make them suitable for allogeneic cell therapy. Meanwhile *CD52* gene is also disrupted to generate allogeneic cells resistant to the anti-CD52 monoclonal antibody alemtuzumab, which can be used to eliminate host T cells expressing CD52 and avoid allorejection. (C) Schematics of stem cell-derived allogeneic cellular product manufacturing. Human $CD34^+$ HSCs are collected from either cord blood or from granulocyte-colony stimulating factor (G-CSF)-mobilized human periphery blood. These HSCs are genetic engineered and then cultured in 'off-the-shelf' *in vitro* culture system (e.g., OP9-DL, ATO, or feeder-free culture) to generate mature effector immune cells. The immune cells could also be derived from ESCs/iPSCs using culture conditions that first promote hematopoietic differentiation and then target cell differentiation, followed by target cell maturation and activation. Abbreviations: ATO, artificial thymic organoid; CARs, chimeric antigen receptors; GvHD, graft-versus-host disease; HLA, human leukocyte antigen; HSCs, hematopoietic stem cells; iNKT, invariant natural killer T; NK, natural killer; PBSCs, peripheral blood stem cells; PBMCs, peripheral blood mononuclear cells; TCR, T cell receptor.

stem/progenitor cells (HSPCs) and mature immune cells [21,22]. HSCs are the most primitive of blood lineage cells. They can be obtained from umbilical cord blood (UCB), bone marrow of a donor, or granulocyte colony stimulating factor (G-CSF) mobilized peripheral blood [denoted as peripheral blood stem cells (PBSCs)] [23,24]. Immune cell-derived iPSCs, including T cell-derived iPSCs (T-iPSCs) [25–27], iNKT cell-derived iPSCs (iNKT-iPSCs) [28], and non-T peripheral blood cell-derived iPSCs (PBC-iPSCs) [29] can be reprogrammed from a highly accessible human cell source, peripheral blood mononuclear cells (PBMCs). Multiple approaches have been applied to stem cell engineering and differentiation (Box 1).

Viral vector and virus transduction

Efficient genetic modification of stem cells relies on permanent gene insertion and expression in stem cells and their progeny. Vectors from *retroviridae* family, including γ-retroviral vectors (such as murine leukemia viruses), lentiviral vectors (such as human immunodeficiency virus), and spumaviral vectors (such as human foamy virus), have been applied for stable and effective gene transfer into stem cells [30].

Human $CD34^+$ HSPCs collected from UCBs or PBSCs, or generated from PSCs, are enriched by $CD34^+$ immunoaffinity selection, cultured in a cocktail medium with human cytokines including Fms-like tyrosine kinase 3 ligand (FLT-3L), human stem cell factor (SCF), and thrombopoietin (TPO), and then transduced with one or more gene delivery vectors. At the completion of virus transduction, these HSPCs are collected and formulated for either direct transplantation, *in vitro* differentiation, or cryopreservation [24,30].

Box 1. Culture systems to differentiate stem cells into immune cells

BLT humanized mouse model

BLT model is established through cotransplantation of human fetal thymus, liver, and $CD34^+$ hematopoietic stem cells (HSCs) to immunodeficient mice. This model supports a sustained human hematopoiesis and functional human immune system in immunodeficient mice [121,122]. By engineering HSCs and adoptively transferring HSCs to BLT mouse, TCR-engineered, antigen-specific T cells could be generated in mice [79,83,123,124]. One defect of the BLT model is that the education of T cells in a human thymus does not cause tolerance to the mouse host, therefore generating self-reactive T cells that eventually kill the mouse due to GvHD [125]. To address this issue, human HSCs could be transplanted into sub-lethally irradiated NSG neonatal mice, where the generated human thymocytes are educated in the mouse thymus, resulting in a reduced TCR repertoire compared with the BLT model [79,125].

OP9-DL culture system

The OP9-DL system was based on a mouse bone marrow-derived stromal cell line OP9, engineered to overexpress the Notch ligand, Delta-like ligand 1 (DLL-1) or 4 (DLL-4) [126–128]. The OP9-DL system allows the generation of human HSPC-derived T cells *in vitro* [129,130].

Artificial thymic organoid (ATO) culture system

ATO culture system supports effective and reproducible *in vitro* differentiation and positive selection of conventional human T cells from HSCs and ESCs/iPSCs [115,131]. This culture system is based on a DLL1-expressing murine bone marrow-derived stromal cell line, and serum-free, off-the-shelf components that include B27, Fms-related tyrosine kinase 3 (FLT3) ligand, IL-7, and ascorbic acid. T cell differentiation in ATO system mirrors the natural T cell commitment following a phenotypic progression which closely recapitulates human thymopoiesis [131]. The ATO-derived mature T cells display an antigen-naïve phenotype, a diverse TCR repertoire, and a potent antigenic stimuli response [131]. ATO system also supports generation of TCR-engineered, antigen-specific T cells through genetically engineering stem cells [115,131].

Feeder-free culture system

Using feeder-free culture system to generate T cells from stem cells has been investigated to expedite the clinical application of allogeneic 'off-the-shelf' T cells. A clinically relevant Notch-mediated *ex vivo* expansion system using serum-free Stemspan media with the addition of SCF, FLT3L, IL-6, IL-3, TPO, and lipoprotein has been reported [132]. The feeder-free culture system supports significant expansion of $CD34^+$ stem/progenitor cells *in vitro* and sufficient engraftment of these cells in immunodeficient mice [132].

CAR engineering

CARs are synthetic receptors that redirect lymphocytes to target the cells expressing a cognate ligand [10]. Stable retroviral or lentiviral transduction of a prearranged tumor antigen-specific CAR to stem cells can provide an attractive method for generating effector T cells with defined antigen specificity [31,32]. Compared to mature PBMC T cells, it is more attractive to use stem cells as the engineering target for CARs because the regenerative nature of stem cells may serve as a long lasting, even life-long supply for engineered effector T cells targeting the antigen of interest.

Multiple strategies have been used to improve the safety, efficacy, and applicability of CAR-engineered cell therapy. The evolution of CAR construct designs aims to enhance the efficacy and safety of CAR-engineered cell products, broaden the range of cancers amenable to such therapy, and facilitate more reliable and efficient generation of these products [10].

Gene knock-out techniques involving short hairpin RNAs (shRNAs) or CRISPR–Cas9 genome-editing system have been used to enhance the antitumor capability of CAR-engineered cells [33–35]. The CRISPR/Cas9 genome-editing system has been used to ablate the expression of the TCR α chain, TCR β chain, β2M, and PD-1 in CAR-T cells [14,33,34,36–38]. Insertion of the CAR gene construct into the *TRAC* locus has been accomplished by inserting the CAR construct and knocking out the TCR gene in one step [39]. These gene knock-out techniques could also be applied to stem cells to achieve stable and efficient gene ablation in stem cell-differentiated immune cells.

Suicide gene modifications have been incorporated into CAR therapy to avoid the risks of insertional oncogenesis [40]. The most widely adopted suicide gene is from the herpes simplex virus thymidine kinase (HSV-TK) gene, which confers sensitivity to an antiviral nucleoside analogue ganciclovir (GCV) and allows positron emission tomography (PET) visualization for modified cell tracking [41–43]. Alternative suicide switch systems, such as fusion protein expressing Fas signaling moieties [44] or caspase components under the post-transcriptional regulation of small molecule ligands [45] have also been developed.

TCR engineering

Compared to CAR engineering, TCR engineering can recognize a broader variety of tumor-specific antigens, including both surface and secreted antigens (e.g., MART-1, NY-ESO-1, MAGE-A3, and CEA) [46]. Therefore, engineering stem cells to continuously generate TCR-modified T cells may benefit the current T cell-related cancer immunotherapies. In addition, the stem cell-engineered T cells display a near-complete lack of endogenous TCR expression likely due to allelic exclusion, thereby avoiding the off-target cytotoxicity or blunted surface expression of the engineered TCRs due to TCR mispairing [47].

Nevertheless, the disadvantages of TCR engineering are that TCR expression is limited to T cells, as the surface display of TCRs needs CD3 coexpression, and the TCR recognition is MHC-restricted, as the TCR/antigen recognition replies on the presentation by MHC molecules [46]. However, CARs can be expressed on more hematopoietic lineages such as NK and myeloid cells, enhancing the potential antitumor capacity [19]. Generation of NK and myeloid cells from transplanted HSCs would be rapid and serve as an early response for antitumor immunity [18,48]. CAR-engineered NK and myeloid cells have similar antigen-specific cytotoxicity to CAR-engineered T cells [18,48]. In addition, the maturation and activation of NK and myeloid cells do not depend on thymopoiesis, thus amplifying their antitumor ability directed by CARs [18,19].

Allogeneic HSCT (allo-HSCT)

HSCT has been widely and effectively used for hematological malignancy and solid tumors, including leukemia, multiple myeloma, lymphoma, breast, ovarian, prostate, brain, lung, colorectal cancers, and melanoma [49–56]. The initial incorporation of HSCT into cancer therapies was because transplanted HSCs could replace the defective HSCs and reconstitute the entire hematopoietic system in cancer patients. Therefore, HSCT allows patients to tolerate high-dose chemotherapy or radiotherapy for tumor eradication [49,52]. The success of haploidentical HSCT has made it possible to widely use allo-HSCT with reduced risk of GvHD; the graft-versus-leukemia (GvL) effect of allo-HSCT have been comparable to HSCT with matched sibling donors [57]. Now a variety of cell-based therapeutic approaches have been developed to induce long-term immune tolerance, further minimize the risk of GvHD, and improve the GvL effect [58,59]. For example, several clinical trials have used CD19 CAR-T cell therapy as a bridge to allo-HSCT or applied CD19 CAR-T cell infusion to treat post-transplant relapse [60–64]. Approaches to co-infuse allogeneic CAR-T cells with allogeneic HSCs from a haploidentical donor into relapsed or refractory B cell acute lymphoblastic leukemia (R/R B-ALL) patients has also been performed [65–67]. The engraftment of CD19 CAR-T cells eradicates leukemia cells and the patients' B cells, potentially benefiting from HSCs engraftment. In turn, infusion of allogeneic HSCs promotes the amplification and persistence of allogeneic CD19 CAR-T cells [65–67]. In addition, a platform combining TCR αβ/CD19-depleted haplo-HSCT and TCR αβ-depleted CD19 CAR-T cells was developed, showing high antileukemia activity and low transplantation-related mortality and GvHD incidence [58,68]. Therefore, the combination of HSC-engineering (e.g., TCR αβ and CD19 ablation), allo-HSCT, and allogeneic CAR-T cell therapy leads to a promising direction of next-generation cancer treatment. Importantly, considering the manufacturing, limited yields, and potential GvHD risk of PBMC-derived allogeneic CAR-T cells, a 'third-party' stem cell-derived CAR-T cell product could be generated and combined with allo-HSCT for treating cancer patients (Figure 2). Engineering stem cells to generate allogeneic conventional αβ T cells will be discussed in other sections of this review.

By contrast, the risk of GvHD induced by allogeneic T cells is a concern of allo-HSCT. The commonly used immunosuppressive agents for GvHD could weaken the antileukemic effects of T cells post-HSCT and increase the risk of tumor relapse. Recently, other immune cell subsets, including regulatory T (Treg), iNKT, mucosal associated invariant T (MAIT), NK cells, and myeloid-derived suppressor cells (MDSCs) have been shown to ameliorate GvHD but maintain GvL effect during allo-HSCT [58,69–71]. Therefore, incorporating 'third-party' stem cell-derived immune suppressor cells, or stem cell-derived CAR-engineered immune suppressor cells (e.g., CAR-NK, CAR-iNKT, and CAR-MAIT cells) could potentially ameliorate GvHD and promote antitumor capacity in allo-HSCT (Figure 2).

Engineering stem cells for conventional T cell-based cancer immunotherapy

The current strategies for developing allogeneic T cell therapies can be divided into two categories: peripheral blood T cells from healthy donors and stem cell-derived T cells. Both candidates are being actively explored within academia, clinical research, and industry. A conventional T cell-based universal CD19-CAR engineered T cell product (UCART19) was recently tested in Phase I clinical trials treating $CD19^+$ B cell malignancies, showing the feasibility, antileukemic activity, and manageable safety profile of UCART19 [16]. To generate UCART19, both *TRAC* and *CD52* genes are disrupted to reduce the risk of GvHD and to endow the cells with resistance to Alemtuzumab treatment, which targets CD52-expressing cells [16,72,73]. In comparison to the development of healthy donor peripheral blood T cells, the progress of stem cell-derived T cell is still in the preclinical stage [74].

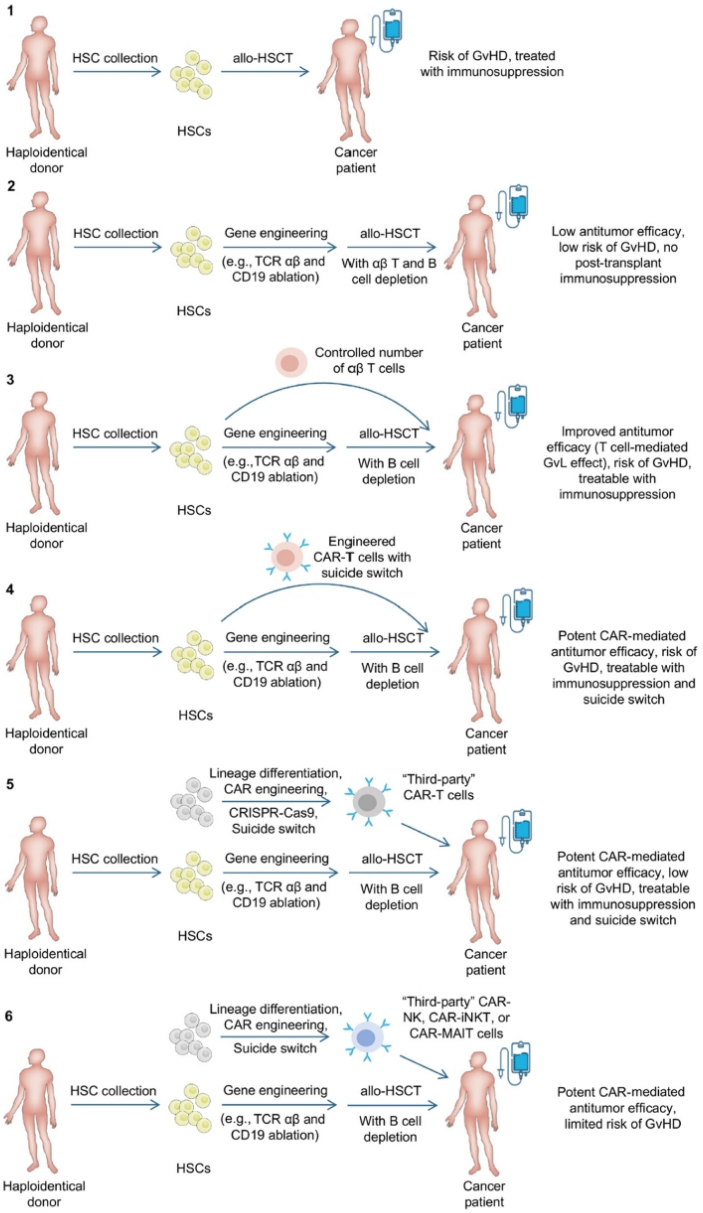

Trends in Cancer

(See figure legend at the bottom of the next page.)

T cells have been successfully differentiated from ESCs-derived hematopoietic zones using OP9-DL culture system *in vitro* [75]. The resulting cells express typical T cell markers, proliferate, and secrete cytokines in response to mitogens [75]. The unlimited production of antigen-specific human $CD8^+$ T lymphocytes from T cell-derived iPSCs (T-iPSCs) has also been reported [25–27]. These 'rejuvenated' T cells have the same TCR gene rearrangement patterns as that in the original T cell clone, and exhibit potent antigen-specific killing activity [25,27,76]. Notably, CD19 CAR-engineered T cells have been generated from T-iPSCs, showing powerful antileukemic capability [22]. The development of off-the-shelf CAR-T or tumor specific TCR-T cells will provide opportunities for upscaling of manufacturing and banking of the product. These reformations in manufacturing could significantly enlarge the access of cancer patients to CAR-T or TCR-T cell therapies and may also reduce the substantial costs of CAR-T or TCR-T cell therapies.

Engineering stem cells for unconventional T cell-based cancer immunotherapy

In addition to conventional T and NK cells, new cell carriers have been explored for cancer immunotherapy, particularly unconventional T cells, such as iNKT cell, gamma delta T (γδ T) cell, and MAIT cell. These cells serve as great candidates for off-the-shelf cancer therapy.

iNKT cell-based immunotherapy

iNKT cells are a unique T cell subpopulation specialized with CD1d-restriction that can recognize lipid antigens [77,78]. Activated iNKT cells lead to the activation of both innate and adaptive immune cells, which has been a driving force behind the development of iNKT-based immunotherapy. In addition, because iNKT cells do not recognize mismatched MHC molecules and protein autoantigens, these cells are not expected to cause GvHD [70,78,79]. Adoptive iNKT transfer is associated with reduced GvHD in multiple clinical trials [70,78,80–82]. However, the application of iNKT cell-based immunotherapy is restricted by its extremely low number in the peripheral blood. Yang laboratory developed a new approach that increases the number of circulating iNKT cells through iNKT TCR-engineering of HSCs [79,83]. It has been demonstrated that both mouse and human HSCs engineered with iNKT TCR can successfully differentiate into mouse and human iNKT cells *in vivo*. The HSC-derived iNKT cells resembled the characters of endogenous PBMC-derived iNKT cells, deploying antitumor efficacy and no toxicity [79,83]. Alternatively, Kaneko *et al*. and the Fujii Group reported the generation of human iNKT cells from iPSCs. The iPSC-derived iNKT cells showed rapid proliferation in response to α-GalCer stimulation and possessed strong antitumor activity to the K562 leukemia cell line [27,28,84,85].

γδ T cell-based immunotherapy

Another candidate considered as an idea cell carrier for developing off-the-shelf allogeneic cell therapy is γδ T cells, particularly the Vγ9Vδ2 subtype. Unlike conventional αβ T cells, γδ T cells are a small subpopulation of T lymphocytes that express γδ TCR. They respond to small phosphorylated nonpeptide antigens which are widely expressed on malignant cells. γδ T cells recognize phosphoantigen (pAg) presented by butyrophilin 3A1 (BTN3A1/CD277), which is structurally

Figure 2. Schematics of combination therapy of allo-HSCT and allogeneic CAR-T therapy. Six strategies of allo-HSCT and allogeneic CAR-T combination therapy and their pros and cons are presented. GvHD is the most frequent complication following traditional allo-HSCT (Panel 1). Therefore, a TCRαβ/CD19-depleted allo-HSCT platform has been employed (Panel 2). CAR-T cells are generated from depleted αβ conventional T cells, while simultaneously inactivating the TCR and rejoining the graft of haplo-HSCT (Panels 3 and 4). A 'third-party' CAR-engineered T, iNKT, MAIT, or NK cells could also be incorporated to allo-HSCT (Panels 5 and 6), improving CAR-mediated antitumor capacity, reducing the risk of GvHD, and upscaling manufacturing. Abbreviations: CAR, chimeric antigen receptor; GvHD, graft-versus-host disease; HSCs, hematopoietic stem cells; HSCT, hematopoietic stem cell transplantation; iNKT, invariant NK T; MAIT, mucosal associated invariant T; NK, natural killer; TCR, T cell receptors.

homologous to the B7 superfamily of proteins [86]. In addition to their unique TCR, γδ T cells also express NK receptors and FcγRIII, providing additional manners against tumor cells. However, the current approach of γδ T-based adoptive therapy only involves *ex vivo* expansion of PBMC γδ T cells using a synthetic aminobisphosphonate drug, Zoledronate [86–88]. The low yield and highly variability of current γδ T production methods make it important to develop new approaches that can stably generate pure and clonal γδ T cells. Similar to generating conventional αβ T cells, NK cells and iNKT cells from genetically engineered stem cells, engineering stem cells to produce γδ T cells, might be a feasible approach that can facilitate the γδ T cell-based cancer therapy.

MAIT cell-based immunotherapy

Another innate T lymphocyte population, MAIT cells, express the semi-invariant TCR, classically consisting of Vα7.2-Jα33/Jα12/Jα20 in humans, and Vα19-Jα33 in mice, which are paired with a restricted Vβ repertoire [89–91]. MAIT TCRs recognize riboflavin metabolite-based antigens and folate derivatives presented by monomorphic MHC I-related protein 1 (MR1) [89–91]. Similar to iNKT and γδ T cells, MAIT cells have shown powerful antitumor capacity independent of tumor antigen- and MHC-restriction [90,92]. Because MAIT cells do not recognize mismatched MHC molecules and protein autoantigens, these cells are not expected to cause GvHD [93,94]. These unique features provide MAIT cells with great potential for developing off-the-shelf cellular therapy for cancer. Wakao *et al.* have shown successful generation of human MAIT cells through iPSCs reprogramming and redifferentiation. The resulting iPSC-derived MAIT cells showed resembling phenotypes and functionality resembling those of PBMC-derived MAIT cells [76]. However, contradictorily, a recent study has found that MAIT cells displayed tumor-promoting function by suppressing T and/or NK cells [95]. Thus, more research is needed to explore the roles of MAIT cells in cancer treatment.

In conclusion, engineering unconventional innate-type T cells (e.g., iNKT, γδ T, and MAIT cells) that have powerful antitumor capacity while free of GvHD risk represents an attractive direction for developing allogeneic cell therapy for cancer especially for solid tumors [80,96–98]. Yang lab has successfully developed HSC-engineered iNKT, γδ T, and MAIT cell therapy for cancer, using either *in vivo* bone marrow–liver–thymus (BLT) mouse model or *in vitro* 'off-the-shelf' culture systems [79,83]. These approaches demonstrate the feasibility, safety, and cancer therapy potential of the proposed HSC-iNKT, γδ T, and MAIT cell therapy and laid a foundation for future translational and clinical development (Figure 3).

Engineering stem cells for NK cell-based cancer immunotherapy

NK cells are potent innate immune cells endowed with powerful antitumor activity. Unlike conventional αβ T cells expressing rearranged, antigen-specific receptors, NK cell function is dictated by the integration of signals from activating and inhibitory receptors [3,99]. NK cells recognize and target abnormal or stressed cells independent of MHC restriction and prior sensitization, thereby eliminating the risk of GvHD [3,99]. The functional activity of NK cell-mediated immunotherapy can be enhanced by stimulating activating receptors, by methods such as exposure to cytokines like IL-2 or IL-15 [3,100,101], directing antibody-dependent cellular cytotoxicity (ADCC) through the NK cell Fc receptor CD16 (FcγRIIIa) [102], blocking NK inhibitory receptors using anti-killer cell immunoglobulin-like receptor (KIR) or anti-NKG2A monoclonal antibodies [3,102], or arming the NK cells with CARs [103–105].

Current clinical grade NK cells can be produced from various sources, such as NK92 cell line, PBMCs, UCB, $CD34^+$ HSCs, and iPSCs [100]. Particularly, due to the fast-paced advancement of CAR engineering, generating CAR-NK cells from genetically engineered stem cells has opened

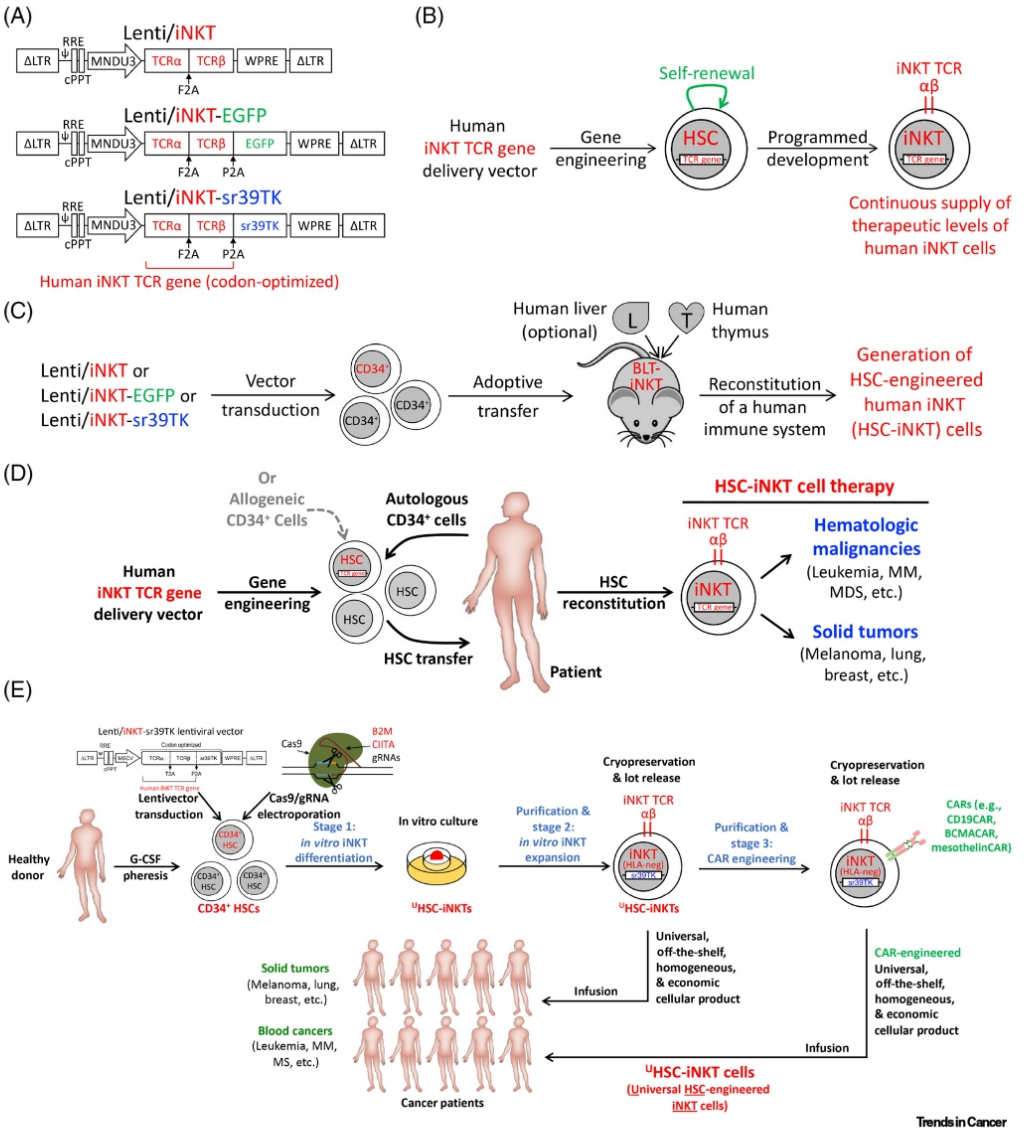

Figure 3. HSC-engineered iNKT cell therapy for cancer. The same strategies outlined for iNKT cell therapy could be applied to generate HSC-engineered γδ T, MAIT, and TCR-specific αβ T (e.g., NY-ESO-1-T) cells. (A) Schematics of the Lenti/iNKT vectors. (B) Generation of HSC-engineered iNKT cells. (C) Experimental design to generate HSC-iNKT cells in a BLT humanized mouse model. (D) Proposed HSC-iNKT cell therapy. Autologous or allogeneic human HSCs could be collected and engineered with Lenti/iNKT vectors, followed by adoptive transfer into cancer patients. (E) Proposed allogeneic 'off-the-shelf' HSC-iNKT cell therapy. G-CSF-mobilized

(Figure legend continued at the bottom of the next page.)

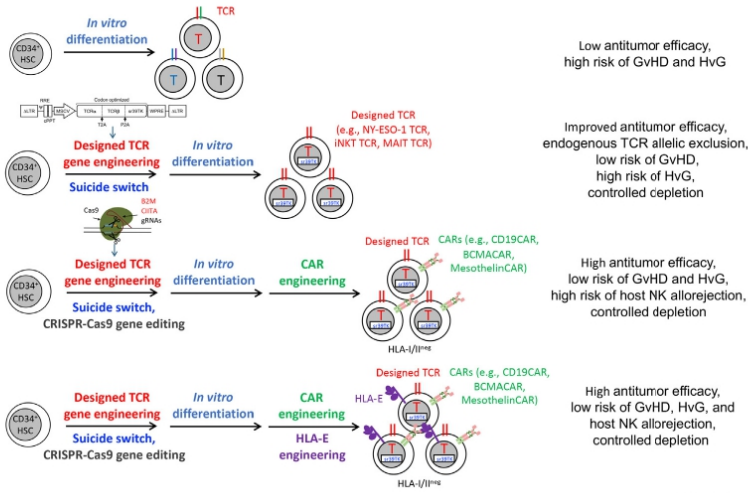

Figure 4. Development of 'off-the-shelf' HSC-engineered T cell-based therapy for cancer. Transferring the TCR gene (e.g., NY-ESO-1, iNKT, MAIT, and γδ T TCR genes) into HSCs provides a promising approach to long-term generation of T cells with endogenous TCR allelic exclusion and defined tumor antigen specificity. Suicide switch and CARs could also be engineered on HSCs or differentiated T cells to enhance their safety profile and antitumor capacity. In order to avoid HvG effect, HSC-engineered T cell products could be further engineered to achieve total ablation of their surface HLA-I/II molecules by knocking out *B2M* and *CIITA* genes using CRISPR–Cas9–gRNAs system. However, one potential caveat of this modification is that the lack of HLA expression in the cell product may trigger the risk of rejection by the host NK cells. An *HLA-E* transgene can also be incorporated into the final T cell products to further increase their resistance to host NK cell-mediated allorejection. Abbreviations: CAR, chimeric antigen receptor; HLA, human leukocyte antigen; HSCs, hematopoietic stem cells; HvG, host-versus-graft; γδ T, gamma delta T; GvHD, graft-versus-host disease; iNKT, invariant NK T; MAIT, mucosal associated invariant T; NK, natural killer; TCR, T cell receptors.

a new era of cancer immunotherapy. Most clinical trials use NK92 cell line and autologous/haploidentical NK cells without genetic modification [100]. However, NK92 being a tumor cell line has potential tumorigenicity risk and requires lethal irradiation before infusion; the self-human leukocyte antigen (HLA) signals in tumor environment may inhibit the antitumor activity of autologous NK cells. Nevertheless, $CD34^+$ HSCs isolated from mobilized periphery blood (PB) or UCB provide stable sources for NK cells and retain the flexibility of selecting donors with certain HLA types. HSC-derived NK cells express specific NK receptor profiles [105] and perform similar functions as PB-derived NK cells [106]. Of note, HSC-derived NK cells are less mature and exhibit lower cytotoxicity with lower expression of Perforin, Granzyme B, and higher expression of certain inhibitory molecules.

Another attractive direction for allogeneic NK cell therapy is to generate NK cells from PSCs, which will not be restricted by the limited $CD34^+$ cell number and complicated harvesting

$CD34^+$ HSCs could be collected from healthy donors, engineered with Lenti/iNKT vectors and a CRISPR–Cas9/B2M–CIITA–gRNAs complex, then be differentiated into iNKT cells in an *in vitro* culture (e.g., ATO and feeder-free culture). The iNKT cells will then be purified and further expanded *in vitro*, followed by cryopreservation and lot release. CAR engineering could also be incorporated into HSC-iNKT cells to enhance the antitumor capacity of these cells. Note that knockout of *B2M* and *CIITA* genes could efficiently ablate HLA-I/II expression on HSC-iNKT cells to avoid HvG responses following the autologous transfer of iNKT cells. Abbreviations: ATO, artificial thymic organoid; BLT, bone marrow–liver–thymus; CAR, chimeric antigen receptor; HLA, human leukocyte antigen; HSCs, hematopoietic stem cells; γδ T, gamma delta T; iNKT, invariant NK T; MAIT, mucosal associated invariant T; MDS, myelodysplastic syndromes; MM, multiple myeloma; NK, natural killer; TCR, T cell receptors.

procedures. Studies have demonstrated the successful generation of NK cells from PSCs, including ESCs [21,107,108] and iPSCs [109,110]. ES-derived NK cells express comparable maturation markers such as KIRs, CD16, and natural cytotoxic receptors, and exhibit antitumor activity through both direct cell-mediated cytotoxicity and ADCC [108]. Genetic engineered iPSCs can stably differentiate into hematopoietic progenitor cells in medium supplemented with SCF, bone morphogenetic protein 4 (BMP4), and vascular endothelial growth factor (VEGF). Following activation with artificial antigen presenting cells (APCs) and stimulation with IL-15, IL-7, SCF, and FLT-3L, a large number of highly homogeneous CAR-NK cells can be generated for clinical use [21,107,111]. iPSC-derived NK cells exhibit an immature phenotype with lower expression of KIR and CD16 while expressing higher levels of NKG2A compared to PB-derived NK cells. In combination with CAR engineering, CAR-iPSC-NK cells significantly inhibited tumor growth and prolonged survival in an ovarian cancer xenograft model [109]. This finding is pending validation in clinical studies. If successful, the experience will provide a platform of knowledge to treat other cancers and to create the next-generation of NK cell-based immunotherapy.

Despite the optimistic outcomes from most recent studies, there are still many challenges remaining. How can expansion methods be standardized for robust NK generation? How can screens identify the best donors from various NK phenotypes? And how do we resolve the rejection of allogeneic NK cells post infusion by recipients? All of these questions are left for future studies.

Engineering stem cells for innate immune cell-based cancer immunotherapy

Several studies have reported that CAR-equipped myeloid cells exhibit similar antigen-specific cytotoxicity in comparison with CAR-T cells [18,48]. Since non-T cells, such as myeloid and NK cells, do not rely on thymopoiesis to acquire active cytotoxic effectors, CAR-engineered myeloid and NK cells could exponentially magnify their antitumor capacity [19].

Dendritic cells (DCs) are derived from hematopoietic stem/progenitors, and genetic engineering of HSCs with specific antigen genes followed by HSCT could reconstitute host lymphoid–hematopoietic systems and allow continuous generation of antigen-expressing DCs [112]. The administration of appropriate DC stimulatory cytokines could promote maturation and expansion of antigen-expressing DCs, and subsequently evoke powerful antitumor immune responses [113,114]. Therefore, utilizing HSC gene engineering in the context of HSCT and DC activation adjuvant may facilitate the translational and clinical development toward generating/redirecting desired antigen-specific immune responses.

Concluding remarks

Stem cells including HSCs, ESCs, and iPSCs remain attractive targets for cancer immunotherapy. Current studies and early clinical trials support the feasibility of engineered stem cells for developing potent effector cells and antitumor immunity for cancer eradication. Stem cell engineering not only provides an unlimited source of therapeutic cellular products, but it also creates a versatile and flexible platform for performing additional engineering in order to improve the antitumor potency of resulting cellular products. It remains to be proven in clinical trials whether the stem cell-engineered approaches will possess additional efficacy compared to those utilizing mature human PBMC-derived immune cells as targets. Certainly, the two approaches may be complementary when applied together in some cases. Clinical trials are being developed that will provide some preliminary assessments.

Transferring TCR gene into HSCs provides an attractive method of sustained long-term generation of T cells with defined antigen specificity [31,32]. These HSC-engineered T cells display near-complete lack of endogenous TCR expression likely due to allelic exclusion [47,115–117].

Outstanding questions

How can one further enhance the safety profile and reduce the potential toxicity of stem cell-derived cellular products?

How can the *in vivo* persistence of stem cell-derived cellular products be elevated post adoptive transfer?

How can resistance to host T and NK cell-mediated allorejection be improved and be used to increase engraftment of resulting cells post infusion?

How can tumor antigen specificity and exhaustion resistance increase when using stem cell-derived cellular products to treat cancer?

How can the tumor suppressive microenvironment be altered to enhance therapeutic cell trafficking?

How can preparation and storage conditions be improved without affecting the viability and cytotoxicity of the resulting cellular products?

Will combination therapy, such as with traditional chemotherapy and checkpoint inhibitor blockade, enhance antitumor ability of stem cell-derived cellular products?

A systemic comparison between PBMC-derived and stem cell-derived cellular products, including their antitumor capacity, *in vivo* persistence, safety, availability, manufacturing, and costs, etc., should be investigated in clinical studies to customize the ideal treatment plan to individual patients.

Therefore, these HSC-engineered T cells would have limited risk of inducing GvHD. Zhu *et al.* have generated functional clonal HSC-iNKT cells with high purity and high yield through iNKT-TCR engineering of human HSCs and differentiation of HSCs to iNKT cells [79]. Besides getting rid of the alloreactive endogenous TCR, the next generation of product can benefit from ablating surface MHC molecules and making the cells resistant to the clearance by host cells. These can be achieved by disrupting *B2M* and *CIITA* genes [14,118]. However, one possible caveat of this modification is that the lack of HLA expression in the cell product may trigger the risk of rejection by the host NK cells [119,120]. An *HLA-E* or *HLA-G transgene* can also be incorporated into the *B2M/CIITA* knockout cell products to further increase their resistance to host NK cell-mediated allorejection. The stem cell engineering platform is robust and versatile, allowing the plug-in of additional engineering approaches. For example, incorporation of multiple tumor targeting molecules (e.g., CARs and TCRs) and functional enhancement factors (e.g., overexpression of immune enhancement genes like *IL15* and *IL7*, and ablation of immune inhibitory genes like *PDCD1* and *CTLA4*) may improve the cancer therapy potential. Therefore, developing new techniques to achieve high engineering efficacy of multiple genes is necessary for next-generation stem cell-based cancer immunotherapies (Figure 4).

In conclusion, stem cells can be engineered to stably express various antitumor agents, overcoming the shortage of conventional PBMC-derived agents. However, widely using stem cell-based therapy will require further developing our understanding of fundamental stem cell mechanisms and the relationships between normal and cancer stem cells, as well as applying new techniques to engineer stem cells and improve stem cell engineering efficacy (see Outstanding questions) more precisely. With more intensive and rapid progress of stem cell research, engineering stem cells provide great promise for developing novel, efficient, and safe strategies for successful cancer immunotherapy.

Acknowledgments

This work was supported by a Director's New Innovator Award from the NIH (DP2 CA196335, to L.Y.), a Partnering Opportunity for Translational Research Projects Award from the California Institute for Regenerative Medicine (CIRM TRAN1-08533, to L.Y.), a Stem Cell Research Award from the Concern Foundation (to L.Y.), a Research Career Development Award from the STOP CANCER Foundation (to L.Y.), and a BSCRC-RHF Research Award from the Rose Hills Research Foundation (to L.Y.). Y.-R.L. is a predoctoral fellow supported by the UCLA Whitcome Predoctoral Fellowship in Molecular Biology.

Declaration of interests

No interests to declare.

References

1. Restifo, N.P. *et al.* (2012) Adoptive immunotherapy for cancer: Harnessing the T cell response. *Nat. Rev. Immunol.* 12, 269–281
2. Sadelain, M. *et al.* (2013) The basic principles of chimeric antigen receptor design. *Cancer Discov.* 3, 388–398
3. Shimasaki, N. *et al.* (2020) NK cells for cancer immunotherapy. *Nat. Rev. Drug Discov.* 19, 200–218
4. Brentjens, R.J. *et al.* (2011) Safety and persistence of adoptively transferred autologous CD19-targeted T cells in patients with relapsed or chemotherapy refractory B-cell leukemias. *Blood* 118, 4817–4828
5. Lin, Q. *et al.* (2019) Recent updates on CAR T clinical trials for multiple myeloma. *Mol. Cancer* 18, 154
6. Schaft, N. (2020) The landscape of car-t cell clinical trials against solid tumors—a comprehensive overview. *Cancers (Basel)* 12, 2567
7. Brentjens, R.J. *et al.* (2013) CD19-targeted T cells rapidly induce molecular remissions in adults with chemotherapy-refractory acute lymphoblastic leukemia. *Sci. Transl. Med.* 5, 177ra38
8. Kochenderfer, J.N. *et al.* (2012) B-cell depletion and remissions of malignancy along with cytokine-associated toxicity in a clinical trial of anti-CD19 chimeric-antigen-receptor-transduced T cells. *Blood* 119, 2709–2720
9. Kalos, M. *et al.* (2011) T cells with chimeric antigen receptors have potent antitumor effects and can establish memory in patients with advanced leukemia. *Sci. Transl. Med.* 3, 95ra73
10. Rafiq, S. *et al.* (2020) Engineering strategies to overcome the current roadblocks in CAR T cell therapy. *Nat. Rev. Clin. Oncol.* 17, 147–167
11. Aftab, B.T. *et al.* (2020) Toward 'off-the-shelf' allogeneic CAR T cells. *Adv. Cell Gene Ther.* 3, e86
12. Basar, R. *et al.* (2020) Next-generation cell therapies: the emerging role of CAR-NK cells. *Blood Adv.* 4, 5868–5876
13. Lanza, R. *et al.* (2019) Engineering universal cells that evade immune detection. *Nat. Rev. Immunol.* 19, 723–733
14. Ren, J. *et al.* (2017) Multiplex genome editing to generate universal CAR T cells resistant to PD1 inhibition. *Clin. Cancer Res.* 23, 2255–2266
15. Depil, S. *et al.* (2020) 'Off-the-shelf' allogeneic CAR T cells: development and challenges. *Nat. Rev. Drug Discov.* 19, 185–199

16. Benjamin, R. *et al.* (2020) Genome-edited, donor-derived allogeneic anti-CD19 chimeric antigen receptor T cells in paediatric and adult B-cell acute lymphoblastic leukaemia: results of two phase 1 studies. *Lancet* 396, 1885–1894
17. Liu, E. *et al.* (2020) Use of CAR-transduced natural killer cells in CD19-positive lymphoid tumors. *N. Engl. J. Med.* 382, 545–553
18. Roberts, M.R. *et al.* (1998) Antigen-specific cytolysis by neutrophils and NK cells expressing chimeric immune receptors bearing zeta or gamma signaling domains. *J. Immunol.* 161, 375–384
19. Adair, J.E. *et al.* (2017) Hematopoietic stem cell approaches to cancer. *Hematol. Oncol. Clin. North Am.* 31, 897–912
20. Takahashi, K. *et al.* (2007) Induction of pluripotent stem cells from adult human fibroblasts by defined factors. *Cell* 131, 861–872
21. Hermanson, D.L. *et al.* (2016) Induced pluripotent stem cell-derived natural killer cells for treatment of ovarian cancer. *Stem Cells* 34, 93–101
22. Themeli, M. *et al.* (2013) Generation of tumor-targeted human T lymphocytes from induced pluripotent stem cells for cancer therapy. *Nat. Biotechnol.* 31, 928–933
23. Notta, F. *et al.* (2011) Isolation of single human hematopoietic stem cells capable of long-term multilineage engraftment. *Science* 333, 218–221
24. Larson, S. and De Oliveira, S.N. (2014) Gene-modified hematopoietic stem cells for cancer immunotherapy. *Hum. Vaccines Immunother.* 10, 982–985
25. Nishimura, T. *et al.* (2013) Generation of rejuvenated antigen-specific T cells by reprogramming to pluripotency and redifferentiation. *Cell Stem Cell* 12, 114–126
26. Nishimura, T. and Nakauchi, H. (2019) Generation of antigen-specific T cells from human induced pluripotent stem cells. *Methods Mol. Biol.* 1899, 25–40
27. Vizcardo, R. *et al.* (2013) Regeneration of human tumor antigen-specific T cells from iPSCs derived from mature CD8+ T cells. *Cell Stem Cell* 12, 31–36
28. Kitayama, S. *et al.* (2016) Cellular adjuvant properties, direct cytotoxicity of re-differentiated Vα24 invariant NKT-like cells from human induced pluripotent stem cells. *Stem Cell Reports* 6, 213–227
29. Zeng, J. *et al.* (2017) Generation of 'off-the-shelf' natural killer cells from peripheral blood cell-derived induced pluripotent stem cells. *Stem Cell Reports* 9, 1796–1812
30. Kohn, D.B. *et al.* (2013) Gene therapy through autologous transplantation of gene-modified hematopoietic stem cells. *Biol. Blood Marrow Transplant.* 19, S64–S69
31. Yang, L. and Baltimore, D. (2005) Long-term *in vivo* provision of antigen-specific T cell immunity by programming hematopoietic stem cells. *Proc. Natl. Acad. Sci. U. S. A.* 102, 4518–4523
32. Yang, L. *et al.* (2002) Generation of functional antigen-specific T cells in defined genetic backgrounds by retrovirus-mediated expression of TCR cDNAS in hematopoietic precursor cells. *Proc. Natl. Acad. Sci. U. S. A.* 99, 6204–6209
33. Rupp, L.J. *et al.* (2017) CRISPR/Cas9-mediated PD-1 disruption enhances antitumor efficacy of human chimeric antigen receptor T cells. *Sci. Rep.* 7, 737
34. Stadtmauer, E.A. *et al.* (2020) CRISPR-engineered T cells in patients with refractory cancer. *Science* 367, eaba7365
35. Cherkassky, L. *et al.* (2016) Human CAR T cells with cell-intrinsic PD-1 checkpoint blockade resist tumor-mediated inhibition. *J. Clin. Invest.* 126, 3130–3144
36. Qasim, W. *et al.* (2017) Molecular remission of infant B-ALL after infusion of universal TALEN gene-edited CAR T cells. *Sci. Transl. Med.* 9, eaaj2013
37. Georgiadis, C. *et al.* (2018) Long terminal repeat CRISPR-CAR-coupled 'universal' T cells mediate potent antileukemic effects. *Mol. Ther.* 26, 1215–1227
38. Liu, X. *et al.* (2017) CRISPR-Cas9-mediated multiplex gene editing in CAR-T cells. *Cell Res.* 27, 154–157
39. Eyquem, J. *et al.* (2017) Targeting a CAR to the TRAC locus with CRISPR/Cas9 enhances tumour rejection. *Nature* 543, 113–117
40. Mukherjee, S. and Thrasher, A.J. (2013) Gene therapy for PIDs: progress, pitfalls, and prospects. *Gene* 525, 174–181
41. Traversari, C. *et al.* (2007) The potential immunogenicity of the TK suicide gene does not prevent full clinical benefit associated with the use of TK-transduced donor lymphocytes in HSCT for hematologic malignancies. *Blood* 109, 4708–4715
42. Berger, C. *et al.* (2006) Analysis of transgene-specific immune responses that limit the *in vivo* persistence of adoptively transferred HSV-TK-modified donor T cells after allogeneic hematopoietic cell transplantation. *Blood* 107, 2294–2302
43. Bonini, C. *et al.* (1997) HSV-TK gene transfer into donor lymphocytes for control of allogeneic graft-versus-leukemia. *Clin. Trial Sci.* 376, 1719–1724
44. Straathof, K.C. *et al.* (2005) An inducible caspase 9 safety switch for T-cell therapy. *Blood* 105, 4247–4254
45. Thomis, D.C. *et al.* (2001) A Fas-based suicide switch in human T cells for the treatment of graft-versus-host disease. *Blood* 97, 1249–1257
46. Zhao, L. and Cao, Y.J. (2019) Engineered T cell therapy for cancer in the clinic. *Front. Immunol.* 10, 2250
47. Giannoni, F. *et al.* (2013) Allelic exclusion and peripheral reconstitution by TCR transgenic T cells arising from transduced human hematopoietic stem/progenitor cells. *Mol. Ther.* 21, 1044–1054
48. Hege, K.M. *et al.* (1996) Systemic T cell-independent tumor immunity after transplantation of universal receptor-modified bone marrow into SCID mice. *J. Exp. Med.* 184, 2261–2269
49. Nabhan, C. *et al.* (2001) The role of bone marrow transplantation in acute promyelocytic leukemia. *Bone Marrow Transplant.* 28, 219–226
50. Shelburne, N. and Bevans, M. (2009) Non-myeloablative hematopoietic stem cell transplantation. *Semin. Oncol. Nurs.* 25, 120–128
51. Nieto, Y. *et al.* (2004) Prognostic analysis of early lymphocyte recovery in patients with advanced breast cancer receiving high-dose chemotherapy with an autologous hematopoietic progenitor cell transplant. *Clin. Cancer Res.* 10, 5076–5086
52. Popat, U. *et al.* (2003) Haemopoietic stem cell transplantation for acute lymphoblastic leukaemia. *Cancer Treat. Rev.* 29, 3–10
53. Rizzo, J.D. *et al.* (2002) Autologous stem cell transplantation for small cell lung cancer. *Biol. Blood Marrow Transplant.* 8, 273–280
54. Frickhofen, N. *et al.* (2006) Phase I/II trial of multicycle high-dose chemotherapy with peripheral blood stem cell support for treatment of advanced ovarian cancer. *Bone Marrow Transplant.* 38, 493–499
55. McNiece, I. *et al.* (2000) *Ex vivo* expanded peripheral blood progenitor cells provide rapid neutrophil recovery after high-dose chemotherapy in patients with breast cancer. *Blood* 96, 3001–3007
56. Hale, G.A. (2005) Autologous hematopoietic stem cell transplantation for pediatric solid tumors. *Expert. Rev. Anticancer. Ther.* 5, 835–846
57. Luo, Y. *et al.* (2014) T-cell-replete haploidentical HSCT with low-dose anti-T-lymphocyte globulin compared with matched sibling HSCT and unrelated HSCT. *Blood* 124, 2735–2743
58. Zhang, M. and Huang, H. (2020) How to combine the two landmark treatment methods—allogeneic hematopoietic stem cell transplantation and chimeric antigen receptor T cell therapy together to cure high-risk B cell acute lymphoblastic leukemia? *Front. Immunol.* 11
59. Bertaina, A. and Roncarolo, M.G. (2019) Graft engineering and adoptive immunotherapy: New approaches to promote immune tolerance after hematopoietic stem cell transplantation. *Front. Immunol.* 10, 611710
60. Gu, B. *et al.* (2021) Allogeneic haematopoietic stem cell transplantation improves outcome of adults with relapsed/refractory Philadelphia chromosome-positive acute lymphoblastic leukemia entering remission following CD19 chimeric antigen receptor T cells. *Bone Marrow Transplant.* 56, 91–100
61. Hay, K.A. *et al.* (2019) Factors associated with durable EFS in adult B-cell ALL patients achieving MRD-negative CR after CD19 CAR T-cell therapy. *Blood* 133, 1652–1663
62. Turtle, C.J. *et al.* (2016) CD19 CAR-T cells of defined CD4+: CD8+ composition in adult B cell ALL patients. *J. Clin. Invest.* 126, 2123–2138

1.2 Development of hematopoietic stem cell-engineered iNKT cell therapy for cancer

(This project is published on Cell Stem Cell in 2019)

Article

Cell Stem Cell

Development of Hematopoietic Stem Cell-Engineered Invariant Natural Killer T Cell Therapy for Cancer

Graphical Abstract

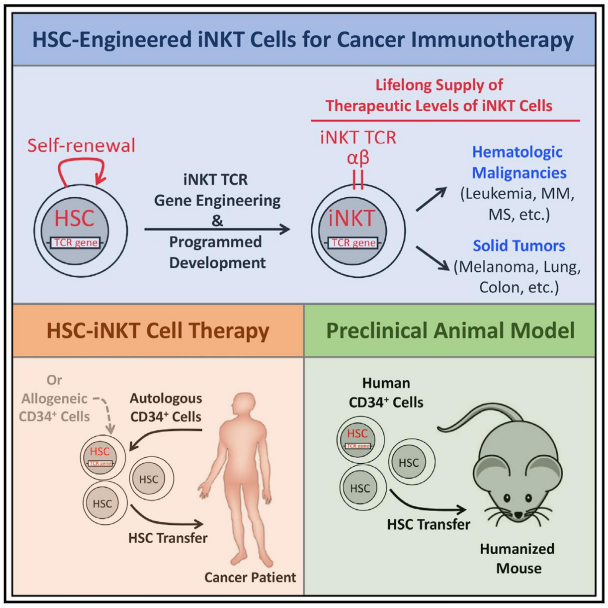

Highlights

- HSC-iNKT cell therapy can provide patients with a lifelong supply of iNKT cells
- HSC-iNKT cell therapy can potentially be utilized to treat a broad range of cancers
- HSC-iNKT cells can target tumor cells through multiple mechanisms
- A preclinical study demonstrated feasibility, safety, and cancer therapy potential

Authors

Yanni Zhu, Drake J. Smith, Yang Zhou, ..., Donald B. Kohn, Owen N. Witte, Lili Yang

Correspondence

liliyang@ucla.edu

In Brief

Yang and colleagues reported the preclinical development of a hematopoietic stem cell-engineered-invariant natural killer T (HSC-iNKT) cell therapy. HSC-iNKT cell therapy has the potential to treat a broad range of cancers through providing cancer patients with therapeutic levels of iNKT cells for a lifetime.

Please cite this article in press as: Zhu et al., Development of Hematopoietic Stem Cell-Engineered Invariant Natural Killer T Cell Therapy for Cancer, Cell Stem Cell (2019), https://doi.org/10.1016/j.stem.2019.08.004

Cell Stem Cell
Article

Development of Hematopoietic Stem Cell-Engineered Invariant Natural Killer T Cell Therapy for Cancer

Yanni Zhu,[1,17] Drake J. Smith,[1,17] Yang Zhou,[1] Yan-Ruide Li,[1] Jiaji Yu,[1] Derek Lee,[1] Yu-Chen Wang,[1] Stefano Di Biase,[1] Xi Wang,[1] Christian Hardoy,[1] Josh Ku,[1] Tasha Tsao,[1] Levina J. Lin,[1] Alexander T. Pham,[1] Heesung Moon,[1] Jami McLaughlin,[1] Donghui Cheng,[1] Roger P. Hollis,[1] Beatriz Campo-Fernandez,[1] Fabrizia Urbinati,[1] Liu Wei,[2,3] Larry Pang,[2,3] Valerie Rezek,[4,5] Beata Berent-Maoz,[5] Mignonette H. Macabali,[5] David Gjertson,[6,7] Xiaoyan Wang,[5] Zoran Galic,[4,5] Scott G. Kitchen,[4,5] Dong Sung An,[5,8,9] Siwen Hu-Lieskovan,[5] Paula J. Kaplan-Lefko,[5,10] Satiro N. De Oliveira,[11] Christopher S. Seet,[4,5] Sarah M. Larson,[12] Stephen J. Forman,[13] James R. Heath,[14] Jerome A. Zack,[1,4,5,15] Gay M. Crooks,[4,6,10,11] Caius G. Radu,[2,3,10] Antoni Ribas,[2,4,10,16] Donald B. Kohn,[1,4,11] Owen N. Witte,[1,4,10,15,16] and Lili Yang[1,4,10,15,18,*]

[1]Department of Microbiology, Immunology & Molecular Genetics, University of California, Los Angeles, Los Angeles, CA 90095, USA
[2]Department of Molecular and Medical Pharmacology, University of California, Los Angeles, Los Angeles, CA 90095, USA
[3]Ahmanson Translational Imaging Division, University of California, Los Angeles, Los Angeles, CA 90095, USA
[4]Eli and Edythe Broad Center of Regenerative Medicine and Stem Cell Research, University of California, Los Angeles, Los Angeles, CA 90095, USA
[5]Department of Medicine, University of California, Los Angeles, Los Angeles, CA 90095, USA
[6]Department of Pathology and Laboratory Medicine, University of California, Los Angeles, Los Angeles, CA 90095, USA
[7]Department of Biostatistics, University of California, Los Angeles, Los Angeles, CA 90095, USA
[8]School of Nursing, University of California, Los Angeles, Los Angeles, CA 90095, USA
[9]AIDS Institute, University of California, Los Angeles, Los Angeles, CA 90095, USA
[10]Jonsson Comprehensive Cancer Center, David Geffen School of Medicine, University of California, Los Angeles, Los Angeles, CA 90095, USA
[11]Department of Pediatrics, University of California, Los Angeles, Los Angeles, CA 90095, USA
[12]Department of Internal Medicine, University of California, Los Angeles, Los Angeles, CA 90095, USA
[13]Hematological Malignancies and Hematopoietic Stem Cell Transplantation Institute, City of Hope, Duarte, CA 91010, USA
[14]Institute for Systems Biology, Seattle, WA 98109, USA
[15]Molecular Biology Institute, University of California, Los Angeles, Los Angeles, CA 90095, USA
[16]Parker Institute for Cancer Immunotherapy, University of California, Los Angeles, Los Angeles, CA 90095, USA
[17]These authors contributed equally
[18]Lead Contact
*Correspondence: liliyang@ucla.edu
https://doi.org/10.1016/j.stem.2019.08.004

SUMMARY

Invariant natural killer T (iNKT) cells are potent immune cells for targeting cancer; however, their clinical application has been hindered by their low numbers in cancer patients. Here, we developed a proof-of-concept for hematopoietic stem cell-engineered iNKT (HSC-iNKT) cell therapy with the potential to provide therapeutic levels of iNKT cells for a patient's lifetime. Using a human HSC engrafted mouse model and a human iNKT TCR gene engineering approach, we demonstrated the efficient and long-term generation of HSC-iNKT cells *in vivo*. These HSC-iNKT cells closely resembled endogenous human iNKT cells, could deploy multiple mechanisms to attack tumor cells, and effectively suppressed tumor growth *in vivo* in multiple human tumor xenograft mouse models. Preclinical safety studies showed no toxicity or tumorigenicity of the HSC-iNKT cell therapy. Collectively, these results demonstrated the feasibility, safety, and cancer therapy potential of the proposed HSC-iNKT cell therapy and laid a foundation for future clinical development.

INTRODUCTION

Invariant natural killer T (iNKT) cells are a small population of αβ T lymphocytes highly conserved from mice to humans (Bendelac et al., 2007; Kronenberg and Gapin, 2002). These cells have several unique features, making them exceedingly attractive agents for developing cancer immunotherapy (King et al., 2018; Krijgsman et al., 2018; Lam et al., 2017). First, iNKT cells have a strong relevance to cancer. There is compelling evidence suggesting a significant role of iNKT cells in tumor surveillance in mice (Berzins et al., 2011; Vivier et al., 2012). In humans, iNKT cell frequencies are decreased in patients with solid tumors (including melanoma, colon, lung, breast, and head and neck cancers) and hematologic malignancies (including leukemia, multiple myeloma, and myelodysplastic syndromes), while increased iNKT cell numbers are associated with a better prognosis (Berzins et al., 2011; Krijgsman et al., 2018; Lam et al., 2017). Second, iNKT cells have the remarkable capacity to target

Please cite this article in press as: Zhu et al., Development of Hematopoietic Stem Cell-Engineered Invariant Natural Killer T Cell Therapy for Cancer, Cell Stem Cell (2019), https://doi.org/10.1016/j.stem.2019.08.004

multiple types of cancer independent of tumor antigen and major histocompatibility complex (MHC) restrictions (Fujii et al., 2013). iNKT cells recognize glycolipid antigens presented by non-polymorphic CD1d, which frees them from MHC restriction (Bendelac et al., 2007). Many tumor tissues express conserved glycolipid antigens that can be recognized by iNKT cells, although the nature of these glycolipids remain to be identified (Gapin, 2010; Mallevaey and Selvanantham, 2012; Wu et al., 2003). Third, iNKT cells can deploy multiple mechanisms to attack tumor cells, including direct killing of $CD1d^+$ tumors and immune adjuvant effects such as activating NK cells, activating DCs and thereby stimulating cytotoxic T lymphocytes (CTLs), and inhibiting tumor-associated macrophages (TAMs) (Brennan et al., 2013; Cortesi et al., 2018; Fujii et al., 2013; Krijgsman et al., 2018; Song et al., 2009; Vivier et al., 2012).

Attracted by the potent and broad anticancer functions of iNKT cells, researchers have conducted a series of clinical trials utilizing iNKT cells to treat various forms of cancer, ranging from solid tumors to hematologic malignancies (Nair and Dhodapkar, 2017; Waldowska et al., 2017). These clinical trials have utilized α-galactosylceramide (αGC, a synthetic glycolipid ligand specifically stimulating iNKT cells) alone, or αGC-pulsed DCs alone or in combination with *ex vivo*-expanded patient iNKT cells, and have shown these treatments to be safe and well tolerated. Several recent trials reported encouraging antitumor immunity in patients with melanoma, non-small cell lung cancer, and head and neck squamous cell carcinomas, attesting to the therapeutic potential of iNKT cell-based immunotherapies (Exley et al., 2017; Kunii et al., 2009; Motohashi et al., 2006; Yamasaki et al., 2011). However, most other trials yielded unsatisfactory results. Overall, these trials have all worked through the direct stimulation or *ex vivo*-expansion of patients' endogenous iNKT cells, thus yielding only short-term, limited clinical benefits to a small number of patients. The extremely low frequencies of iNKT cells in cancer patients (~0.001%–0.1% in blood), as well as the rapid depletion of these cells post-stimulation, are considered the major factors limiting the success of these trials (Krijgsman et al., 2018). In order to unleash the full potential of iNKT cells for cancer immunotherapy, innovative therapies that can overcome these limitations are in high demand.

In this study, we aim to overcome the current limitations by genetically engineering human hematopoietic stem cells (HSCs) to produce iNKT cells targeting cancer (Figure S1A). Because of the longevity and self-renewal of HSCs, by adoptively transferring iNKT T cell receptor (TCR) gene-engineered HSCs into cancer patients, this new therapy has the potential to provide patients with therapeutic levels of iNKT cells for a lifetime (Figure S1A) (Morrison et al., 1995). This TCR-engineered HSC transfer approach takes advantage of two molecular mechanisms governing T cell development, TCR allelic exclusion, and TCR instruction, to genetically program HSCs to produce T cells of designated antigen specificity and T cell subtype identity (Yang and Baltimore, 2005). Previously, we and others have successfully utilized this strategy to generate tumor antigen-specific CD4 helper and CD8 cytotoxic T cells of both mouse and human origins (Bettini et al., 2012; Giannoni et al., 2013; Vatakis et al., 2011; Yang and Baltimore, 2005). Human clinical trials are ongoing, testing NY-ESO-1 TCR-engineered HSC adoptive therapy for treating multiple cancers (Baltimore et al., 2010; Puig-Saus et al., 2019). Recently, we successfully generated iNKT cells in mice through iNKT TCR-engineered bone marrow transfer and proved cancer therapy potential of the engineered iNKT cells in a mouse melanoma lung metastasis model (Smith et al., 2015). Based on these previous works, as well as the scientific rationale that human iNKT cells also follow a "TCR-instructed" developmental path similar to that of the mouse iNKT cells (Godfrey and Berzins, 2007), we hypothesized that it would be possible to engineer human HSCs with a human iNKT TCR gene to produce human iNKT cells targeting cancer. Here, we report the preclinical development of the proposed HSC-engineered iNKT cell therapy, demonstrating its feasibility, safety, and cancer therapy potential.

RESULTS

Cloning of Human iNKT TCR Genes

Single human iNKT cells were sorted from healthy donor peripheral blood mononuclear cells (PBMCs) using flow cytometry based on a stringent combination of surface markers, gated as $hTCR\alpha\beta^+6B11^+$hTCR $V\beta11^+hCD161^{hi}$ (Figure 1A) (Bendelac et al., 2007). 6B11 is a monoclonal antibody that specifically recognizes the human iNKT TCR invariant alpha chain (hTCR Vα24-Jα18) (Chan et al., 2013; Montoya et al., 2007). We included hTCR Vβ11 staining to focus on the dominant $V\beta11^+$ population of human iNKT cells (Bendelac et al., 2007). The sorted single human iNKT cells were then subjected to TCR cloning using an established single-cell TCR cloning technology (Figure 1B) (Smith et al., 2015). A validated pair of iNKT TCR α and β chain genes (thereafter collectively referred to as the human iNKT TCR gene) were selected for further development.

Construction of Human iNKT TCR Gene Delivery Vectors

A pMNDW lentiviral vector designated for HSC-based gene therapy was chosen to deliver the iNKT TCR gene (Figure 1C) (Cartier et al., 2009). Three vectors were constructed: (1) a Lenti/iNKT vector encoding the iNKT TCR gene, which is intended for eventual clinical usage; (2) a Lenti/iNKT-EGFP vector encoding the iNKT TCR gene together with an EGFP reporter gene, which allows for convenient tracking of vector-engineered HSCs and their progeny cells using flow cytometry and thus is valuable for preclinical studies; and (3) a Lenti/iNKT-sr39TK vector encoding the iNKT TCR gene together with an sr39TK suicide and positron emission tomography (PET) imaging reporter gene, which allows for monitoring vector-engineered HSCs and their progeny cells using PET imaging and for depleting engineered cells through ganciclovir (GCV) administration in case of an adverse side effect and thus is valuable for early clinical development (Figure 1C) (Black et al., 1996; Gschweng et al., 2014; Larson et al., 2017). The gene-delivery capacity of these lentivectors, as well as the functionality of the encoded human iNKT TCR gene and EGFP and sr39TK reporter genes, was studied by transducing 293T cells (Figure 1D) and primary human PBMC T cells (Figures 1E–1G) with individual lentivectors followed by functional tests. Notably, all three lentivectors mediated efficient expression of the human iNKT TCR gene (Figure 1D); the resulting transgenic human iNKT TCRs recognized αGC and responded to αGC stimulation, as evidenced by hCD1d-PBS-57 tetramer binding and induced interferon (IFN)-γ production

Please cite this article in press as: Zhu et al., Development of Hematopoietic Stem Cell-Engineered Invariant Natural Killer T Cell Therapy for Cancer, Cell Stem Cell (2019), https://doi.org/10.1016/j.stem.2019.08.004

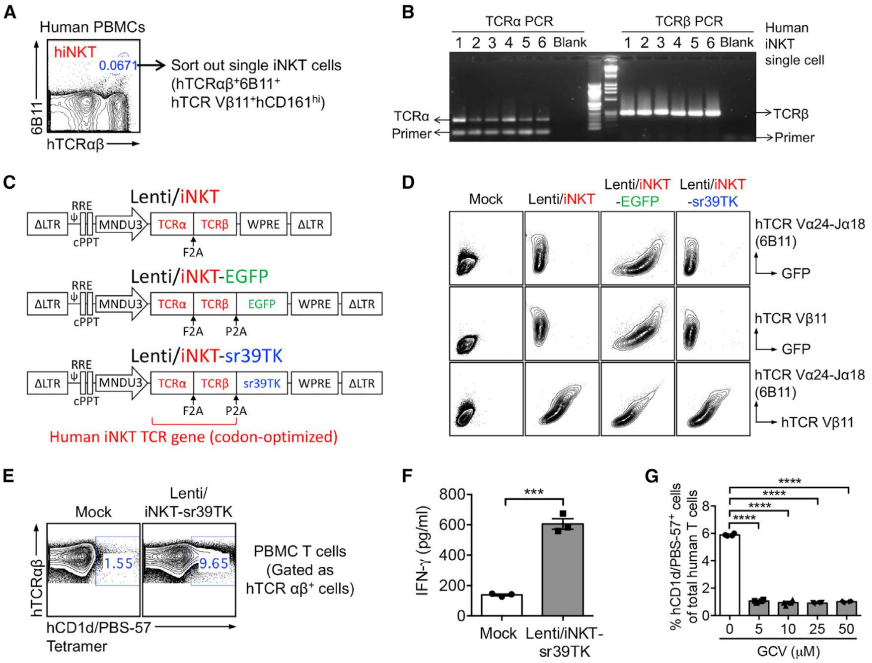

Figure 1. Cloning of Human Invariant Natural Killer T Cell Receptor Genes and Construction of Lentiviral Gene Delivery Vectors

(A and B) Cloning of human iNKT TCR genes using a single-cell RT-PCR approach. (A) Fluorescence-activated cell sorting (FACS) of single human iNKT cells. (B) Representative DNA gel image showing the human TCR α and β chain PCR products from six sorted single iNKT cells.

(C) Schematics of the Lenti/iNKT, Lenti/iNKT-EGFP, and Lenti/iNKT-sr39TK vectors.

(D) FACS detection of intracellular expression of iNKT TCRs (identified as hTCR Vβ11+6B11+) in 293T cells transduced with the indicated iNKT TCR gene delivery lentivectors.

(E–G) Functional characterization of the Lenti/iNKT-sr39TK vector by transducing human PBMC T cells. (E) FACS detection of surface iNKT TCR expression on vector-transduced PBMC T cells. (F) ELISA analysis of IFN-γ production by vector-transduced PBMC T cells post-αGC stimulation (n = 3). (G) FACS quantification of the depletion of vector-transduced PBMC T cells post-GCV treatment (n = 4).

Data are representative of 2 experiments. See also Figure S1.

(Figures 1E and 1F); and the encoded sr39TK enabled efficient GCV-induced depletion of gene-engineered cells (Figure 1G). In the present study, these three lentivectors were utilized simultaneously or individually, depending on the purpose of a given experiment.

iNKT TCR Gene Engineering of Human HSCs

iNKT TCR gene-delivery lentivectors were of high titer and could transduce human CD34+ hematopoietic stem and progenitor cells (referred to as HSCs thereafter) of various donors robustly and efficiently (Figures S1B–S1D). Gene-engineering rate of HSCs could be conveniently adjusted through titrating lentivectors utilized for transduction, resulting in 0%–50% iNKT TCR+ HSCs with an average vector copy number (VCN) of 0–3 per cell (Figure S1E).

Production of BLT-iNKT Humanized Mice

We utilized a BLT (human bone marrow-liver-thymus engrafted NOD/SCID/γc$^{-/-}$ mice) humanized mouse model that supports the engraftment of human HSCs and supports the development of human T cells, to study the *in vivo* generation of HSC-engineered human iNKT cells (Lan et al., 2006; Melkus et al., 2006; Smith et al., 2016). Human HSCs, either mock-transduced or transduced with human iNKT TCR gene-delivery vectors, were adoptively transferred into NOD/SCID/γc$^{-/-}$ (NSG) mice engrafted with human thymus to produce standard BLT mice or iNKT TCR gene-engineered BLT mice (denoted as BLT or BLT-iNKT mice, respectively) (Figure 2A). These BLT and BLT-iNKT humanized mice were then utilized for further study.

Generation of HSC-iNKT Cells in BLT-iNKT Humanized Mice

We detected efficient and comparable reconstitution of human immune cells, in particular, human αβ T cells, in both BLT and BLT-iNKT mice (Figure 2B). BLT mice contained minimal numbers of endogenous human iNKT cells below detection level (Figure 2B). Numbers of human iNKT cells were greatly increased in BLT-iNKT mice; these iNKT cells started to appear in the

Please cite this article in press as: Zhu et al., Development of Hematopoietic Stem Cell-Engineered Invariant Natural Killer T Cell Therapy for Cancer, Cell Stem Cell (2019), https://doi.org/10.1016/j.stem.2019.08.004

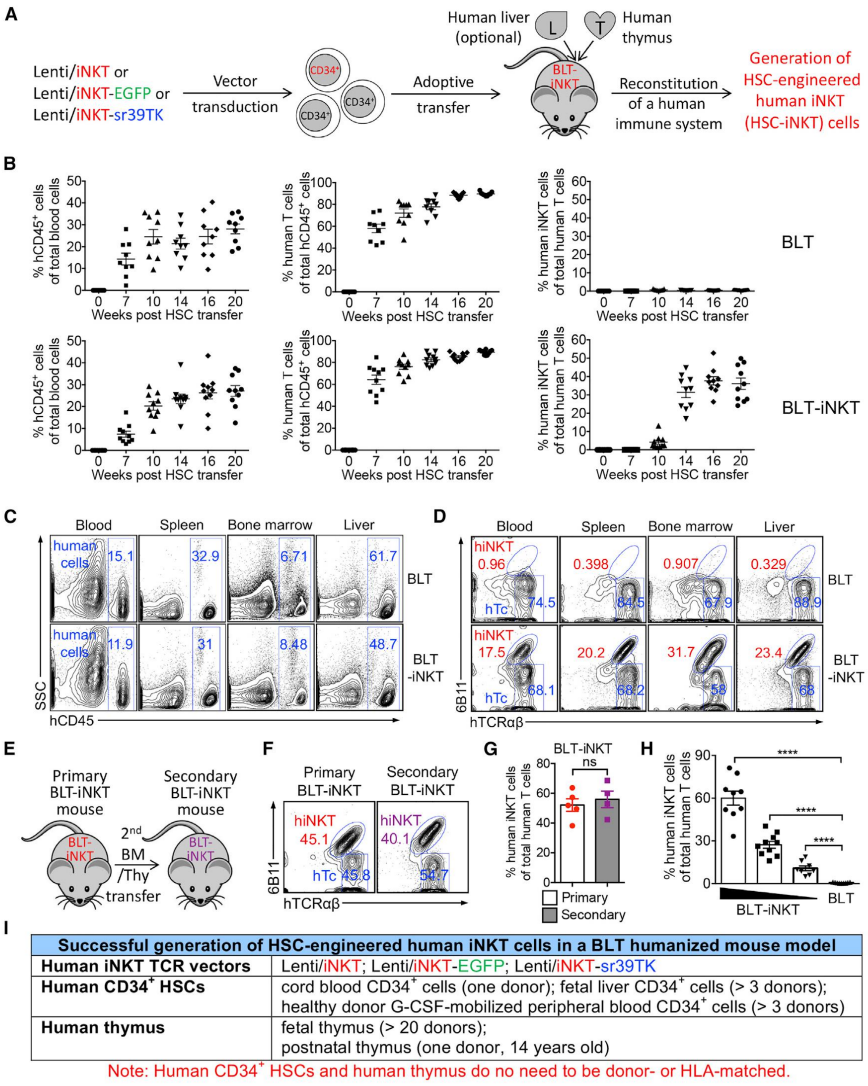

I

Successful generation of HSC-engineered human iNKT cells in a BLT humanized mouse model	
Human iNKT TCR vectors	Lenti/iNKT; Lenti/iNKT-EGFP; Lenti/iNKT-sr39TK
Human CD34$^+$ HSCs	cord blood CD34$^+$ cells (one donor); fetal liver CD34$^+$ cells (> 3 donors); healthy donor G-CSF-mobilized peripheral blood CD34$^+$ cells (> 3 donors)
Human thymus	fetal thymus (> 20 donors); postnatal thymus (one donor, 14 years old)

Note: Human CD34$^+$ HSCs and human thymus do no need to be donor- or HLA-matched.

Figure 2. Generation of Hematopoietic Stem Cell-Engineered Human iNKT (HSC-iNKT) Cells in BLT-iNKT Humanized Mice

(A) Experimental design to generate HSC-iNKT cells in a BLT humanized mouse model.

(B–D) Generation of HSC-iNKT cells in BLT-iNKT mice. (B) Time-course FACS monitoring of human immune cells (gated as hCD45$^+$ cells), human αβ T cells (gated as hCD45$^+$hTCRαβ$^+$ cells), and human iNKT cells (gated as hCD45$^+$hTCRαβ$^+$6B11$^+$ cells) in the peripheral blood of BLT-iNKT mice and control BLT mice post-HSC transfer (n = 9–10). (C) FACS detection of human immune cells in various tissues of BLT-iNKT and control BLT mice, at week 20 post-HSC transfer. (D) FACS detection of HSC-iNKT cells in various tissues of BLT-iNKT mice, at week 20 post-HSC transfer. hiNKT, human iNKT cells; hTc, conventional human αβ T cells (gated as hCD45$^+$hTCRαβ$^+$6B11$^-$ cells).

(E–G) Long-term production of HSC-iNKT cells in BLT-iNKT mice. (E) Experimental design. BM, total bone marrow cells harvested from the primary BLT-iNKT mice; Thy, human thymus implants collected from the primary BLT-iNKT mice. (F) FACS detection of HSC-iNKT cells in the peripheral blood of the secondary BLT-iNKT mice at week 16 after the secondary BM and Thy transfer. (G) Quantification of (F) (n = 4–5).

peripheral blood of BLT-iNKT mice around 2 months post-HSC transfer and then peaked and stabilized around 3 months, indicating that they were derived from the iNKT TCR gene-engineered HSCs (Figure 2B). Analysis of BLT-iNKT mice revealed a tissue distribution of HSC-engineered human iNKT cells (referred to as HSC-iNKT cells thereafter) that was typical of human iNKT cells: besides circulating in blood, HSC-iNKT cells homed to lymphoid organs such as the bone marrow and spleen, as well as other peripheral organs such as the liver (Figures 2C and 2D) (Godfrey and Berzins, 2007). The *in vivo* production of HSC-iNKT cells was stable and long-lasting, evident in the persistence of high levels of iNKT cells in the primary BLT-iNKT mice for over 5 months after the initial HSC transfer (Figure 2B), and in the secondary BLT-iNKT mice after the secondary HSC transfer (Figures 2E–2G). These results indicate that the iNKT TCR gene-engineered HSCs retain their longevity and self-renewal capacity and are able to produce iNKT cells over time, highlighting the long-term therapeutic potential of the HSC-engineered iNKT cell approach. Moreover, by titrating the iNKT TCR gene-engineering rate of HSCs used for adoptive transfer, we could generate BLT-iNKT mice that contained gradient levels of human iNKT cells ranging from 5% to over 60% of total human αβ T cells (Figures 2H and S1E). The capacity to control the outputs of engineered human iNKT cells could be very valuable for the clinical application of HSC-iNKT cell therapy, allowing dosing the engineered iNKT cells in cancer patients according to therapeutic and safety needs.

The method of generating human iNKT cells through TCR gene engineering of HSCs is highly robust. In our experiments, we have succeeded in generating HSC-iNKT cells in BLT-iNKT mice engineered with all three iNKT TCR gene delivery lentivectors (Lenti/iNKT, Lenti/iNKT-EGFP, and Lenti/iNKT-sr39TK), using human $CD34^+$ HSCs isolated from various cell sources of multiple donors (cord blood, fetal liver, and granulocyte colony-stimulating factor [G-CSF]-mobilized peripheral blood), and using human thymus implants collected from various tissue sources of multiple donors (fetal thymus and post-natal thymus) (Figure 2I). Notably, there was no need to match human $CD34^+$ HSCs with human thymus implants for donors, or tissue sources, or human leukocyte antigens (HLAs), making the generation of BLT-iNKT mice highly adaptable (Figure 2I). The BLT-iNKT humanized mouse model therefore can be utilized as a powerful and versatile tool for the preclinical development of HSC-iNKT cell therapy, and for the study of human iNKT cell biology and other human iNKT cell-based immunotherapies. Importantly, the success of generating human iNKT cells through TCR gene engineering of G-CSF-mobilized peripheral blood $CD34^+$ HSCs (referred to as PBSCs thereafter) from multiple human donors directly indicates the robustness and translational potential of the proposed HSC-iNKT cell therapy (Figures 2I and S1A). Because of their possible relevance to early clinical development, in this report, we focused on studying HSC-iNKT cells generated in BLT-iNKT mice produced with Lenti/iNKT-sr39TK vector-transduced PBSCs (and implanted with human fetal thymus), unless otherwise indicated.

Safety Study of HSC-iNKT Cell Therapy in BLT-iNKT Humanized Mice

Safety of the HSC-iNKT cell therapy was evaluated by long-term monitoring and terminal pathology analysis of the BLT-iNKT humanized mice in comparison with the control BLT mice (Figure S2). Over a period of 5 months, BLT-iNKT mice showed a steady body weight increase and a survival rate comparable to that of the control BLT mice (Figures S2A and S2B). Pathological analysis of the various tissues of the BLT-iNKT mice collected at the end of 5 months showed no increase of tissue inflammation, hematopoietic neoplasm, or non-hematopoietic neoplasm, comparable to that of the control BLT mice (Figure S2C). 5 months after HSC transfer, BLT mice gradually developed graft-versus-host disease (GvHD) and eventually died of this disease due to the xenoreactive nature of the engrafted human conventional αβ T cells (Lan et al., 2006; Melkus et al., 2006; Smith et al., 2016). Intriguingly, compared to the control BLT mice, BLT-iNKT mice were significantly protected from GvHD, evidenced by the reduced auto-activation of engrafted human conventional αβ T cells in BLT-iNKT mice (Figures S2D–S2F) and the resulting elongated survival of these mice (Figure S2G). This phenomenon agreed with the clinical observation that in leukemia patients who received allogenic HSC transfer, levels of donor-derived iNKT cells positively correlated with the therapeutic effects of graft-versus-leukemia (GvL) and negatively correlated with the incidences and severity of GvHD, presumably attributed to the regulatory function of human iNKT cells (de Lalla et al., 2011; Haraguchi et al., 2004; Rubio et al., 2012). Reduced GvHD in BLT-iNKT mice suggest that, like native human iNKT cells, HSC-iNKT cells promote a favorable balance of GvL compared to GvHD. Taken together, these results demonstrate the safety of HSC-iNKT cell therapy in the BLT-iNKT pre-clinical animal model. The results also suggest a possible pro-GvL/anti-GvHD dual benefit of HSC-iNKT cell therapy in an allogeneic HSC transfer therapeutic setting (Figure S1A).

Biodistribution and Controlled Depletion of HSC-iNKT Cells in BLT-iNKT Humanized Mice Visualized by PET Imaging

Incorporation of an sr39TK suicide and PET imaging reporter gene in the human iNKT TCR gene delivery vector provides an additional safety control for HSC-iNKT cell therapy, allowing the depletion of gene-engineered human immune cells through GCV treatment in case the therapy needs to be terminated due to safety concerns (Figure 3A). It also provides an opportunity to visualize the biodistribution and *in vivo* dynamics of the gene-engineered human HSCs and their progeny cells in Lenti/iNKT-sr39TK vector-engineered BLT-iNKT mice (denoted as BLT-$iNKT^{TK}$ mice) using non-invasive PET imaging, a clinically applicable technology (Figure 3A). Using PET imaging combined with computed

(H) Controlled production of HSC-iNKT cells in BLT-iNKT mice. BLT-iNKT mice were generated with PBSCs transduced with titrated amounts of Lenti/iNKT-sr39TK vector (4×10^8, 2×10^8, or 1×10^8 transduction unit [TU] per 1×10^6 PBSCs). FACS quantification of human iNKT cells in the blood of indicated BLT-iNKT mice at week 16 post-HSC transfer were presented (n = 8–10).

(I) Table summarizing experiments that have successfully generated HSC-iNKT cells in the BLT human mouse model.

Data are representative of 2 (E–G, H) and over 10 (B–D) experiments.

Please cite this article in press as: Zhu et al., Development of Hematopoietic Stem Cell-Engineered Invariant Natural Killer T Cell Therapy for Cancer, Cell Stem Cell (2019), https://doi.org/10.1016/j.stem.2019.08.004

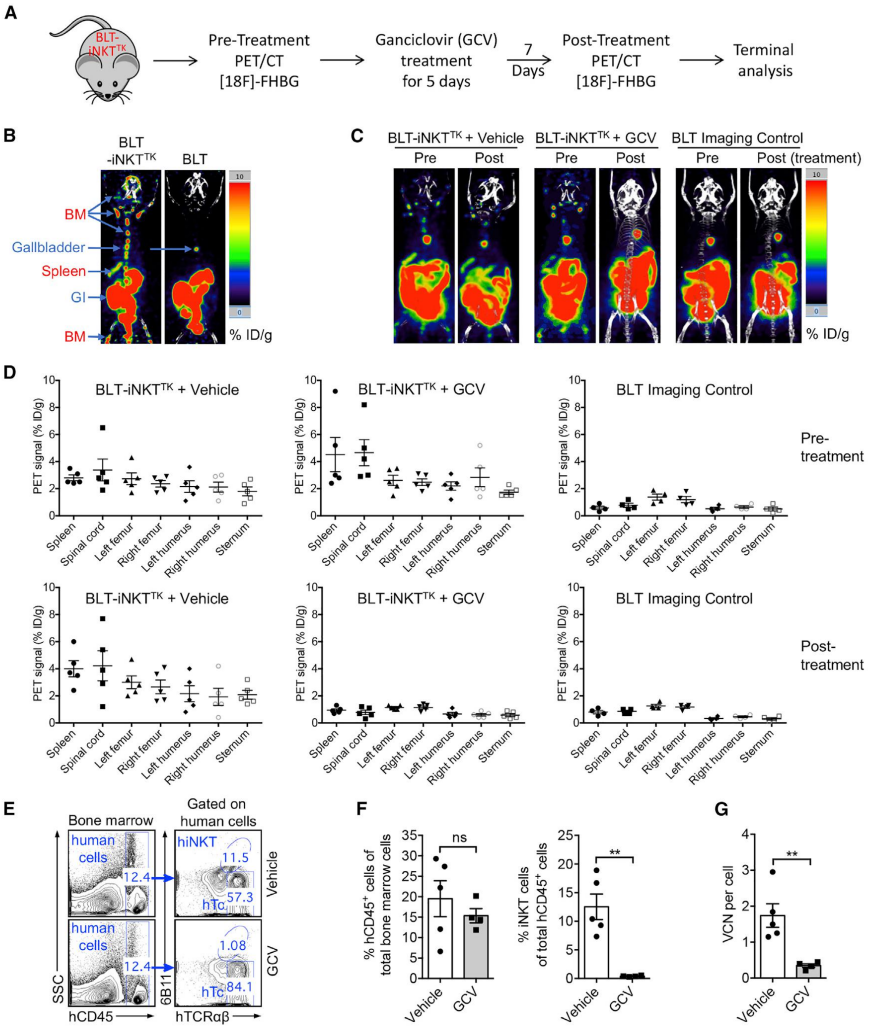

Figure 3. Biodistribution and Controlled Depletion of HSC-iNKT Cells in BLT-iNKT Humanized Mice Visualized by PET Imaging

(A) Experimental design. BLT-iNKT^{TK}, BLT-iNKT mice generated with Lenti/iNKT-sr39TK vector-transduced PBSCs.

(B) Biodistribution of vector-engineered human immune cells. Representative PET and CT images were presented. Note that there were background signals in the gastrointestinal tract (GI) and gallbladder of all mice. BM, bone marrow.

(C and D) PET and CT analysis of controlled depletion of vector-engineered human immune cells in BLT-iNKT^{TK} mice via GCV treatment. (C) Representative PET and CT images. (D) Quantification of (C) (n = 4–5).

(E and F) FACS validation of controlled depletion of HSC-iNKT cells in BLT-iNKT^{TK} mice via GCV treatment. (E) Representative FACS plots of bone marrow cells. (F) Quantification of (E) (n = 4–5).

(G) Droplet Digital PCR (ddPCR) validation of controlled depletion of vector-engineered human immune cells in BLT-iNKT^{TK} mice via GCV treatment (n = 4–5). VCN, vector copy number.

Data are representative of 2 experiments. See also Figures S2 and S3.

Please cite this article in press as: Zhu et al., Development of Hematopoietic Stem Cell-Engineered Invariant Natural Killer T Cell Therapy for Cancer, Cell Stem Cell (2019), https://doi.org/10.1016/j.stem.2019.08.004

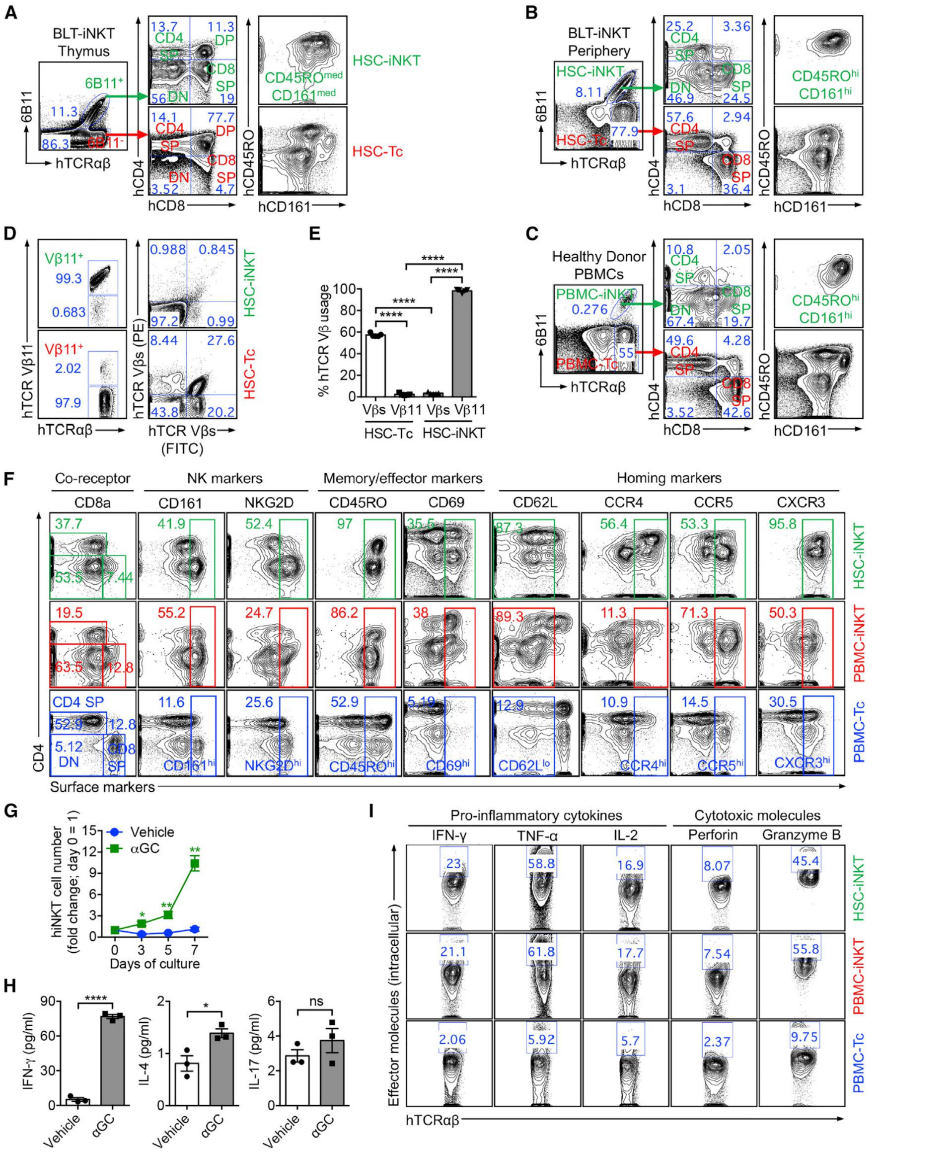

Figure 4. Development, Phenotype, and Functionality of HSC-iNKT Cells

(A–C) Development of HSC-iNKT cells. (A) FACS analysis of developing HSC-iNKT cells in the human thymus implants of BLT-iNKT mice. (B) FACS analysis of mature HSC-iNKT cells in the periphery (blood) of BLT-iNKT mice. (C) FACS analysis of control native human iNKT (PBMC-iNKT) cells in the blood of a representative healthy human donor.

(D and E) Allelic exclusion of endogenous TCRs in HSC-iNKT cells. (D) FACS plots showing the TCR Vβ usage by HSC-iNKT cells and HSC-T_C (human HSC-derived conventional αβ T cells) cells harvested from the liver of BLT-iNKT mice. hTCR Vβs (FITC) and hTCR Vβs (PE) staining antibodies collectively stained human TCR Vβ 1, 2, 3, 4, 5.1, 5.2, 5.3, 7.1, 7.2, 8, 9, 12, 13.1, 13.2, 13.6, 16, 17, 18, 20, 21.3, and 23. (E) Quantification of (D) (n = 5).

Please cite this article in press as: Zhu et al., Development of Hematopoietic Stem Cell-Engineered Invariant Natural Killer T Cell Therapy for Cancer, Cell Stem Cell (2019), https://doi.org/10.1016/j.stem.2019.08.004

tomography (CT) scan, we detected the distribution of gene-engineered human immune cells across the lymphoid tissues of BLT-iNKT^{TK} mice, particularly in the bone marrow and spleen (Figure 3B). Treating BLT-iNKT^{TK} mice with GCV effectively depleted gene-engineered human cells across the body (Figures 3C, 3D, S3A, and S3B). The depletion of gene-engineered human cells in bone marrow was confirmed by droplet digital PCR (Figure 3G). Importantly, the GCV-induced cell depletion was specific, evidenced by the selective depletion of HSC-iNKT cells but not the overall human immune cells in BLT-iNKT^{TK} mice as measured by flow cytometry (Figures 3E, 3F, S3C, and S3D).

Development of HSC-iNKT Cells in BLT-iNKT Humanized Mice

Utilizing the BLT-iNKT mouse model, we set out to study the *in vivo* development of HSC-iNKT cells. Analysis of the human thymus implants in BLT-iNKT mice detected the presence of developing HSC-iNKT cells; these cells followed a typical iNKT cell development path defined by CD4/CD8 co-receptor expression: from DN (double-negative) to DP (double-positive) then to SP (single-positive) or back to DN cells (Figures 4A and S4A) (Godfrey and Berzins, 2007). In the periphery, HSC-iNKT cells further upregulated memory T cell and NK cell markers (CD45RO and CD161, respectively), a signature of iNKT cell development resembling that of endogenous human iNKT cells (Figures 4B, 4C, S4A, and S4B) (Godfrey and Berzins, 2007).

We have previously shown that overexpression of a transgenic mouse iNKT TCR gene in mouse HSCs induced allelic exclusion and blocked the rearrangement of endogenous TCR genes in the resulting HSC-engineered mouse iNKT cells (Smith et al., 2015). Study of the human HSC-iNKT cells generated in BLT-iNKT mice revealed that these cells expressed the transgenic human iNKT TCRs (hTCR Vβ11$^+$) but not the other human TCR Vβ chains analyzed in our experiments, indicating that allelic exclusion also occurred during the development of human HSC-iNKT cells (Figures 4D and 4E). Utilizing BLT-iNKT mice engineered with the Lenti/iNKT-EGFP vector (denoted as BLT-iNKT^{GFP} mice), we studied the lineage differentiation of iNKT TCR-engineered human HSCs by tracking GFP$^+$ human HSCs and their progeny human immune cells. Analysis of human $\alpha\beta$ T cell population in the periphery of BLT-iNKT^{GFP} mice revealed that GFP$^+$ cells were exclusively human iNKT cells (Figures S4C and S4D). Analysis of bone marrow cells of BLT-iNKT^{GFP} mice showed that GFP$^+$ and GFP$^-$ cells comprised a similar composition of all lineages of human immune cells analyzed, including HSCs, T cells, B cells, myeloid cells, monocytes, dendritic cells, and NK cells (Figures S4E and S4F). Taken together, these results indicate that iNKT TCR-engineered human HSCs have the full potential to remain as long-term HSCs or to differentiate into various lineages of human immune cells; however, once going down the path of T cell development, the engineered T cell progenitor cells will commit to become iNKT cells but not other T cells following a TCR-instruction mechanism (Smith et al., 2015). Notably, because only T cells express the CD3 molecules that are required to support the surface display of TCRs and the downstream TCR signaling events, the expression of transgenic human iNKT TCRs is functionally restricted to the therapeutic HSC-iNKT cells without interfering with the activities of other lineages of human immune cells, which is a desirable feature for gene- and cell-based therapies.

Phenotype and Functionality of HSC-iNKT Cells

Next, we studied the phenotype and functionality of HSC-iNKT cells, in comparison with that of endogenous human iNKT cells and conventional $\alpha\beta$ T cells isolated from the peripheral blood of healthy human donors (denoted as PBMC-iNKT and PBMC-Tc cells, respectively). HSC-iNKT cells displayed a surface phenotype closely resembling PBMC-iNKT cells but distinct from PBMC-Tc cells: they expressed a mixed pattern of CD4/CD8 co-receptors (DN, CD4 SP, and CD8 SP); they expressed high levels of NK cell markers (CD161 and NKG2D); they upregulated T cell memory and activation markers (CD45RO and CD69); and they downregulated lymphoid organ homing marker (CD62L) and upregulated peripheral tissue and inflammatory site homing markers (CCR4, CCR5, and CXCR3) (Figure 4F). When stimulated with αGC, HSC-iNKT cells proliferated vigorously (Figure 4G). They secreted high levels of T_H0/T_H1 cytokines such as IFN-γ, limited amounts of T_H2 cytokines such as IL-4, and minimal amounts of T_H17 cytokines such as IL-17, indicating a T_H0/T_H1-prone effector function of these cells (Figure 4H). Intracellular staining showed that at the single-cell level, HSC-iNKT cells produced excess amounts of effector molecules, in particular pro-inflammatory cytokines (IFN-γ, TNF-α, and IL-2) and cytotoxic molecules (Perforin and Granzyme B), at levels comparable to that produced by the native PBMC-iNKT cells (Figure 4I). The capacity to produce excess amounts of pro-inflammatory and cytotoxic effector molecules is a signature of iNKT cells, which is attractive to cancer therapy (King et al., 2018; Krijgsman et al., 2018; Lam et al., 2017). Analysis of transcription factor expression pattern revealed that HSC-iNKT cells expressed high levels of PLZF, the "master" transcription factor regulating iNKT cell development and functionality, resembling that of native iNKT cells while differing from that of native conventional $\alpha\beta$ T cells and $\gamma\delta$ T cells isolated from healthy donor peripheral blood (Figure S4G) (Kovalovsky et al., 2008; Savage et al., 2008).

Tumor-Attacking Mechanisms of HSC-iNKT Cells

One of the most attractive features of iNKT cells is that they can attack tumors through multiple mechanisms (Brennan et al., 2013; Fujii et al., 2013; Krijgsman et al., 2018; Vivier et al.,

(F) Phenotype of HSC-iNKT cells. FACS plots are presented, showing the surface markers of HSC-iNKT cells isolated from the spleen of BLT-iNKT mice, compared to those of endogenous human iNKT (PBMC-iNKT) and conventional $\alpha\beta$ T (PBMC-Tc) cells isolated from healthy donor peripheral blood.
(G and H) Antigen responses of HSC-iNKT cells. Spleen cells of BLT-iNKT mice were cultured *in vitro* in the presence or absence of αGC for 7 days. (G) FACS quantification of HSC-iNKT cell expansion over time (n = 3). (H) ELISA analysis of cytokine production at day 7 (n = 3).
(I) Production of effector molecules by HSC-iNKT cells. BLT-iNKT mice spleen cells and healthy donor PBMCs were stimulated *in vitro* with αGC for 7 days. FACS plots are presented, showing the intracellular production of effector cytokines and cytotoxic molecules in HSC-iNKT cells compared to that in the PBMC-iNKT and PBMC-Tc cells.
Data are representative of 2 experiments. See also Figure S4.

2012). We therefore studied HSC-iNKT cells for their capacity to deploy these various tumor-attacking mechanisms, including (1) direct killing of $CD1d^+$ tumor cells, (2) adjuvant effects on enhancing NK-mediated killing of tumor cells, (3) adjuvant effects on boosting dendritic cell and cytotoxic T lymphocyte (DC and CTL) antitumor activities, and (4) inhibition of tumor-associated macrophages (TAMs) (Figure 5A).

We utilized an *in vitro* tumor cell killing assay to study the direct killing of $CD1d^+$ tumor cells. A human multiple myeloma (MM) cell line, MM.1S, was chosen as the model tumor target, because MM has a strong clinical relevance to iNKT cells, and because primary human MM tumor cells are $CD1d^+$ and are proven targets of native human iNKT cell killing (Dhodapkar et al., 2003; Dhodapkar and Richter, 2011; Spanoudakis et al., 2009). Notably, most MM cell lines, including MM.1S, have lost CD1d expression (Dhodapkar et al., 2003). We therefore engineered MM.1S cells to overexpress CD1d. We also engineered these cells to overexpress the firefly luciferase (Fluc) and EGFP reporters to enable the sensitive measurement of tumor killing using luminescence reading or flow cytometry. The resulting MM.1S-FG and MM.1S-hCD1d-FG cell lines were then used for the *in vitro* tumor cell killing assay (Figures S5A and S5B). In the presence of αGC, HSC-iNKT cells killed tumor cells aggressively in an CD1d-dependent manner, attesting to the strong tumor-killing potency of HSC-iNKT cells triggered by CD1d-antigen recognition (Figures 5B, 5C, S5C, and S5D). Importantly, even without the addition of αGC, HSC-iNKT cells could still effectively kill MM.1S-hCD1d-FG tumor cells, although tumor killing was less aggressive and required the addition of IL-15 (Figures 5D and 5E). Besides its role as an essential homeostatic cytokine in supporting the peripheral maintenance of iNKT cells, IL-15 is critical in supporting the function of iNKT cells, especially when iNKT cells respond to sub-optimal antigen stimulations (Liu et al., 2012; Matsuda et al., 2002). The direct killing of MM.1S-hCD1d-FG tumor cells by HSC-iNKT cells was dependent on the presence of CD1d on tumor cells (Figures 5E), indicating that HSC-iNKT cells can directly kill $CD1d^+$ tumor cells by recognizing tumor cell-derived lipid antigens presented by CD1d.

Next, we studied the capacity of HSC-iNKT cells for enhancing NK cell-mediated killing of tumor cells, utilizing an *in vitro* NK adjuvant effect assay (Figure 5F). A K562 human myelogenous leukemia cell line, which did not express HLA-I or CD1d, was engineered to express Fluc and EGFP and utilized as the model tumor target to assess NK cell-mediated killing (Figures S5E–S5G). αGC was used as a surrogate tumor-derived lipid antigen to stimulate HSC-iNKT cells. Antigen-stimulated HSC-iNKT cells significantly enhanced the activation (measured by CD69 upregulation) and tumor cell-killing efficacy of NK cells (Figures 5G–5I), likely through secreting NK cell-activation cytokines, including IFN-γ and IL-2 (Figure S5H) (Krijgsman et al., 2018; Vivier et al., 2012). Therefore, HSC-iNKT cells can function as an effective cellular adjuvant to enhance NK cell-mediated killing of tumor cells.

Subsequently, we evaluated the ability of HSC-iNKT cells for boosting DC- and CTL-mediated antitumor activities, using an *in vitro* DC and CTL adjuvant effect assay (Figure 5J). DC-stimulated CTL response to NY-ESO-1, a well-studied tumor antigen common in many cancers, was analyzed (Bethune et al., 2018). Monocyte-derived dendritic cells (MoDCs) were generated from $HLA\text{-}A2^+$ healthy donor PBMCs (Figures S6A and S6B); these MoDCs expressed CD1d as well as HLA-A2 and thus could present αGC to stimulate HSC-iNKT cells, and also present NY-ESO-1 peptide (ESOp) to activate ESO-specific $CD8^+$ CTLs (denoted as ESO-T cells) (Figures S6C–S6F). In the presence of αGC, HSC-iNKT cells efficiently promoted the maturation of MoDCs as evidenced by the upregulation of co-stimulatory marker CD86 on MoDCs (Figures 5K and 5L). MoDCs matured by HSC-iNKT cells showed significantly enhanced capacity to present ESOp tumor antigens, thereby inducing greatly increased activation and expansion of ESO-T cells as well as resulting in enhanced ESO-T cell mediated killing of target tumor cells (Figures 6M, 6N, S6G, and S6H). Therefore, HSC-iNKT cells can function as an effective cellular adjuvant to boost DC and CTL antitumor activities.

Last, we evaluated the potential of HSC-iNKT cells in inhibiting tumor-associated macrophages (TAMs), utilizing an *in vitro* macrophage inhibition assay (Figure 5O). Human $CD14^+$ monocytes isolated from healthy donor PBMCs were used in this study (Figure S6I). These monocytes expressed CD1d (Figure S6J); when loaded with αGC as a surrogate tumor-derived lipid antigen, these monocytes stimulated HSC-iNKT cells (evidenced by upregulation of CD69 on HSC-iNKT cells; Figures 6P and 6Q) and were quickly killed by HSC-iNKT cells (Figures 6R and 6S). Therefore, HSC-iNKT cells have the potential to inhibit TAMs in a CD1d-antigen-dependent manner.

Taken together, these results indicate that HSC-iNKT cells are capable of deploying multiple mechanisms to attack tumor cells, attesting to their multifaceted cancer therapy potential.

In Vivo Antitumor Efficacy of HSC-iNKT Cells against Hematologic Malignancies in a Human Multiple Myeloma Xenograft Mouse Model

In vivo antitumor efficacy of HSC-iNKT cells against hematologic malignancies was studied using a human multiple myeloma (MM) xenograft NSG mouse model (Figure 6A). The pre-established MM.1S-hCD1d-FG human MM cell line was utilized for this study (Figure S5A). MM.1S-hCD1d-FG cells were inoculated intravenously (i.v.) into NSG mice to establish disease, followed by i.v. injection of HSC-iNKT cells and monitoring of HSC-iNKT cell therapeutic effects (Figure 6A). This tumor model allowed the *in vivo* study of direct killing of $CD1d^+$ blood cancer cells by HSC-iNKT cells (Figure S5A). HSC-iNKT cells showed a robust suppression of MM, as evidenced by a significant decrease of total body luminescence measured by bioluminescence live animal imaging (BLI) (Figures 6B and 6C). Terminal tissue collection and flow cytometry analysis confirmed a significant reduction of GFP^+ tumor cells in multiple tissues, particularly in the bone marrow, which is the primary site of MM, and in the liver, which is another major MM site in this model (Figures 6D and 6E). Correspondingly, flow cytometry analysis detected the presence of HSC-iNKT cells in various tumor-residing tissues (Figure 6F). In particular, high numbers of HSC-iNKT cells homed to the areas of MM involvement, including bone marrow and liver (Figure 6F), where these HSC-iNKT cells displayed an activated phenotype ($CD62L^{lo}CD69^{hi}$) correlating with their antitumor function (Figures 6G–6I). The antitumor efficacy of HSC-iNKT cells was robust and consistent for all three donors that we studied (Figure 6A). The suppression of MM in the MM.1S-CD1d-FG model was mediated by HSC-iNKT cells through a

Please cite this article in press as: Zhu et al., Development of Hematopoietic Stem Cell-Engineered Invariant Natural Killer T Cell Therapy for Cancer, Cell Stem Cell (2019), https://doi.org/10.1016/j.stem.2019.08.004

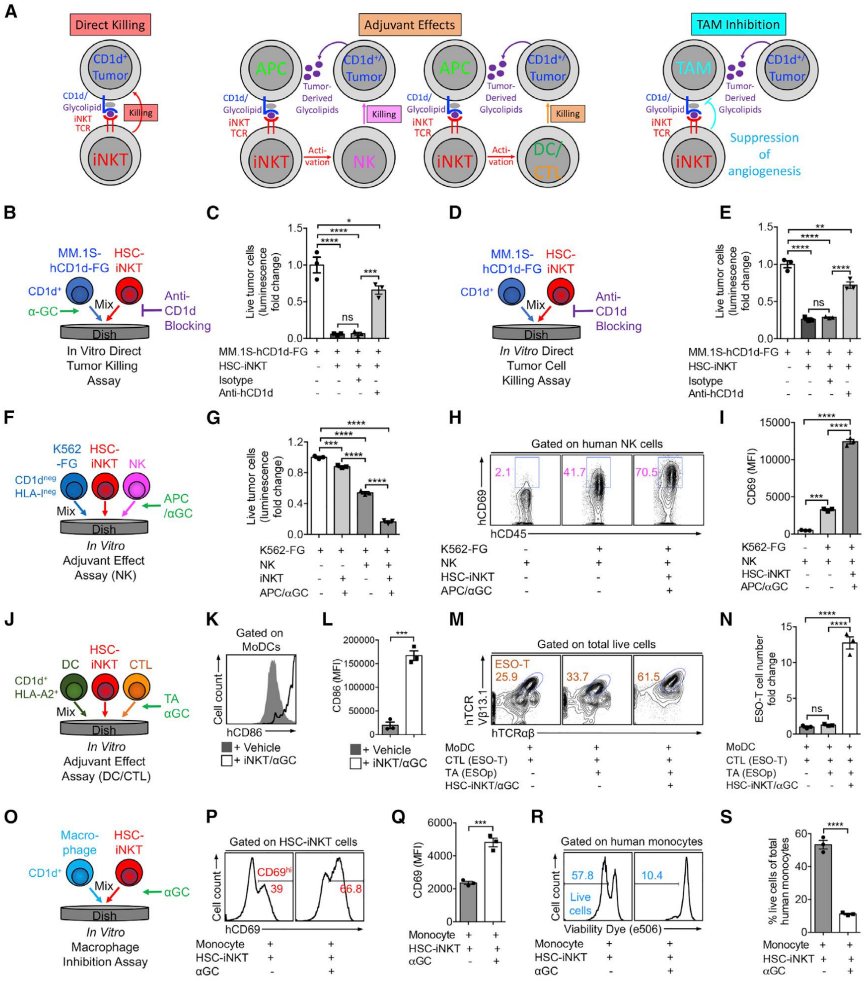

Figure 5. Tumor-Attacking Mechanisms of HSC-iNKT Cells

(A) Diagram showing the possible mechanisms utilized by human iNKT cells to attack tumor cells. APC, antigen presenting cell; NK, natural killer cell; DC, dendritic cell; CTL, cytotoxic T lymphocyte; TAM, tumor-associated macrophage.

(B–E) Studying the direct killing of $CD1d^+$ tumor cells by HSC-iNKT cells (tumor:iNKT ratio 1:10). (B) Experimental design to study CD1d-dependent killing of MM.1S-hCD1d-FG cells in the presence of αGC. (C) Tumor killing data from (B) (n = 3). (D) Experimental design to study CD1d-dependent killing of MM.1S-hCD1d-FG cells in the absence of αGC. (E) Tumor killing data from (D) (n = 3).

(F–I) Studying the adjuvant effects of HSC-iNKT cells on enhancing NK cell-mediated killing of tumor cells (tumor:NK:iNKT ratio 1:2:2). (F) Experimental design. (G) Tumor killing (n = 3). (H) FACS plots showing CD69 expression on NK cells. (I) Quantification of (H) (n = 3).

(J–N) Studying the adjuvant effects of HSC-iNKT cells on boosting DC and CTL antitumor reactions (DC:CTL:iNKT ratio 1:1:1). (J) Experimental design. (K) FACS plots showing CD86 expression on MoDCs. (L) Quantification of (K) (n = 3). (M) FACS plots showing the detection of ESO-T cells in the mixed cell culture. (N) Quantification of (M) (n = 3).

(O–S) Studying the inhibition of macrophages by HSC-iNKT cells (macrophage:iNKT ratio 1:1). Monocytes isolated from healthy donor PBMCs were studied. (O) Experimental design. (P) FACS plots showing CD69 expression on HSC-iNKT cells. (Q) Quantification of (P) (n = 3). (R) FACS plots showing the viability of monocytes. (S) Quantification of (R) (n = 3).

Data are representative of 2 experiments. See also Figures S5 and S6.

Please cite this article in press as: Zhu et al., Development of Hematopoietic Stem Cell-Engineered Invariant Natural Killer T Cell Therapy for Cancer, Cell Stem Cell (2019), https://doi.org/10.1016/j.stem.2019.08.004

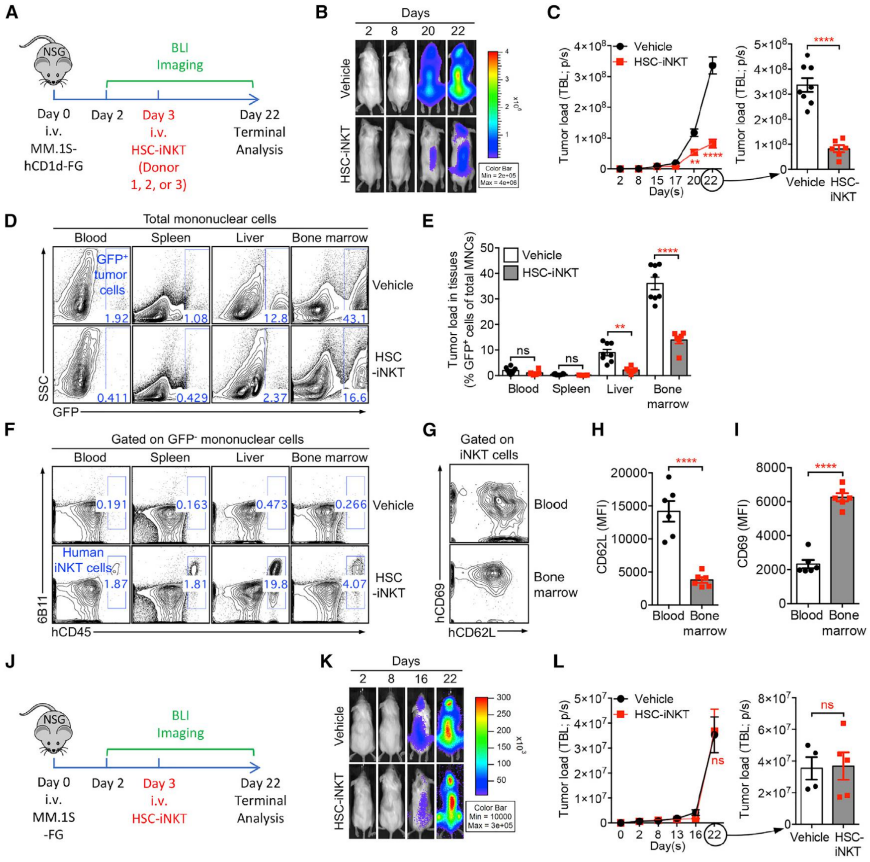

Figure 6. *In Vivo* Antitumor Efficacy of HSC-iNKT Cells against Hematologic Malignancies in a Human Multiple Myeloma (MM) Xenograft Mouse Model

(A–I) *In vivo* antitumor efficacy of HSC-iNKT cells was studied using an MM.1S-hCD1d-FG human MM xenograft NSG mouse model. HSC-iNKT cells derived from PBSCs of three different donors were studied, to verify the robustness of the HSC-iNKT cell therapy. Data from one representative donor were presented. (A) Experimental design. BLI, live animal bioluminescence imaging. (B) BLI images showing tumor loads in experimental mice over time. (C) Quantification of (B) (n = 6–8). TBL, total body luminescence. (D) FACS plots showing the detection of tumor cells (gated as GFP^+ cells) in various tissues of experimental mice. (E) Quantification of (D) (n = 6–8). MNCs, mononuclear cells. (F) FACS plots showing the detection of HSC-iNKT cells in various tissues of experimental mice. (G) FACS plots showing the expression of CD62L and CD69 on HSC-iNKT cells isolated from the blood and bone marrow of tumor-bearing mice. (H and I) Quantification of (G) (n = 6).

(J–L) *In vivo* antitumor efficacy of HSC-iNKT cells was studied using a control MM.1S-FG human MM xenograft NSG mouse model. HSC-iNKT cells derived from PBSCs of a representative donor were studied. (J) Experimental design. (K) BLI images showing tumor loads in experimental mice over time. (L) Quantification of (K) (n = 4–5).

Data are representative of 3 (A–I) and 2 (J–L) experiments.

CD1d-dependent tumor recognition and suppression mechanism, because HSC-iNKT cells did not exhibit tumor suppression effects and were not enriched at tumor sites in the control MM.1S-FG model, which lacked the expression of CD1d (Figures 6J–6L). These data demonstrated the *in vivo* antitumor efficacy of HSC-iNKT cells and support their therapeutic potential against hematologic malignancies.

In Vivo Antitumor Efficacy of HSC-iNKT Cells against Solid Tumors in a Human Melanoma Xenograft Mouse Model

In vivo antitumor efficacy of HSC-iNKT cells against solid tumors was studied using a human melanoma xenograft NSG mouse model (Figure 7A). An A375-hCD1d-hIL-15-FG human melanoma cell line and a control A375-hIL-15-FG melanoma cell

Please cite this article in press as: Zhu et al., Development of Hematopoietic Stem Cell-Engineered Invariant Natural Killer T Cell Therapy for Cancer, Cell Stem Cell (2019), https://doi.org/10.1016/j.stem.2019.08.004

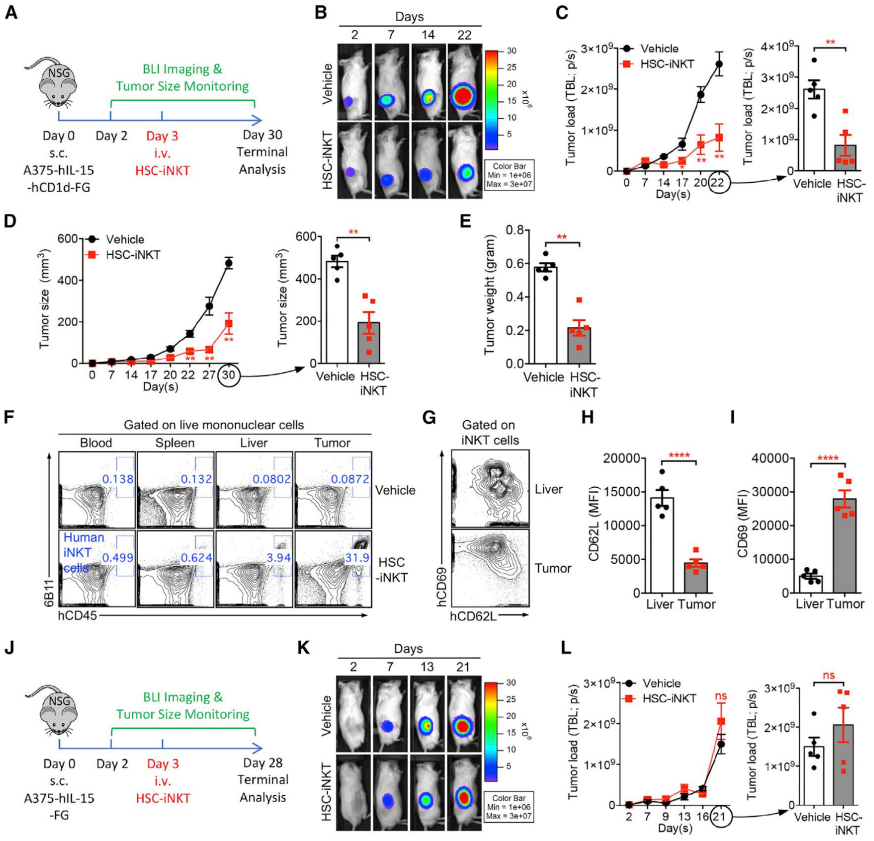

Figure 7. *In Vivo* Antitumor Efficacy of HSC-iNKT Cells against Solid Tumors in a Human Melanoma Xenograft Mouse Model

(A–I) *In vivo* antitumor efficacy of HSC-iNKT cells was studied using an A375-hIL-15-hCD1d-FG human melanoma xenograft NSG mouse model. (A) Experimental design. (B) BLI images showing tumor loads in experimental mice over time. Note that beyond day 22, BLI signals were saturated and thus were not included for quantification. (C) Quantification of (B) (n = 5). (D) Measurements of tumor size over time (n = 5). (E) Measurements of tumor weight at the terminal harvest on day 30 (n = 5). (F) FACS plots showing the detection of HSC-iNKT cells in various tissues of experimental mice. (G) FACS plots showing the expression of CD62L and CD69 on HSC-iNKT cells isolated from the livers and tumors of tumor-bearing mice. (H and I) Quantification of (G) (n = 5).

(J–L) *In vivo* antitumor efficacy of HSC-iNKT cells was studied using a control A375-hIL-15-FG human melanoma xenograft NSG mouse model. (J) Experimental design. (K) BLI images showing tumor loads in experimental mice over time. Note that beyond day 21, BLI signals were saturated and thus were not included for quantification. (L) Quantification of (K) (n = 5).

Data are representative of 2 experiments. See also Figure S7.

line were generated for this study (Figures S7A and S7B). When co-cultured *in vitro*, HSC-iNKT cells effectively killed the A375-hCD1d-hIL-15-FG cells in a CD1d-antigen-dependent manner (Figures S7C–S7F). For the *in vivo* study, A375-hIL-15-hCD1d-FG cells loaded with αGC were subcutaneously inoculated into NSG mice to form solid tumors, followed by i.v. injection of HSC-iNKT cells and monitoring of tumor growth (Figure 7A). We detected a significant suppression of tumor growth by HSC-iNKT cells, analyzed by time-course BLI (Figures 7B and 7C), measurement of tumor size over time (Figure 7D), and terminal tumor weight assessment (Figure 7E). Terminal tissue collection and flow cytometry analysis revealed a highly efficient infiltration of HSC-iNKT cells into solid tumors (Figure 7F). The targeted homing of HSC-iNKT cells to the tumor sites was impressive, as much smaller numbers of HSC-iNKT cells were detected in all other tissues examined (blood, spleen, and liver), likely due to the expression of inflammatory site-homing markers on HSC-iNKT cells (Figures 7F and 4F). HSC-iNKT cells isolated from tumors displayed a highly active phenotype ($CD62L^{lo}CD69^{hi}$) compared to HSC-iNKT cells isolated from non-tumor tissues like the liver, corresponding with their anti-tumor activities (Figures 7G–7I). The suppression of solid tumor

growth in the A375-hIL-15-hCD1d-FG model was mediated by HSC-iNKT cells through a CD1d-dependent direct killing mechanism, because HSC-iNKT cells did not induce tumor suppression in the control A375-hIL-15-FG model, which lacked the expression of CD1d (Figures 7J–7L, S7G, and S7H). Taken together, these *in vivo* results demonstrated the therapeutic potential of HSC-iNKT cells for treating solid tumors. In particular, the capacity of HSC-iNKT cells effectively trafficking to the tumor sites and infiltrating solid tumors is highly desirable for cancer immunotherapy.

DISCUSSION

HSC transplantation (HSCT) has a history of over half a century and has been utilized routinely to treat a variety of malignant and non-malignant hematopoietic disorders (Chabannon et al., 2018). Over the last decade, gene-engineered HSCT has undergone rapid development and has shown great promise for treating diseases like monogene-related immunodeficiencies (Chabannon et al., 2018). Safe and efficient gene delivery vectors have been developed, and robust HSC gene modification protocols have been established (Chabannon et al., 2018). In 2016, the first gene-engineered HSCT therapy product received marketing authorization from the European Medicines Agency, marking a major milestone and paving the way for this new class of cell therapy drugs (Chabannon et al., 2018). Therefore, both the technology and clinical platforms are ready to translate the intended HSC-iNKT cell therapy.

Generation of HSC-engineered iNKT cells requires a functional thymus. Aging-related degeneration of human thymus in many cancer patients therefore may be a concern (Lynch et al., 2009). Clinical studies of adult cancer patients receiving HSC transfer were reported previously, showing the reconstitution of iNKT cells in these patients (Beziat et al., 2010; Haraguchi et al., 2004). These clinical data support the likelihood that HSC-iNKT therapy can benefit aged cancer patients.

Increasing iNKT cells in cancer patients may have certain risks, including possible toxicity and interference of immune surveillance. The levels of iNKT cells achievable in cancer patients may also be limited by the availability of host supporting factors such as homeostatic cytokines. These concerns can be greatly alleviated through controlling the iNKT cell outputs via controlling the HSC gene-engineering rates (Figures 2H and S1E). For clinical trial design, an initial dose targeting ~5% iNKT cells in blood may be a rational starting point: (1) this level exists in healthy individuals and therefore should be physiological safe and possible to achieve (Chan et al., 2009); and (2) this level represents an over 100- to 1,000-fold increase of iNKT cells in cancer patients and likely can exhibit certain therapeutic effects (Vivier et al., 2012). After the 5% initial dose proven feasible and tolerable, dose escalation (up or down) may follow. Of course, all need to be tested clinically. Notably, besides the dosage control, we have engineered an additional safety control for the intended HSC-iNKT cell therapy, by incorporating an sr39TK suicide gene in the iNKT TCR gene delivery vector (Figures 1C and 1G). This engineered safety control will allow the effective depletion of engineered iNKT cells (and their engineered progenitor HSCs) through GCV administration in case of a safety need (Figures 3 and S3).

HSC-iNKT cell therapy can certainly combine with other therapeutic modalities. For instance, adoptive transfer of αGC-loaded DCs into cancer patients has been demonstrated to be safe and effective in stimulating human iNKT cells *in vivo;* therefore, it is plausible to propose that a combination of HSC-iNKT cell therapy with αGC-loaded DC vaccination would maximize the therapeutic potential of the engineered HSC-iNKT cells (Nair and Dhodapkar, 2017; Waldowska et al., 2017). Alternatively, iNKT cells in cancer patients have been shown to express high levels of T cell-exhaustion marker PD-1 (Kamata et al., 2016). It is therefore conceivable that a combination of HSC-iNKT cell therapy with the PD-1/PD-L1 blockade therapy may also produce synergistic therapeutic effects (Durgan et al., 2011). Moreover, recent studies showed promising cancer therapy potential of chimeric antigen receptor (CAR)-engineered iNKT cells; therefore, further engineering HSC-iNKT cells to express CAR to enhance their tumor-targeting effectiveness may represent another attractive approach (Heczey et al., 2014; Rotolo et al., 2018; Tian et al., 2016).

In summary, here we report the pre-clinical development of an HSC-iNKT cell therapy that has the potential to treat a broad range of hematologic malignancies and solid tumors and that is ready to translate into clinical development. Our study also established a humanized BLT-iNKT mouse model that can be utilized as a valuable tool to study human iNKT cell biology and human iNKT cell-based immunotherapy.

STAR★METHODS

Detailed methods are provided in the online version of this paper and include the following:

- KEY RESOURCES TABLE
- LEAD CONTACT AND MATERIALS AVAILABILITY
- EXPERIMENTAL MODEL AND SUBJECT DETAILS
  - Mice
  - Human Tumor Cell Lines
  - Human PBMCs, $CD34^+$ HSCs, and Thymus Tissues
  - Materials and Reagents
- METHOD DETAILS
  - Lentiviral Vectors
  - Antibodies and Flow Cytometry
  - Human iNKT Cell TCR Vβ Repertoire Analysis
  - ELISA
  - Ganciclovir (GCV) *In Vitro* Killing Assay
  - Single-Cell Human iNKT TCR Cloning
  - Generation of BLT and BLT-iNKT Humanized Mice
  - Generation of Secondary BLT-iNKT Humanized Mice
  - Safety Study of HSC-iNKT Cell Therapy in BLT-iNKT Mice
  - Biodistribution and Controlled Depletion of HSC-iNKT Cells in BLT-iNKT Humanized Mice Visualized by PET/CT Imaging
  - HSC-iNKT Cell Phenotype and Functional Study
  - HSC-iNKT Cell *In Vitro* Expansion
  - HSC-iNKT Cell Tumor-Attacking Mechanism Study: *In Vitro* Direct Tumor Cell Killing Assay
  - HSC-iNKT Cell Tumor-Attacking Mechanism Study: *In Vitro* NK Adjuvant Effect Assay

Please cite this article in press as: Zhu et al., Development of Hematopoietic Stem Cell-Engineered Invariant Natural Killer T Cell Therapy for Cancer, Cell Stem Cell (2019), https://doi.org/10.1016/j.stem.2019.08.004

SUPPLEMENTAL INFORMATION

Supplemental Information can be found online at https://doi.org/10.1016/j.stem.2019.08.004.

ACKNOWLEDGMENTS

We gratefully thank D. Baltimore (California Institute of Technology) and J. Economou (UCLA) for advising this study. We thank the University of California, Los Angeles (UCLA) animal facility for providing animal support; the UCLA Translational Pathology Core Laboratory (TPCL) for providing histology support; the UCLA AIDS Institute/CFAR Virology Core/Gene and Cell Therapy Core/Humanized Mouse Core for providing human cells and tissues and humanized mice services; the UCLA BSCRC Flow Cytometry Core Facility for cell-sorting support; the NIH Tetramer Core Facility for providing the hCD1d/PBS-57 tetramer reagents; N. Rozengurt (UCLA) for providing pathology analysis support; P. Wang (University of Southern California, USC) for critical reading of this manuscript; and E.L. Siegler for editing the manuscript. This work was supported by a Director's New Innovator Award from the NIH (DP2 CA196335, to L.Y.), a Partnering Opportunity for Translational Research Projects Award from the California Institute for Regenerative Medicine (CIRM TRAN1-08533, to L.Y.), a Stem Cell Research Award from the Concern Foundation (to L.Y.), a Research Career Development Award from the STOP CANCER Foundation (to L.Y.), and a BSCRC-RHF Research Award from the Rose Hills Research Foundation (to L.Y.). D.J.S. is a predoctoral fellow supported by the UCLA Tumor Immunology Training Grant (USHHS Ruth L. Kirschstein Institutional National Research Service Award #T32 CA009056). J.Y. is a predoctoral fellow supported by the UCLA Broad Stem Cell Research Center (BSCRC) Predoctoral Fellowship.

AUTHOR CONTRIBUTIONS

Y.Z., D.J.S., and L.Y. designed the experiments, analyzed the data, and wrote the manuscript. L.Y. conceived and oversaw the study, with assistance from Y.Z. and with suggestions from Z.G., S.G.K., D.S.A., S.H.-L., P.J.K.-L., S.N.D., C.S.S., S.M.L., S.J.F., J.R.H., J.A.Z., G.M.C., C.G.R., A.R., D.B.K., and O.N.W. Y.Z. and D.J.S. performed all experiments, with assistance from Y. Zhou, Y.-R.L., J.Y., D.L., Y.-C.W., S.D.B., Xi Wang, C.H., J.K., T.T., L.J.L., A.T.P., and H.M. J.M. assisted with TCR cloning. D.C. performed cell sorting. R.P.H. helped with lentivirus production. B.C.-F. and F.U. helped with vector copy analysis. L.W. and L.P. performed PET and CT imaging and analyzed data. V.R. performed BLT surgeries. B.B.-M. and M.H.M. helped with PBSC isolation. D.G. and Xiaoyan Wang helped with the statistical analysis of data.

DECLARATION OF INTERESTS

Y.Z., D.J.S., and L.Y. are inventors on patents relating to this study filed by UCLA. D.J.S. and S.D.B. are currently employees of Kite, a Gilead Company. F.U. is currently an employee of PACT Pharma. S.H.-L. is a consultant for Amgen and Merck. S.M.L. is on the speaker bureau for Takeda and is a consultant for Bristol-Meyers Squibb. J.R.H is a founder and board member of Isoplexis and PACT Pharma. C.G.R. is a founder and stockholder of Sofie Biosciences and Trethera Corporation. A.R. is a consultant for Amgen, Bristol-Meyers Squibb, Chugai, Genentech-Roche, Merck-MSD, Novartis, and Sanofi; a scientific advisory board member and stockholder for Advaxis, Apricity, Arcus, Bioncotech, Compugen, CytomX, Five Prime, FLX-Bio, ImaginAb, Isoplexis, Kite-Gilead, Merus, and Rgenix; and a co-founder and scientific advisory board member of Lutris, PACT Pharma, and Tango Therapeutics. D.B.K. is an inventor on intellectual property licensed by UCLA to Orchard Therapeutics and is a member of their scientific advisory board; D.B.K. is also a scientific advisory board member of Allogene Therapeutics. O.N.W. is a consultant, stockholder, and/or board member with Trethera Corporation, Kronos Biosciences, Sofie Biosciences, and Allogene Therapeutics. All other authors declare no competing interests. None of the declared companies contributed to or directed any of the research reported in this article.

Received: February 11, 2019
Revised: June 19, 2019
Accepted: August 9, 2019
Published: September 5, 2019

REFERENCES

Baltimore, D., Witte, O.N., Yang, L., Economou, J., and Ribas, A. (2010). Overcoming barriers to programming a therapeutic cellular immune response to fight melanoma. Pigment Cell Melanoma Res. *23*, 288–289.

Bendelac, A., Savage, P.B., and Teyton, L. (2007). The biology of NKT cells. Annu. Rev. Immunol. *25*, 297–336.

Berzins, S.P., Smyth, M.J., and Baxter, A.G. (2011). Presumed guilty: natural killer T cell defects and human disease. Nat. Rev. Immunol. *11*, 131–142.

Bethune, M.T., Li, X.H., Yu, J., McLaughlin, J., Cheng, D., Mathis, C., Moreno, B.H., Woods, K., Knights, A.J., Garcia-Diaz, A., et al. (2018). Isolation and characterization of NY-ESO-1-specific T cell receptors restricted on various MHC molecules. Proc. Natl. Acad. Sci. USA *115*, E10702–E10711.

Bettini, M.L., Bettini, M., and Vignali, D.A. (2012). T-cell receptor retrogenic mice: a rapid, flexible alternative to T-cell receptor transgenic mice. Immunology *136*, 265–272.

Beziat, V., Nguyen, S., Exley, M., Achour, A., Simon, T., Chevallier, P., Sirvent, A., Vigouroux, S., Debré, P., Rio, B., and Vieillard, V.; French Minicord Study Group (2010). Shaping of iNKT cell repertoire after unrelated cord blood transplantation. Clin. Immunol. *135*, 364–373.

Black, M.E., Newcomb, T.G., Wilson, H.M., and Loeb, L.A. (1996). Creation of drug-specific herpes simplex virus type 1 thymidine kinase mutants for gene therapy. Proc. Natl. Acad. Sci. USA *93*, 3525–3529.

Brennan, P.J., Brigl, M., and Brenner, M.B. (2013). Invariant natural killer T cells: an innate activation scheme linked to diverse effector functions. Nat. Rev. Immunol. *13*, 101–117.

Cartier, N., Hacein-Bey-Abina, S., Bartholomae, C.C., Veres, G., Schmidt, M., Kutschera, I., Vidaud, M., Abel, U., Dal-Cortivo, L., Caccavelli, L., et al. (2009). Hematopoietic stem cell gene therapy with a lentiviral vector in X-linked adrenoleukodystrophy. Science *326*, 818–823.

Chabannon, C., Kuball, J., Bondanza, A., Dazzi, F., Pedrazzoli, P., Toubert, A., Ruggeri, A., Fleischhauer, K., and Bonini, C. (2018). Hematopoietic stem cell transplantation in its 60s: A platform for cellular therapies. Sci. Transl. Med *10*, eaap9630.

Chan, A.C., Serwecinska, L., Cochrane, A., Harrison, L.C., Godfrey, D.I., and Berzins, S.P. (2009). Immune characterization of an individual with an exceptionally high natural killer T cell frequency and her immediate family. Clin. Exp. Immunol. *156*, 238–245.

Chan, W.K., Rujkijyanont, P., Neale, G., Yang, J., Bari, R., Das Gupta, N., Holladay, M., Rooney, B., and Leung, W. (2013). Multiplex and genome-wide analyses reveal distinctive properties of KIR+ and CD56+ T cells in human blood. J. Immunol. *191*, 1625–1636.

Cooper, A.R., Patel, S., Senadheera, S., Plath, K., Kohn, D.B., and Hollis, R.P. (2011). Highly efficient large-scale lentiviral vector concentration by tandem tangential flow filtration. J. Virol. Methods *177*, 1–9.

Cortesi, F., Delfanti, G., Grilli, A., Calcinotto, A., Gorini, F., Pucci, F., Lucianò, R., Grioni, M., Recchia, A., Benigni, F., et al. (2018). Bimodal

Seet, C.S., He, C., Bethune, M.T., Li, S., Chick, B., Gschweng, E.H., Zhu, Y., Kim, K., Kohn, D.B., Baltimore, D., et al. (2017). Generation of mature T cells from human hematopoietic stem and progenitor cells in artificial thymic organoids. Nat. Methods *14*, 521–530.

Smith, D.J., Liu, S., Ji, S., Li, B., McLaughlin, J., Cheng, D., Witte, O.N., and Yang, L. (2015). Genetic engineering of hematopoietic stem cells to generate invariant natural killer T cells. Proc. Natl. Acad. Sci. USA *112*, 1523–1528.

Smith, D.J., Lin, L.J., Moon, H., Pham, A.T., Wang, X., Liu, S., Ji, S., Rezek, V., Shimizu, S., Ruiz, M., et al. (2016). Propagating Humanized BLT Mice for the Study of Human Immunology and Immunotherapy. Stem Cells Dev. *25*, 1863–1873.

Song, L., Asgharzadeh, S., Salo, J., Engell, K., Wu, H.W., Sposto, R., Ara, T., Silverman, A.M., DeClerck, Y.A., Seeger, R.C., and Metelitsa, L.S. (2009). Valpha24-invariant NKT cells mediate antitumor activity via killing of tumor-associated macrophages. J. Clin. Invest. *119*, 1524–1536.

Spanoudakis, E., Hu, M., Naresh, K., Terpos, E., Melo, V., Reid, A., Kotsianidis, I., Abdalla, S., Rahemtulla, A., and Karadimitris, A. (2009). Regulation of multiple myeloma survival and progression by CD1d. Blood *113*, 2498–2507.

Tian, G., Courtney, A.N., Jena, B., Heczey, A., Liu, D., Marinova, E., Guo, L., Xu, X., Torikai, H., Mo, Q., et al. (2016). CD62L+ NKT cells have prolonged persistence and antitumor activity in vivo. J. Clin. Invest. *126*, 2341–2355.

Vatakis, D.N., Koya, R.C., Nixon, C.C., Wei, L., Kim, S.G., Avancena, P., Bristol, G., Baltimore, D., Kohn, D.B., Ribas, A., et al. (2011). Antitumor activity from antigen-specific CD8 T cells generated in vivo from genetically engineered human hematopoietic stem cells. Proc. Natl. Acad. Sci. USA *108*, E1408–E1416.

Vivier, E., Ugolini, S., Blaise, D., Chabannon, C., and Brossay, L. (2012). Targeting natural killer cells and natural killer T cells in cancer. Nat. Rev. Immunol. *12*, 239–252.

Waldowska, M., Bojarska-Junak, A., and Roliński, J. (2017). A brief review of clinical trials involving manipulation of invariant NKT cells as a promising approach in future cancer therapies. Cent. Eur. J. Immunol. *42*, 181–195.

Wu, D.Y., Segal, N.H., Sidobre, S., Kronenberg, M., and Chapman, P.B. (2003). Cross-presentation of disialoganglioside GD3 to natural killer T cells. J. Exp. Med. *198*, 173–181.

Yamasaki, K., Horiguchi, S., Kurosaki, M., Kunii, N., Nagato, K., Hanaoka, H., Shimizu, N., Ueno, N., Yamamoto, S., Taniguchi, M., et al. (2011). Induction of NKT cell-specific immune responses in cancer tissues after NKT cell-targeted adoptive immunotherapy. Clin. Immunol. *138*, 255–265.

Yang, L., and Baltimore, D. (2005). Long-term in vivo provision of antigen-specific T cell immunity by programming hematopoietic stem cells. Proc. Natl. Acad. Sci. USA *102*, 4518–4523.

Yang, L., Yang, H., Rideout, K., Cho, T., Joo, K.I., Ziegler, L., Elliot, A., Walls, A., Yu, D., Baltimore, D., and Wang, P. (2008). Engineered lentivector targeting of dendritic cells for in vivo immunization. Nat. Biotechnol. *26*, 326–334.

HLA-haploidentical stem cell transplantation defines distinct CD4+ and CD4- subset dynamics and correlates with remission state. J. Immunol. *186*, 4490–4499.

Dhodapkar, M.V., and Richter, J. (2011). Harnessing natural killer T (NKT) cells in human myeloma: progress and challenges. Clin. Immunol. *140*, 160–166.

Dhodapkar, M.V., Geller, M.D., Chang, D.H., Shimizu, K., Fujii, S., Dhodapkar, K.M., and Krasovsky, J. (2003). A reversible defect in natural killer T cell function characterizes the progression of premalignant to malignant multiple myeloma. J. Exp. Med. *197*, 1667–1676.

Durgan, K., Ali, M., Warner, P., and Latchman, Y.E. (2011). Targeting NKT cells and PD-L1 pathway results in augmented anti-tumor responses in a melanoma model. Cancer Immunol. Immunother. *60*, 547–558.

Exley, M.A., Friedlander, P., Alatrakchi, N., Vriend, L., Yue, S., Sasada, T., Zeng, W., Mizukami, Y., Clark, J., Nemer, D., et al. (2017). Adoptive Transfer of Invariant NKT Cells as Immunotherapy for Advanced Melanoma: A Phase I Clinical Trial. Clin. Cancer Res. *23*, 3510–3519.

Fujii, S., Shimizu, K., Okamoto, Y., Kunii, N., Nakayama, T., Motohashi, S., and Taniguchi, M. (2013). NKT cells as an ideal anti-tumor immunotherapeutic. Front. Immunol. *4*, 409.

Gapin, L. (2010). iNKT cell autoreactivity: what is 'self' and how is it recognized? Nat. Rev. Immunol. *10*, 272–277.

Giannoni, F., Hardee, C.L., Wherley, J., Gschweng, E., Senadheera, S., Kaufman, M.L., Chan, R., Bahner, I., Gersuk, V., Wang, X., et al. (2013). Allelic exclusion and peripheral reconstitution by TCR transgenic T cells arising from transduced human hematopoietic stem/progenitor cells. Mol. Ther. *21*, 1044–1054.

Godfrey, D.I., and Berzins, S.P. (2007). Control points in NKT-cell development. Nat. Rev. Immunol. *7*, 505–518.

Gschweng, E.H., McCracken, M.N., Kaufman, M.L., Ho, M., Hollis, R.P., Wang, X., Saini, N., Koya, R.C., Chodon, T., Ribas, A., et al. (2014). HSV-sr39TK positron emission tomography and suicide gene elimination of human hematopoietic stem cells and their progeny in humanized mice. Cancer Res. *74*, 5173–5183.

Haraguchi, K., Takahashi, T., Hiruma, K., Kanda, Y., Tanaka, Y., Ogawa, S., Chiba, S., Miura, O., Sakamaki, H., and Hirai, H. (2004). Recovery of Valpha24+ NKT cells after hematopoietic stem cell transplantation. Bone Marrow Transplant. *34*, 595–602.

Heczey, A., Liu, D., Tian, G., Courtney, A.N., Wei, J., Marinova, E., Gao, X., Guo, L., Yvon, E., Hicks, J., et al. (2014). Invariant NKT cells with chimeric antigen receptor provide a novel platform for safe and effective cancer immunotherapy. Blood *124*, 2824–2833.

Kamata, T., Suzuki, A., Mise, N., Ihara, F., Takami, M., Makita, Y., Horinaka, A., Harada, K., Kunii, N., Yoshida, S., et al. (2016). Blockade of programmed death-1/programmed death ligand pathway enhances the antitumor immunity of human invariant natural killer T cells. Cancer Immunol. Immunother. *65*, 1477–1489.

King, L.A., Lameris, R., de Gruijl, T.D., and van der Vliet, H.J. (2018). CD1d-Invariant Natural Killer T Cell-Based Cancer Immunotherapy: α-Galactosylceramide and Beyond. Front. Immunol. *9*, 1519.

Kovalovsky, D., Uche, O.U., Eladad, S., Hobbs, R.M., Yi, W., Alonzo, E., Chua, K., Eidson, M., Kim, H.J., Im, J.S., et al. (2008). The BTB-zinc finger transcriptional regulator PLZF controls the development of invariant natural killer T cell effector functions. Nat. Immunol. *9*, 1055–1064.

Krijgsman, D., Hokland, M., and Kuppen, P.J.K. (2018). The Role of Natural Killer T Cells in Cancer-A Phenotypical and Functional Approach. Front. Immunol. *9*, 367.

Kronenberg, M., and Gapin, L. (2002). The unconventional lifestyle of NKT cells. Nat. Rev. Immunol. *2*, 557–568.

Lam, P.Y., Nissen, M.D., and Mattarollo, S.R. (2017). Invariant Natural Killer T Cells in Immune Regulation of Blood Cancers: Harnessing Their Potential in Immunotherapies. Front. Immunol. *8*, 1355.

Lan, P., Tonomura, N., Shimizu, A., Wang, S., and Yang, Y.G. (2006). Reconstitution of a functional human immune system in immunodeficient mice through combined human fetal thymus/liver and CD34+ cell transplantation. Blood *108*, 487–492.

Larson, S.M., Truscott, L.C., Chiou, T.T., Patel, A., Kao, R., Tu, A., Tyagi, T., Lu, X., Elashoff, D., and De Oliveira, S.N. (2017). Pre-clinical development of gene modification of haematopoietic stem cells with chimeric antigen receptors for cancer immunotherapy. Hum. Vaccin. Immunother. *13*, 1094–1104.

Liu, D., Song, L., Wei, J., Courtney, A.N., Gao, X., Marinova, E., Guo, L., Heczey, A., Asgharzadeh, S., Kim, E., et al. (2012). IL-15 protects NKT cells from inhibition by tumor-associated macrophages and enhances antimetastatic activity. J. Clin. Invest. *122*, 2221–2233.

Lynch, H.E., Goldberg, G.L., Chidgey, A., Van den Brink, M.R., Boyd, R., and Sempowski, G.D. (2009). Thymic involution and immune reconstitution. Trends Immunol. *30*, 366–373.

Mallevaey, T., and Selvanantham, T. (2012). Strategy of lipid recognition by invariant natural killer T cells: 'one for all and all for one'. Immunology *136*, 273–282.

Matsuda, J.L., Gapin, L., Sidobre, S., Kieper, W.C., Tan, J.T., Ceredig, R., Surh, C.D., and Kronenberg, M. (2002). Homeostasis of V alpha 14i NKT cells. Nat. Immunol. *3*, 966–974.

Melkus, M.W., Estes, J.D., Padgett-Thomas, A., Gatlin, J., Denton, P.W., Othieno, F.A., Wege, A.K., Haase, A.T., and Garcia, J.V. (2006). Humanized mice mount specific adaptive and innate immune responses to EBV and TSST-1. Nat. Med. *12*, 1316–1322.

Montoya, C.J., Pollard, D., Martinson, J., Kumari, K., Wasserfall, C., Mulder, C.B., Rugeles, M.T., Atkinson, M.A., Landay, A.L., and Wilson, S.B. (2007). Characterization of human invariant natural killer T subsets in health and disease using a novel invariant natural killer T cell-clonotypic monoclonal antibody, 6B11. Immunology *122*, 1–14.

Morrison, S.J., Uchida, N., and Weissman, I.L. (1995). The biology of hematopoietic stem cells. Annu. Rev. Cell Dev. Biol. *11*, 35–71.

Motohashi, S., Ishikawa, A., Ishikawa, E., Otsuji, M., Iizasa, T., Hanaoka, H., Shimizu, N., Horiguchi, S., Okamoto, Y., Fujii, S., et al. (2006). A phase I study of in vitro expanded natural killer T cells in patients with advanced and recurrent non-small cell lung cancer. Clin. Cancer Res. *12*, 6079–6086.

Nair, S., and Dhodapkar, M.V. (2017). Natural Killer T Cells in Cancer Immunotherapy. Front. Immunol. *8*, 1178.

Puig-Saus, C., Parisi, G., Garcia-Diaz, A., Krystofinski, P.E., Sandoval, S., Zhang, R., Champhekar, A.S., McCabe, J., Cheung-Lau, G.C., Truong, N.A., et al. (2019). IND-Enabling Studies for a Clinical Trial to Genetically Program a Persistent Cancer-Targeted Immune System. Clin. Cancer Res. *25*, 1000–1011.

Rotolo, A., Caputo, V.S., Holubova, M., Baxan, N., Dubois, O., Chaudhry, M.S., Xiao, X., Goudevenou, K., Pitcher, D.S., Petevi, K., et al. (2018). Enhanced Anti-lymphoma Activity of CAR19-iNKT Cells Underpinned by Dual CD19 and CD1d Targeting. Cancer Cell *34*, 596–610.

Rubio, M.T., Moreira-Teixeira, L., Bachy, E., Bouillié, M., Milpied, P., Coman, T., Suarez, F., Marcais, A., Sibon, D., Buzyn, A., et al. (2012). Early post-transplantation donor-derived invariant natural killer T-cell recovery predicts the occurrence of acute graft-versus-host disease and overall survival. Blood *120*, 2144–2154.

Savage, A.K., Constantinides, M.G., Han, J., Picard, D., Martin, E., Li, B., Lantz, O., and Bendelac, A. (2008). The transcription factor PLZF directs the effector program of the NKT cell lineage. Immunity *29*, 391–403.

KEY RESOURCES TABLE

REAGENT or RESOURCE	SOURCE	IDENTIFIER
Antibodies		
Anti-human IFN-γ (ELISA, capture)	BD Biosciences	CAT#551221, RRID: AB_394099
Anti-human IFN-γ (ELISA, detection)	BD Biosciences	CAT#554550, RRID: AB_395472
Anti-human IL-4 (ELISA, capture)	BD Biosciences	CAT#554515; RRID: AB_398567
Anti-human IL-4 (ELISA, detection)	BD Biosciences	CAT#554483; RRID: AB_395422
Anti-human IL-2 (ELISA, capture)	BD Biosciences	CAT#554563; RRID: AB_398570
Anti-human IL-2 (ELISA, detection)	BD Biosciences	CAT#555040; RRID: AB_395666
Anti-human CD3 (Clone HIT3a; LEAF purified)	Biolegend	CAT#300314, RRID: AB_314050
Anti-human CD28 (Clone CD28.2; LEAF purified)	Biolegend	CAT#302902, RRID: AB_314304
Anti-human CD45 (Clone H130)	Biolegend	CAT#304026, RFID: AB_893337
Anti-human TCR(alpha)(beta) (Clone I26)	Biolegend	CAT#306716, RRID: AB_1953257
Anti-human CD4 (Clone OKT4)	Biolegend	CAT#317414, RRID: AB_571959
Anti-human CD8 (Clone SK1)	Biolegend	CAT#344714, RRID: AB_2044006
Anti-human CD45RO (Clone UCHL1)	Biolegend	CAT#304216, RRID: AB_493659
Anti-human CD45RA (Clone HI100)	Biolegend	CAT#304126, RRID: AB_10708879
Anti-human CD161 (Clone HP-3G10)	Biolegend	CAT#339928, RRID: AB_2563967
Anti-human CD69 (Clone FN50)	Biolegend	CAT#310914, RRID: AB_314849
Anti-human CD56 (Clone HCD56)	Biolegend	CAT#318304, RRID: AB_604100
Anti-human CD62L (Clone DREG-56)	Biolegend	CAT#304822, RRID: AB_830801
Anti-human CD14 (Clone HCD14)	Biolegend	CAT#325608, RRID: AB_830681
Anti-human CD11b (Clone ICRF44)	Biolegend	CAT#301330, RRID: AB_2561703
Anti-human CD11c (Clone N418)	Biolegend	CAT#337234, RRID: AB_2566656
Anti-human CD20 (Clone 2H7)	Biolegend	CAT#555623, RRID: AB_395989
Anti-human HLA-A2 (Clone BB7.2)	Biolegend	CAT#558570, RRID: AB_647220
Anti-human CD1d (Clone 51.1)	Biolegend	CAT#350308, RRID: AB_10642829
Anti-human PD-1 (Clone EH12.2H7)	Biolegend	CAT#329908, RRID: AB_940475
Anti-human CCR4 (Clone L291H4)	Biolegend	CAT#359409, RRID: AB_2562430
Anti-human CCR5 (Clone HEK/1/85a)	Biolegend	CAT#313705, RRID: AB_345305
Anti-human CXCR3 (Clone G025H7)	Biolegend	CAT#306513, RRID: AB_2089652
Anti-human NKG2D (Clone 1D11)	Biolegend	CAT#320812, RRID: AB_2234394
Anti-human IFNγ (Clone B27)	Biolegend	CAT#506518, RRID: AB_2123321
Anti-human Granzyme B (Clone QA16A02)	Biolegend	CAT#372204, RRID: AB_2687028
Anti-human Perforin (Clone dG9)	Biolegend	CAT#308126, RRID: AB_2572049
Anti-human TNFα (Clone Mab11)	Biolegend	CAT#502912, RRID: AB_315264
Anti-human IL-2 (Clone MQ1-17H12)	Biolegend	CAT#500341, RRID: AB_2562854
Anti-human IL-4 (Clone MP4-25D2)	Biolegend	CAT#500812, RRID: AB_315131
Anti-human IL-17 (Clone BL168)	Biolegend	CAT#512334, RRID: AB_2563986
Anti-human CD34 (Clone 581)	BD Biosciences	CAT#555822, RRID: AB_396151
Anti-human TCR V(alpha)24-J(alpha)18 (Clone 6B11)	BD Biosciences	CAT#552825, RRID: AB_394478
Anti-human TCR V(beta)11	Beckman-Coulter	CAT#A66905
Anti-human PLZF (Clone 9E12)	eBioscience	CAT#19-9322-82, RRID: AB_2637113
Anti-human T-bet (Clone 4B10)	eBioscience	CAT#25-5825-80, RRID: AB_11041809
Anti-mouse CD1d (Clone 1B1)	eBioscience	CAT#17-0011-82, RRID: AB_2573135
Mouse IgG2b, κ isotype control antibody (Clone MPC-11)	Biolegend	CAT#400320
Rat IgG2b, κ isotype control antibody (Clone eB149/10H5)	eBioscience	CAT#17-4031-82, RRID: AB_470176

(*Continued on next page*)

Continued

REAGENT or RESOURCE	SOURCE	IDENTIFIER
Human Fc Receptor Blocking Solution (TrueStain FcX)	Biolegend	CAT#422302
Mouse Fc Block (anti-mouse CD16/32)	BD Biosciences	CAT#553142, RRID: AB_394657
Anti-human CD1d antibody (Clone 51.1; LEAF purified)	Biolegend	CAT#350304, RRID: AB_10641291
Mouse IgG2b, κ isotype control antibody (Clone MG2b-57; LEAF purified)	Biolegend	CAT#401212
Tetramer/Dextramer		
hCD1d/PBS-57 tetramer	NIH Tetramer Core Facility	N/A
HLA-A2/NY-ESO-$1_{157-165}$ dextramer	This paper	N/A
Bacterial and Virus Strains		
Lenti/iNKT	This paper	N/A
Lenti/iNKT-EGFP	This paper	N/A
Lenti/iNKT-sr39TK	This paper	N/A
Lenti/FG	This paper	N/A
Lenti/CD1d	This paper	N/A
Lenti/IL-15-FG	This paper	N/A
Lenti/ESO-sr39TK	This paper	N/A
Lenti/HLA-A2	This paper	N/A
Lenti/NY-ESO-1	This paper	N/A
Biological Samples		
Human peripheral blood mononuclear cells (PBMCs)	UCLA	N/A
Human fetal liver	UCLA	N/A
Human cord blood $CD34^+$ hematopoietic stem and progenitor cells (CB HSCs)	UCLA	N/A
Fetal thymus tissues	UCLA	N/A
Postnatal human thymus	CHLA	N/A
G-CSF-mobilized peripheral blood units	CCHMC	CAT#M001F-GCSF-3
G-CSF-mobilized leukopak	HemaCare	CAT#M001CLPG-4-KIT
Chemicals, Peptides, and Recombinant Proteins		
Streptavidin-HRP conjugate	Invitrogen	CAT#SA10001
Recombinant IL-2 (ELISA, standard)	eBioscience	CAT#570409
Recombinant human IL-4 (ELISA, standard)	eBioscience	CAT#571809
Recombinant human IL-17 (ELISA, standard)	eBioscience	CAT#570509
Recombinant human IFN-γ (ELISA, standard)	eBioscience	CAT#570209
Tetramethylbenzidine (TMB)	KPL	CAT#5120-0053
Ganciclovir (GCV)	Sigma	CAT#ADV465749843
α-Galactosylceramide (KRN7000)	Avanti Polar Lipids	SKU#867000P-1mg
Recombinant human IL-2	Peprotech	CAT#200-02
Recombinant human IL-3	Peprotech	CAT#200-03
Recombinant human IL-4	Peprotech	CAT#200-04
Recombinant human IL-7	Peprotech	CAT#200-07
Recombinant human IL-15	Peprotech	CAT#200-15
Recombinant human Flt3-Ligand	Peprotech	CAT#300-19
Recombinant human SCF	Peprotech	CAT#300-07
Human NY-ESO-$1_{157-165}$ peptide	ThermoFisher	N/A
Recombinant human TPO	Peprotech	CAT#300-18
Recombinant human GM-CSF	Peprotech	CAT#300-03
X-VIVO 15 Serum-free Hematopoietic Cell Medium	Lonza	CAT#04-418Q
RPMI1640 cell culture medium	Corning Cellgro	CAT#10-040-CV
DMEM cell culture medium	Corning Cellgro	CAT#10-013-CV

(*Continued on next page*)

Continued

REAGENT or RESOURCE	SOURCE	IDENTIFIER
Fetal Bovine Serum (FBS)	Sigma	CAT#F2442
Penicillin-Streptomycine-Glutamine (P/S/G)	GIBCO	CAT#10378016
MEM non-essential amino acids (NEAA)	GIBCO	CAT#11140050
HEPES Buffer Solution	GIBCO	CAT#15630056
Sodium Pyruvate	GIBCO	CAT#11360070
Beta-Mercaptoethanol	Sigma	SKU#M6250
Normocin	Invivogen	CAT#ant-nr-2
Fixable Viability Dye eFluor506	affymetrix eBioscience	CAT#65-0866-14
Cell Fixation/Permeabilization Kit	BD Biosciences	CAT#554714
RetroNectin recombination human fibronectin fragment, 2.5mg	Takara	CAT#T100B
10% neutral-buffered formalin	Richard-Allan Scientific	CAT#5705
D-Luciferin	Caliper LIfe Science	CAT#XR-1001
Isoflurane	Zoetis	CAT#50019100
Phosphate Buffered Saline (PBS) pH 7.4 (1X)	GIBCO	CAT#10010-023
Phorbol-12-myristate-13-acetate (PMA)	Calbiochem	CAT#524400
Ionomycin, Calcium salt, Streptomyces conglobatus	Calbiochem	CAT#407952
Critical Commercial Assays		
IOTest beta Mark TCR Vβ Repertoire Kit	Beckman-Coulter	CAT#IM3497
OneStep RT-PCR kit	QIAGEN	CAT#210212
NK Cell Isolation Kit	Miltenyi Biotec	CAT#130-092-657
Human CD14 Microbeads	Miltenyi Biotec	CAT# 130-050-201
Fixation/Permeabilization Solution Kit	BD Sciences	CAT#55474
Human IL-17A ELISA MAX Deluxe Kit	Biolegend	CAT#433915
Experimental Models: Cell Lines		
Human multiple myeloma (MM) cell line MM.1S	ATCC	CRL-2974
Human chronic myelogenous leukemia cancer cell line K562	ATCC	CCL-243
Human melanoma cell line A375	ATCC	CRL-1619
Human multiple myeloma (MM) cell line MM.1S-FG	This paper	N/A
Human multiple myeloma (MM) cell line MM.1S-hCD1d-FG	This paper	N/A
Human chronic myelogenous leukemia cancer cell line K562-FG	This paper	N/A
Human melanoma cell line A375-hIL-15-FG	This paper	N/A
Human melanoma cell line A375-hIL-15-hCD1d-FG	This paper	N/A
Human melanoma cell line A375-A2-ESO-FG	This paper	N/A
Experimental Models: Organisms/Strains		
NOD.Cg-Prkdcscid Il2rgtm1Wjl/SzJ	The Jackson Laboratory	Stock #: 005557
Human bone marrow-liver-thymus (BLT) engrafted NSG mice	This paper	N/A
Human iNKT TCR gene-engineered bone marrow-liver-thymus (BLT) mice	This paper	N/A
Secondary BLT-iNKT mice	This paper	N/A
BLT-iNKT mice generated using Lenti/iNKT-sr39TK vector-transduced PBMCs	This paper	N/A
Oligonucleotides		
Primer: TCRα Forward: GCTCTCTGCACATCACAGCCT CCCAG	IDT	N/A
Primer: TCRβ Forward: CCACAGAGAAGGGAGATCTTT CCTCTGAGTC	IDT	N/A

(*Continued on next page*)

Continued		
REAGENT or RESOURCE	SOURCE	IDENTIFIER
Recombinant DNA		
Vector: parental lentivector pMNDW	Giannoni et al., 2013 and Lan et al., 2006	N/A
Software and Algorithms		
FlowJo Software	FlowJo	https://www.flowjo.com/solutions/flowjo/downloads
OsiriX Imaging Software	OsiriX	https://www.osirix-viewer.com/
Living Imaging 2.50 software	Xenogen/PerkinElmer	https://www.perkinelmer.com/lab-products-and-services/resources/in-vivo-imaging-software-downloads.html
Prism 6	Graphpad	https://www.graphpad.com/scientific-software/prism/
I-control 1.7 Microplate Reader Software	Tecan	https://www.selectscience.net/tecan/i-control–microplate-reader-software/81307

LEAD CONTACT AND MATERIALS AVAILABILITY

Further information and requests for new reagents generated in this study may be directed to and will be fulfilled by the Lead Contact, Lili Yang (liliyang@ucla.edu).

EXPERIMENTAL MODEL AND SUBJECT DETAILS

Mice

NOD.Cg-Prkdc^{SCID}Il2rg^{tm1Wjl}/SzJ (NOD/SCID/IL-2R$\gamma^{-/-}$, NSG) mice were maintained in the animal facilities at the University of California, Los Angeles (UCLA). Six- to ten-week-old females were used for all experiments unless otherwise indicated. All animal experiments were approved by the Institutional Animal Care and Use Committee of UCLA.

Human Tumor Cell Lines

Human multiple myeloma (MM) cell line MM.1S, human chronic myelogenous leukemia cancer cell line K562, and human melanoma cell line A375 were all purchased from the American Type Culture Collection (ATCC). MM.1S and K562 cells were cultured in R10 medium. A375 cells were cultured in D10 medium.

To make stable tumor cell lines overexpressing human CD1d, human HLA-A2.1, human NY-ESO-1, human IL-15, and/or firefly luciferase and enhanced green fluorescence protein (Fluc-EGFP) dual-reporters, the parental tumor cell lines were transduced with lentiviral vectors encoding the intended gene(s) (Yang et al., 2008). 72h post lentivector transduction, cells were subjected to flow cytometry sorting to isolate gene-engineered cells for making stable cell lines. Six stable tumor cell lines were generated for this study, including MM.1S-FG, MM.1S-hCD1d-FG, A375-hIL-15-FG, A375-hIL-15-hCD1d-FG, A375-A2-ESO-FG, and K562-FG.

Human PBMCs, CD34$^+$ HSCs, and Thymus Tissues

Human peripheral blood mononuclear cells (PBMCs), human fetal liver or cord blood CD34$^+$ hematopoietic stem and progenitor cells (referred to as HSCs), and fetal thymus tissues were obtained from the CFAR Gene and Cellular Therapy Core Laboratory at UCLA, without identification information under federal and state regulations. Postnatal human thymus was obtained under IRB exemption as anonymized, discarded waste from patients undergoing cardiac surgery at Children's Hospital Los Angeles (CHLA). G-CSF-mobilized healthy donor peripheral blood units were purchased from HemaCare or Cincinnati Children's Hospital Medical Center (CCHMC), followed by isolation of CD34$^+$ HSCs through magnetic-activated cell sorting using a CliniMACS (Miltenyi Biotec) according to the manufacturer's instructions. For all isolates, the purity of CD34$^+$ cells were more than 97% as evaluated by flow cytometry.

Materials and Reagents

α-Galactosylceramide (αGC, KRN7000) was purchased from Avanti Polar Lipids. Fluorochrome-conjugated hCD1d/PBS-57 tetramer reagents were provided by the NIH Tetramer Core Facility (Emory University, Atlanta, GA). Recombinant human IL-2, IL-3, IL-4, IL-7, IL-15, Flt3-Ligand, Stem Cell Factor (SCF), Thrombopoietin (TPO), and Granulocyte-Macrophage Colony-Stimulating Factor (GM-CSF) were purchased from Peprotech.

X-VIVO 15 Serum-free Hematopoietic Cell Medium was purchased from Lonza. RPMI1640 and DMEM cell culture medium were purchased from Corning Cellgro. Fetal bovine serum (FBS) was purchased from Sigma. Medium supplements, including Penicillin-Streptomycine-Glutamine (P/S/G), MEM non-essential amino acids (NEAA), HEPES Buffer Solution, and Sodium Pyruvate, were

purchased from GIBCO. Beta-Mercaptoethanol (β-ME) was purchased from Sigma. Normocin was purchased from InvivoGen. Complete lymphocyte culture medium (denoted as C10 medium) was made of RPMI 1640 supplemented with FBS (10% vol/vol), P/S/G (1% vol/vol), MEM NEAA (1% vol/vol), HEPES (10 mM), Sodium Pyruvate (1 mM), β-ME (50 μM), and Normocin (100 μg/ml). Medium for culturing monocyte-derived dendritic cells (MoDC) and non-adherent tumor cells (denoted as R10 medium) was made of RPMI 1640 supplemented with FBS (10% vol/vol) and P/S/G (1% vol/vol). Adherent cell culture medium (denoted as D10 medium) was made of DMEM supplemented with FBS (10% vol/vol) and P/S/G (1% vol/vol).

METHOD DETAILS

Lentiviral Vectors

Lentiviral vectors used in this study were all constructed from a parental lentivector pMNDW, that contains the MND retroviral LTR U2 region as an internal promoter and contains an additional truncated Woodchuck Responsive Element (WPRE) to stabilize viral mRNA (Giannoni et al., 2013; Smith et al., 2016). The pMNDW lentivector mediates high and stable expression of transgene in human HSCs and their progeny human immune cells (Cartier et al., 2009). The Lenti/iNKT vector was constructed by inserting into pMNDW a synthetic bicistronic gene encoding human iNKT TCRα-F2A-TCRβ; the Lenti/iNKT-EGFP vector was constructed by inserting into pMNDW a synthetic tricistronic gene encoding human iNKT TCRα-F2A-TCRβ-P2A-EGFP; the Lenti/iNKT-sr39TK vector was constructed by inserting into pMNDW a synthetic tricistronic gene encoding human iNKT TCRα-F2A-TCRβ-P2A-sr39TK; the Lenti/FG vector was constructed by inserting into pMNDW a synthetic bicistronic gene encoding Fluc-P2A-EGFP; the Lenti/CD1d vector was constructed by inserting into pMNDW a synthetic gene encoding human CD1d; the Lenti/IL-15-FG vector was constructed by inserting into pMNDW a synthetic tricistronic gene encoding human IL-15-F2A-Fluc-P2A-EGFP; the Lenti/ESO-sr39TK vector was constructed by inserting into pMNDW a synthetic tricistronic gene encoding human NY-ESO-1-specific TCRα-F2A-TCRβ-P2A-sr39TK; the Lenti/HLA-A2 vector was constructed by inserting into pMNDW a synthetic gene encoding human HLA-A2.1; and the Lenti/NY-ESO-1 vector was constructed by inserting into pMNDW a synthetic gene encoding human NY-ESO-1. The synthetic gene fragments were obtained from GenScript and IDT. Lentiviruses were produced using 293T cells, following a standard calcium precipitation protocol and an ultracentrifugation concentration protocol or a tandem tangential flow filtration concentration protocol as previously described (Cooper et al., 2011; Smith et al., 2016). Lentivector titers were measured by transducing HT29 cells with serial dilutions and performing digital qPCR, following established protocols (Cooper et al., 2011; Smith et al., 2016).

Antibodies and Flow Cytometry

Fluorochrome-conjugated antibodies specific for human CD45 (clone H130), TCRαβ (clone I26), CD4 (clone OKT4), CD8 (clone SK1), CD45RO (clone UCHL1), CD45RA (clone HI100), CD161 (clone HP-3G10), CD69 (clone FN50), CD56 (clone HCD56), CD62L (clone DREG-56), CD14 (clone HCD14), CD11b (clone ICRF44), CD11c (clone N418), CD20 (clone 2H7), HLA-A2 (clone BB7.2), CD1d (clone 51.1), PD-1 (clone EH12.2H7), CCR4 (clone L291H4), CCR5 (clone HEK/1/85a), CXCR3 (clone G025H7), NKG2D (clone 1D11), IFN-γ (clone B27), Granzyme B (clone QA16A02), Perforin (clone dG9), TNF-α (clone Mab11), IL-2 (clone MQ1-17H12), IL-4 (clone MP4-25D2) and IL-17 (clone BL168) were purchased from BioLegend; fluorochrome-conjugated antibodies specific for human CD34 (clone 581), TCR Vα24-Jα18 (clone 6B11) were purchased from BD Biosciences; fluorochrome-conjugated antibodies specific for human PLZF (alone 9E12), T-bet (clone 4B10), and CD1d (clone 1B1) were purchased from eBioscience. A fluorochrome-conjugated antibody specific for human Vβ11 was purchased from Beckman-Coulter. Human Fc Receptor Blocking Solution (TruStain FcX) was purchased from BioLegend, while mouse Fc Block (anti-mouse CD16/32) was purchased from BD Biosciences. Fixable Viability Dye eFluor506 (e506) were purchased from affymetrix eBioscience. Cells were stained as previously described (Yang and Baltimore, 2005). Intracellular cytokines were measured using a Cell Fixation/Permeabilization Kit (BD Biosciences) according to the manufacturer's instructions. Stained cells were analyzed using a MACSQuant Analyzer 10 flow cytometer (Miltenyi Biotec). FlowJo software was used to analyze the data.

Human iNKT Cell TCR Vβ Repertoire Analysis

Human iNKT cell TCR Vβ repertoire was analyzed through flow cytometry using an IOTest® Beta Mark TCR V beta Repertoire Kit (Beckman-Coulter), following the manufacturer's instructions. Tube G was not used in staining because it included an antibody for Vβ11, which was stained separately. All other combined hTCR Vβs (FITC) and hTCR Vβs (PE) antibodies collectively stained for human TCR Vβ 1, 2, 3, 4, 5.1, 5.2, 5.3, 7.1, 7.2, 8, 9, 12, 13.1, 13.2, 13.6, 16, 17, 18, 20, 21.3, and 23.

ELISA

The ELISAs for detecting human cytokines were performed following a standard protocol from BD Biosciences. The capture and biotinylated antibody pairs for detecting human IFN-γ, IL-4, and IL-17 were purchased from BD Biosciences. The streptavidin-HRP conjugate was purchased from Invitrogen. Human IFN-γ, IL-4 and IL-17 standards were purchased from eBioscience. The tetramethylbenzidine (TMB) substrate was purchased from KPL. The samples were analyzed for absorbance at 450 nm using an Infinite M1000 microplate reader (Tecan).

Ganciclovir (GCV) *In Vitro* Killing Assay

Healthy donor PBMC T cells were cultured *in vitro* in C10 medium for 8 days, in the presence of 1 μg/ml anti-human CD3 (Clone HIT3a; LEAF^{TM} purified; Biolegend), 1 μg/ml anti-human CD28 (Clone CD28.2; LEAF^{TM} purified; Biolegend), and 10 ng/ml recombinant human IL-2. On days 2 and 3, concentrated Lenti/iNKT-sr39TK vectors were added into the cell culture. On day 4, titrated amounts of GCV (0-50 μM) were added into the cell culture. On day 8, selective killing of lentivector-transduced T cells (identified as hCD1d/PBS-57^{+} cells among total T cells) were analyzed using flow cytometry.

Single-Cell Human iNKT TCR Cloning

The single-cell iNKT TCR RT-PCR was performed based on an established protocol, with certain modifications (Smith et al., 2015). Single human iNKT cells were sorted from healthy donor PBMCs based on a stringent forum of surface markers (hTCRαβ^{+}hTCR Vα24-Jα18^{+}hTCR Vβ11^{+}CD161^{+}) using a FACSAria II flow cytometer (BD Biosciences). Single cells were sorted directly into PCR plates containing cell lysis buffer. The plates were then immediately flash frozen and stored at −80°C until use. Upon thawing, the cell lysate from each cell was split in half on the same PCR plate and processed directly into iNKT TCR cloning for both α and β chain genes using a OneStep RT-PCR kit (QIAGEN), following the manufacturer's instructions and using the human iNKT TCR gene-specific primers. These primers were designed to amplify the ~200-300 bps spanning the CDR3 regions of the iNKT TCR α and β chain cDNAs and were customer-synthesized by IDT: for TCRα (FW primer: 5′- GCT CTC TGC ACA TCA CAG CCT CCC AG −3′; BW primer: 5′- CGG TGA ATA GGC AGA CAG ACT TGT CAC TG −3′) and for TCRβ (FW: 5′- CCA CAG AGA AGG GAG ATC TTT CCT CTG AGT C −3′; BW: 5′- CCT GTG GCC AGG CAC ACC AGT G −3′). Verified sequences (productive germline Vα24-Jα18-Cα assembly for TCRα and Vβ11-D/J/N-Cβ assembly for TCRβ) were used to construct the complete cDNA sequences encoding the TCR α and β chains from a single cell, based on information about human TCR genomic segments [the international ImMunoGeneTics information system (IMGT), http://www.imgt.org/]. The selected iNKT TCR α and β pair cDNAs were then synthesized as a single bicistonic gene, with codon optimization and an F2A sequence linking the TCRα and TCRβ cDNAs to enable their co-expression (GenScript).

Generation of BLT and BLT-iNKT Humanized Mice

BLT (human bone marrow-liver-thymus engrafted NSG mice) and BLT-iNKT (human iNKT TCR gene-engineered BLT mice) humanized mice were generated as previously described, with some modifications (Lan et al., 2006; Melkus et al., 2006; Smith et al., 2016). In brief, human CD34^{+} HSCs were cultured for no more than 48 hours in X-VIVO 15 Serum-free Hematopoietic Cell Medium (Lonza) containing recombinant human Flt3 ligand (50 ng/mL), SCF (50 ng/mL), TPO (50 ng/mL), and IL-3 (20 ng/mL) in non-tissue culture-treated plates coated with Retronectin (20 μg/ml) (Takara). Viral transduction, when applicable, was performed at 24 hours by adding concentrated lentivectors (Lenti/iNKT, Lenti/iNKT-EGFP, or Lenti/iNKT-sr39TK) directly to the culture medium. At around 48 hours, CD34^{+} cells were collected and i.v. injected into NSG mice (~0.5-1 × 10^{6} cells per recipient) that had received 270 rads of total body irradiation. 1-2 fragments of human fetal or postnatal thymus (~1 mm^{3}) were implanted under the kidney capsule of each recipient NSG mouse. The mice were maintained on trimethoprim/sulfmethoxazole (TMS) chow in a sterile environment for 8-12 weeks until analysis or use for further experiments. Unless otherwise indicated, data from BLT-iNKT mice produced with human fetal thymus and Lenti/iNKT-sr39TK vector-transduced PBSCs were presented.

Generation of Secondary BLT-iNKT Humanized Mice

Secondary BLT-iNKT mice were generated through harvesting total bone marrow cells and human thymus implants from primary BLT-iNKT mice followed by adoptive transfer into NSG recipient mice (Smith et al., 2016). Primary BLT-iNKT mice were produced with human fetal thymus and Lenti/iNKT-sr39TK vector-transduced PBSCs. Recipient NSG mice were pre-conditioned with 270 rads of total body irradiation. 10 × 10^{6} primary BLT-iNKT mice bone marrow cells were i.v. injected into each NSG recipient mouse. Human thymus implants were dissected from the kidney capsule of primary BLT-iNKT mice, cut into fragments (~1 mm^{3}), then surgically implanted under the kidney capsule of the NSG recipient mice (1-2 fragments per recipient). The mice were maintained on TMS chow in a sterile environment for 8-12 weeks until analysis or further experiments.

Safety Study of HSC-iNKT Cell Therapy in BLT-iNKT Mice

BLT-iNKT mice and control BLT mice were monitored for body weight and survival rate over a period of 5 months after HSC transfer. At the end of 5 months, mice were terminated and various tissues were collected, including bone marrow, spleen, lleum, pancreas, kidney, lung, liver, heart, and brain. Tissues were fixed with 10% neutral-buffered formalin and embedded in paraffin for sectioning (5 μm thickness), followed by hematoxylin and eosin staining using standard procedures (UCLA Translational Pathology Core Laboratory). The sections were examined by a mouse pathologist (N.R.) who was blinded to the sample group assignments during initial scoring. Scores were assigned on the basis of a combination of criteria, including inflammation, hematopoietic neoplasm, and non-hematopoietic neoplasm. An ordinal scale scoring system was used: 0, no abnormal findings; 1, mild; 2, moderate; and 3, severe.

In another set of longer-term experiments, BLT-iNKT mice and control BLT mice were maintained for a period of over 8 months, to monitor graft-versus-host (GvH) reactions in these animals. Over time, mouse survival rates were recorded. At 6 months post-HSC transfer, a subset of animals were terminated and their tissues (e.g., liver) were collected and processed for flow cytometry analysis

following established protocols (Smith et al., 2016). Activation status of engrafted human conventional αβ T cells (identified as hCD45$^+$hTCRαβ$^+$6B11$^-$ cells) was assessed through measuring T cell expression of CD45RA and CD45RO surface markers (CD45RA^{lo}CD45RO^{hi} indicating T cell activation).

Biodistribution and Controlled Depletion of HSC-iNKT Cells in BLT-iNKT Humanized Mice Visualized by PET/CT Imaging

BLT-iNKT^{TK} mice (BLT-iNKT mice generated using Lenti/iNKT-sr39TK vector-transduced PBSCs) were utilized for this study. Regular BLT mice were included as imaging controls. To study controlled depletion of vector-engineered human HSCs and their progeny immune cells, experimental animals received i.p. injection of nucleoside prodrug ganciclovir (GCV) for five consecutive days (50 mg/kg per injection per day). PET/CT imaging data were collected one day prior to GCV treatment, and 7 days post GCV treatment. PET/CT scans were performed using a microPET/CT system Genisys 8 (Sofie Bioscience). Mice were anesthetized using 1.5%–2% isoflurane. 20 μCi of 18F-FHBG probes was administrated via tail vein. Acquisition of static PET images was started 60 min after probe injection. Maximum-likelihood expectation maximization with 60 iterations was used for PET image reconstruction. All images were corrected for photon attenuation. The CT acquisition parameters were 40 kVp, 190 mA, and 720 projections with an exposure time of 55 ms at each projection. For image analysis, PET/CT images were analyzed using OsiriX Imaging Software (Version 3.9.3; Pixmeo SARL).

HSC-iNKT Cell Phenotype and Functional Study

HSC-engineered human iNKT cells (denoted as HSC-iNKT cells) were isolated from the spleen of BLT-iNKT mice. Phenotype of HSC-iNKT cells was studied using flow cytometry, through analyzing cell surface markers including co-receptors (CD4 and CD8), NK cell markers (CD161 and NKG2D), memory/effector T cell markers (CD45RO and CD69), and homing markers (CD62L, CCR4, CCR5, and CXCR3). Native human iNKT cells and conventional T cells isolated from healthy donor PBMCs (denoted as PBMC-iNKT and PBMC-Tc cells, respectively) were included as FACS analysis controls.

Response of HSC-iNKT cells to antigen stimulation was studied by culturing BLT-iNKT spleen cells *in vitro* in C10 medium for 7 days, in the presence or absence of αGC (100 ng/ml). Proliferation of HSC-iNKT cells (identified as hCD45$^+$hTCRαβ$^+$6B11$^+$ cells of total cell culture) was measured by cell counting and flow cytometry over time. Cytokine production was assessed by ELISA analysis of cell culture supernatants collected on day 7 (for human IFN-γ, IL-4, and IL-17).

Capacity of HSC-iNKT cells to produce effector molecules was studied in comparison with that of native PBMC-iNKT cells and PBMC-Tc cells. BLT-iNKT spleen cells and healthy donor PBMCs were cultured *in vitro* in C10 medium for 7 days with αGC stimulation (100 ng/ml). On day 7, cells were collected and analyzed for intracellular production of various pro-inflammatory cytokines (IFN-γ, TNF-α, and IL-2) and cytotoxic molecules (Perforin and Granzyme B) using a Cytofix/Cytoperm Fixation/Permeabilization Kit (BD Biosciences) (Smith et al., 2015). The CD4/CD8 co-receptor expression patterns on HSC-iNKT cells and PBMC-iNKT cells pre- and post-αGC stimulation were studied using flow cytometry.

HSC-iNKT Cell *In Vitro* Expansion

Various tissues (spleen, lymph nodes, liver, bone marrow) were collected from BLT-iNKT mice, processed into single mononuclear cells, and pooled together for *in vitro* culture. Healthy donor PBMCs were loaded with αGC (by culturing 1 × 10^8 PBMCs in 5 mL C10 medium containing 5 μg/ml αGC for 1 hour), irradiated at 6,000 rads, then used to stimulate HSC-iNKT cells (denoted as αGC/PBMCs). To expand HSC-iNKT cells, pooled BLT-iNKT mouse tissue cells were mixed with αGC/PBMCs (ratio 1:1 or 1:1.5) and cultured in C10 medium for 7 days. Recombinant human IL-7 (10 ng/ml) and IL-15 (10 ng/ml) were added to cell cultures from day 2. On day 7, cell cultures were collected and HSC-iNKT cells were sorted out using flow cytometry (identified as hCD45$^+$hTCRαβ$^+$6B11$^+$ cells). The sorted HSC-iNKT cells (> 99% purify based on flow cytometry analysis) were expanded further with αGC/APCs and IL-7/IL-15 for another 7 to 14 days, then were aliquoted and frozen in LN2 storage tanks. For mechanistic and efficacy studies, HSC-iNKT cells were thawed from frozen stock and utilized for the intended assays.

HSC-iNKT Cell Tumor-Attacking Mechanism Study: *In Vitro* Direct Tumor Cell Killing Assay

MM.1S-FG or MM.1S-hCD1d-FG tumor cells (5-10 × 10^3 cells per well) were co-cultured with HSC-iNKT cells (ratio 1:10, unless otherwise indicated) in Corning 96-well clear bottom black plates for 24-48 hours, in X-VIVO^{TM} 15 medium with or without the addition of αGC (100 ng/ml). At the end of culture, live tumor cells were quantified by adding D-Luciferin (150 μg/ml) (Caliper Life Science) to cell cultures and reading out luciferase activities using an Infinite M1000 microplate reader (Tecan) according to the manufacturer's instructions. In tumor cell killing assays involving blocking CD1d, 10 μg/ml LEAF^{TM} purified anti-human CD1d antibody (Clone 51.1, Biolegend) or LEAF^{TM} purified mouse IgG2b κ isotype control antibody (Clone MG2b-57, Biolegend) was added to tumor cell cultures one hour prior to adding HSC-iNKT cells.

HSC-iNKT Cell Tumor-Attacking Mechanism Study: *In Vitro* NK Adjuvant Effect Assay

Primary human NK cells were isolated from healthy donor PBMCs through magnetic-activated cell sorting (MACS sorting), using an NK Cell Isolation Kit (Miltenyi Biotec) according to the manufacturer's instructions. K562-FG cells (5 × 10^4 cells per well) were co-cultured with NK cells and HSC-iNKT cells (ratio 1:2:2) in Corning 96-well clear bottom black plates for 24 hours, in C10 medium with or without the addition of αGC-loaded irradiated PBMCs as antigen presenting cells (APCs). Live tumor cells were quantified

by adding D-Luciferin (150 μg/ml) (Caliper Life Science) to the cell cultures and reading out luciferase activities using an Infinite M1000 microplate reader (Tecan). NK cell activation status was monitored through measuring NK cell expression of CD69 using flow cytometry. Cytokine production from co-cultured NK and HSC-iNKT cells was analyzed through collecting cell culture supernatants and assaying cytokines (IFN-γ and IL-2) using ELISA.

HSC-iNKT Cell Tumor-Attacking Mechanism Study: *In Vitro* DC/CTL Adjuvant Effect Assay

$CD1d^+$/$HLA\text{-}A2^+$ human monocyte-derived dendritic cells (MoDCs) were generated by isolating $CD14^+$ monocytes from $HLA\text{-}A2^+$ healthy donor PBMCs using MACS sorting, followed by culturing monocytes in R10 medium supplemented with recombinant human GM-CSF (100 ng/ml) and IL-4 (20 ng/ml) for 4 days (Yang et al., 2008). NY-ESO-1 specific $CD8^+$ human cytotoxic T lymphocytes (CTLs, or ESO-T cells) were generated through engineering human $CD34^+$ HSCs with a TCR gene encoding a 1G4 TCR (HLA-A2-restricted, NY-ESO-1 tumor antigen-specific) and differentiating the TCR gene-engineered HSCs into $CD8^+$ CTLs in an Artificial Thymic Organoid (ATO) culture, following an established protocol (Bethune et al., 2018; Seet et al., 2017). The resulting ESO-T CTLs were co-cultured with $CD1d^+$/$HLA\text{-}A2^+$ MoDCs in C10 medium for 3 days, with or without the addition of HSC-iNKT cells (cell ratio 1:1:1) and αGC (100 ng/ml). Activation of MoDCs was analyzed at 24 hours through measuring MoDC surface expression of CD86 using flow cytometry. Expansion of ESO-T cells was quantified at 72 hours through cell counting and flow cytometry analysis (ESO-T cells were gated as $hTCR\alpha\beta^+$$hTCR\ V\beta13.1^+$ cells of the total cell cultures). Tumor-killing potential of ESO-T cells was measured by adding A375-A2-ESO-FG tumor cells (1:1 ratio to input ESO-T cells) to the ESO-T/MoDC co-culture 24 hours post co-culture setup, and quantifying live tumor cells via luciferase activity reading in another 24 hours.

HSC-iNKT Cell Tumor-Attacking Mechanism Study: *In Vitro* Macrophage Inhibition Assay

$CD14^+$ monocytes were isolated from healthy donor PBMCs through MACS sorting, followed by co-culturing with HSC-iNKT cells (ratio 1:1) for 24-48 hours in C10 medium with or without the addition of αGC (100 ng/ml). At the end of culture, cells were collected for flow cytometry analysis, to assess the activation of HSC-iNKT cells (gated as $hTCR\alpha\beta^+6B11^+$ cells of total cell culture) by measuring their expression of CD69, and to assess the viability of monocytes (gated as $CD14^+$ cells of total cell culture) with the eBioscience Fixable Viability Dye eFluor 506 (e506).

Bioluminescence Live Animal Imaging (BLI)

BLI was performed using an IVIS 100 imaging system (Xenogen/PerkinElmer). Live animal imaging was acquired 5 minutes after intraperitoneal injection of D-Luciferin (1 mg per mouse). Imaging results were analyzed using a Living Imaging 2.50 software (Xenogen/PerkinElmer).

HSC-iNKT Cell *In Vivo* Antitumor Efficacy Study: MM.1S Human Multiple Myeloma Xenograft NSG Mouse Model

NSG mice were inoculated with 0.5-1 × 10^6 MM.1S-hCD1d-FG or MM.1S-FG cells intravenously (day 0) and were allowed to develop MM over the course of about 3 weeks. Prior to tumor inoculation (day 0), mice were pre-conditioned with 175 rads of total body irradiation. Three days post-tumor inoculation (day 3), mice received i.v. injection of vehicle (PBS) or 1 × 10^7 HSC-iNKT cells. Recombinant human IL-15 was supplemented to experimental animals through i.p injection to support the peripheral maintenance of HSC-iNKT cells twice per week starting from day 3 (500 ng per animal per injection). Over time, tumor loads in experimental animals were monitored using BLI, twice per week starting from day 2. At around week 3, mice were terminated. Various mouse tissues (blood, spleen, liver, and bone marrow) were harvested and processed for flow cytometry analysis to detect tissue-residing tumor cells (identified as GFP^+ cells) and HSC-iNKT cells (identified as $hCD45^+6B11^+$ cells), following established protocols (Smith et al., 2016). Activation status of HSC-iNKT cells was monitored through measuring cell surface expression of CD62L and CD69 markers using flow cytometry.

HSC-iNKT Cell *In Vivo* Antitumor Efficacy Study: A375 Human Melanoma Xenograft NSG Mouse Model

NSG mice were inoculated with 1 × 10^6 αGC-loaded A375-hIL-15-hCD1d-FG cells or 1 × 10^6 αGC-loaded A375-hIL-15-FG cells subcutaneously (day 0) and were allowed to grow solid tumors over the course of approximately 4 weeks. Three days post-tumor inoculation (day 3), mice received 100 rads of total body irradiation followed by i.v. injection of vehicle (PBS) or 1 × 10^7 HSC-iNKT cells. Note that inclusion of a human IL-15 gene in the tumor cells aimed to provide human IL-15 within solid tumors *in vivo*, because the on-site presence of IL-15 has been indicated to be critical in maintaining iNKT cell survival in the hypoxic solid tumor microenvironment. Recombinant human IL-15 was also supplemented to experimental animals through i.p injection to support the peripheral maintenance of HSC-iNKT cells twice per week starting from day 3 (500 ng per animal per injection). Over time, tumor loads in experimental animals were monitored twice per week starting from day 2 by measuring total body luminescence using BLI (shown as TBL p/s), and by measuring tumor size using a Fisherbrand™ Traceable™ digital caliper (Thermo Fisher Scientific) (tumor volume calculated as (W(2) x L)/2 mm^3). At approximately week 4, mice were terminated. Solid tumors were retrived, weighted using a PA84 precision balance (Ohaus), then processed for flow cytometry analysis to detect tumor-infiltrating HSC-iNKT cells (identified as $hCD45^+6B11^+$ cells). Various mouse tissues (blood, spleen, and liver) were also collected and processed for flow cytometry analysis to detect tissue-residing HSC-iNKT cells (identified as $hCD45^+6B11^+$ cells), following established protocols (Smith et al., 2016). Activation status of HSC-iNKT cells was monitored through measuring cell surface expression of CD62L and CD69 markers using flow cytometry.

QUANTIFICATION AND STATISTICAL ANALYSIS

A Prism 6 software (Graphpad) was used for all statistical analysis. Pairwise comparisons were made using a 2-tailed Student's t test. Multiple comparisons were performed using an ordinary 1-way ANOVA, followed by Tukey's multiple comparisons test. Kaplan-Meier survival curves were analyzed by log rank (Mantel-Cox) test adjusted for multiple comparisons. Data are presented as the mean ± SEM, unless otherwise indicated. In all figures and figure legends, "n" represents the number of samples or animals utilized in the indicated experiments. A P value of less than 0.05 was considered significant. ns, not significant; * $p < 0.05$; ** $p < 0.01$; *** $p < 0.001$; **** $p < 0.0001$.

DATA AND CODE AVAILABILITY

All data associated with this study are present in the paper or Supplemental Information.

Cell Stem Cell, Volume *25*

Supplemental Information

Development of Hematopoietic Stem Cell-Engineered Invariant Natural Killer T Cell Therapy for Cancer

Yanni Zhu, Drake J. Smith, Yang Zhou, Yan-Ruide Li, Jiaji Yu, Derek Lee, Yu-Chen Wang, Stefano Di Biase, Xi Wang, Christian Hardoy, Josh Ku, Tasha Tsao, Levina J. Lin, Alexander T. Pham, Heesung Moon, Jami McLaughlin, Donghui Cheng, Roger P. Hollis, Beatriz Campo-Fernandez, Fabrizia Urbinati, Liu Wei, Larry Pang, Valerie Rezek, Beata Berent-Maoz, Mignonette H. Macabali, David Gjertson, Xiaoyan Wang, Zoran Galic, Scott G. Kitchen, Dong Sung An, Siwen Hu-Lieskovan, Paula J. Kaplan-Lefko, Satiro N. De Oliveira, Christopher S. Seet, Sarah M. Larson, Stephen J. Forman, James R. Heath, Jerome A. Zack, Gay M. Crooks, Caius G. Radu, Antoni Ribas, Donald B. Kohn, Owen N. Witte, and Lili Yang

Vβ11$^+$) using flow cytometry (C). 14 days later, the remaining HSCs were collected and analyzed for average vector copy number (VCN) per cell using droplet digital PCR (ddPCR) (D; n = 3).

(E) Titrated transduction of HSCs with the Lenti/iNKT-sr39TK vector. Representative data studying G-CSF-mobilized peripheral blood CD34$^+$ HSCs from a selected donor were presented. Titrated amount of concentrated Lenti/iNKT-sr39TK vector were added to HSC cultures. Three days later, a portion of HSCs were collected and analyzed for intracellular expression of iNKT TCR (identified as hTCR Vβ11$^+$) using flow cytometry. 14 days later, the remaining HSCs were collected and analyzed for average VCN per cell using ddPCR. Note the correlation between vector titers and transduction rates. Average VCN per cell at all transduction rates remained between 1-3, which is considered to be a relative safe range for lentivector-mediated gene therapy.

Representative of 2 experiments. Data were presented as the mean ± SEM. ns, not significant, by 1-way ANOVA (D).

A

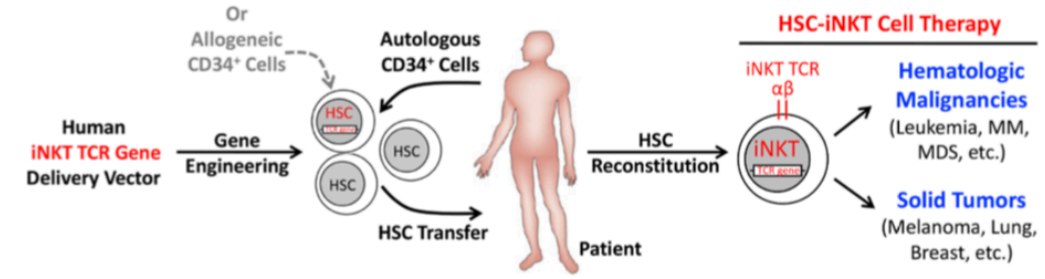

B

Vector Titer (Lenti/iNKT-sr39TK)			
Titer (TU/ml)	**Average**	**STDEV**	**%CV**
Un-Concentrated Supernatant (4 L)	8.27×10^5	6.40×10^4	7.73%
Concentrated Supernatant (2000x fold; 2 ml)	5.30×10^9	2.55×10^8	4.90%

C

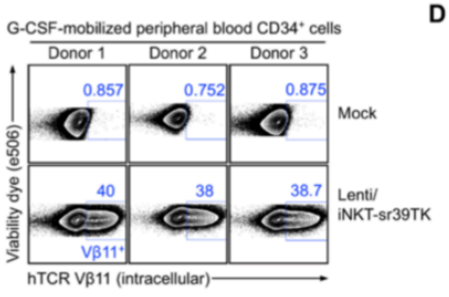

D

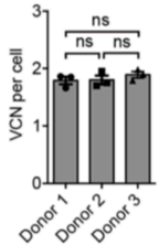

E

Transduction of G-CSF mobilized CD34⁺ HSCs (1 x 10^6)				
Lenti/iNKT-sr39TK (TU)	0	1 x 10^8	2 x 10^8	4 x 10^8
% Vβ11⁺	0	19%	39%	51%
VCN	0	1.28	1.73	1.98

Figure S1. Development of a Hematopoietic Stem Cell-Engineered Invariant Natural Killer T (HSC-iNKT) Cell Therapy, Related to Figure 1.

(A) Schematic representation of the concept of HSC-iNKT cell therapy. Autologous or allogeneic human CD34$^+$ HSCs will be collected and engineered *in vitro* with a human iNKT TCR gene, followed by adoptive transfer into cancer patients. Post-HSC reconstitution, iNKT TCR gene-engineered HSCs will continuously produce human iNKT cells. This therapy has the potential to provide cancer patients with therapeutic levels of iNKT cells for a lifetime. HSC-iNKT cell therapy may benefit patients with a broad range of cancers, including various hematologic malignancies and solid tumors. MM, multiple myeloma; MDS, myelodysplastic syndromes.

(B) Titer of the Lenti/iNKT-sr39TK vector. A 4-liter batch of Lenti/iNKT-sr39TK lentiviral vector was produced using a 293T virus packaging cell line transient transfection method, followed by concentration to 2 ml (2000x fold) using an established tandem tangential filtration method. Vector titers prior to and post-concentration were measured by transducing HT29 cells with serial dilutions and performing digital QPCR (n = 3). TU, transduction unit.

(C-D) Transduction of HSCs with the Lenti/iNKT-sr39TK vector. G-CSF-mobilized peripheral blood CD34$^+$ HSCs from three healthy donors were studied. Concentrated Lenti/iNKT-sr39TK vector were added to HSC cultures (2 x 10^8 TU per 1 x 10^6 HSCs). Three days later, a portion of HSCs were collected and analyzed for intracellular expression of iNKT TCR (identified as hTCR

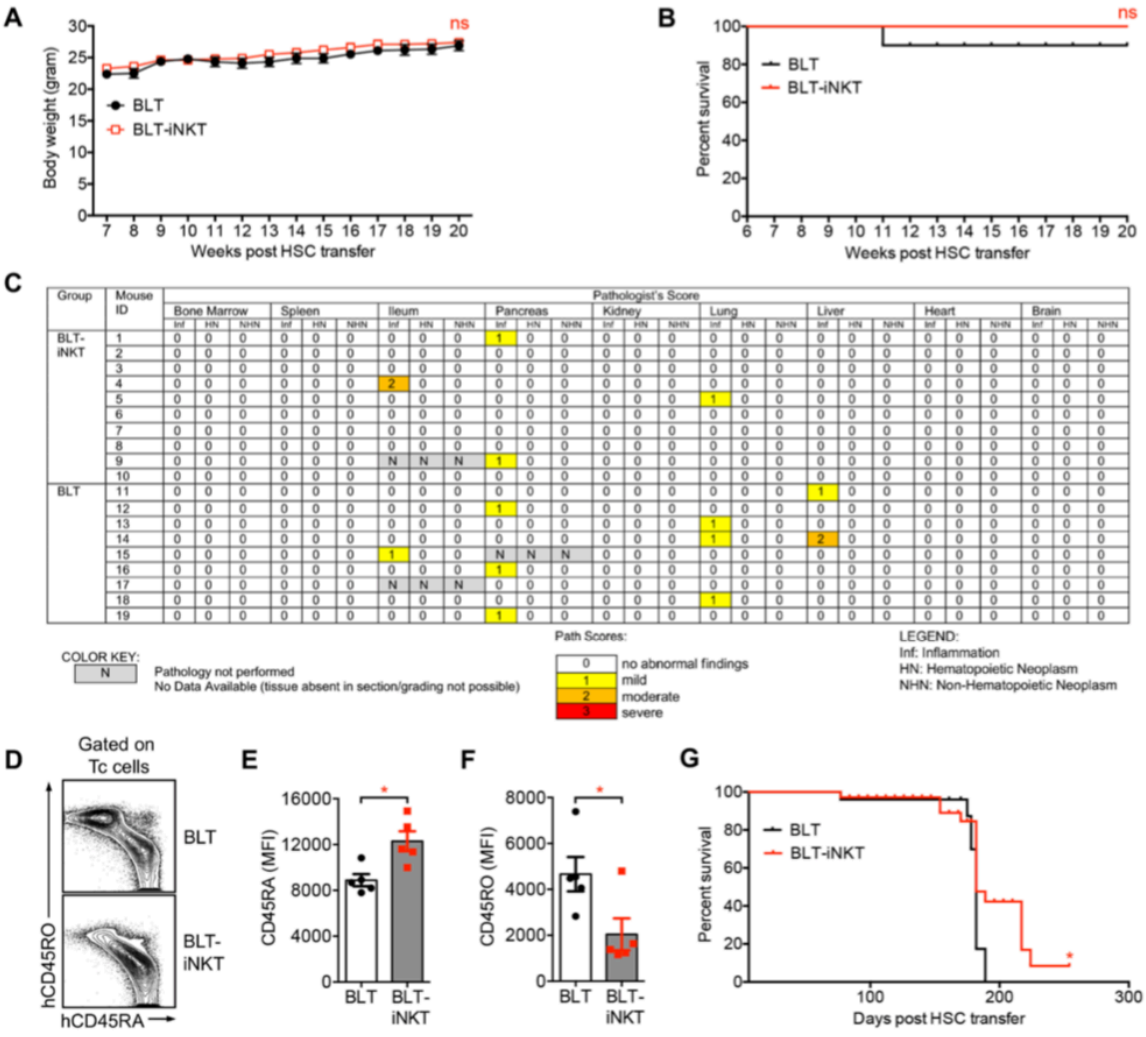

Figure S2. Safety Study of HSC-iNKT Cell Therapy in BLT-iNKT Humanized Mice, Related to Figure 3.

Representative data were presented, studying BLT-iNKT mice produced with human fetal thymus and Lenti/iNKT-sr39TK vector-transduced PBSCs. BLT mice generated in parallel using the same fetal thymus and PBSCs (mock-transduced) were included as a control.

(A-C) Monitoring of BLT-iNKT mice and control BLT mice over a period of 5 months post-HSC transfer, followed by tissue collection and pathological analysis. (A) Mouse body weight (n = 9-10). (B) Kaplan-Meier analysis of mouse survival rate (n = 9-10). (C) Mouse pathology. Various tissues were collected and analyzed by the UCLA Pathology Core. Tissues were analyzed for inflammation (Inf), hematopoietic neoplasm (HN), and non-hematopoietic neoplasm (NHN). Data were presented as pathologist's scores of individual mouse tissues (n = 9-10). 0, no abnormal findings; 1, mild; 2, moderate; 3, severe.

(D-F) Analysis of the auto-activation of human conventional T cells in BLT-iNKT and control BLT mice at 6 months post-HSC transfer. (D) FACS plots showing the expression of CD45RA and CD45RO markers on human T cells isolated from the liver of experimental mice. Tc, human

conventional αβ T cells (gated as hCD45^{+}hTCRαβ^{+}6B11^{-} cells). (E-F) Quantification of D (n = 5). Note that compared to Tc cells isolated from the control BLT mice, Tc cells isolated from the BLT-iNKT mice displayed a less antigen-experienced phenotype (marked as hCD45RA^{lo}hCD45RO^{hi}), indicating their reduced graft-versus-host (GvH) responses in BLT-iNKT mice.

(G) Kaplan-Meier survival curves of BLT-iNKT mice and control BLT mice over a period of 8 months post-HSC transfer. N = 14-19. Mice were combined from 2 independent experiments.

Representative of 2 experiments. Data are presented as the mean ± SEM. ns, not significant, *P < 0.05, by Student's *t* test (A, E, F) or by log rank (Mantel-Cox) test adjusted for multiple comparisons (B, G).

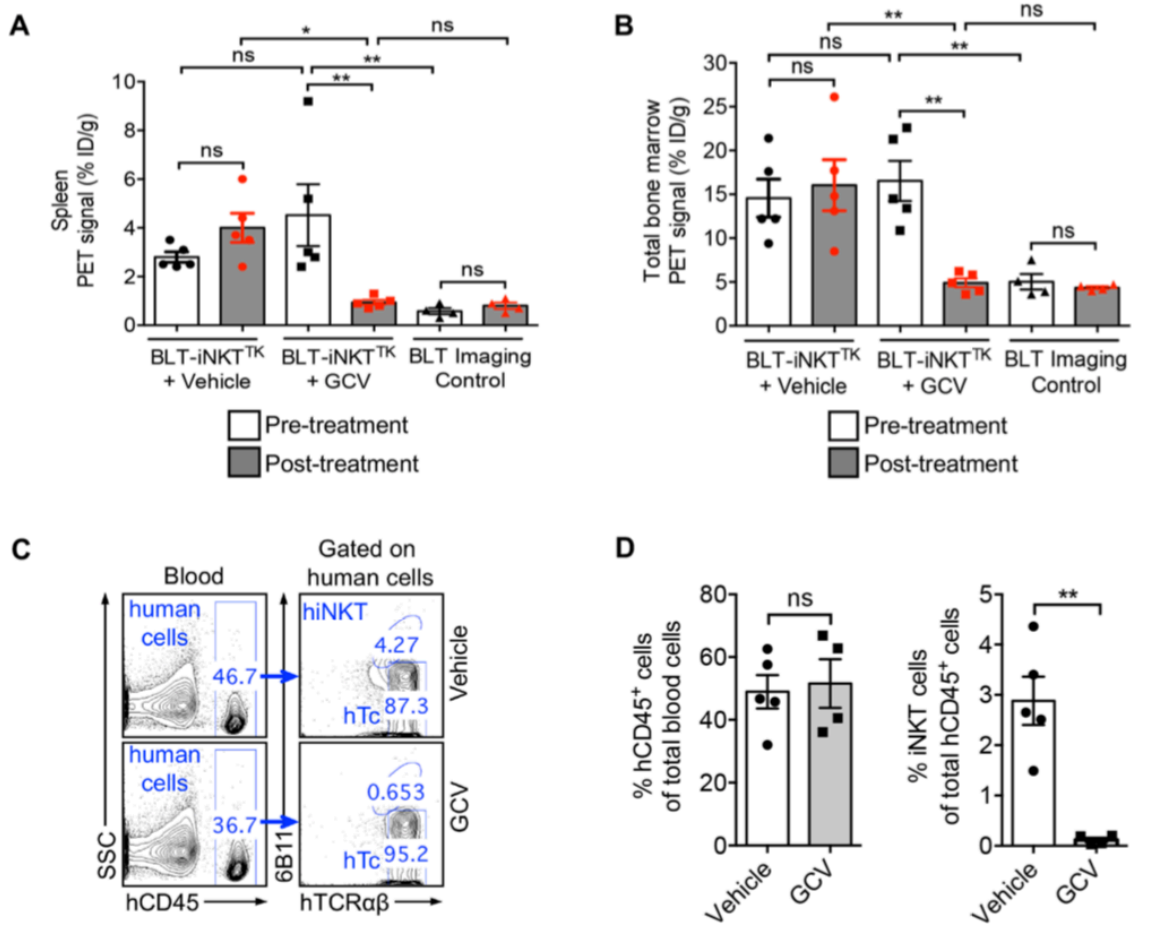

Figure S3. Controlled Depletion of HSC-iNKT Cells in BLT-iNKT Humanized Mice, Related to Figure 3.

Representative data were presented, studying BLT-iNKT^{TK} mice produced with human fetal thymus and Lenti/iNKT-sr39TK vector-transduced PBSCs. BLT mice generated in parallel using the same fetal thymus and PBSCs (mock-transduced) were included as a control.

(A) Statistical analysis of PET/CT signals in the spleen of BLT-iNKT^{TK} and control BLT mice pre- and post-GCV treatment (n= 4-5).

(B) Statistical analysis of PET/CT signals in the bone marrow of BLT-iNKT^{TK} and control BLT mice pre- and post-GCV treatment (n = 4-5).

(C-D) FACS validation of controlled depletion of HSC-engineered human iNKT (HSC-iNKT) cells in BLT-iNKT^{TK} mice via GCV treatment. (C) Representative FACS plots of blood cells. (D) Quantification of C (n= 4-5). Note the selective depletion of HSC-iNKT cells (gated as hCD45$^+$ hTCR$\alpha\beta^+$6B11$^+$ cells) but not the overall human immune cells (gated as total hCD45$^+$ cells) in BLT-iNKT^{TK} mice post-GCV treatment.

Representative of 2 experiments. Data are presented as the mean ± SEM. ns, not significant, *P < 0.05, **P < 0.01, by 1-way ANOVA (A, B) or by Student's *t* test (D).

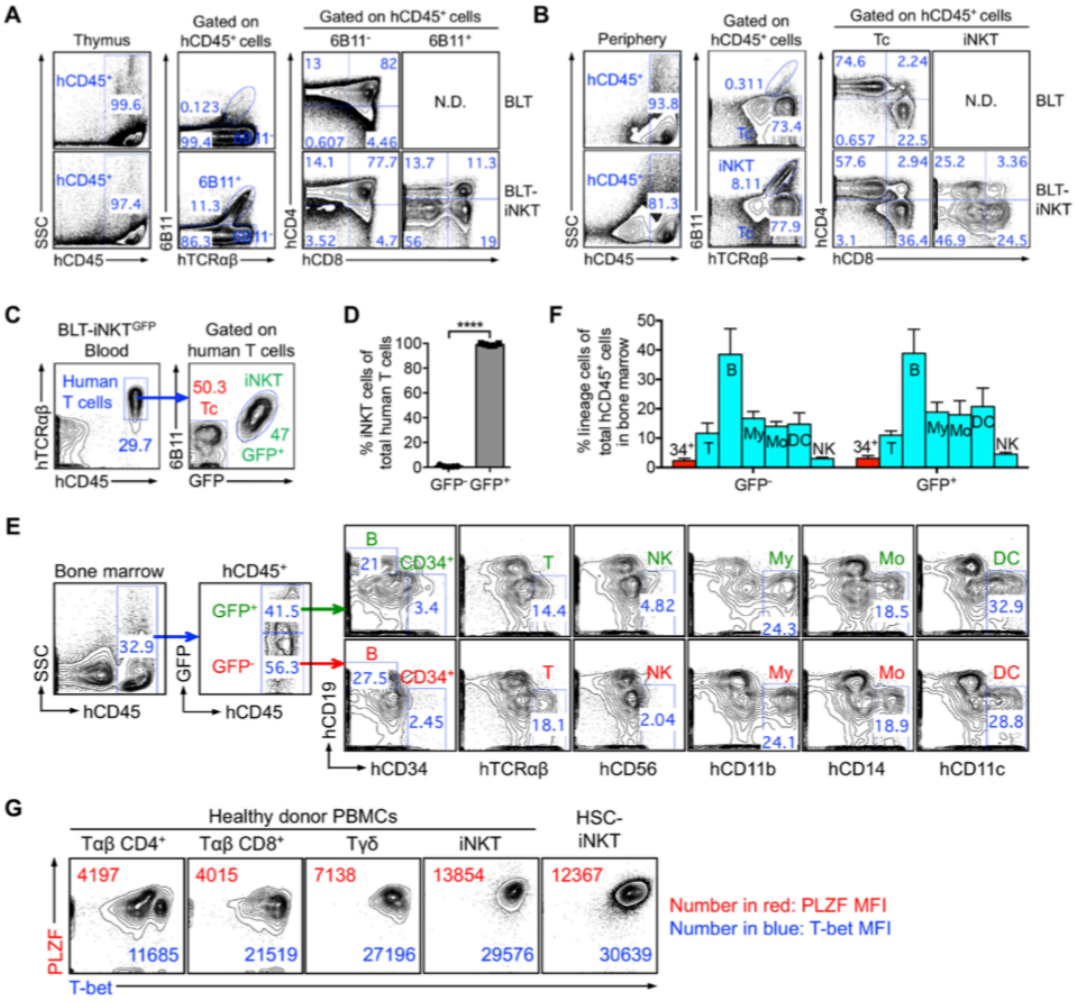

Figure S4. Development, Phenotype, and Functionality of HSC-iNKT Cells; Related to Figure 4.

Representative data were presented, studying HSC-iNKT cells generated from BLT-iNKT mice produced with Lenti/iNKT-sr39TK vector (A-B, G) or Lenti/iNKT-EGFP vector (C-F) transduced PBSCs.

(A) FACS plots showing the analysis of cells isolated from the human thymus implants of BLT-iNKT mice and control BLT mice. Note the detection of developing HSC-iNKT cells (gated as $hCD45^+hTCR\alpha\beta^+6B11^+$) in BLT-iNKT mice but not in control BLT mice. N.D., not detected.

(B) FACS plots showing the analysis of cells isolated from the periphery (blood) of BLT-iNKT mice and of control BLT mice. Note the detection of mature HSC-iNKT cells (gated as $hCD45^+hTCR\alpha\beta^+6B11^+$) in BLT-iNKT mice but not in control BLT mice. N.D., not detected.

(C-F) Lineage commitment of iNKT TCR gene-engineered human HSCs. BLT-iNKT mice generated with Lenti/iNKT-EGFP vector-transduced PBSCs were studied (denoted as BLT-iNKT^{GFP} mice). (C) FACS plots showing the analysis of human αβ T cells (pre-gated as hTCR45$^+$hTCRαβ$^+$ cells) present in the blood of BLT-iNKT^{GFP} mice, studying the correlation of GFP expression and iNKT cell (gated as 6B11$^+$) commitment. (D) Quantification of C (n = 5). (E) FACS plots showing the analysis of bone marrow cells of BLT-iNKT^{GFP} mice. (F) Quantification of E, showing the quantification of various lineages of human immune cells within the GFP$^-$ and GFP$^+$ subpopulations (pre-gated as hCD45$^+$GFP$^-$ and hCD45$^+$GFP$^+$, respectively) (n = 5). CD34$^+$ (34$^+$), CD34$^+$ hematopoietic stem and progenitor cells (gated as Lin$^-$hCD34$^+$); T, T cells (gated as hTCRαβ$^+$); B, B cells (gated as hCD19$^+$); My, myeloid cells (gated as hCD11b$^+$); Mo, monocytes/macrophages (gated as hCD14$^+$); DC, dendritic cells (gated as hCD11c$^+$); NK, natural killer cells (gated as hCD56$^+$).

(G) FACS plots showing the intracellular expression of master transcription factors PLZF and T-bet in HSC-iNKT cells. Various lineages of native human T cells isolated from healthy donor peripheral blood were studied as controls, including iNKT cells (identified as hTCRαβ$^+$6B11$^+$ cells), conventional CD4$^+$ αβ T cells (Tαβ CD4$^+$; identified as hTCRαβ$^+$6B11$^-$CD4$^+$CD8$^-$ cells), conventional CD8$^+$ αβ T cells (Tαβ CD4$^+$; identified as hTCRαβ$^+$6B11$^-$CD4$^-$CD8$^+$ cells), and gamma-delta T cells (Tγδ; identified as hTCRγδ$^+$ cells).

Representative of 2 experiments. Data were presented as the mean ± SEM. ****P < 0.0001, by Student's *t* test.

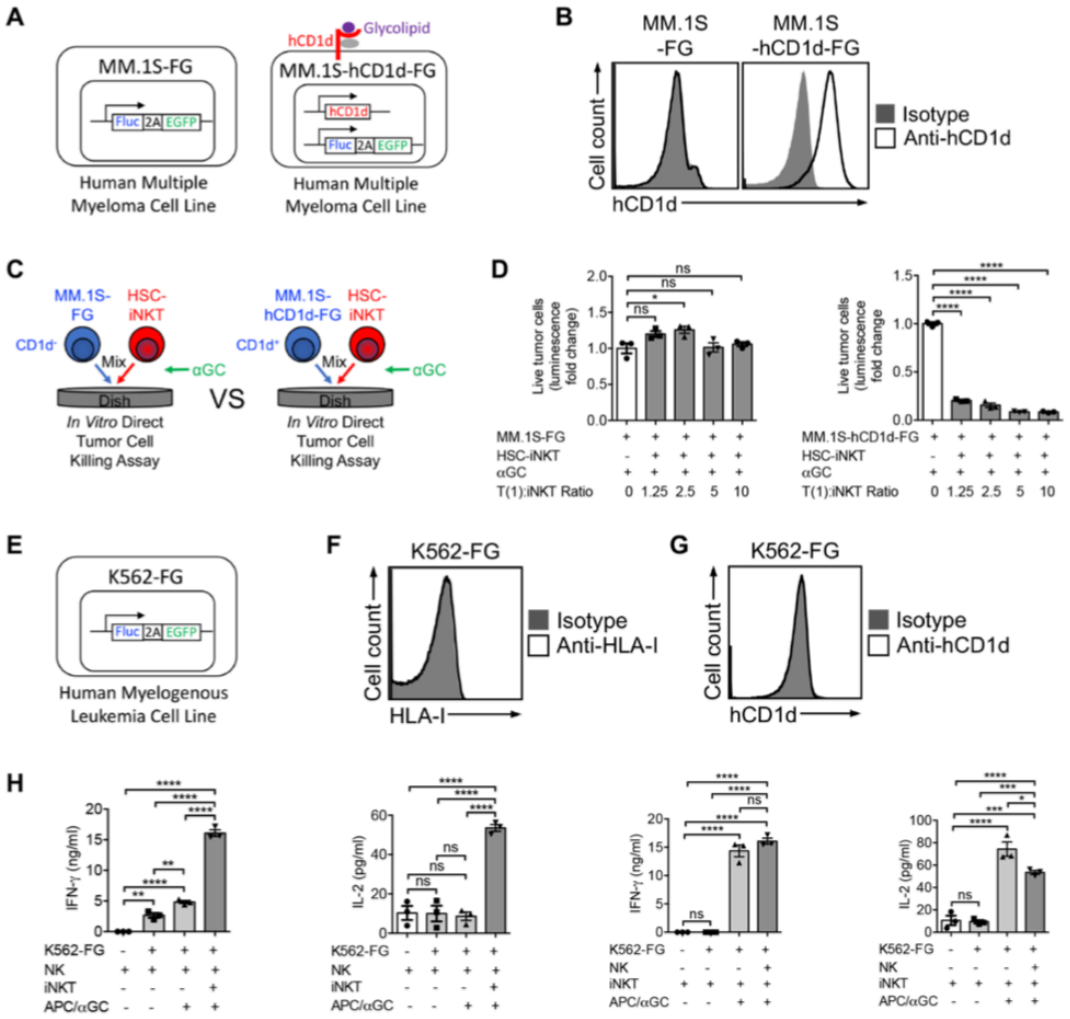

Figure S5. Tumor-Attacking Mechanisms of HSC-iNKT Cells: Direct Killing of CD1d$^+$ Tumor Cells and NK Adjuvant Effects, Related to Figure 5, B-I.

(A-D) Schematics showing the engineered MM.1S-FG and MM.1S-hCD1d-FG cell lines. MM.1S is a human multiple myeloma cell line. MM.1S-FG cell line was generated by stably transducing the parental MM.1S cell line with a Lenti/FG lentiviral vector encoding a firefly luciferase (Fluc) reporter gene and an enhanced green fluorescent protein (EGFP) reporter gene. MM.1S-hCD1d-FG cell line was generated by stably transducing the MM.1S-FG cell line with another Lenti/CD1d lentiviral vector encoding the human CD1d gene.

(B) FACS plots showing the detection of CD1d on MM.1S-hCD1d-FG cells, but not on MM.1S-FG cells.

(C-D) Studying the CD1d/αGC-mediated killing of tumor cells by HSC-iNKT cells. (C) Experimental design. (D) Tumor killing data from C (n = 3). Note the aggressive killing of tumor cells in a CD1d-dependant manner in the presence of αGC.

(E) Schematic of the K562-FG cell line. K562 is a human myelogenous leukemia cell line that is sensitive to NK cell-mediated tumor killing. The K562-FG cell line was generated by stably transducing the parental K562 cell line with a Lenti/FG lentiviral vector encoding Fluc and EGFP dual reporter genes.

(F) FACS plot showing the absence of MHC class I (HLA-I) expression on K562-FG cells.

(G) FACS plot showing the absence of CD1d expression on K562-FG cells.

(H) ELISA analysis of IFN-γ and IL-2 in the supernatants of various mixed cell cultures (tumor:NK:iNKT ratio 1:2:2), showing the massive production of these cytokines by HSC-iNKT cells post-APC/αGC stimulation (n = 3).

Representative of 2 experiments. Data were presented as the mean $\pm$ SEM. ns, not significant, *P < 0.05, **, P<0.01, ***P < 0.001, ****P < 0.0001, by 1-way ANOVA.

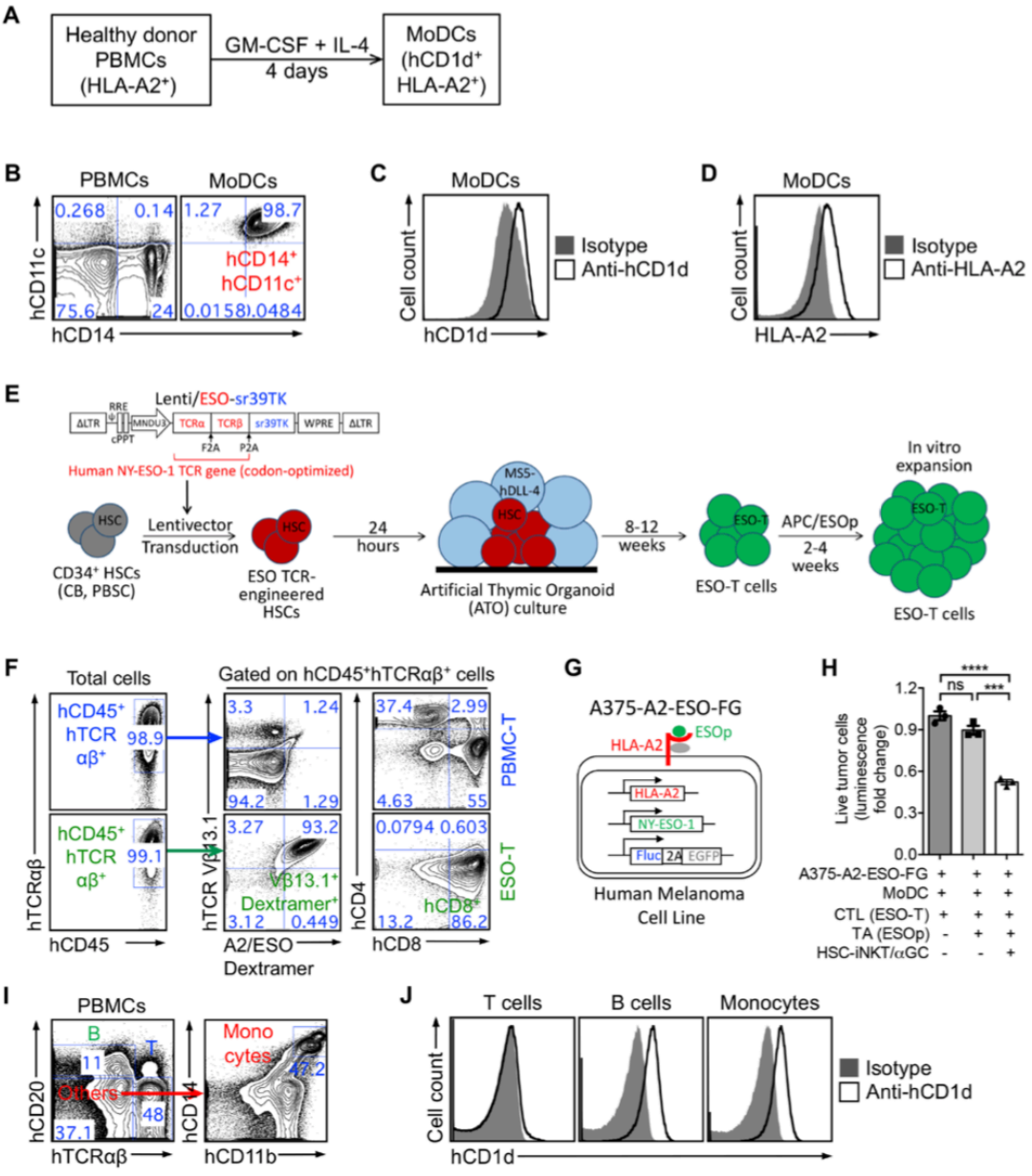

Figure S6. Tumor-Attacking Mechanisms of HSC-iNKT Cells: Adjuvant Effects of HSC-iNKT Cells on Boosting DC/CTL Antitumor Reactions and Inhibiting TAMs, Related to Figure 5, J-S.

(A) Diagram showing the experimental design to generate HLA-A2$^+$hCD1d$^+$ human MoDCs. PBMCs, peripheral blood mononuclear cells; MoDCs, monocyte-derived dendritic cells.

(B) FACS plots showing the lineage verification of MoDCs (identified as $hCD14^+hCD11c^+$). PBMCs were included as a staining control.

(C) FACS plot showing the detection of CD1d on MoDCs.

(D) FACS plot showing the detection of HLA-A2 on MoDCs.

(E) Diagram showing the experimental design to generate NY-ESO-1-specific human CD8 cytotoxic T lymphocytes (denoted as ESO-T cells). Human $CD34^+$ HSCs were transduced with a Lenti/ESO-sr39TK vector, then differentiated into ESO-T cells in an artificial thymic organoid (ATO) culture, following by *in vitro* expansion of ESO-T cells with APC/ESOp stimulation. Human $CD34^+$ HSCs were isolated from cord blood (CB) or G-CSF-mobilized peripheral blood (denoted as peripheral blood stem cells, PBSCs). Lenti/ESO-sr39TK, lentivector encoding a human NY-ESO-1 TCR gene as well as an sr39TK suicide/PET imaging reporter gene; MS5-hDLL4, MS5 murine bone marrow stromal cell line engineered to express human Delta Like Canonical Notch Ligand 4; APC/ESOp, antigen-presenting cell (irradiated $HLA\text{-}A2^+$ healthy donor PBMCs) loaded with NY-ESO-$1_{157\text{-}165}$ peptide (ESOp). The transgenic NY-ESO-1 TCR recognizes NY-ESO-1 peptide presented by HLA-A2.1, and comprises a $V\beta\ 13.1^+$ beta chain.

(F) FACS plots showing the phenotype of ESO-T cells (characterized as $hCD45^+hTCR\alpha\beta^+hTCR\ V\beta13.1^+$A2/ESO $Dextramer^+hCD4^-hCD8^+$). Human T cells expanded from healthy donor PBMCs through anti-CD3/CD28 Dynabeads stimulation were included as a staining control (denoted as PBMC-T cells). HLA-A2.1/NY-ESO-$1_{157\text{-}165}$ (A2/ESO) dextramer is a FACS staining reagent that detects HLA-A2.1-restricted and NY-ESO-1-specific human TCRs.

(G) Schematic showing the engineered A375-A2-ESO-FG cell line. A375 is a human melanoma cell line. A375-A2-ESO-FG cell line was generated by stably transducing the parental A375 cell line with lentivectors encoding an HLA-A2.1 gene, a NY-ESO-1 gene, and the Fluc and EGFP dual reporter genes.

(H) Tumor killing by ESO-T cells (n = 3). ESO-T cells were stimulated with MoDC/ESOp in the presence or absence of HSC-iNKT/αGC, followed by co-culture with A375-A2-ESO-FG tumor cells and analysis of tumor killing (tumor:DC:CTL:iNKT ratio 1:1:1:0.5).

(I) FACS plots showing the identification of T cells (gated as $hTCR\alpha\beta^+$ cells), B cells (gated as $hCD20^+$ cells), and monocytes (gated as $hCD14^+$ cells) from healthy donor peripheral blood mononuclear cells (PBMCs).

(J) FACS plots showing the measurement of CD1d expression on PBMC T cells, B cells, and monocytes gated from A. Note CD1d was highly expressed on antigen presenting cells (APCs) like B cells and monocytes, but not on T cells.

Representative of 2 experiments. Data were presented as the mean ± SEM. ns, not significant, ***P < 0.001, ****P < 0.0001, by 1-way ANOVA (H).

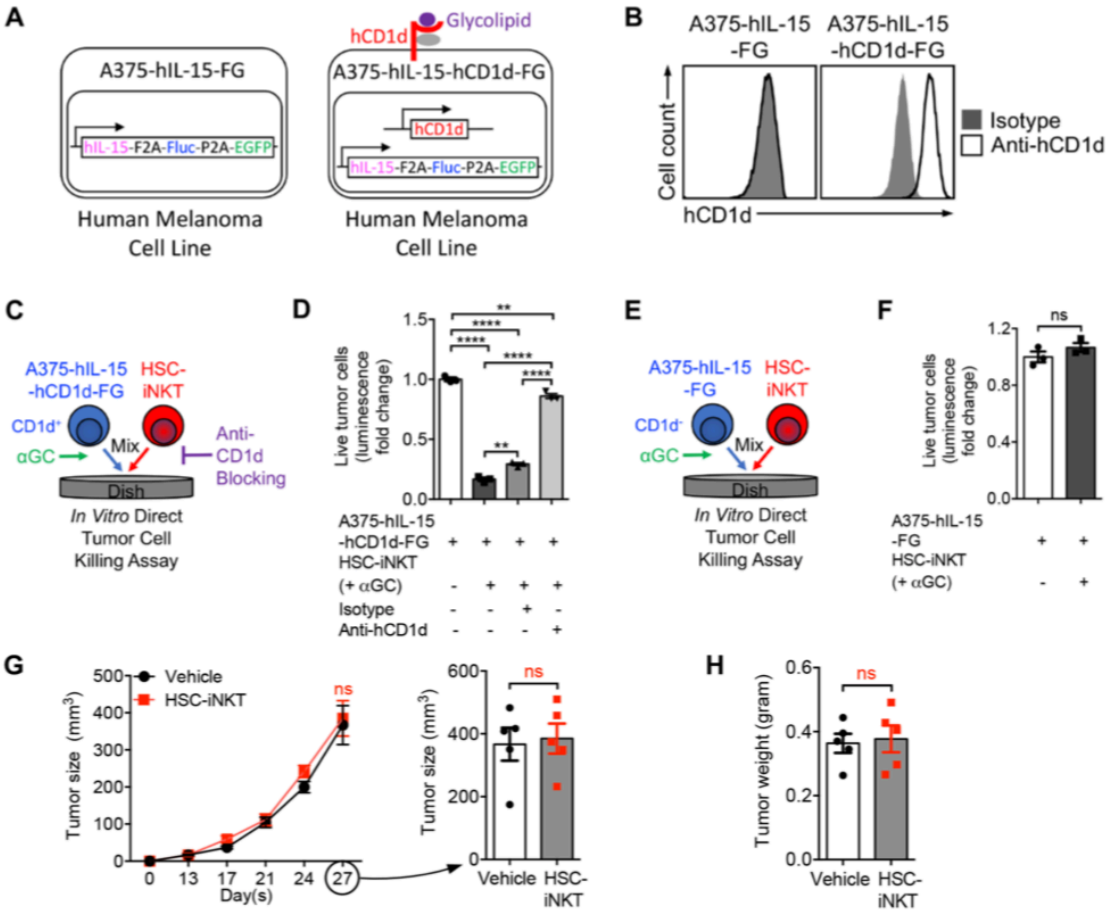

Figure S7. *In Vivo* Antitumor Efficacy of HSC-iNKT Cells Against Solid Tumors in a Human Melanoma Xenograft Mouse Model, Related to Figure 7.

(A) Schematics showing the engineered A375-hIL-15-FG and A375-hIL-15-hCD1d-FG cell lines. A375 is a human melanoma cell line. A375-hIL-15-FG cell line was engineered by stably transducing the parental A375 cell line with a Lenti/hIL-15-FG lentiviral vector encoding a human IL-15 gene, a Fluc reporter gene, and an EGFP reporter gene. A375-hIL-15-hCD1d-FG cell line was generated by stably transducing the A375-hIL-15-FG cell line with a Lenti/CD1d lentiviral vector encoding the human CD1d gene.

(B) FACS plots showing the detection of CD1d on A375-hIL-15-hCD1d-FG cells, but not on A375-hIL-15-FG cells.

(C-D) Studying the *in vitro* direct killing of A375-hIL-15-hCD1d-FG cells by HSC-iNKT cells in the presence of αGC (tumor:iNKT ratio 1:2). (C) Experimental design. (D) Tumor killing (n = 3). Note that tumor killing was dependent on CD1d.

(E-F) Studying the *in vitro* direct killing of A375-hIL-15-FG cells by HSC-iNKT cells in the presence of αGC (tumor:iNKT ratio 1:2). (E) Experimental design. (F) Tumor killing (n = 3). Note the lack of tumor killing in the absence of CD1d.

(G-H) Studying the *in vivo* antitumor efficacy of HSC-iNKT cells in the control A375-hIL-15-FG human melanoma xenograft NSG mouse model (related to main Figures 7J-7L). (G) Measurements of tumor size over time (n = 5). (H) Measurements of tumor weight at the terminal harvest on day 28 (n = 5).

Representative of 2 experiments. Data were presented as the mean ± SEM. ns, not significant, **P < 0.01, ****P < 0.0001, by 1-way ANOVA (D) or by Student's *t* test (F, G, H).

CHAPTER 2:

Development of allogeneic HSC-engineered iNKT cells
for off-the-shelf cancer immunotherapy

Cell Reports
Medicine

Article

Development of allogeneic HSC-engineered iNKT cells for off-the-shelf cancer immunotherapy

Graphical abstract

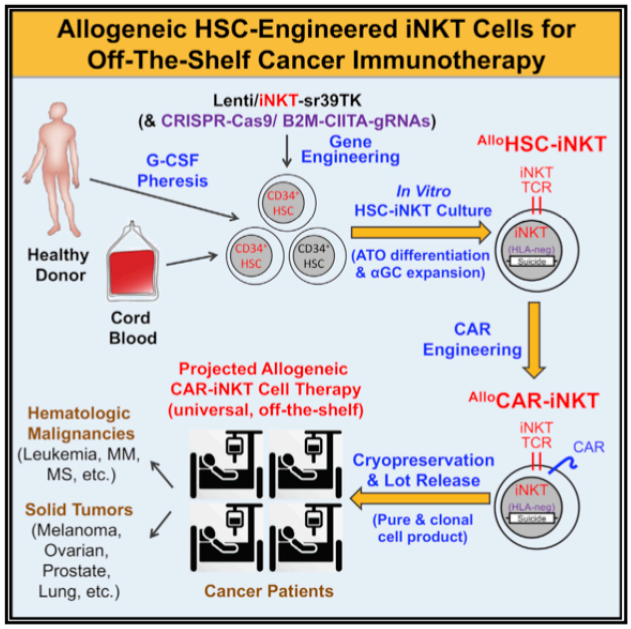

Highlights

- Allogeneic HSC-iNKT cells are generated *in vitro* at high yield and purity
- Allogeneic HSC-iNKT cells effectively target tumor cells using multiple mechanisms
- Allogeneic HSC-iNKT cells exhibit high safety and low immunogenicity
- A preclinical study demonstrated feasibility, safety, and cancer therapy potential

Authors

Yan-Ruide Li, Yang Zhou, Yu Jeong Kim, ..., Owen Witte, Pin Wang, Lili Yang

Correspondence

liliyang@ucla.edu

In brief

Li et al. report the preclinical development of allogeneic-hematopoietic-stem-cell-engineered invariant natural killer T (HSC-iNKT) cells for off-the-shelf cancer therapy. Allogeneic HSC-iNKT cells demonstrate cancer therapy potential and a high safety profile.

Article

Development of allogeneic HSC-engineered iNKT cells for off-the-shelf cancer immunotherapy

Yan-Ruide Li,[1,14] Yang Zhou,[1,14] Yu Jeong Kim,[1] Yanni Zhu,[1] Feiyang Ma,[2] Jiaji Yu,[1] Yu-Chen Wang,[1] Xianhui Chen,[3] Zhe Li,[1] Samuel Zeng,[1] Xi Wang,[1] Derek Lee,[1] Josh Ku,[1] Tasha Tsao,[1] Christian Hardoy,[1] Jie Huang,[1] Donghui Cheng,[4] Amélie Montel-Hagen,[6] Christopher S. Seet,[4,5,7] Gay M. Crooks,[4,6,7,8] Sarah M. Larson,[9] Joshua P. Sasine,[4,7,10] Xiaoyan Wang,[5] Matteo Pellegrini,[2,4] Antoni Ribas,[4,7,11,12] Donald B. Kohn,[1,4,10] Owen Witte,[1,4,7,12,13] Pin Wang,[3] and Lili Yang[1,4,7,13,15,*]

[1]Department of Microbiology, Immunology & Molecular Genetics, University of California, Los Angeles, Los Angeles, CA 90095, USA
[2]Department of Molecular, Cell and Developmental Biology, College of Letters and Sciences, University of California, Los Angeles, Los Angeles, CA 90095, USA
[3]Department of Pharmacology and Pharmaceutical Sciences, University of Southern California, Los Angeles, CA 90089, USA
[4]Eli and Edythe Broad Center of Regenerative Medicine and Stem Cell Research, University of California, Los Angeles, Los Angeles, CA 90095, USA
[5]Department of Medicine, University of California, Los Angeles, Los Angeles, CA 90095, USA
[6]Department of Pathology and Laboratory Medicine, University of California, Los Angeles, Los Angeles, CA 90095, USA
[7]Jonsson Comprehensive Cancer Center, David Geffen School of Medicine, University of California, Los Angeles, Los Angeles, CA 90095, USA
[8]Department of Pediatrics, University of California, Los Angeles, Los Angeles, CA 90095, USA
[9]Department of Internal Medicine, University of California, Los Angeles, Los Angeles, CA 90095, USA
[10]Division of Hematology/Oncology, Department of Pediatrics, David Geffen School of Medicine, University of California, Los Angeles, Los Angeles, CA 90095, USA
[11]Department of Molecular and Medical Pharmacology, University of California, Los Angeles, Los Angeles, CA 90095, USA
[12]Parker Institute for Cancer Immunotherapy, University of California, Los Angeles, Los Angeles, CA 90095, USA
[13]Molecular Biology Institute, University of California, Los Angeles, Los Angeles, CA 90095, USA
[14]These authors contributed equally
[15]Lead contact
*Correspondence: liliyang@ucla.edu
https://doi.org/10.1016/j.xcrm.2021.100449

SUMMARY

Cell-based immunotherapy has become the new-generation cancer medicine, and "off-the-shelf" cell products that can be manufactured at large scale and distributed readily to treat patients are necessary. Invariant natural killer T (iNKT) cells are ideal cell carriers for developing allogeneic cell therapy because they are powerful immune cells targeting cancers without graft-versus-host disease (GvHD) risk. However, healthy donor blood contains extremely low numbers of endogenous iNKT cells. Here, by combining hematopoietic stem cell (HSC) gene engineering and *in vitro* differentiation, we generate human allogeneic HSC-engineered iNKT (^{Allo}HSC-iNKT) cells at high yield and purity; these cells closely resemble endogenous iNKT cells, effectively target tumor cells using multiple mechanisms, and exhibit high safety and low immunogenicity. These cells can be further engineered with chimeric antigen receptor (CAR) to enhance tumor targeting or/and gene edited to ablate surface human leukocyte antigen (HLA) molecules and further reduce immunogenicity. Collectively, these preclinical studies demonstrate the feasibility and cancer therapy potential of ^{Allo}HSC-iNKT cell products and lay a foundation for their translational and clinical development.

INTRODUCTION

Over the past decade, immunotherapy has become the new-generation cancer medicine.[1–3] In particular, T-cell-based cancer therapy has shown great promise.[4] An outstanding example is the chimeric antigen receptor (CAR)-engineered T (CAR-T) cell adoptive therapy, which targets certain blood cancers at impressive efficacy and has been approved by the US Food and Drug Administration (FDA) to treat CD19$^+$ B cell malignancies.[4–6] Adoptive transfer of *in vitro* expanded tumor-infiltrating T lymphocytes (TILs) and T cell receptor (TCR)-engineered T cells also show promise in treating some blood cancers and solid tumors in the clinic.[7,8] However, most of the current T cell therapies fall in the category of autologous cell therapy, wherein T cells collected from a patient are manufactured and used to treat that single patient. Such an approach is time consuming, logistically challenging, and costly; furthermore, for patients with heavily lymphopenic pretreatment or rapidly proliferative disease,

it might not always be possible to produce autologous cell products.[5,9] Allogenic cell products that can be manufactured at large scale and distributed readily to treat a broad range of cancer patients therefore are in great demand.

Conventional αβ T cells have been utilized for generating allogeneic cell products; however, these T cells risk inducing graft-versus-host disease (GvHD) in allogeneic hosts due to histocompatibility leukocyte antigen (HLA) incompatibility, thereby requiring additional gene editing to ablate their endogenous TCR expression that may potentially increase manufacture complexity.[10–13] Innate immune cells such as natural killer (NK) cells that have no GvHD risk have been investigated; however, NK cells may have limited *in vivo* clonal expansion and antitumor performance compared to T cells.[14,15]

Invariant NK T (iNKT) cells are a small population of αβ T lymphocytes.[16] iNKT cells have several unique features, making them ideal for developing off-the-shelf cellular therapy for cancer. Compared to conventional T cells, iNKT cells can attack tumor cells using multiple mechanisms and at higher efficacy; can more effectively traffic to and infiltrate solid tumors; can alter solid tumor immunosuppressive microenvironment; and, most importantly, do not induce GvHD.[17–25] However, human blood contains extremely low numbers of iNKT cells (0.001%–1%), making it very difficult to reliably grow large numbers of allogeneic iNKT cells for cell therapies.[26] Moreover, allogeneic iNKT products expanded from blood may contain bystander allogeneic conventional αβ T cells and thus risk inducing GvHD. Technology breakthroughs are needed to exploit the allogeneic cell therapy potential of iNKT cells.

Previously, we have established a method to generate large numbers of iNKT cells through TCR gene engineering of hematopoietic stem cells (HSCs) followed by *in vivo* reconstitution; using this method, we have successfully generated both mouse and human HSC-engineered iNKT (HSC-iNKT) cells.[27,28] However, such an *in vivo* approach cannot be used to produce off-the-shelf mature allogeneic iNKT cells.[27,28] Here, we intended to build on the HSC-iNKT engineering approach and develop an *in vitro* culture method to produce large numbers of off-the-shelf human iNKT cells for allogeneic cell therapy applications. We report the preclinical development of the proposed allogeneic HSC-iNKT cell therapy, demonstrating its manufacture feasibility, cancer therapy potential, and high safety profile.

RESULTS

Generation of allogeneic HSC-engineered iNKT (^{Allo}HSC-iNKT) cells

Human $CD34^+$ cells collected from either cord blood (CB) or granulocyte-colony-stimulating factor (G-CSF)-mobilized human peripheral blood stem cells (PBSCs) were transduced with a Lenti/iNKT-sr39TK vector and then cultured *in vitro* in a two-stage artificial thymic organoid (ATO)/α-galactosylceramide (αGC) culture system (Figure 1A). Note $CD34^+$ cells comprise both hematopoietic stem and progenitor cells; in this report we refer to $CD34^+$ cells as HSCs. The Lenti/iNKT-sr39TK vector has been previously used to develop an autologous HSC-engineered iNKT cell therapy for cancer[28]; ATO is an *in vitro* 3D culture that supports the human HSC differentiation into T cells,[29,30] while αGC is a synthetic agonist glycolipid ligand that specifically stimulates iNKT cells.[16] We routinely achieved over 50% lentivector transduction rate of HSCs (Figure 1B). Transduced HSCs were then placed in the stage 1 ATO culture, where they differentiated into human iNKT cells over a course of 8 weeks with over 100-fold expansion (Figures 1A and 1C). At the end of stage 1 culture, ATOs were dissociated into single cells that were then placed in the stage 2 αGC expansion culture for another 2–3 weeks, resulting in another 100- to 1,000-fold expansion and an ^{Allo}HSC-iNKT cell product of high yield and purity (Figures 1A and 1D).

In the ATO/αGC culture, ^{Allo}HSC-iNKT cells followed a typical iNKT cell development path defined by CD4/CD8 co-receptor expression.[31] During stage 1, ^{Allo}HSC-iNKT cells transited from $CD4^-CD8^-$ (DN) to $CD4^+CD8^+$ (DP), then toward $CD4^-CD8^{+/-}$ (Figure 1E). At the end of stage 2, the majority (>99%) of ^{Allo}HSC-iNKT cells showed a $CD4^-CD8^{+/-}$ (CD8 SP/DN) phenotype (Figure 1E). Note that the end ^{Allo}HSC-iNKT cell product did not contain a $CD4^+CD8^-$ (CD4 SP) population that are present in the endogenous human iNKT cells (Figure 1E).[31] In general, CD8 SP/DN human iNKT cells are considered to be proinflammatory and highly cytotoxic and thereby are desirable for cancer immunotherapy.[24,31–35]

Flow cytometry analysis showed that the ^{Allo}HSC-iNKT cell product comprised high-purity transgenic iNKT cells (Figure 1D); single-cell TCR sequencing analysis confirmed that these ^{Allo}HSC-iNKT cells uniformly expressed the transgenic iNKT TCRs while nearly undetectable randomly recombined endogenous αβ TCRs (Figure 1F). In sharp contrast to ^{Allo}HSC-iNKT cells, conventional αβ T cells isolated from health donor periphery blood (denoted as PBMC-Tc cells) expressed highly diverse endogenously recombined αβ TCRs, whereas iNKT cells isolated from health donor periphery blood (denoted as PBMC-iNKT cells) expressed a conserved invariant TCR α chain (Vα24-Jα18) and limited diverse TCR β chains (dominantly Vβ11) (Figure 1F).

The manufacture of ^{Allo}HSC-iNKT cells was highly robust; we generated ^{Allo}HSC-iNKT cell products of high purity and yield from all 12 donors tested (4 CB-HSCs and 8 PBSCs) (Figures 1G and 1H). Based on our results, it was estimated that from one CB donor (comprising ~5×10^6 CB-HSCs), ~5×10^{11} ^{Allo}HSC-iNKT cells could be generated that can potentially be formulated into ~500–5,000 doses (~10^8-10^9 cells per dose based on the approved CAR-T cell therapy doses)[4]; from one PBSC donor (comprising ~5×10^8 PBSCs), ~3×10^{13} ^{Allo}HSC-iNKT cells could be generated that can potentially be formulated into ~30,000–300,000 doses (Figure 1G). The resulting ^{Allo}HSC-iNKT cell product contained pure transgenic iNKT cells and nearly undetectable bystander conventional αβ T cells, thereby lack of GvHD risk and suitable for "off-the-shelf" application.

Phenotype and functionality of ^{Allo}HSC-iNKT cells

Next, we analyzed the phenotype and functionality of ^{Allo}HSC-iNKT cells in comparison with endogenous human PBMC-iNKT and PBMC-Tc cells. ^{Allo}HSC-iNKT cells displayed a phenotype closely resembling PBMC-iNKT cells but distinct from PBMC-Tc cells; they expressed high levels of memory T cell markers

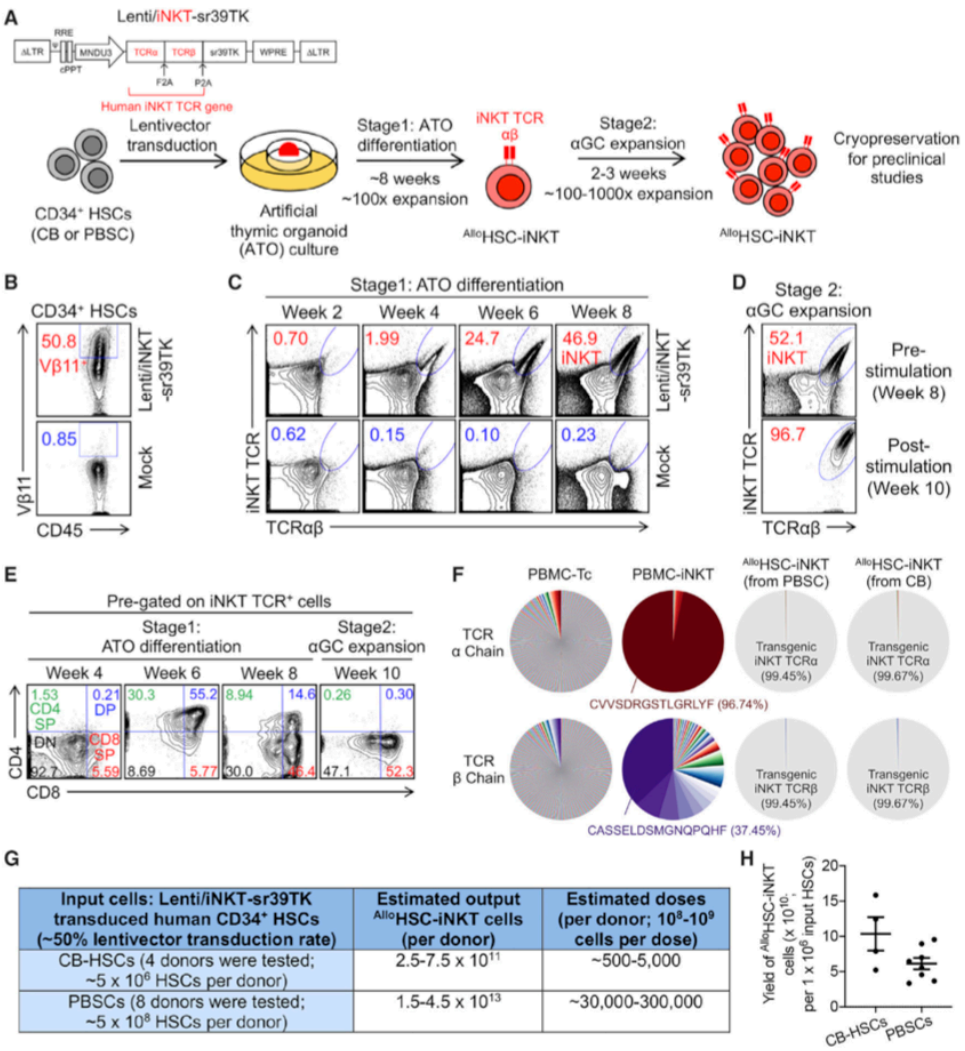

Input cells: Lenti/iNKT-sr39TK transduced human CD34⁺ HSCs (~50% lentivector transduction rate)	Estimated output AlloHSC-iNKT cells (per donor)	Estimated doses (per donor; 10^8-10^9 cells per dose)
CB-HSCs (4 donors were tested; ~5 x 10^6 HSCs per donor)	2.5-7.5 x 10^{11}	~500-5,000
PBSCs (8 donors were tested; ~5 x 10^8 HSCs per donor)	1.5-4.5 x 10^{13}	~30,000-300,000

Figure 1. *In vitro* generation of allogenic HSC-engineered iNKT (AlloHSC-iNKT) cells

(A) Experimental design to generate AlloHSC-iNKT cells *in vitro*. HSC, hematopoietic stem cell; CB, cord blood; PBSC, peripheral blood stem cell; αGC, α-galactosylceramide; Lenti/iNKT-sr39TK, lentiviral vector encoding an iNKT TCR gene and an sr39TK suicide/positron emission tomography (PET) imaging gene.

(B–E) Fluorescence-activated cell sorting (FACS) monitoring of AlloHSC-iNKT cell generation. (B) Intracellular expression of iNKT TCR (identified as Vβ11⁺) in CD34⁺ HSCs at 72 h after lentivector transduction. (C) Generation of iNKT cells (identified as iNKT TCR⁺TCRαβ⁺ cells) during stage 1 ATO differentiation culture. A 6B11 monoclonal antibody was used to stain iNKT TCR. (D) Expansion of iNKT cells during stage 2 αGC expansion culture. (E) Expression of CD4/CD8 co-receptors on AlloHSC-iNKT cells during stage 1 and stage 2 cultures. DN, CD4/CD8 double negative; CD4 SP, CD4 single positive; DP, CD4/CD8 double positive; CD8 SP, CD8 single positive.

(F) Single-cell TCR sequencing analysis of AlloHSC-iNKT cells. Healthy donor peripheral blood mononuclear cell (PBMC)-derived conventional αβ T (PBMC-Tc) and iNKT (PBMC-iNKT) cells were included as controls. The relative abundance of each unique T cell receptor (TCR) sequence among the total unique sequences identified for individual cells is represented by a pie slice.

(G) Table summarizing experiments that have successfully generated AlloHSC-iNKT cells.

(H) Yields of AlloHSC-iNKT cells generated from multiple HSC donors.

Representative of 1 (F) and >10 experiments (A–E).

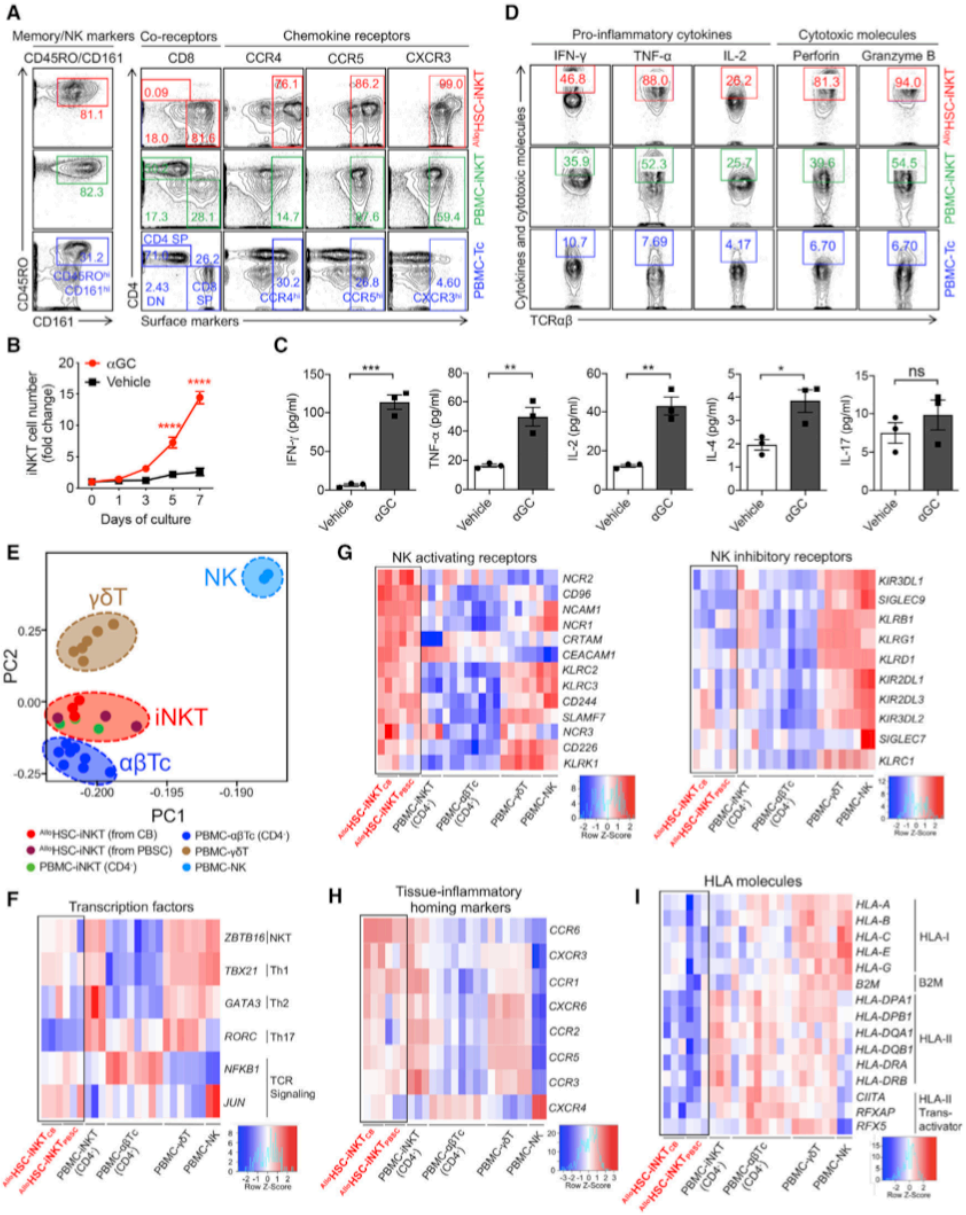

Figure 2. Characterization and gene profiling of ^{Allo}HSC-iNKT cells

(A) FACS detection of surface markers on ^{Allo}HSC-iNKT cells. PBMC-iNKT and PBMC-Tc cells were included as controls.
(B and C) Antigen responses of ^{Allo}HSC-iNKT cells. ^{Allo}HSC-iNKT cells were cultured for 7 days, in the presence or absence of αGC (denoted as αGC or Vehicle, respectively). (B) Cell growth curve (n = 3). (C) ELISA analyses of cytokine (IFN-γ, TNF-α, IL-2, IL-4 and IL-17) production at day 7 post αGC stimulation (n = 3).
(D) FACS detection of intracellular cytokines and cytotoxic molecules in ^{Allo}HSC-iNKT cells. PBMC-iNKT and PBMC-Tc cells were included as controls.
(E–I) Deep RNA-seq analysis of ^{Allo}HSC-iNKT cells generated from CB- or PBSC-derived CD34$^+$ HSCs (n = 3 for each). Healthy donor PBMC-derived conventional CD4$^-$ αβ T (PBMC-αβTc; n = 8), CD4$^-$ iNKT (PBMC-iNKT; n = 3), γδ T (PBMC- γδT; n = 6), and NK (PBMC-NK; n = 2) cells were included as controls. N indicates

(legend continued on next page)

(i.e., CD45RO), NK cell markers (i.e., CD161), and peripheral tissue and inflammatory site homing markers (i.e., CCR4, CCR5 and CXCR3) (Figure 2A). When stimulated with αGC, ^{Allo}HSC-iNKT cells proliferated vigorously (Figure 2B) and secreted high levels of Th0/Th1 cytokines (i.e., interferon-γ [IFN-γ], tumor necrosis factor α [TNF-α], and interleukin-2 [IL-2]) but limited amounts of Th2 cytokines (i.e., IL-4) and Th17 cytokines (i.e., IL-17) (Figure 2C), indicating a Th0/Th1-prone functionality of ^{Allo}HSC-iNKT cells that agrees with their CD8 SP/DN phenotype (Figures 1E and 2A).[24,31–33] Intracellular staining showed that at the single-cell level, ^{Allo}HSC-iNKT cells produced exceedingly high levels of effector cytokines (i.e., IFN-γ, TNF-α, and IL-2) and cytotoxic molecules (i.e., perforin and granzyme B) (Figure 2D). The ability to generate excess amounts of antitumor effector molecules is a promising signature of iNKT cells for cancer immunotherapy.[26,36]

Transcriptome profiling of ^{Allo}HSC-iNKT cells

To fully characterize ^{Allo}HSC-iNKT cells, we performed deep RNA sequencing (RNA-seq) analysis of these cells; ^{Allo}HSC-iNKT cells generated from both CB and PBSC CD34$^+$ HSCs were studied. Healthy donor PBMC-derived endogenous iNKT (PBMC-iNKT), conventional αβ T (PBMC-αβTc), γδ T (PBMC-γδT), and NK (PBMC-NK) cells were included as controls. All cell types were prepared from multiple donors. Because ^{Allo}HSC-iNKT cells were dominantly CD4$^-$ (CD8 SP/DN), the CD4$^-$ subpopulations of PBMC-iNKT (CD8 SP/DN) and PBMC-αβTc (CD8$^+$) cells were analyzed in this experiment.

Principal-component analysis (PCA) of the global gene expression profiles showed that ^{Allo}HSC-iNKT cells (both CB and PBSC-derived) were located the closest to PBMC-iNKT cells, next to PBMC-αβTc and PBMC-γδT cells, and the furthest from PBMC-NK cells, validating the iNKT cell nature of ^{Allo}HSC-iNKT cells (Figure 2E).[37]

"Master" transcription factor gene profiling analysis revealed a distinctive signature of ^{Allo}HSC-iNKT cells; they expressed high levels of *ZBTB16* that encodes PLZF, a signature transcription factor of innate T (e.g., iNKT and γδT) cells and NK cells[38]; they expressed high levels of *TBX21* that encodes T-bet, an essential transcription factor regulating Th1 polarization of T cells[39]; they expressed low levels of *GATA3* and *RORC* that respectively encode GATA3 and RORγ, critical transcription factors regulating Th2 and Th17 polarization of T cells[40]; and they expressed high levels of *NFKB1* and *JUN* that respectively encode NF-κB1 and c-Jun, important transcription factors for TCR signaling (Figure 2F).[41,42] These transcription factors have been indicated to play important roles in regulating iNKT cell development and functionality.[43–45] Of note, the *TBX21*^{high}*GATA3*^{low}*RORC*^{low} expression profile of ^{Allo}HSC-iNKT cells consists with their Th0/Th1-prone cytokine production profile (Figure 2C).

Further analysis of the various genes related to antitumor effector functions (e.g., genes encoding activation/homing markers, cytokines, and cytotoxic molecules) revealed ^{Allo}HSC-iNKT cells to be highly potent effector cells, in agreement with their *in vitro* phenotype and functionality characterization (Figures 2A–2D). In addition, several interesting gene signatures stood out, which are highlighted below.

Typical iNKT cells exert NK function besides T cell function, via surface expression of NK receptors.[16,18,46] Interestingly, compared to PBMC-iNKT and even PBMC-NK cells, ^{Allo}HSC-iNKT cells expressed exceedingly high levels of NK activating receptor genes (e.g., *NCAM1*, *NCR1*, *NCR2*, *KLR2*, and *KLR3*) but low levels of NK inhibitory receptor genes (e.g., *KIR3DL1*, *KIR3DL2*, *KIR2DL1*, and *KIR2DL2*), suggesting that ^{Allo}HSC-iNKT cells might exhibit a superior antitumor NK function (Figure 2G).

Tissue inflammatory homing markers expressed on effector immune cells enable them to access inflammatory tissues including tumor sites.[32,47] ^{Allo}HSC-iNKT cells expressed exceedingly high levels of multiple tissue inflammatory homing marker genes (e.g., *CCR1*, *CCR2*, *CCR3*, *CCR5*, *CCR6*, and *CXCR3*), comparable to those of endogenous innate T cells (i.e., PBMC-iNKT and PBMC-γδT cells) but significantly higher than those of endogenous conventional αβ T and NK cells (i.e., PBMC-αβTc and PBMC-NK cells), suggesting a strong capacity of ^{Allo}HSC-iNKT cells to home to and penetrate tumor sites (Figure 2H).

HLA incompatibility may trigger host T-cell-mediated allorejection of adoptively transferred allogeneic cellular products, thereby limiting their therapeutic efficacy.[48,49] Interestingly, compared to all of the endogenous T cells (i.e., PBMC-iNKT, PBMC-αβTc, and PBMC-γδT cells) and NK cells (i.e., PBMC-NK cells) tested, ^{Allo}HSC-iNKT cells expressed much lower levels of HLA-expression-related genes (e.g., genes encoding HLA-I molecules, B2M, HLA-II molecules, and HLA-II transactivators), suggesting that ^{Allo}HSC-iNKT cells might naturally resist allorejection and thereby have certain advantages over many PBMC-derived allogeneic cell products for off-the-shelf cell therapy (Figure 2I).

Tumor targeting of ^{Allo}HSC-iNKT cells through intrinsic NK function

Following the NK lead of our RNA-seq study (Figure 2G), we investigated the NK phenotype and antitumor function of ^{Allo}HSC-iNKT cells in comparison with those of endogenous PBMC-NK cells. Flow cytometry analysis of cell surface markers showed that ^{Allo}HSC-iNKT cells expressed significantly higher levels of NK activating receptors (i.e., NKG2D and DNAM-1) while nearly undetectable NK inhibitory receptors (i.e., killer cell immunoglobulin-like receptors, KIRs) (Figures 3A and 3B). NK activating receptors recognize stress molecules (e.g., MIC-A/B and UL16-binding protein 1-4, ULBP1-4, recognized by NKG2D and CD112 and CD155 recognized by DNAM-1) upregulated on many tumor cells and trigger tumor targeting,[50–52] while NK inhibitory receptors recognize matched "self" major histocompatibility complex (MHC) molecules and suppress tumor

different donors. (E) Principal-component analysis (PCA) plot showing the ordination of all six cell types. (F–I) Heatmaps showing the expression of selected genes encoding transcription factors (F), NK activating and inhibitory receptors (G), tissue inflammatory homing markers (H), and HLA molecules (I) for all six cell types. Representative of 1 (E–I) and 3 (A–D) experiments. Data are presented as the mean ± SEM ns, not significant, *$p < 0.05$, **$p < 0.01$, ***$p < 0.001$, ****$p < 0.0001$, by Student's t test.

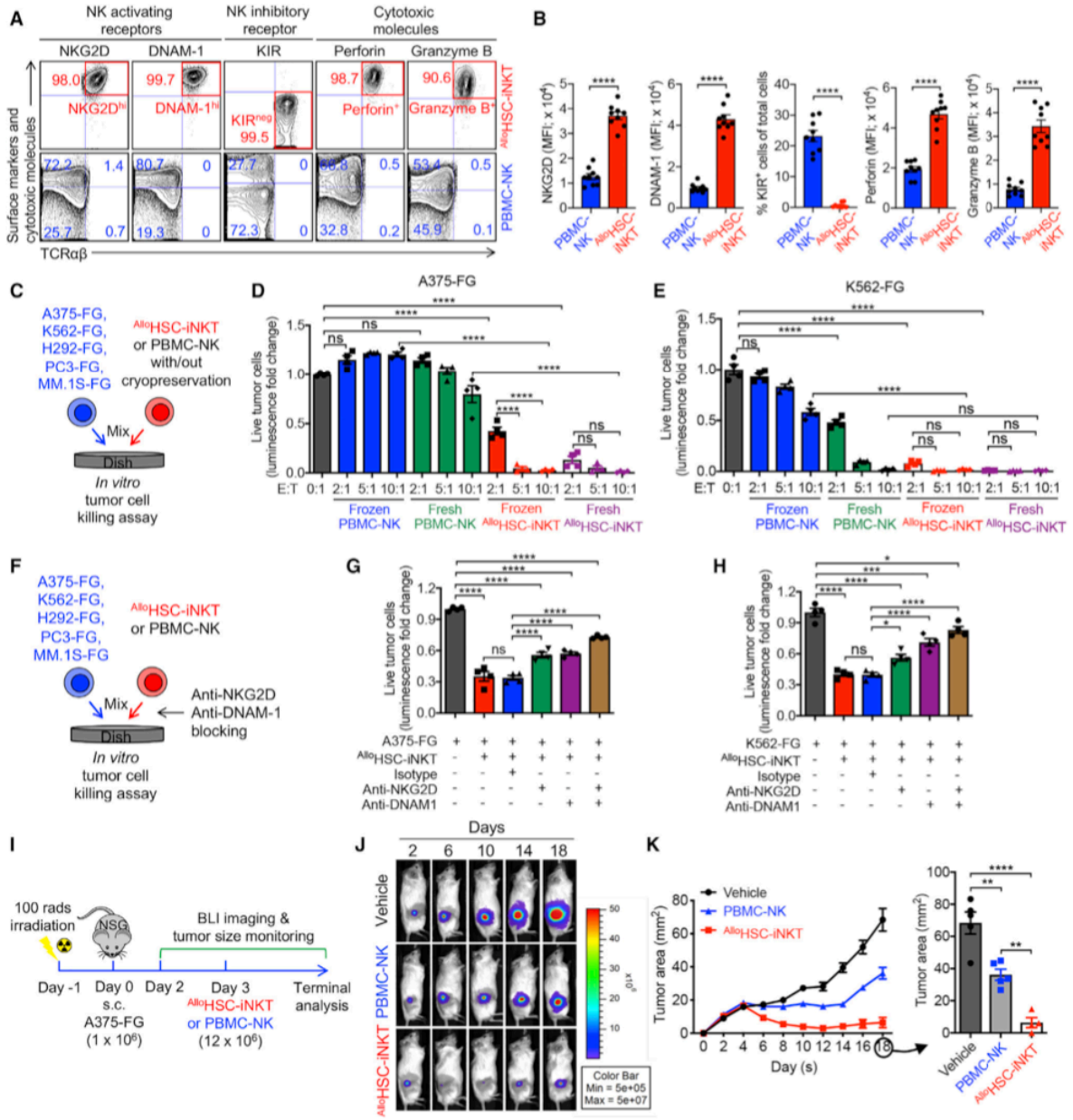

Figure 3. Tumor targeting of AlloHSC-iNKT cells through intrinsic NK function

(A and B) FACS analyses of surface NK receptor expression and intracellular cytotoxic molecule production by AlloHSC-iNKT cells. PBMC-NK cells were included as a control. (A) Representative FACS plots. (B) Quantification of (A) (n = 9).

(C–E) *In vitro* direct killing of human tumor cells by AlloHSC-iNKT cells. PBMC-NK cells were included as a control. Both fresh and frozen-thawed cells were studied. Five human tumor cell lines were studied: A375 (melanoma), K562 (myelogenous leukemia), H292 (lung cancer), PC3 (prostate cancer), and MM.1S (multiple myeloma). All tumor cell lines were engineered to express firefly luciferase and green fluorescence protein (FG) dual reporters. (C) Experimental design. (D and E) Tumor killing data of A375-FG human melanoma cells (D) and K562-FG human myelogenous leukemia cells (E) at 24 h (n = 4).

(F–H) Tumor killing mechanisms of AlloHSC-iNKT cells. NKG2D- and DNAM-1-mediated pathways were studied. (F) Experimental design. (G) Tumor killing data of A375-FG human melanoma cells at 24 h (tumor/iNKT ratio 1:2; n = 4). (H) Tumor killing data of K562-FG human myelogenous leukemia cells at 24 h (tumor/iNKT ratio 1:1; n = 4).

(legend continued on next page)

killing.[53,54] Flow cytometry analysis of intracellular effector molecules showed that compared to PBMC-NK cells, ^{Allo}HSC-iNKT cells produced exceedingly higher levels of cytotoxic molecules (i.e., perforin and granzyme B) (Figures 3A and 3B). Collectively, these results confirmed a promising antitumor potential of ^{Allo}HSC-iNKT cells through their intrinsic NK function.

An attractive feature of NK-cell-based cancer immunotherapy is its capacity to target a broad range of tumor cells independent of HLA and tumor antigen restrictions.[50] However, NK-cell-based therapy also confronts several significant challenges, such as the limited *in vivo* efficacy of NK cells, as well as their intolerance to cryopreservation, that pose a significant technical hurdle to their clinical and commercial applications.[55,56] Based on the "super-active" NK phenotype of ^{Allo}HSC-iNKT cells, we wondered whether these cells might exhibit improved antitumor NK function. Moreover, unlike NK cells, iNKT cells can resist cryopreservation[57]; we therefore wondered whether ^{Allo}HSC-iNKT cells might also improve on this aspect.

Using an *in vitro* tumor cell killing assay, we evaluated the tumor killing efficacy of ^{Allo}HSC-iNKT cells in comparison with PBMC-NK cells (Figure 3C). Five human tumor cell lines were used as targets, including a leukemia cell line (K562), a melanoma cell line (A375), a lung cancer cell line (H292), a prostate cancer cell line (PC3), and a multiple myeloma cell line (MM.1S). All five tumor cell lines were engineered to overexpress the firefly luciferase (Fluc) and enhanced green fluorescence protein (EGFP) dual reporters to enable the convenient monitoring of these tumor cells using either luciferase assay or flow cytometry (Figure S1A). Compared to PBMC-NK cells, ^{Allo}HSC-iNKT cells exhibited a significantly enhanced tumor killing efficacy across all five tumor cell lines (Figures 3D, 3E, and S1B–S1D). Interestingly, ^{Allo}HSC-iNKT cells sustained strong tumor killing efficacy after cryopreservation, whereas PBMC-NK cells were sensitive to freeze-thaw cycles and showed greatly reduced viability and antitumor capacity following cryopreservation (Figures 3D, 3E, and S1B–S1D). Blocking of NK activating receptors (i.e., NKG2D and DNAM-1) reduced tumor killing efficacy of ^{Allo}HSC-iNKT cells (Figures 3F–3H and S1E–S1G), confirming their NK-activating-receptor-mediated tumor-targeting function.

Next we evaluated the *in vivo* antitumor efficacy of ^{Allo}HSC-iNKT cells using a human melanoma xenograft NSG (NOD.Cg-Prkdc^{scid}Il2rg^{tm1Wjl}/SzJ) mouse model. A375-FG tumor cells were subcutaneously inoculated into NSG mice to form solid tumors, followed by a paratumoral injection of ^{Allo}HSC-iNKT or PBMC-NK cells (Figure 3I). ^{Allo}HSC-iNKT cells effectively suppressed tumor growth at an efficacy higher than that of PBMC-NK cells, as evidenced by time-course live animal bioluminescence imaging (BLI) monitoring (Figures 3J and S1H), tumor size measurement (Figure 3K), and terminal tumor weight assessment (Figure S1I).

Taken together, these studies support a cancer therapy potential of ^{Allo}HSC-iNKT cells through their intrinsic NK function, allowing these cells to target a broad range of tumors independent of HLA and tumor antigen restrictions. Attractively, ^{Allo}HSC-iNKT cells may exhibit improved antitumor efficacy and cryopreservation resistance compared to NK-cell-based allogeneic cell therapy products.

Tumor targeting of ^{Allo}HSC-iNKT cells through engineered CARs

CAR-engineered cell therapy has great promise for treating cancer[4–6,58]; we therefore explored the potential of ^{Allo}HSC-iNKT cells as the allogeneic cell carriers for CAR-directed off-the-shelf cell therapy. A second-generation B cell maturation antigen (BCMA)-targeting CAR (BCAR) was used for this study (Figure S2A); this BCAR contains 4-1BB and CD3ζ signaling domains and has shown clinical efficacy in treating human multiple myeloma (MM).[59]

^{Allo}HSC-iNKT cells were generated as previously described (Figure 1A); mature ^{Allo}HSC-iNKT cells were further transduced with a Retro/BCAR-tEGFR retroviral vector to produce the BCAR-engineered ^{Allo}HSC-iNKT cells (denoted as ^{Allo}BCAR-iNKT cells) (Figure 4A). The entire culture time (~10–11 weeks) and cell yield (~10^{11} per CB donor or ~10^{12} per PBSC donor) were similar to those of generating non-CAR-engineered ^{Allo}HSC-iNKT cells (Figures 1A and 1G). The resulting ^{Allo}BCAR-iNKT cells were pure iNKT cells with a high BCAR expression rate (>98% iNKT TCR$^+$ and up to 80% BCAR$^+$; Figure 4B) and displayed a typical human iNKT cell phenotype and functionality similar to those of ^{Allo}HSC-iNKT cells (Figures 2A, 2D, S2C, and S2D). Therefore, ^{Allo}HSC-iNKT cells can be effectively engineered to express CARs without compromising cell yield and quality.

To assess the antitumor capacity of ^{Allo}BCAR-iNKT cells, we used an established *in vitro* MM.1S-CD1d-FG tumor cell killing assay[28]; non-CAR-engineered ^{Allo}HSC-iNKT cells, as well as healthy donor PBMC-derived conventional T cells with or without engineering with the same BCAR (denoted as PBMC-T or BCAR-T cells), were included as controls (Figure 4C). The MM.1S-CD1d-FG cell line was generated by engineering the parental BCMA-positive MM.1S human MM cell line to overexpress human CD1d and the Fluc-EGFP dual reporters,[28] mimicking a large portion of primary patient MM samples that are BCMA$^+$CD1d$^+$ (Figure S2B).[60] This *in vitro* tumor cell killing assay allowed us to evaluate the tumor killing capacity of ^{Allo}BCAR-iNKT cells, as well as investigate their possible NK/TCR/CAR triple mechanisms for targeting MM (Figure 4D).

^{Allo}HSC-iNKT cells without BCAR engineering were able to kill MM.1S-CD1d-FG tumor cells, while PBMC-T cells could not, indicating an intrinsic antitumor NK function of ^{Allo}HSC-iNKT cells (Figures 4E, S1D, and S1G); this intrinsic antitumor NK function was inherited by ^{Allo}BCAR-iNKT cells, as confirmed by NK activating receptor (i.e., DNAM-1) blocking assay (Figure 4F). Meanwhile, the tumor cell killing efficacy of ^{Allo}HSC-iNKT cells was enhanced by the addition of αGC that did not happen to PBMC-T cells, indicating an iNKT TCR-mediated antitumor

(I–K) Studying the *in vivo* antitumor efficacy of ^{Allo}HSC-iNKT cells in an A375-FG human melanoma xenograft NSG mouse model. (I) Experimental design. BLI, live animal bioluminescence imaging. (J) BLI images showing tumor loads in experimental mice over time. (K) Tumor size measurements over time (n = 4–5). Representative of three experiments. Data are presented as the mean ± SEM. ns, not significant; *p < 0.05; **p < 0.01; ***p < 0.001; ****p < 0.0001 by Student's t test (B) or one-way ANOVA (D, E, G, H, and K). See also Figure S1.

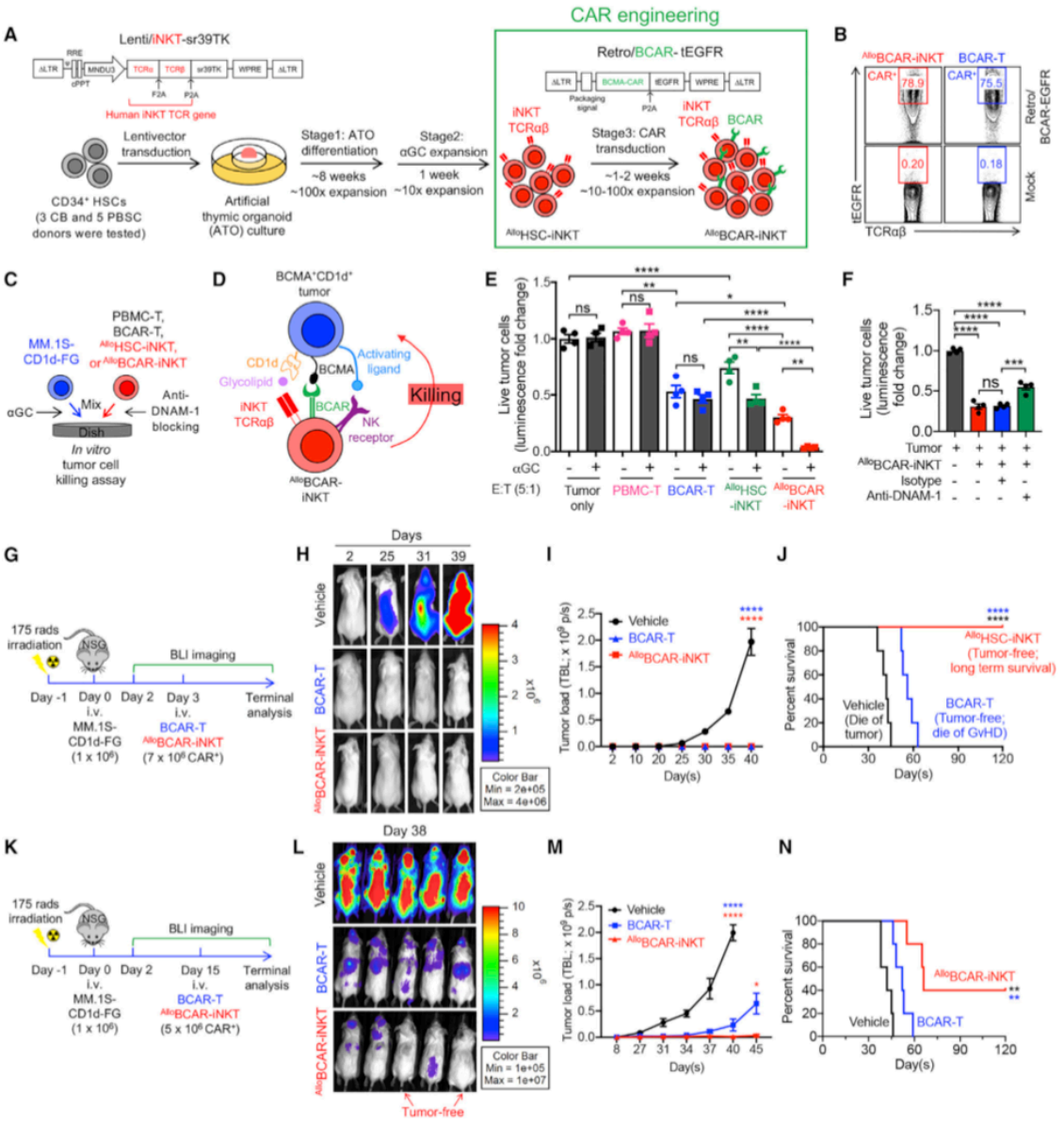

Figure 4. Tumor targeting of ^{Allo}HSC-iNKT cells through engineered chimeric antigen receptors (CARs)

(A) Experimental design to generate BCMA CAR-engineered ^{Allo}HSC-iNKT (^{Allo}BCAR-iNKT) cells *in vitro*. BCMA, B cell maturation antigen; BCAR, BCMA CAR; Retro/BCAR-tEGFR, retroviral vector encoding a BCMA CAR gene as well as a truncated epidermal growth factor receptor (tEGFR) reporter gene. tEGFR was used as a staining marker indicating BCAR expression.

(B) FACS analysis of BCAR expression (identified as tEGFR$^+$) on ^{Allo}BCAR-iNKT at 72 h after retrovector transduction. Healthy donor PBMC-T cells transduced with the same Retro/BCAR-tEGFR vector (denoted as BCAR-T cells) were included as a staining control.

(C–F) *In vitro* killing of human multiple myeloma cells by ^{Allo}BCAR-iNKT cells. MM.1S-CD1d-FG, human MM.1S cell line engineered to overexpress human CD1d as well as FG dual reporters. PBMC-T, BCAR-T, and ^{Allo}HSC-iNKT cells were included as effector cell controls. (C) Experimental design. (D) Diagram showing the tumor-targeting triple mechanisms of ^{Allo}BCAR-iNKT cells, mediated by NK activating receptors, iNKT TCR, and BCAR. (E) Tumor cell killing by the indicated effector cells with/out the addition of αGC (n = 4). (F) Tumor cell killing by ^{Allo}BCAR-iNKT cells with/out the blockade of DNAM-1 (n = 4). Tumor cell killing was analyzed at 8-h after co-culture (effector/tumor ratio 5:1).

(legend continued on next page)

function of ^{Allo}HSC-iNKT cells; this TCR-mediated antitumor function was also inherited by ^{Allo}BCAR-iNKT cells (Figure 4E). Importantly, compared to ^{Allo}HSC-iNKT cells, ^{Allo}BCAR-iNKT cells showed stronger tumor cell killing, indicating a CAR-mediated antitumor function of ^{Allo}BCAR-iNKT cells (Figure 4E). Therefore, ^{Allo}BCAR-iNKT cells are able to target MM tumor cells using the NK/TCR/CAR triple mechanisms, which may grant ^{Allo}BCAR-iNKT cells a higher tumor-targeting efficacy and an enhanced capacity to counteract tumor antigen escape compared to conventional BCAR-T cells (Figures 4D–4F).[25,61,62]

The *in vivo* antitumor efficacy of ^{Allo}BCAR-iNKT cells was studied using an established MM.1S-CD1d-FG xenograft NSG mouse model[28]; conventional BCAR-T cells were included as a control. In low-tumor-load conditions, ^{Allo}BCAR-iNKT cells eliminated MM tumor cells as effectively as BCAR-T cells (Figures 4H and 4I); however, experimental mice treated with BCAR-T cells eventually died of graft-versus-host disease (GvHD) despite being tumor-free, while experimental mice treated with ^{Allo}BCAR-iNKT cells lived long-term with tumor-free and GvHD-free (Figures 4I and 4J). Impressively, in high-tumor-load conditions, ^{Allo}BCAR-iNKT cells still managed to suppress tumor growth effectively and achieved tumor clearance in a fraction of experimental mice (two out of five mice); conventional BCAR-T cells suppressed tumor growth less well and could not achieve tumor clearance (Figures 4K–4N and S2E).

Taken together, these studies support an attractive potential of ^{Allo}HSC-iNKT cells as off-the-shelf cell carriers for CAR-directed cancer immunotherapy. The high antitumor efficacy and multiple tumor-targeting mechanisms of CAR-engineered ^{Allo}HSC-iNKT cells may provide new opportunities to target hard-to-treat tumors and counteract tumor antigen escape.

Safety study of ^{Allo}HSC-iNKT cells

Graft-versus-host (GvH) response is the primary safety concern of an off-the-shelf allogeneic cell therapy.[4] Since iNKT cells do not react to mismatched HLA molecules and protein alloantigens, these cells are not expected to mount GvH responses.[17,19] To verify this safety feature of ^{Allo}HSC-iNKT cells, we performed both *in vitro* and *in vivo* studies. In an *in vitro* mixed lymphocyte reaction (MLR) assay, in sharp contrast to conventional PBMC-Tc cells, ^{Allo}HSC-iNKT cells did not react to all the mismatched healthy donor PBMCs tested, as evidence by their lack of IFN-γ production (Figures 5A and 5B). In an *in vivo* NSG mouse xenograft model, unlike PBMC-Tc cells that induced GvHD and killed experimental mice ~2 months after PBMC-Tc cell transfer, ^{Allo}HSC-iNKT cells did not cause GvHD and sustained long-term survival of experimental mice (Figures 5C and 5D). The lack of GvHD in ^{Allo}HSC-iNKT cell engrafted experimental mice was confirmed by histology analysis showing healthy tissue structures without lymphocyte infiltrations; on the contrary, analyses of PBMC-Tc cell engrafted experimental mice showed severe tissue damages associated with heavy lymphocyte infiltrations (Figures 5E and 5F). To study the influence of CAR engineering, we analyzed the GvH response of ^{Allo}BCAR-iNKT cells; BCAR-T cells were included as a control. Distinct from BCAR-T cells, ^{Allo}BCAR-iNKT cells showed no response in the *in vitro* MLR assay (Figures S3A and S3B) and induced no GvHD in the human MM xenograft NSG mouse model (Figures S3C and S3D), indicating that CAR engineering and tumor encountering do not change the GvH-free safety feature of ^{Allo}HSC-iNKT cells.

Besides GvHD risk, allogeneic cell therapy may confer other safety risks, including those common to cell-based cancer immunotherapy, such as cytokine release syndrome (CRS) and neurotoxicity.[63] Although we did not observe that ^{Allo}HSC-iNKT cells induced tissue toxicity in our NSG xenograft mouse models (Figures 5E and 5F), these safety studies may be limited by the utilized preclinical animal models.[63] Additional safety controls may be necessary, especially for initial clinical development. We therefore have engineered a "safety switch" in ^{Allo}HSC-iNKT cell products by incorporating a suicide gene (i.e., sr39TK) in the human iNKT TCR gene delivery vector, resulting in ^{Allo}HSC-iNKT cells that are 100% labeled with the suicide gene (Figure 1A). In cell culture, addition of guanosine analog (ganciclovir [GCV]) effectively killed ^{Allo}HSC-iNKT cells (Figure S3E); in an NSG mouse xenograft model, administration of GCV effectively depleted ^{Allo}HSC-iNKT cells from all tissues examined (e.g., liver, spleen, and lung; Figures 5G–5I). Of note, GCV has been used clinically as a prodrug to induce sr39TK-mediated suicide effect in cellular products.[64] Other alternative suicide switch systems (e.g., inducible Cas9 and truncated EGFR) can certainly be utilized.[4,65–67]

Taken together, our results show that ^{Allo}HSC-iNKT cells are free of GvHD risk and can be equipped with an additional safety switch, making them suitable for off-the-shelf allogeneic cell therapy.

Immunogenicity study of ^{Allo}HSC-iNKT cells

For allogeneic cell therapies, immunogenicity can be a concern, because allorejection by host T and NK cells can greatly limit the efficacy of therapeutic allogeneic cells.[68] Host conventional CD8 and CD4 $\alpha\beta$ T cells reject allogeneic cells by recognizing mismatched HLA-I and HLA-II molecules, respectively.[69,70] In a classical *in vitro* MLR assay studying T-cell-mediated host-versus-graft (HvG) response via IFN-γ secretion reading, compared to endogenous conventional T and iNKT (i.e., PBMC-Tc and PBMC-iNKT) cells, ^{Allo}HSC-iNKT cells triggered a significantly reduced HvG response (Figures 6A, 6C, and S4A). Our previous RNA-seq study

(G–N) Studying the *in vivo* antitumor efficacy of ^{Allo}BCAR-iNKT cells in an MM.1S-CD1d-FG human multiple myeloma xenograft NSG mouse model. Tumor-bearing mice injected with BCAR-T cells or no cells (vehicle) were included as controls. (G–J) Low-tumor-load condition. (G) Experimental design. (H) BLI images showing tumor loads in experimental mice over time. (I) Quantification of (H) (n = 5). (J) Kaplan-Meier survival curves of experimental mice over a period of 4 months after tumor challenge (n = 5). (K–N) High-tumor-load condition. (K) Experimental design. (L) BLI images showing tumor loads in experimental mice at day 38. (M) Quantification of tumor load in experimental mice over time (n = 5). (N) Kaplan-Meier survival curves of experimental mice over a period of 4 months after tumor challenge (n = 5).

Representative of two experiments (K–N) and three experiments (A–J). Data are presented as the mean ± SEM. ns, not significant; *$p < 0.05$; **$p < 0.01$; ***$p < 0.001$; ****$p < 0.0001$ by one-way ANOVA (E, F, I, and M), or log rank (Mantel-Cox) test adjusted for multiple comparisons (J and N). See also Figure S2.

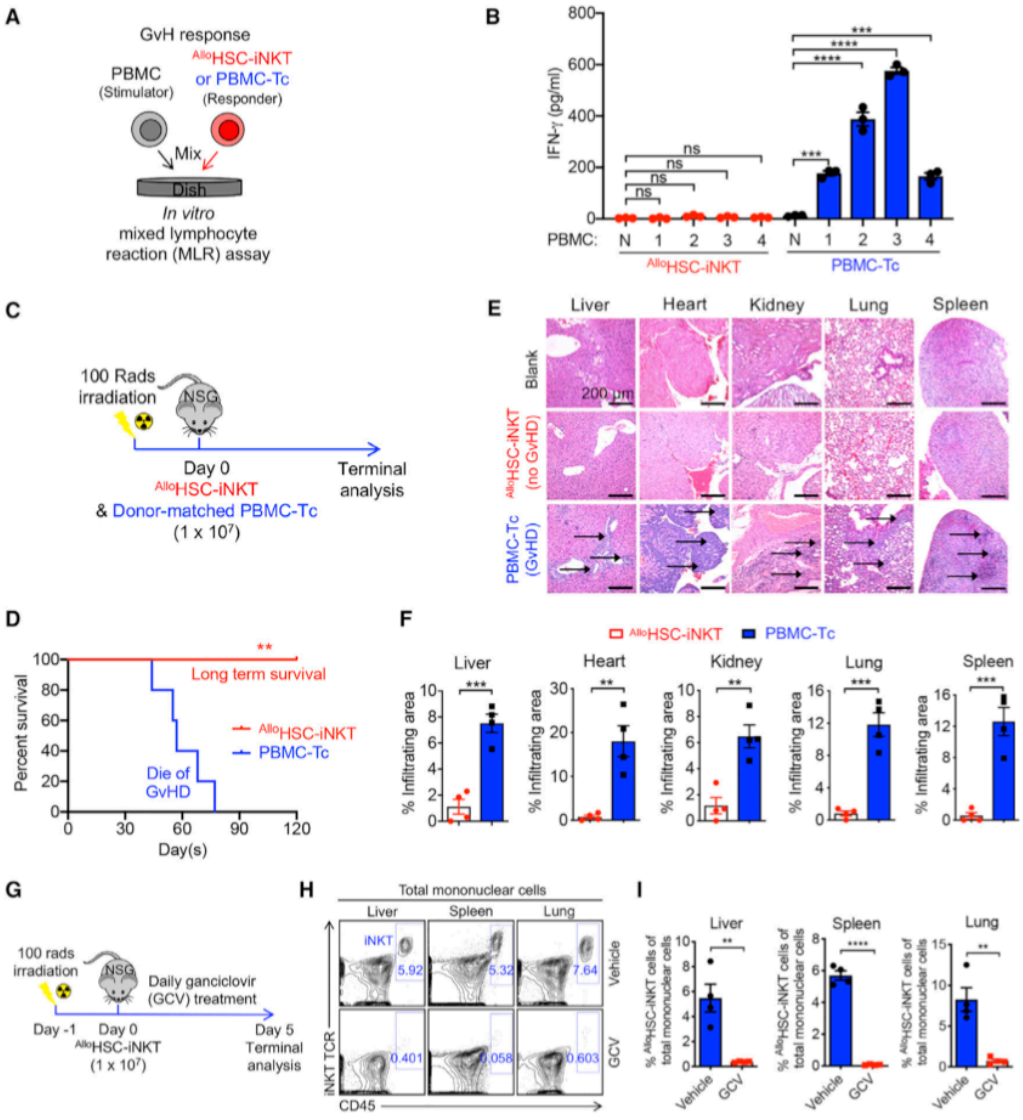

Figure 5. Safety study of AlloHSC-iNKT cells

(A and B) Studying the graft-versus-host (GvH) response of AlloHSC-iNKT cells using an *in vitro* mixed lymphocyte reaction (MLR) assay. PBMC-Tc cells were included as a responder cell control. (A) Experimental design. PBMCs from four different healthy donors were used as stimulator cells. (B) ELISA analyses of IFN-γ production at day 4 (n = 4). N, no stimulator cells.

(C–F) Studying the GvH response of AlloHSC-iNKT cells using an NSG mouse xenograft model. Donor-matched PBMC-Tc cells were included as a control. (C) Experimental design. (D) Kaplan-Meier survival curves of experimental mice over time (n = 5). (E) H&E-stained tissue sections. Blank indicates tissue sections collected from control NSG mice receiving no adoptive cell transfer. Arrows point to mononuclear cell infiltrates. Scale bar, 200 μm. (F) Quantification of (E) (n = 4).

(G–I) *In vivo* controlled depletion of AlloHSC-iNKT cells via GCV treatment. GCV, ganciclovir. (G) Experimental design. (H) FACS detection of AlloHSC-iNKT cells in the liver, spleen, and lung of NSG mice at day 5. (I) Quantification of (G) (n = 4).

Representative of two experiments. Data are presented as the mean ± SEM. ns, not significant; *p < 0.05; **p < 0.01; ***p < 0.001; ****p < 0.0001 by one-way ANOVA (B), Student's t test (F and I), or log rank (Mantel-Cox) test adjusted for multiple comparisons (D). See also Figure S3.

made the interesting observation that compared to endogenous immune cells (i.e., conventional αβT, iNKT, γδT, and NK cells), AlloHSC-iNKT cells globally downregulated the expression of many genes controlling the cell surface display of HLA-I and HLA-II molecules (Figure 2I). Flow cytometry analysis confirmed that compared to PBMC-Tc and PBMC-iNKT cells, AlloHSC-iNKT cells expressed significantly reduced levels of HLA-I molecules and nearly undetectable levels of

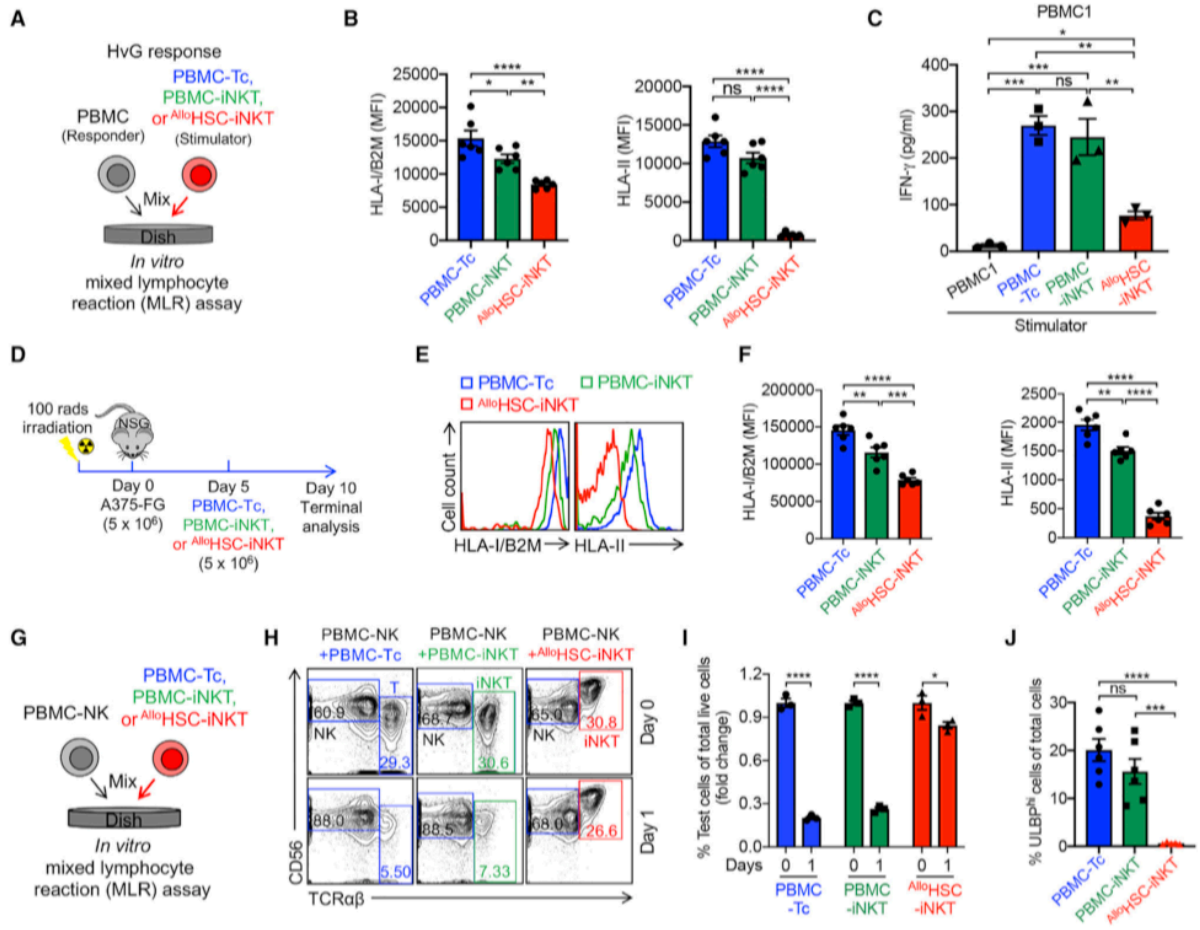

Figure 6. Immunogenicity study of ^{Allo}HSC-iNKT cells

(A–C) Studying allogenic T cell response against ^{Allo}HSC-iNKT cells using an *in vitro* MLR assay. Irradiated ^{Allo}HSC-iNKT cells (as stimulators) were co-cultured with donor-mismatched PBMC cells (as responders). Irradiated PBMC-iNKT and PBMC-Tc cells were included as stimulator cell controls. (A) Experimental design. PBMCs from three different healthy donors were used as responders. (B) FACS analyses of HLA-I and HLA-II expression on the indicated stimulator cells (n = 6). (C) ELISA analyses of IFN-γ production at day 4 (n = 3).

(D–F) Studying HLA-I/II expression on ^{Allo}HSC-iNKT cells *in vivo* in an A375-FG human melanoma xenograft NSG mouse model. PBMC-iNKT and PBMC-Tc cells were included as effector cell controls. (D) Experimental design. (E) FACS analyses of HLA-I/II expression on the indicated effector cells isolated from A375-FG solid tumors. (F) Quantification of (E) (n = 5).

(G–J) Studying allogenic NK cell response against ^{Allo}HSC-iNKT cells using an *in vitro* MLR assay. ^{Allo}HSC-iNKT cells were co-cultured with donor-mismatched PBMC-NK cells. PBMC-iNKT and PBMC-Tc cells were included as controls. (G) Experimental design. (H) FACS analyses of the indicated cells at days 0 and 1. (I) Quantification of (H) (n = 3). (J) FACS analyses of ULBP expression on the indicated cells (n = 5–6).

Representative of two (D–F) and three (A–C and G–J) experiments. Data are presented as mean ± SEM. ns, not significant; *p < 0.05; **p < 0.01; ***p < 0.001; ****p < 0.0001 by Student's t test (I) or one-way ANOVA (B, C, F, and G). See also Figures S4–S6.

HLA-II molecules (Figures 6B and S4B), which may account for their resistance to T-cell-mediated HvG response (Figures 6C and S4A). Because IFNs can upregulate HLA-I expression,[71] we studied HLA-I expression on ^{Allo}HSC-iNKT cells under IFN-γ stimulation (Figure S5A). ^{Allo}HSC-iNKT cells slightly upregulated surface HLA-I expression after IFN-γ stimulation; however, their overall surface HLA-I level still remained significantly lower than those of PBMC-Tc and PBMC-iNKT cells (Figures S5B and S5C). Because an *in vivo* inflammatory tumor microenvironment may upregulate the expression of HLA molecules on tumor-infiltrating immune cells (e.g., via IFN-γ),[72] we also assessed HLA expression on ^{Allo}HSC-iNKT cells in an A375-FG human melanoma xenograft NSG mouse model adapted from a previous study (Figures 3I). A375-FG melanoma cells were subcutaneously inoculated in NSG mice to form solid tumors, followed by injection of ^{Allo}HSC-iNKT cells; PBMC-Tc and PBMC-iNKT cells were included as controls (Figure 6D). Flow cytometry analysis of tumor-infiltrating ^{Allo}HSC-iNKT cells showed that these cells maintained low expression of HLA-I and HLA-II molecules at levels

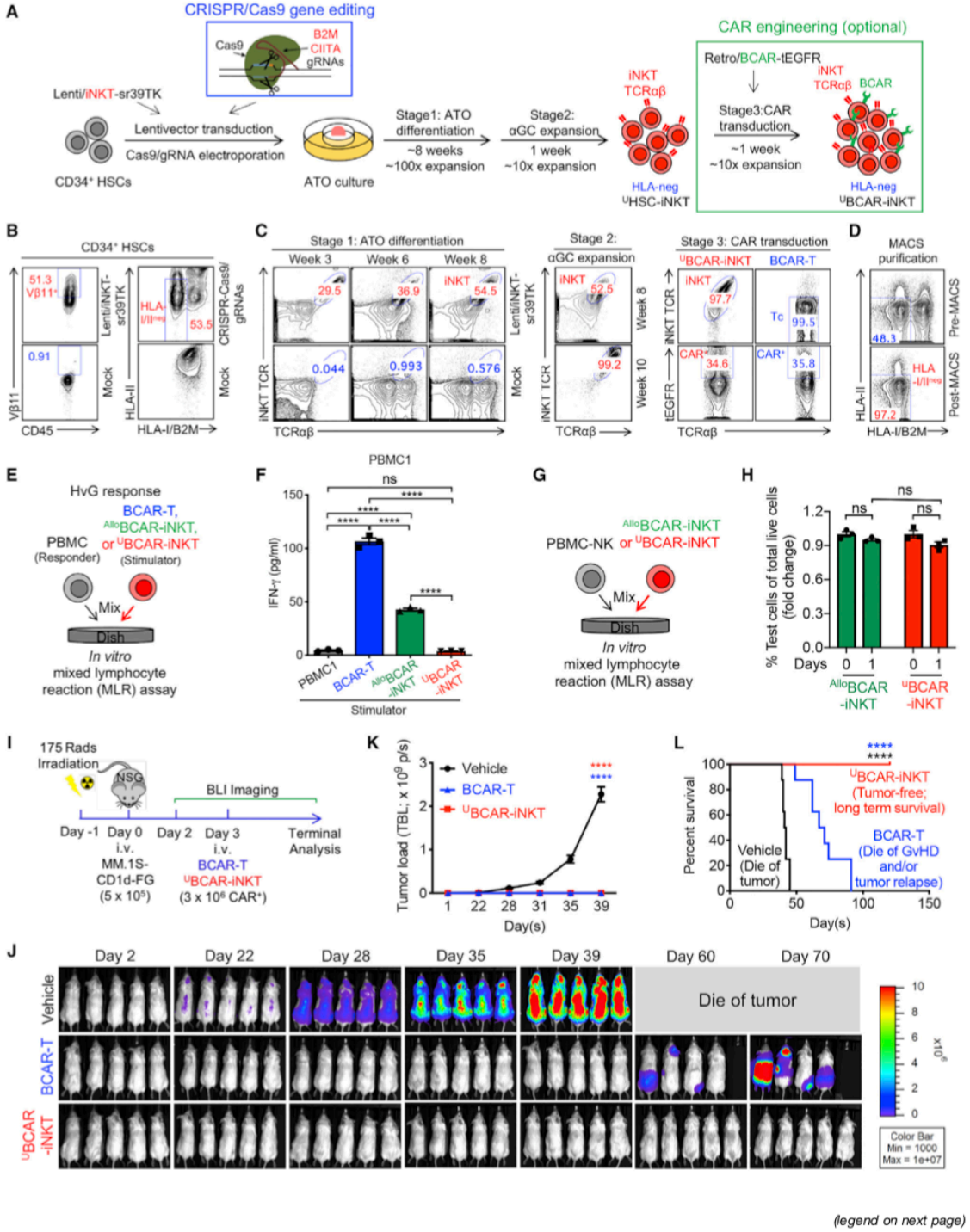

(legend on next page)

significantly lower than those of tumor-infiltrating PBMC-Tc and PBMC-iNKT cells (Figures 6E and 6F).

Next, we studied NK-cell-mediated allorejection. Host NK cells reject allogeneic cells through a double-trigger mechanism: (1) "missing self" (i.e., missing of matching HLA-I molecules on allogeneic cells) triggers the release of KIR inhibition, and (2) a "stress signal" (i.e., upregulated stress molecules on allogeneic cells) triggers the activation of NK activating receptors such as NKG2D.[52,73,74] Because ^{Allo}HSC-iNKT cells expressed low levels of HLA-I molecules, we wondered whether this might make ^{Allo}HSC-iNKT cells susceptible to host NK rejection. Surprisingly, in an *in vitro* MLR assay studying NK-cell-mediated allorejection, compared to endogenous conventional T and iNKT (i.e., PBMC-Tc and PBMC-iNKT) cells, ^{Allo}HSC-iNKT cells survived rejection by mismatched healthy donor PBMC-derived NK cells significantly better (Figures 6G–6I and S6); correspondingly, NK cells co-cultured with ^{Allo}HSC-iNKT cells exhibited less upregulation of NK activation markers (i.e., CD107a) (Figures S4D and S4E). Flow cytometry analysis revealed that compared to PBMC-Tc and PBMC-iNKT cells, ^{Allo}HSC-iNKT cells expressed much reduced and nearly undetectable levels of NKG2D ligands (i.e., ULBP; Figures 6J and S4C),[75] which may be one of the possible mechanisms accounting for their resistance to NK-cell-mediated allorejection.

Collectively, these studies revealed a stable HLA-I/II^{low} phenotype of ^{Allo}HSC-iNKT cells that may grant them advantage to resist host T-cell-mediated rejection compared to other healthy donor PBMC-derived allogeneic cell products; meanwhile, ^{Allo}HSC-iNKT cells also expressed low levels of stress molecules such as NKG2D ligands, making them also resistant to host NK-cell-mediated allorejection. These "low immunogenicity" features of ^{Allo}HSC-iNKT cells support their application for off-the-shelf cell therapy.

Development of HLA-ablated universal HSC-iNKT (^{U}HSC-iNKT) cells and derivatives

Although ^{Allo}HSC-iNKT cells display a stable HLA-I/II^{low} phenotype (Figures 2I, 6B, 6E, 6F, and S4B), their residual HLA-I/II molecules may still make them susceptible to certain levels of host T-cell-mediated allorejection. We therefore explored further engineering of the ^{Allo}HSC-iNKT cell products to achieve total ablation of their surface HLA-I/II molecules. Interestingly, this task can be accomplished by ablation of only two genes: (1) a *B2M* gene encoding the beta 2-microglobulin (B2M) that is required for the surface display of all types of HLA-I molecules,[69] and (2) a *CIITA* gene encoding the class II transactivator (CIITA) that is required for the transcription of all types of HLA-II molecules.[70] Ablation of *B2M* and *CIITA* genes can be achieved by using the powerful gene-editing tools like the CRISPR-Cas9/guide RNA (gRNA) system.[76] We postulated that by combining iNKT TCR gene engineering and B2M/CIITA gene editing, we would produce HLA-ablated "universal" HSC-iNKT (^{U}HSC-iNKT) cells totally resistant to host T-cell-mediated allorejection. We intended to perform both gene engineering and gene editing on the small numbers of starting HSCs upfront of the HSC-iNKT cell culture; this manufacturing design would save on the use of gene-engineering/editing materials (i.e., lentivector and CRISPR-Cas9/gRNA) that can be cost-limiting, and also enable the maximal gene engineering/editing efficiency that can be carried on into the final ^{U}HSC-iNKT cell products. Similar to the generation of ^{Allo}CAR-iNKT cell products (Figure 4A), a CAR engineering step can be incorporated after ^{U}HSC-iNKT cell differentiation, resulting in HLA-ablated universal CAR-engineered HSC-iNKT (^{U}CAR-iNKT) cell products.

CB or PBSC-derived CD34^{+} HSCs were transduced with the Lenti/iNKT-sr39TK lentivector; 24 h later, these HSCs were electroporated with a CRISPR-Cas9/B2M-CIITA-gRNAs complex (Figure 7A). The gene-engineering/editing efficiency was high; we routinely achieved over 50% lentivector transduction rate and over 50% HLA-I/II double-ablation rate (Figures 7B and S7B). The engineered HSCs were then put into the HSC-iNKT differentiation ATO culture for 8 weeks followed by 1 week of αGC expansion (Figures 7A); CRISPR-Cas9 gene editing did not interfere with HSC differentiation into iNKT cells and we obtained high yield of differentiated ^{U}HSC-iNKT cells similar to that of ^{Allo}HSC-iNKT cells (Figures 1C and 7C). CRISPR-Cas9 gene editing also did not interfere with the follow-up CAR engineering; we obtained an efficient BCMA-targeting CAR (BCAR) engineering rate similar to that of engineering PBMC-derived conventional BCAR-T cells (Figure 7C). The high HLA-I/II double-ablation rate of the starting HSCs was inherited by the resulting ^{U}BCAR-iNKT cells (i.e.,

Figure 7. Development of HLA-ablated universal HSC-iNKT (^{U}HSC-iNKT) cells and derivatives

(A) Experimental design to generate ^{U}HSC-iNKT and BCMA CAR-engineered ^{U}HSC-iNKT (^{U}BCAR-iNKT) cells. CRISPR, clusters of regularly interspaced short palindromic repeats; Cas 9, CRISPR-associated protein 9; gRNA, guide RNA; B2M, beta-2-microglobulin; CIITA, class II major histocompatibility complex transactivator.

(B–D) FACS monitoring of ^{U}HSC-iNKT and ^{U}BCAR-iNKT cell generation. (B) Intracellular expression of iNKT TCR (identified as Vβ11^{+}) and surface ablation of HLA-I/II (identified as HLA-I/B2M^{-}HLA-II^{-}) in CD34^{+} HSCs cells at day 5 (72 h after lentivector transduction and 48 h after CRISPR-Cas9 gene editing). (C) Generation of iNKT cells (identified as iNKT TCR^{+}TCRαβ^{+} cells) during stage 1 ATO differentiation culture, stage 2 αGC expansion, and stage 3 CAR transduction. Healthy donor PBMC-T cells transduced with the same Retro/BCAR-tEGFR vector was included as a staining control (denoted as BCAR-T cells). (D) Purification of HLA-I/II-negative ^{U}HSC-iNKT cells using MACS.

(E and F) Studying allogenic T cell response against ^{U}BCAR-iNKT cells using an *in vitro* MLR assay. Irradiated ^{U}BCAR-iNKT cells (as stimulators) were co-cultured with donor-mismatched PBMCs (as responders). Irradiated ^{Allo}BCAR-iNKT and conventional BCAR-T cells were included as stimulator cell controls. (E) Experimental design. PBMCs from three different healthy donors were used as responders. (F) ELISA analyses of IFN-γ production at day 4 (n = 3).

(G and H) Studying allogenic NK cell response against ^{U}HSC-iNKT cells using an *in vitro* MLR assay. ^{U}HSC-iNKT cells were co-cultured with donor-mismatched PBMC-NK cells. ^{Allo}HSC-iNKT cells were included as a control. (G) Experimental design. (H) FACS quantification of the indicated cells (n = 3).

(I–L) Studying the *in vivo* antitumor efficacy of ^{U}BCAR-iNKT cells in an MM.1S-CD1d-FG human multiple myeloma xenograft NSG mouse model. (I) Experimental design. (J) BLI images showing tumor loads in experimental mice over time. (K) Quantification of (J) (n = 5). (L) Kaplan-Meier survival curves of experimental mice over a period of 4 months after tumor challenge (n = 8). Mice were combined from two independent experiments.

Representative of two (I–L) and three (B–H) experiments. Data are presented as mean ± SEM. ns, not significant; ****p < 0.0001 by Student's t test (H), one-way ANOVA (F and K), or log rank (Mantel-Cox) test adjusted for multiple comparisons (L). See also Figure S7.

~50% of the resulting cells were HLA-I/II double negative); if needed, the HLA-I/II double-negative cells could be further enriched (to over 97%) using magnetic-activated cell sorting (MACS) via B2M and HLA-II magnetic beads labeling (Figures 7D).

Despite HLA-I/II ablation, ^{U}BCAR-iNKT cells displayed a typical iNKT phenotype and a highly cytotoxic functionality similar to those of ^{Allo}BCAR-iNKT cells (Figure S7A). As expected, ^{U}BCAR-iNKT cells induced nearly undetectable T-cell-mediated alloresponse when mixed with mismatched healthy donor PBMCs (Figures 7E, 7F, and S7F); meanwhile, ^{U}BCAR-iNKT cells maintained the resistance to NK-cell-mediated allorejection (Figures 7G, 7H, and S7G). Safety features of ^{U}BCAR-iNKT cells resembled those of ^{Allo}BCAR-iNKT cells: ^{U}BCAR-iNKT cells did not mount GvH response (Figures S7C and S7D), and they were sensitive to sr39TK/GCV-induced suicide control (Figure S7E).

To study whether HLA ablation may impact the antitumor efficacy of ^{U}BCAR-iNKT cells, we performed *in vitro* and *in vivo* antitumor assays. In an established *in vitro* MM tumor cell killing assay (Figure 4C), ^{U}BCAR-iNKT cells effectively killed tumor cells at an efficacy comparable to that of ^{Allo}BCAR-iNKT cells (Figures 4E, S7H, and S7I). Similar to ^{Allo}BCAR-iNKT cells, ^{U}BCAR-iNKT cells could also utilize an NK/TCR/CAR triple mechanisms targeting tumor cells (Figures 4E, 4F, S7I, and S7J), which may grant them an advantage over conventional BCAR-T cells to gain additional antitumor efficacy (Figure S7I), as well as to counteract the BCMA antigen escape that has been reported in conventional BCAR-T cell therapy clinical trials.[25,61,62] In an established *in vivo* human MM xenograft NSG mouse model (Figure 4G), ^{U}BCAR-iNKT-cell-treated animals achieved total tumor clearance and long-term survival, while BCAR-T-cell-treated animals only achieved partial tumor suppression that was followed by tumor relapse and GvHD development, leading to limited survival benefit (Figures 7I–7L).

Collectively, these studies support the generation of HLA-ablated universal HSC-iNKT cell products and derivatives (e.g., CAR-iNKT cell products) that are fully resistant to host T-cell-mediated allorejection and thereby may have improved *in vivo* persistence and antitumor efficacy.

DISCUSSION

Here, we report the generation and characterization of allogeneic HSC-engineered iNKT cells and derivatives. Using an *in vitro* HSC-iNKT differentiation cell culture, we generated ^{Allo}HSC-iNKT cells that were of high yield and purity and had high antitumor efficacy, high safety profile (GvH-free and suicide control), and low immunogenicity (largely resistant to T- and NK-cell-mediated allorejection). These ^{Allo}HSC-iNKT cells could be further engineered to express CAR, thereby enhancing their tumor-targeting capacity; these cells can also be further engineered to ablate their surface HLA molecules, thereby enhancing their resistance to host T-cell-mediated allorejection. Collectively, our studies have generated ^{Allo}HSC-iNKT cells and demonstrated them as promising cell carriers for developing off-the-shelf cancer immunotherapy.

Development of allogeneic off-the-shelf cell therapies, many equipped with CARs, is becoming a fast-evolving frontier of cancer immunotherapy. Two major categories of such allogeneic cell products are based on engineering healthy-donor-derived conventional αβ T cells or NK cells.[14,68,69,77] Because conventional αβ T cells risk inducing GvHD in allogeneic hosts due to HLA incompatibility, these T cells need to be gene edited to ablate endogenous TCR expression, usually by disrupting the *TRAC* or/and *TRBC* gene loci, to make them suitable for allogeneic cell therapy but meanwhile may also potentially increase manufacture complexity.[10–13] On the other hand, NK-based allogeneic cell products are considered of low GvHD risk and therefore do not require additional gene editing, but their *in vivo* clonal expansion and antitumor performance may be limited compared to that of conventional αβ T cells.[14] Two such allogeneic cell products, conventional αβ T-cell-based universal CD19-CAR-engineered T cells (UCART19) and NK-cell-based CB-derived CD19-CAR-engineered NK cells, were recently tested in phase 1 clinical trials treating CD19^{+} B cell malignancies.[10,78] These studies reported the feasibility, certain antileukemic activity, and manageable safety profile of the two cell products, showing an encouraging step forward for the field of allogeneic cell therapy.[10,78]

Engineering unconventional innate-type T cells (e.g., iNKT, γδ T, and mucosal-associated invariant T cells) that have potent antitumor capacity while being free of GvHD risk represents another promising direction for developing allogeneic cell therapy for cancer, especially for solid tumors.[25,79–83] In particular, iNKT-cell-based cancer immunotherapy has attracted considerable attention. A preclinical study reported the enhanced anti-lymphoma activity of CAR19-engineered iNKT cells compared to conventional CAR19-T cells.[25] Another preclinical study reported the potent antitumor efficacy to neuroblastoma and no GvHD risk of CAR.GD2-engineered iNKT cells compared to conventional CAR.GD2-T cells.[80] A recent clinical trial testing autologous GD2.CAR-engineered iNKT cells also showed safety and certain efficacy in patients with relapsed or refractory neuroblastoma.[79] These studies suggest the therapeutical potential of iNKT-based cell products and support the development of such cell products for allogeneic cell therapy for cancer even solid tumors.

The *in vitro* HSC-iNKT differentiation cell culture was robust and of high yield (Figure 1G). The resulting ^{Allo}HSC-iNKT cell products were of high purity and nearly free of bystander conventional αβ T cells (Figure 1D), which may allow these cell products to be directly used for allogeneic cell therapy without an additional purification step; if necessary, commercially available human iNKT cell isolation reagents (e.g., human anti-iNKT microbeads from Miltenyi) can be used for further purification. Notably, we detected no expression of endogenous TCRs in ^{Allo}HSC-iNKT cells (Figure 1F), suggesting an induction of allelic exclusion by transgenic iNKT TCRs as previously reported.[27,28] The robustness, high yield, and high purity of ^{Allo}HSC-iNKT cell products will facilitate their next-stage translational and clinical development.

The antitumor efficacy of ^{Allo}HSC-iNKT cells is promising. These cells display a typical iNKT phenotype and functionality; they co-express memory T cell and NK cell markers, express high levels of inflammatory tissue/tumor homing markers, and produce high levels of cytokines and cytotoxic molecules, outperforming T and NK cells (Figures 2 and 3). Interestingly,

compared to endogenous cells (i.e., T, NK, and iNKT cells), ^{Allo}HSC-iNKT cells express exceedingly high levels of NK activating receptors and low levels of NK inhibitory receptors (Figure 2G), which is associated with their superior antitumor NK function *in vitro* and *in vivo* (Figure 3). In addition, the NK/TCR/CAR tumor-targeting triple mechanisms of ^{Allo}HSC-iNKT cells and their derivatives grant these cells a stronger antitumor efficacy (Figures 4D–4F, 7I–7J, and S6G–S6I) and may enable them to counteract tumor antigen escape, which has been observed in T-cell-based cancer therapies.[4,25,61,62] Overall, in both the human blood cancer (i.e., MM) and human solid tumor (i.e., melanoma) preclinical mouse xenograft models utilized in this study, ^{Allo}HSC-iNKT cells or their CAR derivatives (i.e., ^{Allo}BCAR-iNKT and ^{U}BCAR-iNKT cells) showed an enhanced antitumor efficacy compared to healthy donor PBMC-derived NK or CAR-engineered conventional αβ T cells, highlighting their cancer therapy potential (Figures 3I–3K, S1H, S1I, 4G–4N, S2E, and 7I–7L). Notably, a synthetic iNKT cell antagonist, αGC, has been demonstrated to specifically stimulate and expand iNKT cells in both preclinical and clinical studies; αGC is clinically available and may be used as a "designer stimulator" to enhance the *in vivo* performance of ^{Allo}HSC-iNKT cells.[18,23,84–86]

The safety of ^{Allo}HSC-iNKT cells is appealing. In our studies, ^{Allo}HSC-iNKT cells showed no GvH responses against multiple random healthy donor PBMCs in an *in vitro* MLR assay (Figures 5A, 5B, S3A, and S3B) and no GvHD *in vivo* in multiple human tumor xenograft NSG mouse models (Figures 5C–5F, S3C, and S3D), consistent with their iNKT cell nature and high purity (Figure 1).[16] A suicide switch (e.g., sr39TK/GCV) can also be incorporated into ^{Allo}HSC-iNKT cells to provide an additional safety control (Figure 5G, 5I, and S3E). The high safety of ^{Allo}HSC-iNKT cells strongly support their allogeneic application.

A serendipitous feature of ^{Allo}HSC-iNKT cells is their significantly lower immunogenicity compared to PBMC-derived endogenous immune cells (i.e., αβ T, iNKT, γδ T, and NK cells). ^{Allo}HSC-iNKT cells express reduced levels of HLA-I molecules and nearly undetectable levels of HLA-II molecules, which seems to be genomically programmed (Figure 2I) and stable through the *in vitro* culture and *in vivo* persistence even within the tumor microenvironment (Figures 6A–6F); this feature may allow these cells to resist allorejection by host T cells and thereby alleviate the need for additional HLA gene editing or intense host T cell depletion preconditioning treatment (e.g., CD52 antibody treatment).[10,13] Meanwhile, ^{Allo}HSC-iNKT cells also express reduced levels of NK activating receptor ligands (e.g., ULBP) (Figure 6J); this feature may allow these cells to also resist allorejection by host NK cells and increase their suitability for allogeneic cell therapy (Figures 6G–6I). The biological regulations resulting in this low-immunogenicity feature of ^{Allo}HSC-iNKT cells remain to be illustrated; nonetheless, such biological regulations do not seem to interfere with the production or antitumor efficacy of ^{Allo}HSC-iNKT cells both *in vitro* and *in vivo* (Figures 3, 4, and 7).

The ^{Allo}HSC-iNKT cell production platform is robust and versatile, allowing the plug-in of additional engineering approaches. In our studies, we demonstrated the successful generation of CAR-engineered or/and HLA-I/II-ablated ^{Allo}HSC-iNKT cells by incorporating additional CAR gene engineering and CRISPR-Cas9/B2M-CIITA-gRNAs gene-editing steps (Figures 4 and 7). These additional engineering approaches did not interfere with the production and antitumor function of ^{Allo}HSC-iNKT cells, opening up the possibility of developing more advanced ^{Allo}HSC-iNKT cell products. For example, incorporation of multiple tumor-targeting molecules (e.g., CARs and TCRs) and functional enhancement factors (e.g., overexpression of immune enhancement genes like IL-15, and ablation of immune inhibitory genes like PD-1) may improve the cancer therapy potential of ^{Allo}HSC-iNKT cell products.[87,88]

Limitations of the study

Despite their promise, current ^{Allo}HSC-iNKT cell products confront certain limitations that may be further improved; the manufacturing process can benefit from switching to a feeder-free culture system that will greatly simplify and accelerate the clinical and commercial development, the sr39TK/GCV suicide switch can be replaced with an alternative suicide switch system (e.g., inducible Cas9 or truncated EGFR) that is less immunogenic and cell-cycle dependent,[4,65–67,89] an *HLA-E* transgene can also be incorporated into the ^{Allo}HSC-iNKT cell products to further increase their resistance to host NK-cell-mediated allorejection,[73,90] and pluripotent stem cells (i.e., embryonic stem cells and induced pluripotent stem cells [iPSCs]) may be utilized as an alternative "unlimited" cell source to derive HSCs for the generation of ^{Allo}HSC-iNKT cells.[24] Further exploration of ^{Allo}HSC-iNKT cells as allogeneic cell carriers for developing off-the-shelf cell therapy for the treatment of cancer, especially solid tumors, will certainly be an interesting direction for future study.

STAR★METHODS

Detailed methods are provided in the online version of this paper and include the following:

- KEY RESOURCES TABLE
- RESOURCE AVAILABILITY
  - Lead contact
  - Materials availability
  - Data and code availability
- EXPERIMENTAL MODEL AND SUBJECT DETAILS
  - Mice
  - Cell Lines
  - Human CD34^{+} Hematopoietic Stem Cells (HSCs), Periphery Blood Mononuclear Cells (PBMCs), and Patient Bone Marrow Samples
  - Media and Reagents
- METHOD DETAILS
  - Lentiviral and Retroviral Vectors
  - Antibodies and Flow Cytometry
  - Enzyme-Linked Immunosorbent Cytokine Assays (ELISA)
  - *In Vitro* Generation of Allogeneic HSC-Engineered iNKT (^{Allo}HSC-iNKT) Cells
  - *In Vitro* Generation of BCMA CAR-Engineered ^{Allo}HSC-iNKT (^{Allo}BCAR-iNKT) Cells
  - *In Vitro* Generation of HLA-Ablated Universal HSC-iNKT (^{U}HSC-iNKT) Cells

- Generation of PBMC-Derived Conventional αβT, iNKT, γδT, and NK Cells
- Generation of BCMA CAR-Engineered PBMC T (BCAR-T) cells
- Single Cell TCR Sequencing
- Deep RNA Sequencing (Deep RNaseq) and Data Analysis
- ^{Allo}HSC-iNKT Cell Phenotype and Functional Study
- *In Vitro* Tumor Cell Killing Assay
- *In Vitro* Mixed Lymphocyte Reaction (MLR) Assay: Studying Graft-Versus-Host (GvH) Response
- *In Vitro* MLR Assay: Studying Host-Versus-Graft (HvG) Response
- *In Vitro* MLR Assay: Studying NK Cell-Mediated Allorejection
- Bioluminescence Live Animal Imaging (BLI)
- ^{Allo}HSC-iNKT Cell *In Vivo* Antitumor Efficacy Study: A375 Human Melanoma Xenograft NSG Mouse Model
- ^{Allo}BCAR-iNKT Cell *In Vivo* Antitumor Efficacy Study: MM.1S Human MM Xenograft NSG Mouse Model
- ^{U}BCAR-iNKT Cell *In Vivo* Antitumor Efficacy Study: MM.1S Human MM Xenograft NSG Mouse Model
- Ganciclovir (GCV) *In Vitro* and *In Vivo* Killing Assay
- Histological Analysis
- Statistical Analysis

SUPPLEMENTAL INFORMATION

Supplemental information can be found online at https://doi.org/10.1016/j.xcrm.2021.100449.

ACKNOWLEDGMENTS

We thank the University of California, Los Angeles (UCLA) animal facility for providing animal support; the UCLA Translational Pathology Core Laboratory (TPCL) for providing histology support; the UCLA Technology Center for Genomics & Bioinformatics (TCGB) facility for providing RNA-seq services; the UCLA CFAR Virology Core for providing human cells; and the UCLA BSCRC Flow Cytometry Core Facility for cell sorting support. This work was supported by a Director's New Innovator Award from the NIH (DP2 CA196335, to L.Y.), a Partnering Opportunity for Translational Research Projects Award and a Partnering Opportunity for Discovery Stage Award from the California Institute for Regenerative Medicine (CIRM TRAN1-08533 and DISC2-11157, to L.Y.), a Stem Cell Research Award from the Concern Foundation (to L.Y.), a Research Career Development Award from the STOP CANCER Foundation (to L.Y.), a BSCRC-RHF Research Award from the Rose Hills Research Foundation (to L.Y.), and an Ablon Scholars Award (to L.Y.). Y.-R.L. is a predoctoral fellow supported by the UCLA Whitcome predoctoral fellowship in molecular biology. J.Y. is a predoctoral fellow supported by the UCLA Broad Stem Cell Research Center (BSCRC) predoctoral fellowship. D.L. is a predoctoral fellow supported by T32 Microbial Pathogenesis Training Grant (Ruth L. Kirschstein National Research Service Award, T32-AI007323). Z.L. is a postdoctoral fellow supported by the UCLA Tumor Immunology Training Grant (USHHS Ruth L. Kirschstein Institutional National Research Service Award, T32-CA009120). S.Z. is a predoctoral fellow supported by the UCLA Medical Scientist Training Program Grant (T32-GM008042).

AUTHOR CONTRIBUTIONS

Y.-R.L., Y.Zhou, and L.Y. designed the experiments, analyzed the data, and wrote the manuscript. L.Y. conceived and oversaw the study, with assistance from Y.-R.L. and Y.Zhou and suggestions from G.M.C., S.M.L., M.P., A.R., D.B.K., O.N.W., and P.W. Y.-R.L. and Y.Z. performed all experiments, with assistance from Y.J.K., Y. Zhu, F.M., J.Y., Y.-C.W., X.C., Z.L., Z.S., XiWang, D.L., J.K., T.T., C.H., and J.H. D.C. performed cell sorting. A.M.-H. and C.S.S. helped with ATO culture. J.S. provided MM patient BM samples. F.M. helped with analysis of RNA-seq data. Xiaoyan Wang helped with the statistical analysis of data.

DECLARATION OF INTERESTS

Y.-R.L., Y.J.K., J.Y., P.W., Y. Zhu, G.M.C., A.M.-H., C.S.S., and L.Y. are inventors on patents relating to this study filed by UCLA. Y.J.K. is currently an employee of Nkarta. J.Y. and X.W. are currently employees of Appia Bio. X.C. is currently an employee of Atara Bio. Z.L. is currently an employee of Allogene. S.M.L. is a stockholder of 1200 Pharma and TORL BioTherapeutics. A.R. is a consultant for Amgen, Bristol-Meyers Squibb, Chugai, Genentech-Roche, Merck-MSD, Novartis, and Sanofi; a scientific advisory board member of and stockholder with Advaxis, Apricity, Arcus, Bioncotech, Compugen, CytomX, Five Prime, FLX-Bio, ImaginAb, Isoplexis, Kite-Gilead, Merus, Rgenix, and Appia Bio; and a co-founder and scientific advisory board member of Lutris, PACT Pharma, and Tango Therapeutics. J.S. is a consultant for Kite and on the speaker bureau for Kite and BMS. D.B.K. is a stockholder and scientific advisory board member of Allogene Therapeutics, Myogene Bio, ImmunoVec and Pluto Therapeutics. O.N.W. currently has consulting, equity, and/or board relationships with Trethera Corporation, Kronos Biosciences, Sofie Biosciences, Breakthrough Properties, Vida Ventures, Nammi Therapeutics, Two River, Iconovir, Appia BioSciences, Neogene Therapeutics, and Allogene Therapeutics. P.W. is a co-founder, stockholder, consultant, and advisory board member of HRain Biotechnology, TCRCure Biopharma, and Appia Bio. G.M.C., C.S.S., and A.M.-H. are cofounders and stockholders of Pluto Immunotherapeutics. L.Y. is a scientific advisor to AlzChem and Amberstone Biosciensec, and a co-founder, stockholder, and advisory board member of Appia Bio. None of the declared companies contributed to or directed any of the research reported in this article. The remaining authors declare no competing interests.

Received: January 28, 2021
Revised: August 12, 2021
Accepted: October 19, 2021
Published: November 16, 2021

REFERENCES

1. Restifo, N.P., Dudley, M.E., and Rosenberg, S.A. (2012). Adoptive immunotherapy for cancer: harnessing the T cell response. Nat. Rev. Immunol. *12*, 269–281.
2. Kalos, M., and June, C.H. (2013). Adoptive T cell transfer for cancer immunotherapy in the era of synthetic biology. Immunity *39*, 49–60.
3. Maus, M.V., Fraietta, J.A., Levine, B.L., Kalos, M., Zhao, Y., and June, C.H. (2014). Adoptive immunotherapy for cancer or viruses. Annu. Rev. Immunol. *32*, 189–225.
4. Labanieh, L., Majzner, R.G., and Mackall, C.L. (2018). Programming CAR-T cells to kill cancer. Nat. Biomed. Eng. *2*, 377–391.
5. Mikkilineni, L., and Kochenderfer, J.N. (2017). Chimeric antigen receptor T-cell therapies for multiple myeloma. Blood *130*, 2594–2602.
6. June, C.H., and Sadelain, M. (2018). Chimeric antigen receptor therapy. N. Engl. J. Med. *379*, 64–73.
7. Leko, V., and Rosenberg, S.A. (2020). Identifying and Targeting Human Tumor Antigens for T Cell-Based Immunotherapy of Solid Tumors. Cancer Cell *38*, 454–472.
8. Rosenberg, S.A., and Restifo, N.P. (2015). Adoptive cell transfer as personalized immunotherapy for human cancer. Science *348*, 62–68.
9. Lim, W.A., and June, C.H. (2017). The Principles of Engineering Immune Cells to Treat Cancer. Cell *168*, 724–740.
10. Benjamin, R., Graham, C., Yallop, D., Jozwik, A., Mirci-Danicar, O.C., Lucchini, G., Pinner, D., Jain, N., Kantarjian, H., Boissel, N., et al.; UCART19 Group (2020). Genome-edited, donor-derived allogeneic anti-CD19

chimeric antigen receptor T cells in paediatric and adult B-cell acute lymphoblastic leukaemia: results of two phase 1 studies. Lancet *396*, 1885–1894.

11. Qasim, W., Zhan, H., Samarasinghe, S., Adams, S., Amrolia, P., Stafford, S., Butler, K., Rivat, C., Wright, G., Somana, K., et al. (2017). Molecular remission of infant B-ALL after infusion of universal TALEN gene-edited CAR T cells. Sci. Transl. Med. *9*, 1–9.
12. Stadtmauer, E.A., Fraietta, J.A., Davis, M.M., Cohen, A.D., Weber, K.L., Lancaster, E., et al. (2020). CRISPR-engineered T cells in patients with refractory cancer. Science *367*, 1–20.
13. Benjamin, R., Graham, C., Yallop, D., Jozwik, A., Ciocarlie, O., Jain, N., et al. (2018). Preliminary Data on Safety, Cellular Kinetics and Anti-Leukemic Activity of UCART19, an Allogeneic Anti-CD19 CAR T-Cell Product, in a Pool of Adult and Pediatric Patients with High-Risk CD19+ Relapsed/Refractory B-Cell Acute Lymphoblastic Leukemia. Blood *132* (*Supplement 1*), 896.
14. Basar, R., Daher, M., and Rezvani, K. (2020). Next-generation cell therapies: the emerging role of CAR-NK cells. Blood Adv. *4*, 5868–5876.
15. Becker, P.S.A., Suck, G., Nowakowska, P., Ullrich, E., Seifried, E., Bader, P., Tonn, T., and Seidl, C. (2016). Selection and expansion of natural killer cells for NK cell-based immunotherapy. Cancer Immunol. Immunother. *65*, 477–484.
16. Bendelac, A., Savage, P.B., and Teyton, L. (2007). The biology of NKT cells. Annu. Rev. Immunol. *25*, 297–336.
17. Haraguchi, K., Takahashi, T., Hiruma, K., Kanda, Y., Tanaka, Y., Ogawa, S., Chiba, S., Miura, O., Sakamaki, H., and Hirai, H. (2004). Recovery of Valpha24+ NKT cells after hematopoietic stem cell transplantation. Bone Marrow Transplant. *34*, 595–602.
18. Fujii, S., Shimizu, K., Okamoto, Y., Kunii, N., Nakayama, T., Motohashi, S., et al. (2013). NKT cells as an ideal anti-tumor immunotherapeutic. Front. Immunol. *4*, 1–7.
19. de Lalla, C., Rinaldi, A., Montagna, D., Azzimonti, L., Bernardo, M.E., Sangalli, L.M., Paganoni, A.M., Maccario, R., Di Cesare-Merlone, A., Zecca, M., et al. (2011). Invariant NKT cell reconstitution in pediatric leukemia patients given HLA-haploidentical stem cell transplantation defines distinct CD4+ and CD4- subset dynamics and correlates with remission state. J. Immunol. *186*, 4490–4499.
20. Chaidos, A., Patterson, S., Szydlo, R., Chaudhry, M.S., Dazzi, F., Kanfer, E., McDonald, D., Marin, D., Milojkovic, D., Pavlu, J., et al. (2012). Graft invariant natural killer T-cell dose predicts risk of acute graft-versus-host disease in allogeneic hematopoietic stem cell transplantation. Blood *119*, 5030–5036.
21. Rubio, M.T., Bouillié, M., Bouazza, N., Coman, T., Trebeden-Nègre, H., Gomez, A., Suarez, F., Sibon, D., Brignier, A., Paubelle, E., et al. (2017). Pre-transplant donor CD4^{-} invariant NKT cell expansion capacity predicts the occurrence of acute graft-versus-host disease. Leukemia *31*, 903–912.
22. Bae, E.A., Seo, H., Kim, I.K., Jeon, I., and Kang, C.Y. (2019). Roles of NKT cells in cancer immunotherapy. Arch. Pharm. Res. *42*, 543–548.
23. Exley, M.A., Friedlander, P., Alatrakchi, N., Vriend, L., Yue, S., Sasada, T., Zeng, W., Mizukami, Y., Clark, J., Nemer, D., et al. (2017). Adoptive transfer of invariant NKT cells as immunotherapy for advanced melanoma: A phase I clinical trial. Clin. Cancer Res. *23*, 3510–3519.
24. Kitayama, S., Zhang, R., Liu, T.Y., Ueda, N., Iriguchi, S., Yasui, Y., Kawai, Y., Tatsumi, M., Hirai, N., Mizoro, Y., et al. (2016). Cellular Adjuvant Properties, Direct Cytotoxicity of Re-differentiated Vα24 Invariant NKT-like Cells from Human Induced Pluripotent Stem Cells. Stem Cell Reports *6*, 213–227.
25. Rotolo, A., Caputo, V.S., Holubova, M., Baxan, N., Dubois, O., Chaudhry, M.S., Xiao, X., Goudevenou, K., Pitcher, D.S., Petevi, K., et al. (2018). Enhanced Anti-lymphoma Activity of CAR19-iNKT Cells Underpinned by Dual CD19 and CD1d Targeting. Cancer Cell *34*, 596–610.e11.
26. Krijgsman, D., Hokland, M., and Kuppen, P.J.K. (2018). The role of natural killer T cells in cancer-A phenotypical and functional approach. Front. Immunol. *9*, 367.
27. Smith, D.J., Liu, S., Ji, S., Li, B., McLaughlin, J., Cheng, D., Witte, O.N., and Yang, L. (2015). Genetic engineering of hematopoietic stem cells to generate invariant natural killer T cells. Proc. Natl. Acad. Sci. USA *112*, 1523–1528.
28. Zhu, Y., Smith, D.J., Zhou, Y., Li, Y.R., Yu, J., Lee, D., Wang, Y.C., Di Biase, S., Wang, X., Hardoy, C., et al. (2019). Development of Hematopoietic Stem Cell-Engineered Invariant Natural Killer T Cell Therapy for Cancer. Cell Stem Cell *25*, 542–557.e9.
29. Seet, C.S., He, C., Bethune, M.T., Li, S., Chick, B., Gschweng, E.H., Zhu, Y., Kim, K., Kohn, D.B., Baltimore, D., et al. (2017). Generation of mature T cells from human hematopoietic stem and progenitor cells in artificial thymic organoids. Nat. Methods *14*, 521–530.
30. Montel-Hagen, A., Seet, C.S., Li, S., Chick, B., Zhu, Y., Chang, P., Tsai, S., Sun, V., Lopez, S., Chen, H.C., et al. (2019). Organoid-Induced Differentiation of Conventional T Cells from Human Pluripotent Stem Cells. Cell Stem Cell *24*, 376–389.e8.
31. Godfrey, D.I., and Berzins, S.P. (2007). Control points in NKT-cell development. Nat. Rev. Immunol. *7*, 505–518.
32. Lee, P.T., Benlagha, K., Teyton, L., and Bendelac, A. (2002). Distinct functional lineages of human V(α)24 natural killer T cells. J. Exp. Med. *195*, 637–641.
33. Gumperz, J.E., Miyake, S., Yamamura, T., and Brenner, M.B. (2002). Functionally distinct subsets of CD1d-restricted natural killer T cells revealed by CD1d tetramer staining. J. Exp. Med. *195*, 625–636.
34. Fujii, S., Liu, K., Smith, C., Bonito, A.J., and Steinman, R.M. (2004). The linkage of innate to adaptive immunity via maturing dendritic cells in vivo requires CD40 ligation in addition to antigen presentation and CD80/86 costimulation. J. Exp. Med. *199*, 1607–1618.
35. Fujii, S., Shimizu, K., Hemmi, H., and Steinman, R.M. (2007). Innate Valpha14(+) natural killer T cells mature dendritic cells, leading to strong adaptive immunity. Immunol. Rev. *220*, 183–198.
36. Lam, P.Y., Nissen, M.D., and Mattarollo, S.R. (2017). Invariant natural killer T cells in immune regulation of blood cancers: Harnessing their potential in immunotherapies. Front. Immunol. *8*, 1355.
37. Menon, V. (2018). Clustering single cells: a review of approaches on high- and low-depth single-cell RNA-seq data. Brief. Funct. Genomics *17*, 240–245.
38. Alonzo, E.S., and Sant'Angelo, D.B. (2011). Development of PLZF-expressing innate T cells. Curr. Opin. Immunol. *23*, 220–227.
39. Zhang, Y., Zhang, Y., Gu, W., and Sun, B. (2014). TH1/TH2 cell differentiation and molecular signals. Adv. Exp. Med. Biol. *841*, 15–44.
40. Gagliani, N., and Huber, S. (2017). Basic aspects of T helper cell differentiation. Methods Mol. Biol. *1514*, 19–30.
41. Cartwright, T., Perkins, N.D., and L Wilson, C. (2016). NFKB1: a suppressor of inflammation, ageing and cancer. FEBS J. *283*, 1812–1822.
42. Riera-Sans, L., and Behrens, A. (2007). Regulation of alphabeta/gammadelta T cell development by the activator protein 1 transcription factor c-Jun. J. Immunol. *178*, 5690–5700.
43. Park, J.Y., DiPalma, D.T., Kwon, J., Fink, J., and Park, J.H. (2019). Quantitative Difference in PLZF Protein Expression Determines iNKT Lineage Fate and Controls Innate CD8 T Cell Generation. Cell Rep. *27*, 2548–2557.e4.
44. Kovalovsky, D., Uche, O.U., Eladad, S., Hobbs, R.M., Yi, W., Alonzo, E., Chua, K., Eidson, M., Kim, H.J., Im, J.S., et al. (2008). The BTB-zinc finger transcriptional regulator PLZF controls the development of invariant natural killer T cell effector functions. Nat. Immunol. *9*, 1055–1064.
45. Matsuda, J.L., Zhang, Q., Ndonye, R., Richardson, S.K., Howell, A.R., and Gapin, L. (2006). T-bet concomitantly controls migration, survival, and effector functions during the development of Valpha14i NKT cells. Blood *107*, 2797–2805.

46. Vivier, E., Ugolini, S., Blaise, D., Chabannon, C., and Brossay, L. (2012). Targeting natural killer cells and natural killer T cells in cancer. Nat. Rev. Immunol. *12*, 239–252.
47. Thomas, S.Y., Hou, R., Boyson, J.E., Means, T.K., Hess, C., Olson, D.P., Strominger, J.L., Brenner, M.B., Gumperz, J.E., Wilson, S.B., and Luster, A.D. (2003). CD1d-restricted NKT cells express a chemokine receptor profile indicative of Th1-type inflammatory homing cells. J. Immunol. *171*, 2571–2580.
48. Fürst, D., Neuchel, C., Tsamadou, C., Schrezenmeier, H., and Mytilineos, J. (2019). HLA Matching in Unrelated Stem Cell Transplantation up to Date. Transfus. Med. Hemother. *46*, 326–336.
49. Ozdemir, Z.N., and Civriz Bozdağ, S. (2018). Graft failure after allogeneic hematopoietic stem cell transplantation. Transfus. Apheresis Sci. *57*, 163–167.
50. Lee, H.H., Kang, H., and Cho, H. (2017). Natural killer cells and tumor metastasis. Arch. Pharm. Res. *40*, 1037–1049.
51. Liu, H., Wang, S., Xin, J., Wang, J., Yao, C., and Zhang, Z. (2019). Role of NKG2D and its ligands in cancer immunotherapy. Am. J. Cancer Res. *9*, 2064–2078.
52. Paul, S., and Lal, G. (2017). The molecular mechanism of natural killer cells function and its importance in cancer immunotherapy. Front. Immunol. *8*, 1124.
53. Del Zotto, G., Marcenaro, E., Vacca, P., Sivori, S., Pende, D., Della Chiesa, M., Moretta, F., Ingegnere, T., Mingari, M.C., Moretta, A., and Moretta, L. (2017). Markers and function of human NK cells in normal and pathological conditions. Cytometry B Clin. Cytom. *92*, 100–114.
54. Ewen, E.M., Pahl, J.H.W., Miller, M., Watzl, C., and Cerwenka, A. (2018). KIR downregulation by IL-12/15/18 unleashes human NK cells from KIR/HLA-I inhibition and enhances killing of tumor cells. Eur. J. Immunol. *48*, 355–365.
55. Dominguez, E., Lowdell, M.W., Perez-Cruz, I., Madrigal, A., and Cohen, S.B.A. (1997). Natural killer cell function is altered by freezing in DMSO. Biochem. Soc. Trans. *25*, 175S.
56. Li, R., Johnson, R., Yu, G., McKenna, D.H., and Hubel, A.; LI RUI (2019). Preservation of cell-based immunotherapies for clinical trials. Cytotherapy *21*, 943–957.
57. Luo, Y., Wang, P., Liu, H., Zhu, Z., Li, C., and Gao, Y. (2017). The state of T cells before cryopreservation: Effects on post-thaw proliferation and function. Cryobiology *79*, 65–70.
58. Timmers, M., Roex, G., Wang, Y., Campillo-Davo, D., Van Tendeloo, V.F.I., Chu, Y., Berneman, Z.N., Luo, F., Van Acker, H.H., and Anguille, S. (2019). Chimeric antigen receptor-modified T cell therapy in multiple myeloma: Beyond B cell maturation antigen. Front. Immunol. *10*, 1613.
59. Liu, Y., Chen, Z., Fang, H., Wei, R., Yu, K., Jiang, S., et al. (2018). Durable Remission Achieved from Bcma-Directed CAR-T Therapy Against Relapsed or Refractory Multiple Myeloma. Blood *132* (*Supplement 1*), 956.
60. Cohen, A.D. (2018). CAR T Cells and Other Cellular Therapies for Multiple Myeloma: 2018 Update. Am. Soc. Clin. Oncol. Educ. Book *38*, e6–e15.
61. Brudno, J.N., Maric, I., Hartman, S.D., Rose, J.J., Wang, M., Lam, N., Stetler-Stevenson, M., Salem, D., Yuan, C., Pavletic, S., et al. (2018). T cells genetically modified to express an anti–B-Cell maturation antigen chimeric antigen receptor cause remissions of poor-prognosis relapsed multiple myeloma. J. Clin. Oncol. *36*, 2267–2280.
62. Cohen, A.D., Garfall, A.L., Stadtmauer, E.A., Melenhorst, J.J., Lacey, S.F., Lancaster, E., Vogl, D.T., Weiss, B.M., Dengel, K., Nelson, A., et al. (2019). B cell maturation antigen-specific CAR T cells are clinically active in multiple myeloma. J. Clin. Invest. *129*, 2210–2221.
63. Neelapu, S.S., Tummala, S., Kebriaei, P., Wierda, W., Gutierrez, C., Locke, F.L., Komanduri, K.V., Lin, Y., Jain, N., Daver, N., et al. (2018). Chimeric antigen receptor T-cell therapy - assessment and management of toxicities. Nat. Rev. Clin. Oncol. *15*, 47–62.
64. Candolfi, M., Kroeger, K.M., Muhammad, A.K., Yagiz, K., Farrokhi, C., Pechnick, R.N., Lowenstein, P.R., and Castro, M.G. (2009). Gene therapy for brain cancer: combination therapies provide enhanced efficacy and safety. Curr. Gene Ther. *9*, 409–421.
65. Straathof, K.C., Pulè, M.A., Yotnda, P., Dotti, G., Vanin, E.F., Brenner, M.K., Heslop, H.E., Spencer, D.M., and Rooney, C.M. (2005). An inducible caspase 9 safety switch for T-cell therapy. Blood *105*, 4247–4254.
66. Thomis, D.C., Marktel, S., Bonini, C., Traversari, C., Gilman, M., Bordignon, C., and Clackson, T. (2001). A Fas-based suicide switch in human T cells for the treatment of graft-versus-host disease. Blood *97*, 1249–1257.
67. Watanabe, K., Kuramitsu, S., Posey, A.D., Jr., and June, C.H. (2018). Expanding the therapeutic window for CAR T cell therapy in solid tumors: The knowns and unknowns of CAR T cell biology. Front. Immunol. *9*, 2486.
68. Lanza, R., Russell, D.W., and Nagy, A. (2019). Engineering universal cells that evade immune detection. Nat. Rev. Immunol. *19*, 723–733.
69. Ren, J., Liu, X., Fang, C., Jiang, S., June, C.H., and Zhao, Y. (2017). Multiplex genome editing to generate universal CAR T cells resistant to PD1 inhibition. Clin. Cancer Res. *23*, 2255–2266.
70. Steimle, V., Siegrist, C.A., Mottet, A., Lisowska-Grospierre, B., and Mach, B. (1994). Regulation of MHC class II expression by interferon-γ mediated by the transactivator gene CIITA. Science *265*, 106–109.
71. Axelrod, M.L., Cook, R.S., Johnson, D.B., and Balko, J.M. (2019). Biological consequences of MHC-II expression by tumor cells in cancer. Clin. Cancer Res. *25*, 2392–2402.
72. Castro, F., Cardoso, A.P., Gonçalves, R.M., Serre, K., and Oliveira, M.J. (2018). Interferon-gamma at the crossroads of tumor immune surveillance or evasion. Front. Immunol. *9*, 847.
73. Torikai, H., Reik, A., Soldner, F., Warren, E.H., Yuen, C., Zhou, Y., Crossland, D.L., Huls, H., Littman, N., Zhang, Z., et al. (2013). Toward eliminating HLA class I expression to generate universal cells from allogeneic donors. Blood *122*, 1341–1349.
74. Braud, V.M., Allan, D.S., O'Callaghan, C.A., Söderström, K., D'Andrea, A., Ogg, G.S., Lazetic, S., Young, N.T., Bell, J.I., Phillips, J.H., et al. (1998). HLA-E binds to natural killer cell receptors CD94/NKG2A, B and C. Nature *391*, 795–799.
75. Cosman, D., Müllberg, J., Sutherland, C.L., Chin, W., Armitage, R., Fanslow, W., Kubin, M., and Chalupny, N.J. (2001). ULBPs, novel MHC class I-related molecules, bind to CMV glycoprotein UL16 and stimulate NK cytotoxicity through the NKG2D receptor. Immunity *14*, 123–133.
76. Abrahimi, P., Chang, W.G., Kluger, M.S., Qyang, Y., Tellides, G., Saltzman, W.M., and Pober, J.S. (2015). Efficient gene disruption in cultured primary human endothelial cells by CRISPR/Cas9. Circ. Res. *117*, 121–128.
77. Aftab, B.T., Sasu, B., Krishnamurthy, J., Gschweng, E., Alcazer, V., and Depil, S. (2020). Toward "off-the-shelf" allogeneic CAR T cells. Adv. Cell Gene Ther. *3*, 1–11.
78. Liu, E., Marin, D., Banerjee, P., Macapinlac, H.A., Thompson, P., Basar, R., Nassif Kerbauy, L., Overman, B., Thall, P., Kaplan, M., et al. (2020). Use of CAR-Transduced Natural Killer Cells in CD19-Positive Lymphoid Tumors. N. Engl. J. Med. *382*, 545–553.
79. Heczey, A., Courtney, A.N., Montalbano, A., Robinson, S., Liu, K., Li, M., Ghatwai, N., Dakhova, O., Liu, B., Raveh-Sadka, T., et al. (2020). Anti-GD2 CAR-NKT cells in patients with relapsed or refractory neuroblastoma: an interim analysis. Nat. Med. *26*, 1686–1690.
80. Heczey, A., Liu, D., Tian, G., Courtney, A.N., Wei, J., Marinova, E., Gao, X., Guo, L., Yvon, E., Hicks, J., et al. (2014). Invariant NKT cells with chimeric antigen receptor provide a novel platform for safe and effective cancer immunotherapy. Blood *124*, 2824–2833.
81. Deniger, D.C., Moyes, J.S., and Cooper, L.J.N. (2014). Clinical applications of gamma delta T cells with multivalent immunity. Front. Immunol. *5*, 636.
82. Li, Y.-R., Zhou, Y., Kramer, A., and Yang, L. (2021). Engineering stem cells for cancer immunotherapy. Trends Cancer, S2405-8033(21)00171-0.

83. Zhou, Y., Li, Y.-R., Zeng, S., and Yang, L. (2021). Methods for Studying Mouse and Human Invariant Natural Killer T Cells. Methods Mol. Biol. *2388*, 35–57.

84. Kunii, N., Horiguchi, S., Motohashi, S., Yamamoto, H., Ueno, N., Yamamoto, S., Sakurai, D., Taniguchi, M., Nakayama, T., and Okamoto, Y. (2009). Combination therapy of in vitro-expanded natural killer T cells and α-galactosylceramide-pulsed antigen-presenting cells in patients with recurrent head and neck carcinoma. Cancer Sci. *100*, 1092–1098.

85. Motohashi, S., Nagato, K., Kunii, N., Yamamoto, H., Yamasaki, K., Okita, K., Hanaoka, H., Shimizu, N., Suzuki, M., Yoshino, I., et al. (2009). A phase I-II study of α-galactosylceramide-pulsed IL-2/GM-CSF-cultured peripheral blood mononuclear cells in patients with advanced and recurrent non-small cell lung cancer. J. Immunol. *182*, 2492–2501.

86. Yamasaki, K., Horiguchi, S., Kurosaki, M., Kunii, N., Nagato, K., Hanaoka, H., Shimizu, N., Ueno, N., Yamamoto, S., Taniguchi, M., et al. (2011). Induction of NKT cell-specific immune responses in cancer tissues after NKT cell-targeted adoptive immunotherapy. Clin. Immunol. *138*, 255–265.

87. Gordy, L.E., Bezbradica, J.S., Flyak, A.I., Spencer, C.T., Dunkle, A., Sun, J., Stanic, A.K., Boothby, M.R., He, Y.W., Zhao, Z., et al. (2011). IL-15 regulates homeostasis and terminal maturation of NKT cells. J. Immunol. *187*, 6335–6345.

88. Bae, E.A., Seo, H., Kim, B.S., Choi, J., Jeon, I., Shin, K.S., Koh, C.H., Song, B., Kim, I.K., Min, B.S., et al. (2018). Activation of NKT cells in an anti-PD-1–resistant tumor model enhances antitumor immunity by reinvigorating exhausted CD8 T cells. Cancer Res. *78*, 5315–5326.

89. Verzeletti, S., Bonini, C., Marktel, S., Nobili, N., Ciceri, F., Traversari, C., et al. (1998). Herpes Simplex Virus Thymidine Kinase Gene Transfer for Controlled Graft-versus-Host Disease and Leukemia: Clinical Follow-up and Improved New Vectors. Hum. Gene Ther. *9*, 2243–2251.

90. Lee, N., Llano, M., Carretero, M., Ishitani, A., Navarro, F., López-Botet, M., and Geraghty, D.E. (1998). HLA-E is a major ligand for the natural killer inhibitory receptor CD94/NKG2A. Proc. Natl. Acad. Sci. USA *95*, 5199–5204.

STAR★METHODS

KEY RESOURCES TABLE

REAGENT or RESOURCE	SOURCE	IDENTIFIER
Antibodies		
Anti-human IFN-γ (ELISA, capture)	BD Biosciences	CAT#551221, RRID: AB_394099
Anti-human IFN-γ (ELISA, detection)	BD Biosciences	CAT#554550, RRID: AB_395472
Anti-human TNFα (ELISA, capture)	BD Biosciences	CAT#551220, RRID: AB_394098
Anti-human TNFα (ELISA, detection)	BD Biosciences	CAT#554511, RRID: AB_395442
Anti-human IL-2 (ELISA, detection)	BD Biosciences	CAT#554563; RRID: AB_398570
Anti-human IL-2 (ELISA, detection)	BD Biosciences	CAT#555040; RRID: AB_395666
Anti-human IL-4 (ELISA, capture)	BD Biosciences	CAT#554515; RRID: AB_398567
Anti-human IL-4 (ELISA, detection)	BD Biosciences	CAT#554483; RRID: AB_395422
Anti-human CD45 (Clone H130)	Biolegend	CAT#304026, RFID: AB_893337
Anti-human TCRαβ (Clone I26)	Biolegend	CAT#306716, RRID: AB_1953257
Anti-human CD4 (Clone OKT4)	Biolegend	CAT#317414, RRID: AB_571959
Anti-human CD8 (Clone SK1)	Biolegend	CAT#344714, RRID: AB_2044006
Anti-human CD45RO (Clone UCHL1)	Biolegend	CAT#304216, RRID: AB_493659
Anti-human CD161 (Clone HP-3G10)	Biolegend	CAT#339928, RRID: AB_2563967
Anti-human CD69 (Clone FN50)	Biolegend	CAT#310914, RRID: AB_314849
Anti-human CD56 (Clone HCD56)	Biolegend	CAT#318304, RRID: AB_604100
Anti-human CD62L (Clone DREG-56)	Biolegend	CAT#304822, RRID: AB_830801
Anti-human CD14 (Clone HCD14)	Biolegend	CAT#325608, RRID: AB_830681
Anti-human CD11b (Clone ICRF44)	Biolegend	CAT#301330, RRID: AB_2561703
Anti-human CD11c (Clone N418)	Biolegend	CAT#337234, RRID: AB_2566656
Anti-human CD1d (Clone 51.1)	Biolegend	CAT#350308, RRID: AB_10642829
Anti-human CCR4 (Clone L291H4)	Biolegend	CAT#359409, RRID: AB_2562430
Anti-human CCR5 (Clone HEK/1/85a)	Biolegend	CAT#313705, RRID: AB_345305
Anti-human CXCR3 (Clone G025H7)	Biolegend	CAT#306513, RRID: AB_2089652
Anti-human NKG2D (Clone 1D11)	Biolegend	CAT#320812, RRID: AB_2234394
Anti-human DNAM-1 (Clone 11A8)	Biolegend	CAT#338312, RRID: AB_2561952
Anti-human CD158 (KIR2DL1/S1/S3/S5) (Clone HP-MA4)	Biolegend	CAT#339510, RRID: AB_2565577
Anti-human IFN-γ (Clone B27)	Biolegend	CAT#506518, RRID: AB_2123321
Anti-human granzyme B (Clone QA16A02)	Biolegend	CAT#372204, RRID: AB_2687028
Anti-human perforin (Clone dG9)	Biolegend	CAT#308126, RRID: AB_2572049
Anti-human TNFα (Clone Mab11)	Biolegend	CAT#502912, RRID: AB_315264
Anti-human IL-2 (Clone MQ1-17H12)	Biolegend	CAT#500341, RRID: AB_2562854
Anti-human HLAE (Clone 3D12)	Biolegend	CAT#342606, RRID: AB_342606
Anti-human β2-microglobulin (B2M) (Clone 2M2)	Biolegend	CAT#316312, RRID: AB_10641281
Anti-human HLA-DR (Clone L243)	Biolegend	CAT#307618, RRID: AB_493586
Anti-human TCR Vδ2 (Clone B6)	Biolegend	CAT#331417, RRID: AB_2687323
Anti-human CD107a (Clone H4A3)	Biolegend	CAT#328641, RRID: AB_2565965
Anti-human CD34 (Clone 581)	BD Biosciences	CAT#555822, RRID: AB_396151
Anti-human TCR Vα24-Jβ18 (Clone 6B11)	BD Biosciences	CAT#552825, RRID: AB_394478
Anti-human ULBP-2,5,6 (Clone 165903)	R&D Systems	CAT#FAB1298A, RRID: AB_ 2257142
Anti-human Vβ11	Beckman-Coulter	CAT#A66905

(*Continued on next page*)

Continued

REAGENT or RESOURCE	SOURCE	IDENTIFIER
Human Fc Receptor Blocking Solution (TrueStain FcX)	Biolegend	CAT#422302
Mouse Fc Block (anti-mouse CD16/32)	BD Biosciences	CAT#553142, RRID: AB_394657
β-2-Microglobulin Antibody (Clone BBM.1)	Santa Cruz Biotechnology	CAT#sc-13565
LEAF purified anti-human CD1d antibody (Clone 51.1)	Biolegend	CAT#350304
LEAF purified Mouse IgG2b, k isotype ctrl (Clone MG2b-57)	Biolegend	CAT#401212
LEAF purified anti-human NKG2D antibody (Clone 1D11)	Biolegend	CAT#320810, RRID: AB_2133276
LEAF purified anti-human DNAM-1 antibody (Clone DX11)	BD Biosciences	CAT#559786, RRID: AB_397327
Mouse IgG1, κ isotype control antibody (Clone MOPC-21)	Biolegend	CAT#400124
Bacterial and virus strains		
Lenti/iNKT-sr39TK	This paper	N/A
Lenti/BCAR-iNKT-sr39TK	This paper	N/A
Lenti/FG	This paper	N/A
Lenti/CD1d	This paper	N/A
Retro/BCMA-CAR-tEGFR	This paper	N/A
Biological samples		
Human peripheral blood mononuclear cells (PBMCs)	UCLA	N/A
Human cord blood CD34+ hematopoietic stem and progenitor cells (HSCs)	UCLA	N/A
Human multiple myeloma patient bone marrow samples	UCLA	N/A
G-CSF-mobilized peripheral blood units	CCHMC	CAT#M001F-GCSF-3
G-CSF-mobilized leukopak	HemaCare	CAT#M001CLPG-4-KIT
Cord Blood Cryo CD34	HemaCare	CAT#CB34C-3
Chemicals, peptides, and recombinant proteins		
Streptavidin-HRP conjugate	Invitrogen	CAT#SA10001
IFN-γ (ELISA, standard)	eBioscience	CAT#29-8319-65
TNFα (ELISA, standard)	eBioscience	CAT#29-8329-65
IL-2 (ELISA, standard)	eBioscience	CAT#29-8029-65
IL-4 (ELISA, standard)	eBioscience	CAT#39-8049-65
IL-17 (ELISA, standard)	eBioscience	CAT#29-8179-65
Tetramethylbenzidine (TMB)	KPL	CAT#5120-0053
Ganciclovir (GCV)	Sigma	CAT#ADV465749843
α-Galactosylceramide (KRN7000)	Avanti Polar Lipids	SKU#867000P-1mg
Zoledronate	Sigma-Aldrich	CAT#SML0223
Recombinant human IL-2	Peprotech	CAT#200-02
Recombinant human IL-3	Peprotech	CAT#200-03
Recombinant human IL-7	Peprotech	CAT#200-07
Recombinant human IL-15	Peprotech	CAT#200-15
Recombinant human Flt3-Ligand	Peprotech	CAT#300-19
Recombinant human SCF	Peprotech	CAT#300-07
Recombinant human TPO	Peprotech	CAT#300-18
Recombinant human GM-CSF	Peprotech	CAT#300-03

(*Continued on next page*)

Continued

REAGENT or RESOURCE	SOURCE	IDENTIFIER
L-ascorbic acid 2-phosphate	Sigma	CAT#A8960-5G
B27™ Supplement (50X), serum free	ThermoFisher	CAT#17504044
Cas9-NLS purified protein	UC Berkeley	N/A
X-VIVO 15 Serum-free Hematopoietic Cell Medium	Lonza	CAT#04-418Q
RPMI1640 cell culture medium	Corning Cellgro	CAT#10-040-CV
DMEM cell culture medium	Corning Cellgro	CAT#10-013-CV
Fetal Bovine Serum (FBS)	Sigma	CAT#F2442
MACS BSA stock solution	Miltenyi	CAT#130-091-376
30% BSA	Gemini	CAT#50-753-3079
Penicillin-Streptomycine-Glutamine (P/S/G)	GIBCO	CAT#10378016
Penicillin: streptomycin (pen:strep) solution (P/S)	Gemini Bio-products	CAT#400-109
MEM non-essential amino acids (NEAA)	GIBCO	CAT#11140050
HEPES Buffer Solution	GIBCO	CAT#15630056
Sodium Pyruvate	GIBCO	CAT#11360070
Beta-Mercaptoethanol	Sigma	SKU#M6250
Normocin	Invivogen	CAT#ant-nr-2
Fixable Viability Dye eFluor506	affymetrix eBioscience	CAT#65-0866-14
Cell Fixation/Permeabilization Kit	BD Biosciences	CAT#554714
RetroNectin recombination human fibronectin fragment, 2.5mg	Takara	CAT#T100B
10% neutral-buffered formalin	Richard-Allan Scientific	CAT#5705
D-Luciferin	Caliper LIfe Science	CAT#XR-1001
Isoflurane	Zoetis	CAT#50019100
Phosphate Buffered Saline (PBS) pH 7.4 (1X)	GIBCO	CAT#10010-023
Formaldehyde	Sigma-Aldrich	CAT#F8775
Golgistop Protein Transport Inhibitor	BD Biosciences	CAT#554724
Phorbol-12-myristate-13-acetate (PMA)	Calbiochem	CAT#524400
Ionomycin, Calcium salt, Streptomyces conglobatus	Calbiochem	CAT#407952
Critical commercial assays		
Human NK Cell Isolation Kit	Miltenyi Biotec	CAT#130-092-657
Human CD34 MicroBeads Kit	Miltenyi Biotec	CAT#130-046-703
Human CD14 MicroBeads Kit	Miltenyi Biotec	CAT#130-050-201
Human Anti-iNKT MicroBeads	Miltenyi Biotec	CAT#130-094-842
Human Anti-HLA-DR MicroBeads	Miltenyi Biotec	CAT#130-046-101
Fixation/Permeabilization Solution Kit	BD Sciences	CAT#55474
Amaxa™ P3 Primary Cell 4D-Nucleofector™ X Kit S	Lonza	CAT#V4XP-3032
Dynabeads Human T-Activator CD3/CD28	ThermoFisher	CAT#111.61D
miRNeasy Mini Kit	QIAGEN	CAT#217004
Chromium single cell V(D)J enrichment kit, human T cell	10 x Genomics	CAT#1000005
Cryostor cell cryopreservation media	Sigma	CAT#C2874-100ML
Human IL-17A ELISA MAX Deluxe Kit	Biolegend	CAT#433915

(*Continued on next page*)

Continued

REAGENT or RESOURCE	SOURCE	IDENTIFIER
Deposited data		
Deep RNA sequencing	This paper	Gene Expression Omnibus Database: GSE164425
Single cell TCR sequencing	This paper	Gene Expression Omnibus Database: GSE164500
Experimental models: Cell lines		
Human multiple myeloma (MM) cell line MM.1S	ATCC	CRL-2974
Human chronic myelogenous leukemia cancer cell line K562	ATCC	CCL-243
Human melanoma cell line A375	ATCC	CRL-1619
Human adenocarcinoma cell line PC3	ATCC	CRL-1435
Human mucoepidermoid pulmonary carcinoma H292	ATCC	CRL-1848
Mus musculus Leukemia packaging cell PG13	ATCC	CRL-10686
Human multiple myeloma (MM) cell line MM.1S-FG	This paper	N/A
Human multiple myeloma (MM) cell line MM.1S-CD1d-FG	This paper	N/A
Human chronic myelogenous leukemia cancer cell line K562-FG	This paper	N/A
Human adenocarcinoma cell line PC3-FG	This paper	N/A
Human mucoepidermoid pulmonary carcinoma H292-FG	This paper	N/A
Human melanoma cell line A375-FG	This paper	N/A
Mus musculus Leukemia packaging cell PG13-BCAR-tEGFR	This paper	N/A
Mouse bone marrow derived stromal cell line MS5-hDLL4	Amelie et al., 2019	N/A
Experimental models: Organisms/strains		
NOD.Cg-Prkdcscid Il2rgtm1Wjl/SzJ (NSG)	The Jackson Laboratory	Stock #: 005557
Oligonucleotides		
gRNA (B2M): CGCGAGCACAGCUAA GGCCA	Synthego	N/A
gRNA (CIITA): GAUAUUGGCAUAAGC CUCCC	Synthego	N/A
Recombinant DNA		
Vector: parental lentivector pMNDW	N/A	N/A
Vector: parental retrovector pMP71	N/A	N/A
Software and algorithms		
FlowJo Software	FlowJo	https://www.flowjo.com/solutions/flowjo/downloads
Living Imaging 2.50 software	Xenogen/PerkinElmer	https://www.perkinelmer.com/lab-products-and-services/resources/in-vivo-imaging-software-downloads.html
AURA imaging software	Spectral Instruments Imaging	https://spectralinvivo.com/software/
I-control 1.7 Microplate Reader Software	Tecan	https://www.selectscience.net/tecan/i-control-microplate-reader-software/81307
ImageJ	ImageJ	https://imagej.net/Downloads

(*Continued on next page*)

Continued		
REAGENT or RESOURCE	SOURCE	IDENTIFIER
Prism 6	Graphpad	https://www.graphpad.com/scientific-software/prism/
MATLAB	The MathWorks, Inc	https://www.mathworks.com/products/matlab.html
R	R	http://www.R-project.org/

RESOURCE AVAILABILITY

Lead contact

Further information and requests for new reagents generated in this study may be directed to, and will be fulfilled by the Lead Contact, Lili Yang (liliyang@ucla.edu).

Materials availability

All unique/stable reagents generated in this study are available from the Lead Contact with a completed Materials Transfer Agreement.

Data and code availability

- The genomics data generated during this study are available from the public repository Gene Expression Omnibus Database: GSE164425, GSE164500.
- All data reported in this manuscript are available from the Lead Contact without restriction
- No custom computer code was reported in this manuscript.
- Any additional information required to reanalyze the data reported in this work paper is available from the Lead Contact upon request.

EXPERIMENTAL MODEL AND SUBJECT DETAILS

Mice

NOD.Cg-Prkdc^{SCID}Il2rg^{tm1Wjl}/SzJ (NOD/SCID/IL-2R$\gamma^{-/-}$, NSG) mice were maintained in the animal facilities of the University of California, Los Angeles (UCLA). 6-10 weeks old mice were used for all experiments unless otherwise indicated. All animal experiments were approved by the Institutional Animal Care and Use Committee of UCLA. All mice were bred and maintained under specific pathogen-free conditions, and all experiments were conducted in accordance with the animal care and use regulations of the Division of Laboratory Animal Medicine (DLAM) at the UCLA.

Cell Lines

The MS5-DLL4 murine bone marrow derived stromal cell line was obtained from Dr. Gay Crooks' lab (UCLA). Human multiple myeloma cancer cell line MM.1S, chronic myelogenous leukemia cancer cell line K562, melanoma cell line A375, lung carcinoma cell line H292, and prostate cancer cell line PC3 were purchased from the American Type Culture Collection (ATCC). MM.1S cells were cultured in R10 medium. K562 cells were cultured in C10 medium. A375, H292, and PC3 were cultured in D10 medium.

To make stable tumor cell lines overexpressing human CD1d, and/or firefly luciferase and enhanced green fluorescence protein (Fluc-EGFP) dual-reporters, the parental tumor cell lines were transduced with lentiviral vectors encoding the intended gene(s)[28]. 72h post lentivector transduction, cells were subjected to flow cytometry sorting to isolate gene-engineered cells for making stable cell lines. Six stable tumor cell lines were generated for this study, including MM.1S-FG, MM.1S-CD1d-FG, A375-FG, PC3-FG, H292-FG, and K562-FG.

Human CD34$^+$ Hematopoietic Stem Cells (HSCs), Periphery Blood Mononuclear Cells (PBMCs), and Patient Bone Marrow Samples

Cord blood cells were purchased from HemaCare. G-CSF-mobilized healthy donor peripheral blood cells were purchased from HemaCare or Cincinnati Children's Hospital Medical Center (CCHMC). Human CD34$^+$ HSCs were isolated through magnetic-activated cell sorting using ClinMACs CD34$^+$ microbeads (Miltenyi Biotech). Cells were cryopreserved in Cryostor CS10 (Sigma) using CoolCell (BioCision), and were frozen in liquid nitrogen for all experiments and long-term storage. Healthy donor human PBMCs were obtained from the UCLA/CFAR Virology Core Laboratory, without identification information under federal and state regulations. Patient bone marrow samples were collected following UCLA IRB approval (IRB#15-000062).

Media and Reagents

α-Galactosylceramide (αGC, KRN7000) was purchased from Avanti Polar Lipids. Recombinant human IL-2, IL-3, IL-4, IL-7, IL-15, Flt3-Ligand, Stem Cell Factor (SCF), Thrombopoietin (TPO), and Granulocyte-Macrophage Colony-Stimulating Factor (GM-CSF) were purchased from Peprotech. Ganciclovir (GCV) was purchased from Sigma.

X-VIVO 15 Serum-free Hematopoietic Cell Medium was purchased from Lonza. RPMI 1640 and DMEM cell culture medium were purchased from Corning Cellgro. Fetal bovine serum (FBS) was purchased from Sigma. Medium supplements, including Penicillin-Streptomycine-Glutamine (P/S/G), MEM non-essential amino acids (NEAA), HEPES Buffer Solution, and Sodium Pyruvate, were purchased from GIBCO. Beta-Mercaptoethanol (β-ME) was purchased from Sigma. Normocin was purchased from InvivoGen. Complete lymphocyte culture medium (denoted as C10 medium) was made of RPMI 1640 supplemented with FBS (10% vol/vol), P/S/G (1% vol/vol), MEM NEAA (1% vol/vol), HEPES (10 mM), Sodium Pyruvate (1 mM), β-ME (50 mM), and Normocin (100 mg/ml). Medium for culturing human MM.1S tumor cell line (denoted as R10 medium) was made of RPMI 1640 supplemented with FBS (10% vol/vol) and P/S/G (1% vol/vol). Adherent cell culture medium (denoted as D10 medium) was made of DMEM supplemented with FBS (10% vol/vol) and P/S/G (1% vol/vol).

METHOD DETAILS

Lentiviral and Retroviral Vectors

Lentiviral vectors used in this study were all constructed from a parental lentivector pMNDW as previously described[28]. The Lenti/iNKT-sr39TK vector was constructed by inserting into pMNDW vector a synthetic tricistronic gene encoding human iNKT TCRα-F2A-TCRβ-P2A-sr39TK; the Lenti/FG vector was constructed by inserting into pMNDW a synthetic bicistronic gene encoding Fluc-P2A-EGFP; the Lenti/CD1d vector was constructed by inserting into pMNDW a synthetic gene encoding human CD1d. The synthetic gene fragments were obtained from GenScript and IDT. Lentiviruses were produced using HEK293T cells, following a standard calcium precipitation protocol and an ultracentrifugation concentration protocol as previously described[27,28]. Lentivector titers were measured by transducing HT29 cells with serial dilutions and performing digital qPCR, following established protocols[27,28].

The Retro/BCAR-tEGFR vector was constructed by inserting into the parental MP71 vector a synthetic gene encoding human BCMA scFV-41BB-CD3ζ-P2A-tEGFR. The synthetic gene fragments were obtained from IDT. Vsv-g-pseudotyped Retro/BCAR-tEGFR retroviruses were generated by transfecting HEK293T cells following a standard calcium precipitation protocol[27,28]; the viruses were then used to transduce PG13 cells to generate a stable retroviral packaging cell line producing Retro/BCAR-tEGFR retroviruses (denoted as PG13-BCAR-tEGFR cell line). For retrovirus production, the PG13-BCAR-tEGFR cells were seeded at a density of 8×10^5 cells per ml in D10 medium and cultured in a 15 cm-dish (30 mL per dish) for 2 days; virus supernatants were then harvested and stored at −80°C for future use.

Antibodies and Flow Cytometry

All flow cytometry stains were performed in PBS for 15 min at 4°C. The samples were stained with Fixable Viability Dye eFluor506 (e506) mixed with Mouse Fc Block (anti-mouse CD16/32) or Human Fc Receptor Blocking Solution (TrueStain FcX) prior to antibody staining. Antibody staining was performed at a dilution according to the manufacturer's instructions. Fluorochrome-conjugated antibodies specific for human CD45 (Clone H130), TCRαβ (Clone I26), CD4 (Clone OKT4), CD8 (Clone SK1), CD45RO (Clone UCHL1), CD161 (Clone HP-3G10), CD69 (Clone FN50), CD56 (Clone HCD56), CD62L (Clone DREG-56), CD14 (Clone HCD14), CD11b (Clone ICRF44), CD11c (Clone N418), CD1d (Clone 51.1), CCR4 (Clone L291H4), CCR5 (Clone HEK/1/85a), CXCR3 (Clone G025H7), NKG2D (Clone 1D11), DNAM-1 (Clone 11A8), CD158 (KIR2DL1/S1/S3/S5) (Clone HP-MA4), IFN-γ (Clone B27), granzyme B (Clone QA16A02), perforin (Clone dG9), TNF-α (Clone Mab11), IL-2 (Clone MQ1-17H12), HLAE (Clone 3D12), β2-microglobulin (B2M) (Clone 2M2), HLA-DR (Clone L243), TCR Vδ2 (Clone B6) were purchased from BioLegend; Fluorochrome-conjugated antibodies specific for human CD34 (Clone 581) and TCR Vα24-Jβ18 (Clone 6B11) were purchased from BD Biosciences; Fluorochrome-conjugated antibodies specific for human Vβ11 was purchased from Beckman-Coulter; Fluorochrome-conjugated antibodies specific for human ULBP-2,5,6 (Clone 165903) was purchased from R&D Systems. Human Fc Receptor Blocking Solution (TrueStain FcX) was purchased from Biolegend, and Mouse Fc Block (anti-mouse CD16/32) was purchased from BD Biosciences. Fixable Viability Dye e506 were purchased from Affymetrix eBioscience. Intracellular cytokines were stained using a Cell Fixation/Permeabilization Kit (BD Biosciences). Stained cells were analyzed using a MACSQuant Analyzer 10 flow cytometer (Miltenyi Biotech). FlowJo software was utilized to analyze the data.

Enzyme-Linked Immunosorbent Cytokine Assays (ELISA)

The ELISAs for detecting human cytokines were performed following a standard protocol from BD Biosciences. Supernatants from co-culture assays were collected and assayed to quantify IFN-γ, TNF-α, IL-2, IL-4, and IL-17. The capture and biotinylated pairs for detecting cytokines were purchased from BD Biosciences. The streptavidin-HRP conjugate was purchased from Invitrogen. Human cytokine standards were purchased from eBioscience. Tetramethylbenzidine (TMB) substrate was purchased from KPL. The samples were analyzed for absorbance at 450 nm using an Infinite M1000 microplate reader (Tecan).

In Vitro Generation of Allogeneic HSC-Engineered iNKT (^{Allo}HSC-iNKT) Cells

Frozen-thawed human CD34$^+$ HSCs were revived in HSC-culture medium composed of X-VIVO 15 Serum-free Hematopoietic Cell Medium supplemented with SCF (50 ng/ml), FLT3-L (50 ng/ml), TPO (50 ng/ml), and IL-3 (10 ng/ml) for 24 h; the cells were then transduced with Lenti/iNKT-sr39TK viruses for another 24 h following an established protocol[28]. The transduced HSCs were then collected and put into a 2-Stage *in vitro* HSC-iNKT culture.

At Stage 1, gene-engineered HSCs were differentiated into iNKT cells in an artificial thymic organoid (ATO) culture over 8 weeks. ATO was generated following a previously established protocol, with certain modifications[29,30]. Briefly, MS5-DLL4 cells were harvested by trypsinization and resuspended in serum free ATO culture medium (''RB27'') composed of RPMI 1640 (Corning), 4% B27 supplement (ThermoFisher Scientific), 30 mM L-ascorbic acid 2-phosphate sesquimagnesium salt hydrate (Sigma-Aldrich) reconstituted in PBS, 1% penicillin/streptomycin (Gemini Bio-Products), 1% Glutamax (ThermoFisher Scientific), 5 ng/ml rhFLT3L and 5 ng/ml rhIL-7 (Peprotech). RB27 was made fresh weekly. 1.5-6 × 10^5 MS5-DLL4 cells were combined with 0.3-10 × 10^4 transduced HSCs per ATO in 1.5 mL Eppendorf tubes (up to 12 ATOs per tube) and centrifuged at 300 g for 5 min at 4°C in a swinging bucket centrifuge. Supernatants were carefully removed, and the cell pellet was resuspended in 6 mL RB27 per ATO and mixed by brief vortexing. ATOs were plated on a 0.4 mm Millicell transwell insert (EMD Millipore; Cat. PICM0RG50) placed in a 6-well plate containing 1 mL RB27 per well. Medium was changed completely every 3-4 days by aspiration from around the cell insert followed by replacement with 1 mL fresh RB27/cytokines. ATO cells were harvested by adding FACS buffer (PBS/0.5% bovine serum album/2mM EDTA) to each well and briefly disaggregating the ATO by pipetting with a 1 mL ''P1000'' pipet, followed by passage through a 50 mm nylon strainer.

At Stage 2, isolated ATO cells comprising ^{Allo}HSC-iNKT cells were expanded with αGC-loaded PBMCs (αGC-PBMCs). αGC-PBMCs were prepared by incubating 10^7-10^8 PBMCs in 5 mL C10 medium containing 5 μg/ml αGC for 1 h, followed by irradiation at 6,000 rads. ATO cells were mixed with irradiated αGC-PBMCs at ratio 1:1, followed by culturing in C10 medium supplemented with human IL-7 (10 ng/ml) and IL-15 (10 ng/ml) for 2 weeks; cell cultures were split and fresh media/cytokines were added if needed. The Stage 2 expansion culture could be extended to 3 weeks by adding additional αGC-PBMCs at ratio 1:1 at the end of week 2. At the end of Stage 2 culture, the resulting ^{Allo}HSC-iNKT cell products were collected and cryopreserved for future use.

In Vitro Generation of BCMA CAR-Engineered ^{Allo}HSC-iNKT (^{Allo}BCAR-iNKT) Cells

^{Allo}HSC-iNKT cells were generated in the 2-Stage HSC-iNKT culture as described above, followed by an additional Stage 3 CAR engineering culture. At one week into Stage 2 culture, ^{Allo}HSC-iNKT cells were collected and stimulated with CD3/CD28 T-activator beads (ThermoFisher Scientific) in the presence of recombinant human IL-15 (10 ng/ml) and human IL-7 (10 ng/ml) for two days; the cells were then spin-infected with frozen-thawed Retro/BCAR-tEGFR retroviral supernatants supplemented with polybrene (10 μg/ml, Sigma-Aldrich) at 660 g at 30°C for 90 min. Retronectin (Takara) could be pre-coated on plate to increase transduction efficiency. After transduction, the resulting ^{Allo}BCAR-iNKT cells were expanded for another 1-2 weeks in C10 medium supplemented with recombinant human IL-15 (10 ng/ml) and IL-7 (10 ng/ml), and then were collected and cryopreserved for future use.

In Vitro Generation of HLA-Ablated Universal HSC-iNKT (^{U}HSC-iNKT) Cells

^{U}HSC-iNKT cells were generated following the protocol of generating ^{Allo}HSC-iNKT cells, with one additional gene-editing step. CD34$^+$ HSCs were revived in HSC-culture medium on day 1, transduced with Lenti/iNKT-sr39TK viruses on day 2, and then were electroporated with a CRISPR-Cas9/B2M-CIITA-gRNAs complex on day 3, followed by entering the 2-Stage HSC-iNKT culture to generate ^{U}HSC-iNKT cells. A small portion of engineered CD34$^+$ HSCs were cultured in HSC-culture medium for 5 days, and flow cytometry was performed to evaluate the genome-editing efficiencies.

^{U}BCAR-iNKT cells were generated following the protocol of generating ^{Allo}BCAR-iNKT cells, with the same additional gene-editing step. CD34$^+$ HSCs were revived in HSC-culture medium on day 1, transduced with Lenti/iNKT-sr39TK viruses on day 2, and then were electroporated with a CRISPR-Cas9/B2M-CIITA-gRNAs complex on day 3, followed by entering the 3-Stage BCAR-iNKT culture to generate ^{U}BCAR-iNKT cells.

For electroporation, 2 × 10^5 HSCs per condition were pelleted at 90 x g for 10 min at room temperature (RT), resuspended in 20 μL P3 solution (Lonza), mixed with pre-aliquoted B2M and CIITA gRNAs (1 μL of each gRNA at 100 μM) and Cas9 (4 μL at 6.5 mg/ml), and pulsed once at 250 V for 5 ms in an Amaxa 4D Nucleofector X Unit (Lonza). After electroporation, HSCs were rested at RT for 10 min, and then transferred to a 24-well tissue culture treated plate overnight before entering the 2-Stage HSC-iNKT or 3-Stage BCAR-iNKT culture.

If necessary, the resulting ^{U}HSC-iNKT or ^{U}BCAR-iNKT cell products collected at the end of the *in vitro* culture could be purified using Magnetic-Activate Cell Sorting (MACS) via B2M (Santa Cruz Biotechnology) and HLA-II magnetic beads labeling (Miltenyi Biotec), to enrich the HLA-I/II double negative cells in the final ^{U}HSC-iNKT or ^{U}BCAR-iNKT cell products.

Generation of PBMC-Derived Conventional αβT, iNKT, γδT, and NK Cells

Healthy donor PBMCs were obtained from the UCLA/CFAR Virology Core Laboratory, and were used to generate the PBMC-Tc, PBMC-iNKT, PBMC-γδT, and PBMC-NK cells.

To generate PBMC-Tc cells, PBMCs were stimulated with CD3/CD28 T-activator beads (ThermoFisher Scientific) and cultured in C10 medium supplemented with human IL-2 (20 ng/mL) for 2-3 weeks, following the manufacturer's instructions.

To generate PBMC-iNKT cells, PBMCs were MACS-sorted via anti-iNKT microbeads (Miltenyi Biotech) labeling to enrich iNKT cells, which were then stimulated with donor-matched irradiated αGC-PBMCs at the ratio of 1:1, and cultured in C10 medium sup-

plemented with human IL-7 (10 ng/ml) and IL-15 (10 ng/ml) for 2-3 weeks. If needed, the resulting PBMC-iNKT cells could be further purified using Fluorescence-Activated Cell Sorting (FACS) via human iNKT TCR antibody (Clone 6B11; BD Biosciences) staining.

To generate PBMC-γδT cells, PBMCs were stimulated with Zoledronate (5 μM; Sigma-Aldrich) and cultured in C10 medium supplemented with human IL-2 (20 ng/ml) for 2 weeks. If needed, the resulting PBMC-γδT cells could be further purified using FACS via human TCR Vδ2 antibody (Clone B6; Biolegend) staining or via MACS using a human TCRγ/δ T Cell Isolation Kit (Miltenyi Biotech).

To generate PBMC-NK cells, PBMCs were FACS-sorted via human CD56 antibody (Clone HCD56; Biolegend) labeling or MACS-sorted using a human NK Cell Isolation Kit (Miltenyi Biotech).

Generation of BCMA CAR-Engineered PBMC T (BCAR-T) cells

Healthy donor PBMCs were stimulated with CD3/CD28 T-activator beads (ThermoFisher Scientific) in the presence of recombinant human IL-2 (30 ng/ml), following the manufacturer's instructions. On day 2, cells were spin-infected with frozen-thawed Retro/BCAR-tEGFR retroviral supernatants supplemented with polybrene (10 μg/ml, Sigma-Aldrich) at 660 g at 30°C for 90 min. Retronectin (Takara) could be pre-coated on plate to increase transduction efficiency. The resulting BCAR-T cells were expanded for another 7-10 days, and then were cryopreserved for future use.

Single Cell TCR Sequencing

^{Allo}HSC-iNKT (6B11$^+$TCRαβ$^+$), PBMC-iNKT (6B11$^+$TCRαβ$^+$), and PBMC-Tc (6B11$^-$TCRαβ$^+$) cells were sorted using a FACSAria II flow cytometer. Sorted cells were immediately delivered to the UCLA TCGB (Technology Center for Genomics and Bioinformatics) Core to perform single cell TCR sequencing using a 10X Genomics Chromium™ Controller Single Cell Sequencing System (10X Genomics), following the manufacturer's instructions and the TCGB Core's standard protocol. Libraries were constructed using an Illumina TruSeq RNA Sample Prep Kit (Cat#FC-122-1001) and sequenced with 150 bp paired end reads (5,000 reads/cell) on an Illumina NovaSeq. The reads were mapped to the human T cell receptor reference genome (hg38) using Cell Ranger VDJ. The frequencies of the α or β chain recombination were plotted.

Deep RNA Sequencing (Deep RNaseq) and Data Analysis

A total of 25 cell samples were analyzed, as described in the following table:

Sample name	Number of replicates (from different donors)	FACS sorting markers	Description
^{Allo}HSC-iNKT (from PBSC)	3	6B11$^+$TCRαβ$^+$	^{Allo}HSC-iNKT cells derived from G-CSF mobilized peripheral blood CD34$^+$ HSCs
^{Allo}HSC-iNKT (from CB)	3	6B11$^+$TCRαβ$^+$	^{Allo}HSC-iNKT cells derived from cord blood CD34$^+$ HSCs
PBMC-iNKT (CD4$^-$)	3	6B11$^+$TCRαβ$^+$CD4$^-$	PBMC-iNKT cells derived from healthy donor PBMCs (CD4$^-$ cells were analyzed)
PBMC-αβTc (CD4$^-$)	8	6B11$^-$TCRαβ$^+$CD4$^-$	PBMC-αβTc cells derived from healthy donor PBMCs (CD4$^-$ cells were analyzed)
PBMC-NK	2	CD56$^+$TCRαβ$^-$	PBMC-NK cells derived from healthy donor PBMCs
PBMC-γδT	6	TCRγδ$^+$TCRαβ$^-$	PBMC-γδT cells derived from healthy donor PBMCs

Both ^{Allo}HSC-iNKT and PBMC-iNKT cells were activated *in vitro* with αGC, PBMC-αβTc cells were stimulated with CD3/CD28 T-activator beads, and PBMC-γδT cells were stimulated with Zoledronate. Cell samples were sorted using a FACSAria II flow cytometer. Total RNAs were isolated from each cell sample using an miRNeasy Mini Kit (QIAGEN) and delivered to the UCLA TCGB Core to perform Deep RNA sequencing using an Illumina HiSeq3000, following the manufacturer's instructions and the TCGB Core's standard protocol. cDNAs were synthesized using an iScript cDNA Synthesis Kit (1708890, BioRad). Libraries were constructed using an Illumina TruSeq Stranded Total RNA Sample Prep kit and sequenced with 50 bp single end reads (20 M reads/sample) on an Illumina HiSeq3000. The reads were mapped with STAR 2.5.3a to the human genome (hg38). The counts for each gene were obtained using–quantMode GeneCounts in STAR commands, and the other parameters during alignment were set to default. Data quality was checked using Illumina's proprietary software. Sequencing depth normalized counts were obtained from the differential expression analysis and were used for principal component analysis.

^{Allo}HSC-iNKT Cell Phenotype and Functional Study

^{Allo}HSC-iNKT cells and their derivatives (i.e., ^{Allo}BCAR-iNKT, ^{U}HSC-iNKT, and ^{U}BCAR-iNKT cells) were analyzed in comparison with PBMC-Tc, PBMC-NK, PBMC-iNKT, or/and BCAR-T cells. Phenotype of these cells was studied using flow cytometry, by analyzing

cell surface markers including co-receptors (i.e., CD4 and CD8), NK cell receptors (i.e., CD161, NKG2D, DNAM-1, and KIR), memory T cell markers (i.e., CD45RO), and inflammatory tissue/tumor homing markers (i.e., CCR4, CCR5, and CXCR3). Capacity of these cells to produce cytokines (i.e., IFN-γ, TNF-α, and IL-2) and cytotoxic molecules (i.e., perforin and granzyme B) were studied using flow cytometry via intracellular staining.

Response of ^{Allo}HSC-iNKT cells to antigen stimulation was studied by culturing ^{Allo}HSC-iNKT cells *in vitro* in C10 medium for 7 days, in the presence or absence of αGC (100 ng/ml). Proliferation of ^{Allo}HSC-iNKT cells was measured by cell counting and flow cytometry (identified as 6B11$^+$TCRαβ$^+$) over time. Cytokine production was assessed by ELISA analysis of cell culture supernatants collected on day 7 (for human IFN-γ. TNF-α, IL-2, IL-4, and IL-17).

In Vitro Tumor Cell Killing Assay

Tumor cells (1 × 10^4 cells per well) were co-cultured with effector cells (at ratios indicated in figure legends) in Corning 96-well clear bottom black plates for 8-24 h, in C10 medium with or without the addition of αGC (100 ng/ml). At the end of culture, live tumor cells were quantified by adding D-luciferin (150 μg/ml; Caliper Life Science) to cell cultures and reading out luciferase activities using an Infinite M1000 microplate reader (Tecan).

In some experiments, 10 μg/ml of LEAF^{TM} purified anti-human NKG2D (Clone 1D11, Biolegend), anti-human DNAM-1 antibody (Clone 11A8, Biolegend), or LEAF^{TM} purified mouse IgG2bk isotype control antibody (Clone MG2B-57, Biolegend) was added to co-cultures, to study NK activating receptor-mediated tumor cell killing mechanism.

All the PBMC-derived cells and HSC-derived iNKT cells were cryopreserved before use. The cells for comparison (e.g., ^{Allo}HSC-iNKT and PBMC-NK cells in Figure 3) were cryopreserved and thawed for testing side-by-side using Mr. Frosty Freezing Container (Thermo Scientific Nalgene) following the manufacture's instructions.

In Vitro Mixed Lymphocyte Reaction (MLR) Assay: Studying Graft-Versus-Host (GvH) Response

PBMCs of multiple healthy donors were irradiated at 2,500 rads and used as stimulators, to study the GvH response of ^{Allo}HSC-iNKT cells and their derivatives (i.e., ^{Allo}BCAR-iNKT and ^{U}BCAR-iNKT cells) as responders. PBMC-Tc or BCAR-T cells were included as responder controls. Stimulators (5 × 10^5 cells/well) and responders (2 × 10^4 cells/well) were co-cultured in 96-well round bottom plates in C10 medium for 4 days; the cell culture supernatants were then collected to measure IFN-γ production using ELISA.

In Vitro MLR Assay: Studying Host-Versus-Graft (HvG) Response

PBMCs of multiple healthy donors were used as responders, to study the HvG response of ^{Allo}HSC-iNKT cells and their derivatives (i.e., ^{Allo}BCAR-iNKT and ^{U}BCAR-iNKT cells) as stimulators (irradiated at 2,500 rads). PBMC-Tc, PBMC-iNKT or BCAR-T cells were included as stimulator controls. Stimulators (5 × 10^5 cells/well) and responders (2 × 10^4 cells/well) were co-cultured in 96-well round bottom plates in C10 medium for 4 days; the cell culture supernatants were then collected to measure IFN-γ production using ELISA.

In Vitro MLR Assay: Studying NK Cell-Mediated Allorejection

PBMC-NK cells isolated from PBMCs of multiple healthy donors were used to study the NK cell-mediated allorejection of ^{Allo}HSC-iNKT cells and their derivatives (i.e., ^{Allo}BCAR-iNKT and ^{U}BCAR-iNKT cells). Allogeneic PBMC-Tc or PBMC-iNKT cells were included as controls. PBMC-NK cells (2 × 10^4 cells/well) and the corresponding allogeneic cells (2 × 10^4 cells/well) were co-cultured in 96-well round bottom plates in C10 medium for 24 h; the cell cultures were then collected to quantify live cells using flow cytometry.

Bioluminescence Live Animal Imaging (BLI)

BLI was performed using an IVIS 100 imaging system (Xenogen/PerkinElmer) or a Spectral Advanced Molecular Imaging (AMI) HTX imaging system (Spectral instrument Imaging). Live animal imaging was acquired 5 min after intraperitoneal (i.p.) injection of D-Luciferin (1 mg per mouse). Imaging results were analyzed using a Living Imaging 2.50 software (Xenogen/ PerkinElmer) or an AURA imaging software (Spectral Instrument Imaging).

^{Allo}HSC-iNKT Cell *In Vivo* Antitumor Efficacy Study: A375 Human Melanoma Xenograft NSG Mouse Model

NSG mice were pre-conditioned with 100 rads of total body irradiation (day −1), followed by subcutaneous inoculation with 1 × 10^6 A375-FG cells (day 0). On day 3, the tumor-bearing experimental mice received intravenous (i.v.) injection of vehicle (PBS), 1.2 × 10^7 ^{Allo}HSC-iNKT cells, or 1.2 × 10^7 PBMC-NK cells. Over time, tumor loads were monitored by measuring total body luminescence using BLI and by measuring tumor size using a Fisherbrand^{TM} Traceable^{TM} digital caliper (Thermo Fisher Scientific). The tumor size was calculated as W x L mm^2. At around week 3, mice were terminated, and solid tumors were retrieved and weighted using a PA84 precision balance (Ohaus).

^{Allo}BCAR-iNKT Cell *In Vivo* Antitumor Efficacy Study: MM.1S Human MM Xenograft NSG Mouse Model

NSG mice were pre-conditioned with 175 rads of total body irradiation (day −1), followed by intravenous inoculation with 1 × 10^6 MM-CD1d-FGFP cells (day 0). To study antitumor efficacy under low tumor load condition, on day 3, the tumor-bearing experimental mice received i.v. injection of vehicle (PBS), ^{Allo}BCAR-iNKT cells (7 × 10^6 CAR$^+$ cells), or conventional BCAR-T cells (7 × 10^6 CAR$^+$ cells). To study antitumor efficacy under high tumor load condition, on day 15, the tumor-bearing experimental mice received i.v. in-

jection of vehicle (PBS), ^{Allo}BCAR-iNKT cells (5 × 10^6 CAR^+ cells), or conventional BCAR-T cells (5 × 10^6 CAR^+ cells). Over time, experimental mice were monitored for survival, and their tumor loads were measured using BLI.

^{U}BCAR-iNKT Cell *In Vivo* Antitumor Efficacy Study: MM.1S Human MM Xenograft NSG Mouse Model

NSG mice were pre-conditioned with 175 rads of total body irradiation (day −1), followed by intravenous inoculation with 5 × 10^5 MM-CD1d-FGFP cells (day 0). On day 3 the tumor-bearing experimental mice received i.v. injection of vehicle (PBS), ^{Allo}BCAR-iNKT cells (3 × 10^6 CAR^+ cells), or conventional BCAR-T cells (3 × 10^6 CAR^+ cells). Over time, experimental mice were monitored for survival, and their tumor loads were measured using BLI.

Ganciclovir (GCV) *In Vitro* and *In Vivo* Killing Assay

For GCV *in vitro* killing assay, ^{Allo}HSC-iNKT cells were cultured in C10 medium in the presence of titrated amount of GCV (0-50 μM) for 4 days; live ^{Allo}HSC-iNKT cells were then counted using a hematocytometer (VWR) via Trypan Blue staining (Fisher Scientific).

GCV *in vivo* killing assay was performed using an NSG xenograft mouse model. NSG mice received i.v. injection of 1 × 10^{7} ^{Allo}HSC-iNKT cells on day 0, followed by i.p. injection of GCV for 5 consecutive days (50 mg/kg per injection per day). On day 5, mice were terminated. Multiple tissues (i.e., spleen, liver, and lung) were collected and processed for flow cytometry analysis to detect tissue-infiltrating ^{Allo}HSC-iNKT cells (identified as iNKT TCR^+CD45^+), following established protocols.[28]

Histological Analysis

Tissues (i.e., heart, liver, kidney, lung, and spleen) were collected from the experimental mice, fixed in 10% Neutral Buffered Formalin for up to 36 h, then embedded in paraffin for sectioning (5 μm thickness). Tissue sections were prepared and stained with Hematoxylin and Eosin (H&E) by the UCLA Translational Pathology Core Laboratory, following the Core's standard protocols. Stained sections were imaged using an Olympus BX51 upright microscope equipped with an Optronics Macrofire CCD camera (AU Optronics) at 20 x and 40 x magnifications. The images were analyzed using Optronics PictureFrame software (AU Optronics).

Statistical Analysis

GraphPad Prism 6 (Graphpad Software) was used for statistical data analysis. Student's two-tailed t test was used for pairwise comparisons. Ordinary 1-way ANOVA followed by Tukey's or Dunnett's multiple comparisons test was used for multiple comparisons. Log rank (Mantel-Cox) test adjusted for multiple comparisons was used for Meier survival curves analysis. Data are presented as the mean ± SEM, unless otherwise indicated. In all figures and figure legends, "n" represents the number of samples or animals utilized in the indicated experiments. A P value of less than 0.05 was considered significant. ns, not significant; *$p < 0.05$; **$p < 0.01$; ***$p < 0.001$; ****$p < 0.0001$.

Cell Reports Medicine, Volume 2

Supplemental information

Development of allogeneic HSC-engineered iNKT cells for off-the-shelf cancer immunotherapy

Yan-Ruide Li, Yang Zhou, Yu Jeong Kim, Yanni Zhu, Feiyang Ma, Jiaji Yu, Yu-Chen Wang, Xianhui Chen, Zhe Li, Samuel Zeng, Xi Wang, Derek Lee, Josh Ku, Tasha Tsao, Christian Hardoy, Jie Huang, Donghui Cheng, Amélie Montel-Hagen, Christopher S. Seet, Gay M. Crooks, Sarah M. Larson, Joshua P. Sasine, Xiaoyan Wang, Matteo Pellegrini, Antoni Ribas, Donald B. Kohn, Owen Witte, Pin Wang, and Lili Yang

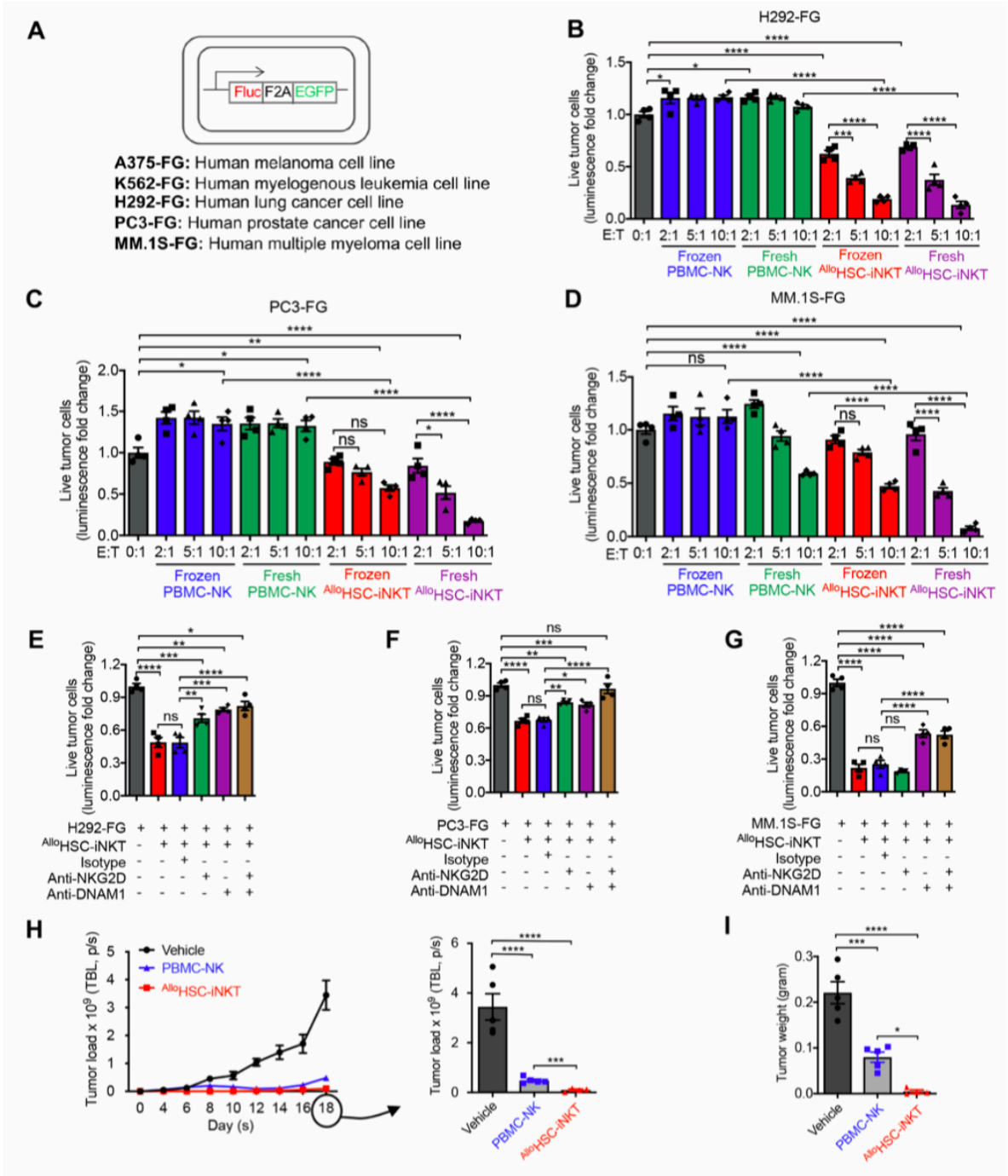

Figure S1. Tumor Targeting of ^{Allo}HSC-iNKT Cells Through Intrinsic NK Function; Related to Figure 3.

(A) Schematics showing the engineered A375-FG, K562-FG, H292-FG, PC3-FG, and MM.1S-FG cell lines. Fluc, firefly luciferase; EGFP, enhanced green fluorescent protein; F2A, foot-and-mouth disease virus 2A self-cleavage sequence.
(B-D) *In vitro* direct killing of human tumor cells by ^{Allo}HSC-iNKT cells. PBMC-NK cells were included as a control. Both fresh and frozen-thawed cells were studied. Tumor cell killing was analyzed at 24-hours post co-culture. Tumor killing data of H292-FG human lung cancer cells (B), PC3-FG human prostate cancer cells (C), and MM.1S-FG human multiple myeloma cells (D) were presented. N = 4. Related to main Figures 3C-3E.
(E-G) Tumor killing mechanisms of ^{Allo}HSC-iNKT cells. NKG2D and DNAM-1 mediated pathways were studied. Tumor cell killing was analyzed at 24-hours post co-culture. Tumor killing data of H292-FG (tumor:iNKT ratio 1:2), PC3-FG (tumor:iNKT ratio 1:10), and MM.1S-FG (tumor:iNKT ratio 1:15) were presented. N = 4. Related to main Figures 3F-3H.
(H-I) *In vivo* antitumor efficacy of ^{Allo}HSC-iNKT cells in an A375-FG human melanoma xenograft NSG mouse model. (H) BLI measurements of tumor loads over time (n = 4 or 5). (I) Tumor weight at the terminal harvest on day 18 (n = 4 or 5). Related to main Figures 3I-3K.
Representative of 3 experiments. Data are presented as the mean ± SEM. ns, not significant, *P < 0.05, **P < 0.01, ***P < 0.001, ****P < 0.0001, by 1-way ANOVA (B-G, I) or by Student's *t* test (H).

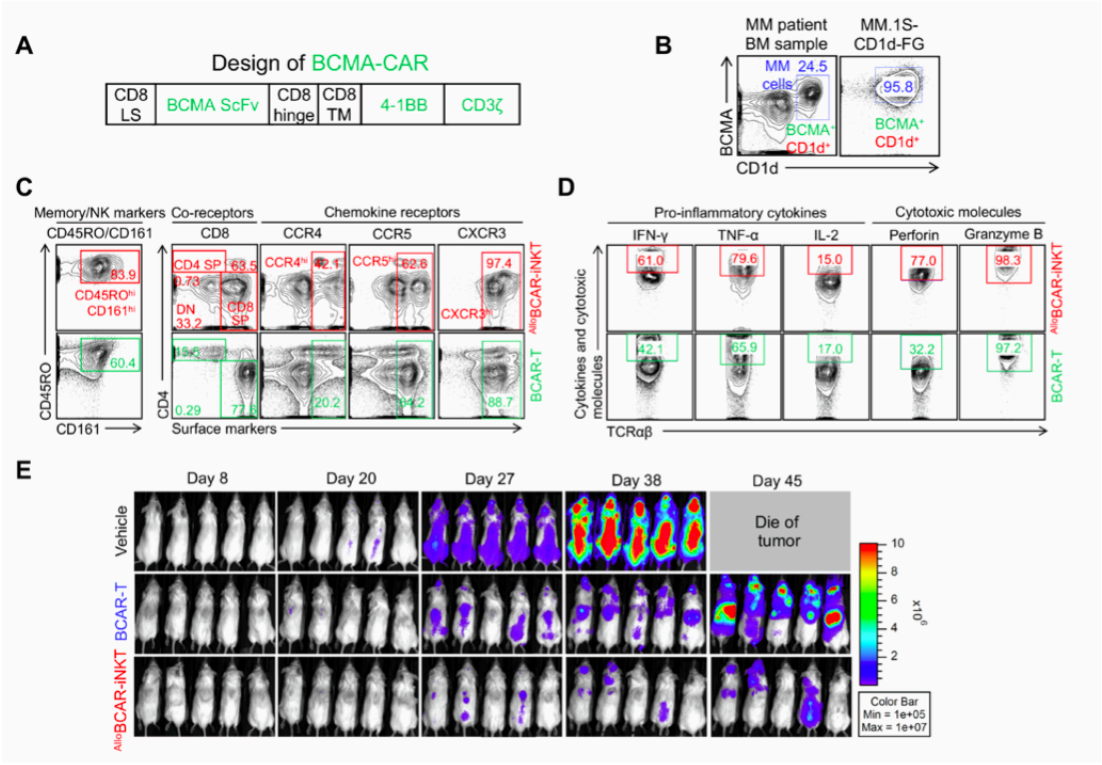

Figure S2. Tumor Targeting of ^{Allo}HSC-iNKT Cells Through Engineered Chimeric Antigen Receptors; Related to Figure 4.

(A) Schematics showing the design of BCMA-CAR. LS, leader sequence; ScFv, single-chain variable fragment; TM, transmembrane domain.

(B) FACS analyses of BCMA and CD1d expression on MM.1S-CD1d-FG cells. A representative MM patient primary bone marrow (BM) sample was included as a control.

(C-D) FACS characterization of ^{Allo}BCAR-iNKT cells. (C) Surface marker expression. (D) Intracellular cytokine and cytotoxic molecule production. BCAR-T cells were included as a control.

(E) *In vivo* antitumor efficacy of ^{Allo}BCAR-iNKT cells in an MM.1S-CD1d-FG human multiple myeloma xenograft NSG mouse model. BLI images were presented showing tumor loads in experimental mice over time. Related to main Figures 4K-4N.

Representative of 2 (E) and 3 (A-D) experiments.

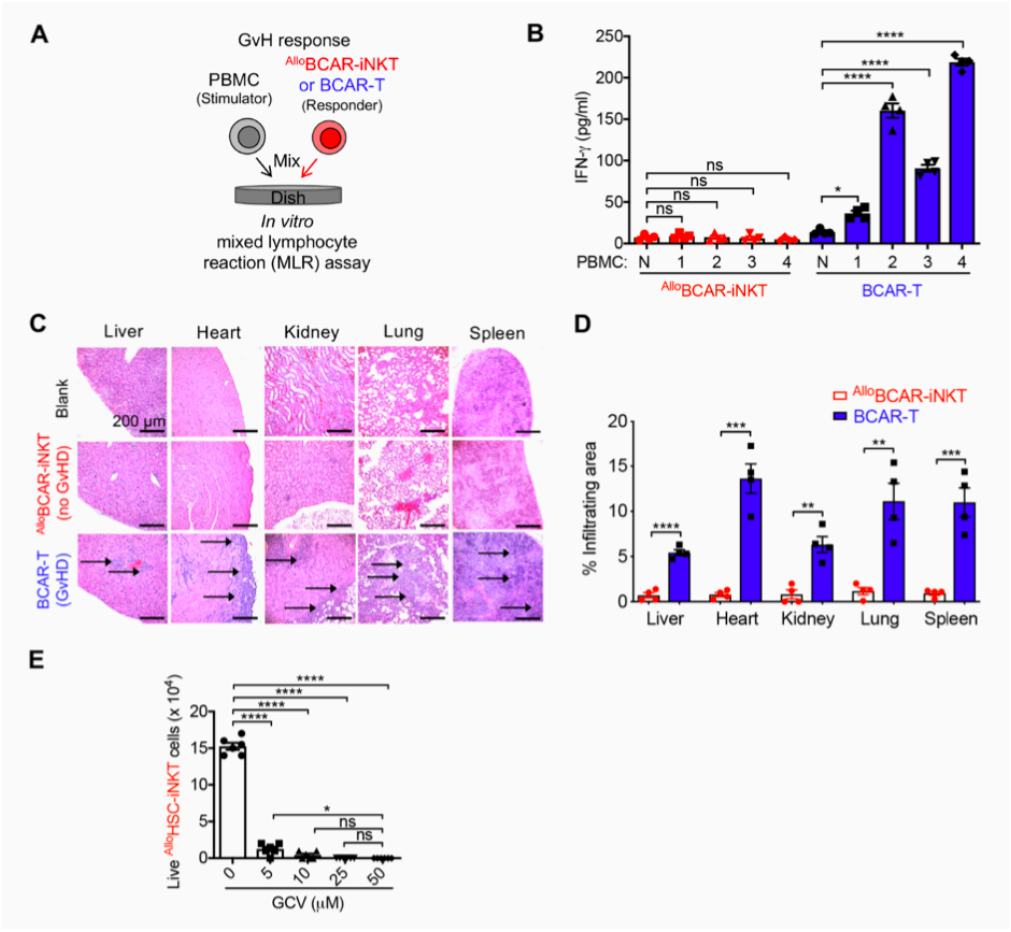

Figure S3. Safety study of ^{Allo}HSC-iNKT cells; Related to Figure 5.

(A-B) Studying the graft-verus-host (GvH) response of ^{Allo}BCAR-iNKT cells using an *in vitro* mixed lymphocyte reaction (MLR) assay. BCAR-T cells were included as a responder cell control. (A) Experimental design. PBMCs from 4 different healthy donors were used as stimulator cells. (B) ELISA analyses of IFN-γ production at day 4 (n = 4).

(C-D) Histology analysis of tissue sections collected from experimental mice as described in Figures 4G-4J. (C) H&E-stained tissue sections. Blank indicates tissue sections collected from NSG mice receiving no adoptive cell transfer. Arrows point to mononuclear cell infiltrates. Scale bar: 200 μm. (D) Quantification of C (n = 4).

(E) *In vitro* GCV killing assay. ^{Allo}HSC-iNKT cells were cultured *in vitro* in the presence of gradient concentrations of GCV for 4 days, followed by quantification of live cells via cell counting (n = 6).

Representative of 2 experiments. Data are presented as the mean ± SEM. ns, not significant, *P < 0.05, **P < 0.01, ***P < 0.001, ****P < 0.0001, by Student's *t* test (D) or by 1-way ANOVA (B and E).

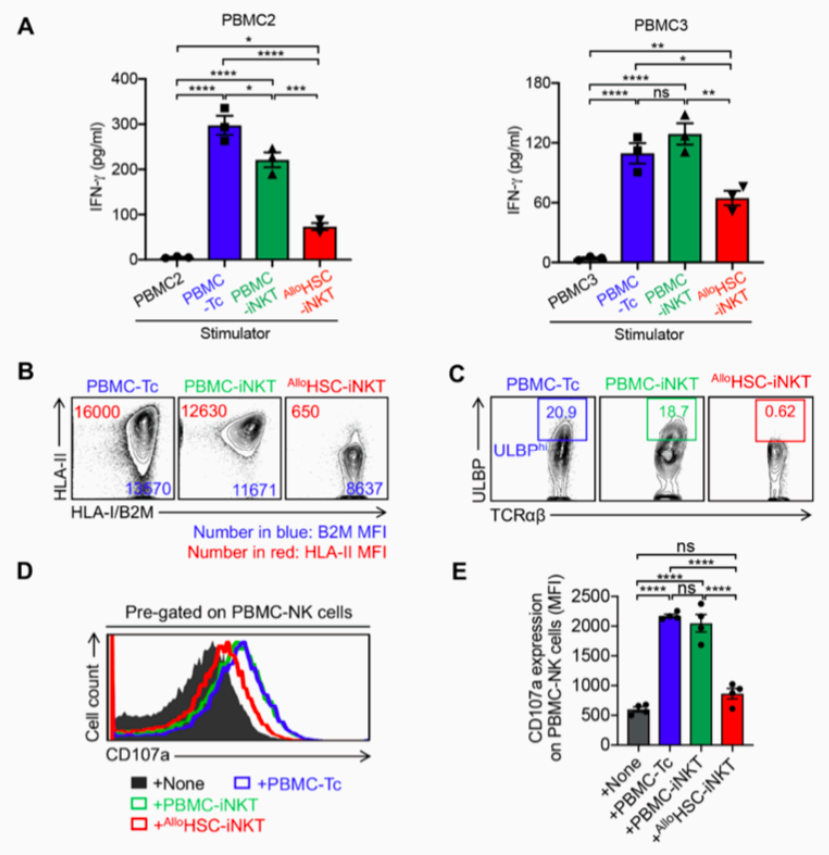

Figure S4. Immunogenicity Study of ^{Allo}HSC-iNKT Cells; Related to Figure 6.

(A) ELISA analyses of IFN-γ production at day 4 in an *in vitro* MLR assay (n = 3). Data of PBMC2 and PBMC3 responders were presented. Related to main Figures 6A and 6C.

(B) FACS analyses of HLA-I/II expression on PBMC-Tc, PBMC-iNKT, and ^{Allo}HSC-iNKT cells. Representative FACS plots were presented. Related to main Figure 6B.

(C) FACS analyses of ULBP expression on PBMC-Tc, PBMC-iNKT, and ^{Allo}HSC-iNKT cells. Representative FACS plots were presented. Related to main Figure 6F.

(D-E) Studying CD107a expressions on PBMC-NK cells using an *in vitro* MLR assay. PBMC-NK cells were co-cultured with ^{Allo}HSC-iNKT, PBMC-iNKT, and PBMC-Tc cells for 24 hours. CD107a antibody was added into the cell cultures and incubated for 2 hours prior to flow cytometry. (D) FACS analyses of CD107a expression on PBMC-NK cells. (E) Quantification of D (n = 4).

Representative of 3 experiments. Data are presented as the mean ± SEM. ns, not significant, *P < 0.05, **P < 0.01, ***P < 0.001, ****P < 0.0001, by one-way ANOVA.

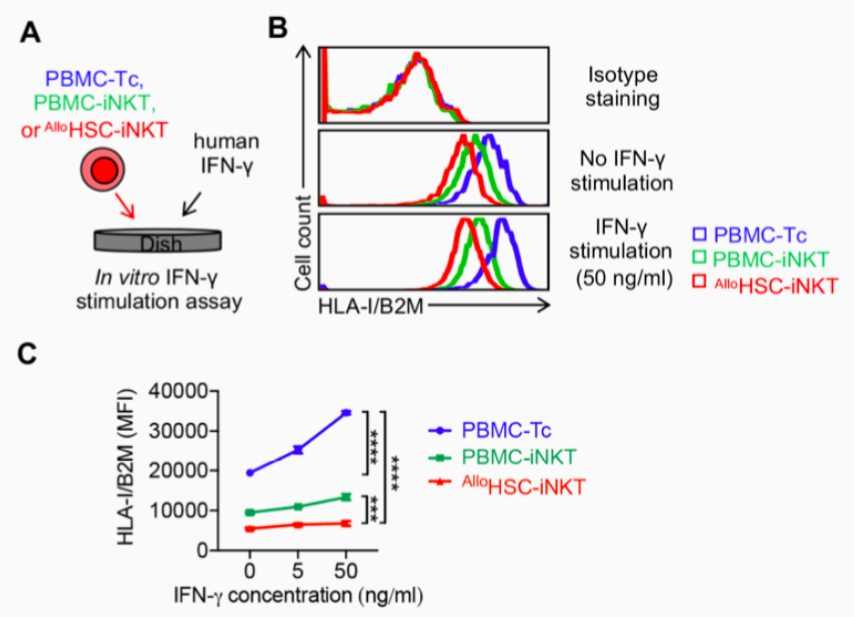

Figure S5. HLA-I Expression Study on ^{Allo}HSC-iNKT Cells Under IFN-γ Stimulation; Related to Figure 6.

(A) Experimental design. ^{Allo}HSC-iNKT cells were stimulated with a range of IFN-γ (0, 5, and 50 ng/ml) for 3 days. PBMC-iNKT and PBMC-Tc cells were included as controls.

(B) FACS analyses of HLA-I expression on the indicated cells.

(C) Quantification of HLA-I expression on the indicated cells stimulated with IFN-γ of indicated concentrations (n = 3).

Representative of 3 experiments. Data are presented as the mean ± SEM. *P < 0.05, ***P < 0.001, ****P < 0.0001, by 1-way ANOVA.

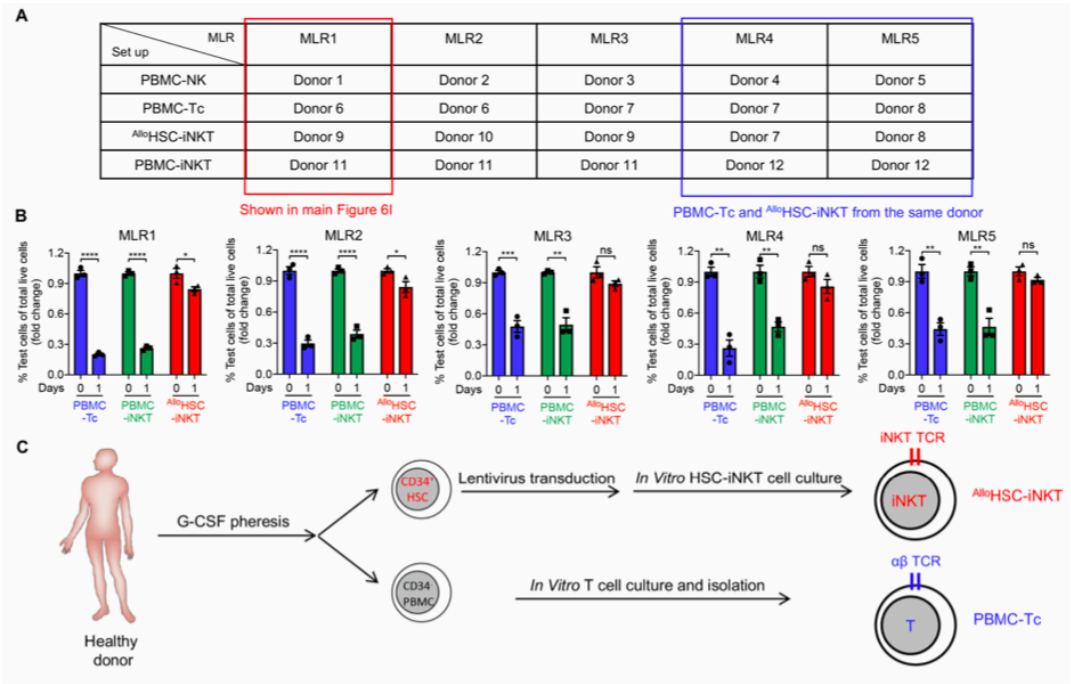

Figure S6. Studying NK cell-mediated allorejection of ^{Allo}HSC-iNKT cells; Related to Figure 6.

(A) Table showing the donor information of MLR assay. Five different sets of MLR assay were performed; three sets used PBMC-Tc and ^{Allo}HSC-iNKT cells from different donors, two sets used PBMC-Tc and ^{Allo}HSC-iNKT cells from the same donors. Data of MLR1 have been shown in Figure 6I.

(B) Quantification of the indicated test cells (n = 3).

(C) Diagram showing the experimental procedure to generate PBMC-Tc and ^{Allo}HSC-iNKT cells from the same donor. Data are presented as the mean ± SEM. ns, not significant, *P < 0.05, **P < 0.01, ***P < 0.001, ****P < 0.0001, by Student's *t* test.

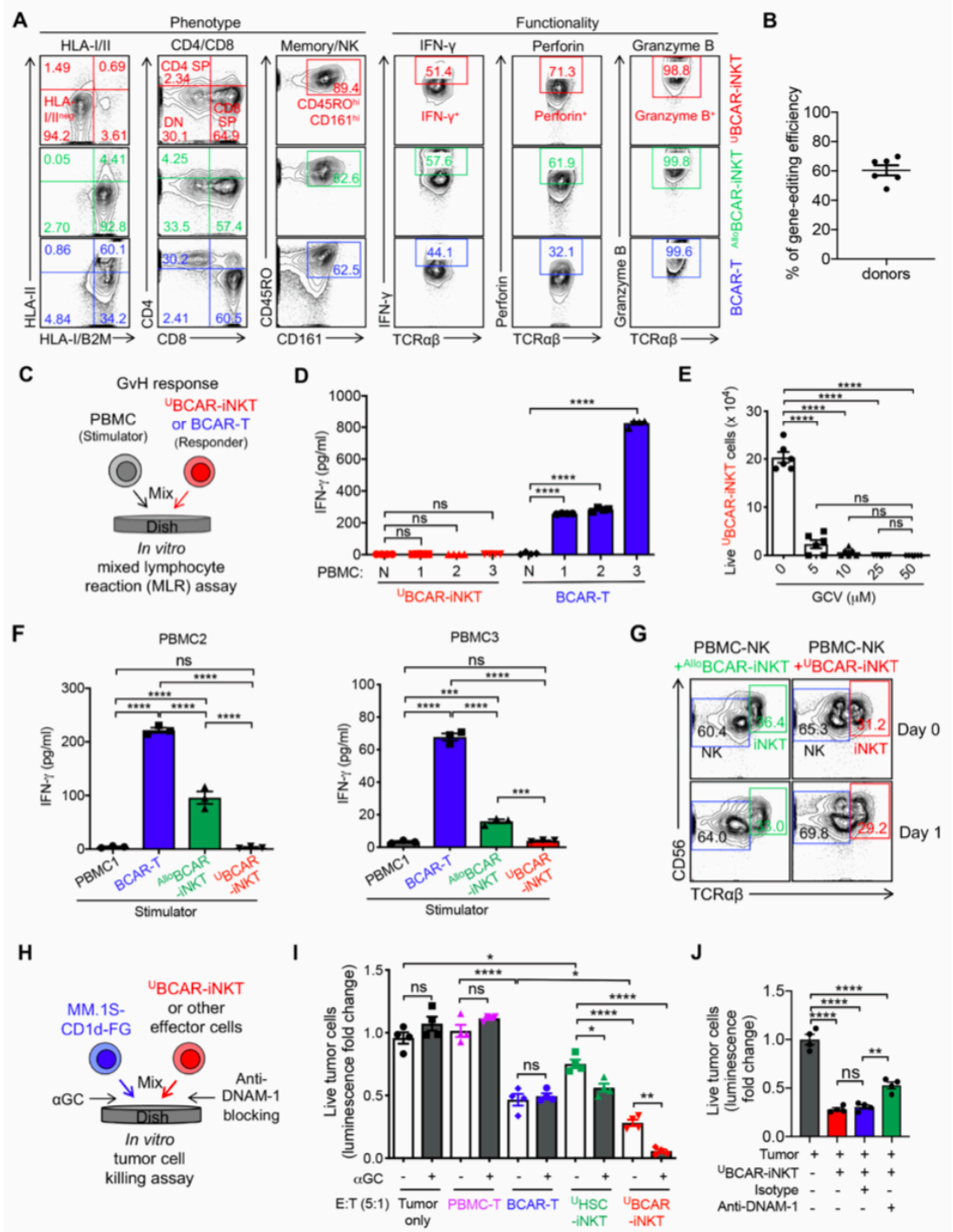

Figure S7. Development of HLA-Ablated Universal HSC-iNKT (^{U}HSC-iNKT) Cells and Derivatives; Related to Figure 7.

(A) FACS analyses of surface marker expression, and Intracellular cytokine and cytotoxic molecule production by ^{U}BCAR-iNKT cells. ^{Allo}BCAR-iNKT and BCAR-T cells were included as controls.
(B) The genome editing efficiencies among multiple HSC donors.
(C-D) Studying the GvH response of ^{u}BCAR-iNKT cells using an *in vitro* MLR assay. BCAR-T cells were included as a responder cell control. (C) Experimental design. PBMCs from 3 different healthy donors were used as stimulator cells. (D) ELISA analyses of IFN-γ production at day 4 (n = 4).
(E) *In vitro* GCV killing assay. ^{U}BCAR-iNKT cells were cultured *in vitro* in the presence of gradient concentrations of GCV for 4 days, followed by quantification of live cells via cell counting (n = 6).
(F) Studying allogenic T cell response against ^{U}BCAR-iNKT cells using an *in vitro* MLR assay. ELISA analyses of IFN-γ production at day 4 were presented (n = 3). Related to main Figures 7E and 7F.
(G) Studying allogenic NK cell response against ^{U}BCAR-iNKT cells using an *in vitro* MLR assay. ^{Allo}BCAR-iNKT cells were included as a control. Representative FACS plots were presented, showing the quantification of the indicated cells at day 0 and day 1. Related to main Figures 7G and 7H.
(H-J) *In vitro* killing of MM.1S-CD1d-FG human multiple myeloma cells by ^{U}BCAR-iNKT cells. PBMC-T, BCAR-T, and ^{U}HSC-iNKT cells were included as effector cell controls. (H) Experimental design. (I) Tumor cell killing by the indicated effector cells with/out the addition of αGC (n = 4). (J) Tumor cell killing by ^{Allo}BCAR-iNKT cells with/out the blockade of DNAM-1 (n = 4). Tumor cell killing was analyzed at 8-hours post co-culture (effector:tumor ratio 5:1).
Representative of 3 experiments. Data are presented as the mean ± SEM. ns, not significant, *P < 0.05, **P < 0.01, ***P < 0.001, ****P < 0.0001, by 1-way ANOVA.

CHAPTER 3:

Scalable HSC-engineered multifunctional and hypoimmunogenic CAR-NKT cells for off-the-shelf cancer immunotherapy

(This project is in submission to *Nature Biotechnology*)

Scalable HSC-engineered multifunctional and hypoimmunogenic CAR-NKT cells for off-the-shelf cancer immunotherapy

Yang Zhou[1,*], Jiaji Yu[1,*], Yan-Ruide Li[1], Feiyang Ma[2], Miao Li[1], Kuangyi Zhou[1], Zhe Li[1], Yu Jeong Kim[1], Derek Lee[1], Xinjian Cen[1], Tiffany Husman[1], Aarushi Bajhaj[1], Yu-Chen Wang[1], Yuchong Zhang[1], Zoe Hanh[1], Zach Dunn[3], Enbo Zhu[1], Wenbin Guo[4], Pin Wang[3], Matteo Pellegrini[4,5] and Lili Yang[1,5,6,7 §]

Author Affiliation:

[1]Department of Microbiology, Immunology & Molecular Genetics, University of California, Los Angeles, Los Angeles, CA 90095, USA

[2]Division of Rheumatology, Department of Internal Medicine, University of Michigan, Ann Arbor, MI 48109, USA

[3]Department of Pharmacology and Pharmaceutical Sciences, University of Southern California, Los Angeles, CA 90089, USA

[4]Department of Molecular, Cell and Developmental Biology, College of Letters and Sciences, University of California, Los Angeles, Los Angeles, CA 90095, USA

[5]Eli and Edythe Broad Center of Regenerative Medicine and Stem Cell Research, University of California, Los Angeles, Los Angeles, CA 90095, USA

[6]Jonsson Comprehensive Cancer Center, David Geffen School of Medicine, University of California, Los Angeles, Los Angeles, CA 90095, USA

[7]Molecular Biology Institute, University of California, Los Angeles, CA 90095, USA

* These authors contributed equally

[§]Corresponding author. Email: liliyang@ucla.edu.

Address Correspondence to:

Lili Yang, Ph.D.

Department of Microbiology, Immunology & Molecular Genetics

University of California, Los Angeles, CA 90095, USA.

Phone: 310-825-8609

Email: liliyang@ucla.edu

Abstract

Although the chimeric antigen receptor (CAR) engineered T (CAR-T) therapy, results impressive clinical outcomes, the current Food and Drug Administration (FDA) approved CAR-T products fall into the autologous category, rendering the therapies high-cost and patient-selective. As such, off-the-shelf assets that are safer, more accessible and affordable to all patients are in great demand. Here, we report a novel feeder-free and serum-free *ex vivo* culture platform to generate allogeneic hematopoietic stem cell (HSC)-engineered CAR-armed natural killer T (^{Allo}CAR-eNKT) cells, providing changes in the allogeneic cell therapy landscape. This platform is robust and compatible for delivering different CAR cargos and additional molecules, such as B cell maturation antigen (BCMA) CAR, and interleukin 15 (IL-15). The allogeneic BCMA CAR NKT (^{Allo}BCAR-eNKT) cells execute potent anti-tumor efficacy without GvHD risk in the human multiple myeloma xenograft mouse model. The IL-15 enhanced BCMA CAR NKT (^{Allo15}BCAR-iNKT) cells displayed remarkable persistence and enhanced therapeutic activity, potentially providing durable protection to patient. The versatile culture platform generates unique hypoimmunogenic ^{Allo}CAR-eNKT cells, resulting in resistance to allo-rejection to favor their allogeneic potential. Therefore, we provide the world the third option apart from T and NK cells for developing "off-the-shelf" cancer immunotherapy and promotes the speedy clinical translation of stem cell-derived cells.

Introduction

Adoptive cell therapy has revolutionized cancer immunotherapy, in particular chimeric antigen receptor (CAR) engineered T (CAR-T) therapy, showing excellent efficacy for treating hematological malignancies[1, 2]. The remarkable clinical outcomes from commercial approved CAR-T cells for leukemia and lymphoma treatment offer hope for patients with other types of cancer. Nevertheless, the autologous nature of current FDA-approved CAR-T cell products render the therapies high-cost, time-consuming and patient selective[2, 3]. The current manufacturing of autologous CAR T cells is in general effective but limited for patients with progressive disease; patients undergo previous treatments may have insufficient or dysfunctional T cells for CAR T production. Thus, allogeneic products that all patients can be accessible and affordable are in great demand. There two approaches to develop allogeneic cellular products. One is to utilize conventional αβT cells via ablating their endogenous TCR expression to diminish their risk of inducing graft-versus-host disease (GvHD)[4, 5]. Alternatively, utilizing other cell types that naturally have no GvHD risk, such as NK and unconventional T cells, to generate off-the-shelf cellular products[6, 7].

Invariant natural killer T (iNKT) cells, a rare population of unconventional T cells[8], are an idea cell carrier for off-the-shelf cell therapy. iNKT cells have shown potent tumor-kiiling capacity potent tumor-killing capacity; tumor infiltrating ability; and bridging innate and adaptive immune responses[9]. Clinically, CAR-iNKT cells induce profound response against relapsed or resistant neuroblastoma without inducing any obvious toxicity as well as cytokine release syndromes[7]. However, the use of iNKT cells is constrained by their low percentages in human blood (0.001-

1%)[8, 10-13]. The number of iNKT cells expanded from PBMC are limited and may contain bystander conventional αβT cells potentially inducing GvHD.

Stem cells, including pluripotent stem cells (PSCs) and hematopoietic stem cells (HSCs), have the flexibility for genetic-engineering and can be differentiated into a certain type of immune cells[14]. Numerous studies have shown their broad scope of application in cancer immunotherapy [5, 15-17]. The stem cell-derived T cells have shown unique innate-like phenotypes, suggesting that stem cell differentiation platform might be more suitable for innate-like T cells generation. Previous studies have shown that by engineering HSCs with iNKT TCR could generate sufficient number of iNKT cells through an artificial thymic organoid (ATO) culture system[17], an important advancement in the *in vitro* T cell differentiation field[15, 18]. However, the dependence of murine derived feeder cells in the system potentiates the risk of cross-species contamination for manufacturing. Here, we report a novel feeder-free and serum-free *ex vivo* culture platform to generate allogeneic HSC-engineered CAR-armed NKT (^{Allo}CAR-eNKT) cells for off-the-shelf cancer immunotherapy. The platform is versatile and compatible to generate unique eNKT cells carrying different CAR cargos, such as B cell maturation antigen (BCMA) CAR (BCAR), CD19 CAR, GD2 CAR, as well as additional molecules, such as interleukin 15 (IL-15) and sr39TK suicide gene. The allogeneic BCMA-targeting ^{Allo}CAR-eNKT (^{Allo}BCAR-eNKT) cells execute potent anti-tumor efficacy without GvHD risk in the human multiple myeloma (MM) xenograft mouse model. The IL-15 enhanced ^{Allo}BCAR-eNKT (^{Allo15}BCAR-eNKT) cells displayed remarkable persistence and enhanced therapeutic activity, potentially providing durable protection to patient. The $^{Allo/15}$BCAR-eNKT cells exhibit a hypoimmunogenic phenotype, resulting in resistance to allo-rejection but without affecting tumor killing capacity. Therefore, we provide the world the third option apart from T and NK cells for developing “off-the-shelf” cancer

immunotherapy and promotes the speedy clinical translation of stem cell-derived cells. The convergence of human stem cell engineering and cell therapy technology holds great promise for the development of a new class of cellular therapeutics.

Results

Generation of allogeneic HSC-engineered NKT (^{Allo}eNKT) and their CAR-armed derivatives (^{Allo}CAR-eNKT cells).

Human cord blood (CB) CD34+ HSCs were transduced with a designated Lenti/iNKT-(CAR)-(Additional Gene) vector, that co-delivers genes encoding an human iNKT TCR, with/out a selected CAR, with/out an optional additional gene for immune modulation (e.g., IL-15) or for safety control (e.g., sr39TK)[17]. Note, $CD34^+$ cells comprise both hematopoietic stem cell and progenitor cells; in this report we refer to $CD34^+$ cells as HSCs. Transduced HSCs were cultured in an *Ex Vivo* HSC-Derived eNKT Cell Culture over ~6 weeks to generate a designated ^{Allo}(CAR)-eNKT cell product (Fig.1a). A StemSpan™ T Cell Generation Kit from StemCell Technologies was utilized to support a feeder-free/serum-free three-stage human T cell differentiation from HSCs (https://www.stemcell.com/products/stemspan-t-cell-generation-kit.html#section-protocols-and-documentation): Stage 1, lymphoid progenitor expansion; Stage 2, T progenitor maturation; and Stage 3, T progenitor deep maturation (Fig.1b). Notably, in this 3-stage T cell generation culture, HSCs without iNKT TCR gene engineering only yielded very limited numbers of mature ($\alpha\beta TCR^+$ $CD4^-CD8^+$) αβT cells that only started to appear at week 8; from one input HSCs, ~2000 mature CD8 single positive (CD8 SP) αβT cells could be generated at the end of week 8. iNKT TCR gene engineering dramatically increased the yield of mature T cells and speeded up their generation; from one gene-engineered input HSCs, ~1000,0000 mature (iNKT $TCR^+CD4^-CD8^{+/-}$) transgenic ^{Allo}(CAR)-eNKT cells could be generated at the end of week 4. Note

at week 4, no endogenous non-transgenic αβT cells would appear (Supplementary Fig. 1). Therefore, the week 4 cell culture comprised pure and mature transgenic ^{Allo}(CAR)-eNKT cells, that were then expanded for ~2 weeks, resulting in a final ^{Allo}(CAR)-eNKT cell product of an impressive yield (~10^{12} product cells per 1 x 10^6 input HSCs) (Fig. 1c). From a standard CB unit containing ~5 x 10^6 $CD34^+$ HSCs, a 10^{12} scale of ^{Allo}(CAR)-eNKT cell product could be generated, that can be formulated into ~1,000-10,000 doses based on a 10^8-10^9 cells per dose estimation according to the current CAR-T therapy clinical experience[19]. Three expansion approaches were tested: 1) an αCD3/αCD28 expansion approach, 2) an αGC/PBMC expansion approach, and 3) an aAPC expansion approach (Fig. 1b). All three expansion approaches produced ^{Allo}(CAR)-eNKT cells at similar yield and quality (Supplementary Fig. 1); in this report, we focused on ^{Allo}(CAR)-eNKT cells generated with the aAPC expansion approach unless otherwise indicated. The reported method of generating HSC-engineered CAR-eNKT cells is robust and versatile. Over 10 CB donors and over 10 Lenti/iNKT-(CAR)-(AG) vectors (each corresponds to a specific cell product) were tested, all successfully resulting in high-yield and high-purity cell products regardless of donor originality and cargo gene variability (Fig.1c).

^{Allo}(CAR)-eNKT cell differentiation followed a typical iNKT developmental path defined by CD4/CD8 co-receptor expression: from $CD4^-CD8^-$ double-negative (DN) stage to a more mature $CD4^+CD8^+$ double-positive (DP) stage, and eventually to be almost all $CD8^+$ single-positive (SP) or DN phenotypes (Fig. 1e and 1f). Note that the end ^{Allo}(CAR)-eNKT cell product did not contain a $CD4^+CD8^-$ (CD4 SP) population that are present in the endogenous human iNKT cells. In general, CD8 SP/DN human iNKT cells are considered to be proinflammatory and highly cytotoxic and thereby are desirable for cancer immunotherapy[20]. The introduction of CAR and enhancer genes at the HSC stage did not interfere with the *ex vivo* development, and the co-

expression of CAR and iNKT TCR genes leads to high CAR expression rates accompanied by the positive selection for the TCR-containing transgene (Fig.1E-H, Fig. S1D). The *ex vivo* eNKT cell culture was compatible with various CAR designs and enhance genes (Fig. 1D). The generation and development of ^{Allo}BCAR-eNKT cells (BCMA-specific 4-1BB co-stimulation CAR), ^{Allo}CAR19-eNKT cells (CD19-specific CD28 co-stimulation CAR), and ^{Allo15}BCAR-eNKT (IL-15 enhanced ^{Allo}BCAR-eNKT) cells followed the same pattern and shared phenotypic results. This approach simplifies gene engineering steps for co-delivering CAR and/or additional genes providing unique advantages over all current allogeneic products production.

Flow cytometry analysis suggested the uniform expression of transgeneic iNKT TCR on the final products; sing-cell TCR sequencing analysis confirmed that ^{Allo}(CAR)-eNKT cells solely expressed the transgenic iNKT TCRs with undetectable randomly rearranged endogenous αβ TCR pairs, suggesting the induction of allelic exclusion through the transgenic iNKT TCR as previously reported[21-23]. In contrast, healthy donor periphery blood mononuclear cell (PBMC)-derived conventional αβ T (PBMC-αβTc) cells expressed highly diverse endogenously rearranged αβ TCRs, and PBMC-derived iNKT (PBMC-iNKT) cells expressed a conserved invariant TCR α chain (Vα24-Jα18) and TCR β chains of limited diversity (predominantly Vβ11).

We also performed deep RNA sequencing to characterize the transcriptome profiles of ^{Allo}(CAR)-eNKT cells in comparison with PBMC derived conventional αβ T (PBMC-αβTc), iNKT (PBMC-iNKT), and NK (PBMC-NK) cells (Fig. 1G). Principal component analysis (PCA) of the global gene expression profiles showed that all ^{Allo}(CAR)-eNKT cells clustered together and located closely to PBMC-iNKT and PBMC-αβTc cells, and the furthest from PBMC-NK cells (Fig. 1G), indicating that engineered eNKT cells are a unique cell population, yet closely resemble PBMC-iNKT and PBMC-αβTc cells. ‘‘Master’’ transcription factor gene profiling analysis

revealed that ^{Allo}(CAR)-eNKT cells expressed high levels of *ZBTB16* that encodes PLZF, a signature transcription factor of innate T (e.g., iNKT and gdT) cells and NK cells; they also expressed high levels of *TBX21* that encodes T-bet, an essential transcription factor regulating Th1 polarization of T cells. These transcription factors have been indicated to play important roles in regulating iNKT cell development and functionality.

Development, phenotype, and functionality of ^{Allo}BCAR-eNKT and their IL-15 enhanced derivative (^{Allo15}BCAR-eNKT cells).

IL-15 plays a critical role in NKT cell survival and homeostasis[24]. It has shown that IL-15-expressing CAR-engineered PBMC-NKT therapy was safe in a recent phase-I clinical trial[25]. No study has ever evaluated whether IL-15-engineering at HSC stage will interfere with iNKT development and affect its functionality. Starting from here, we focus on ^{Allo}BCAR-eNKT and their IL-15 enhanced derivative (^{Allo15}BCAR-eNKT cells) in the main text. All characterizations of ^{Allo}CAR19-eNKT and other products were provided in the SI (Fig. S2).

First, we performed single cell RNA sequence to track the development of engineered CD34$^+$ HSC during the *ex vivo* culture. Uniform manifold approximation and projection (UMAP) visualized the enrichment of $^{Allo/15}$BCAR-eNKT cells during the culture (FIG.2A). At the first two weeks of culture, there were a small portion of CD34$^+$ HSCs expressing myeloid lineage markers, but eventually only eNKT cells grew out. Next, we characterized the phenotype and functionality of $^{Allo/15}$BCAR-eNKT cells compared to the clinically employed PBMC-derived BCAR-T cells. $^{Allo/15}$BCAR-eNKT cells conserved many typical T cell functions while displaying a distinct NKT cell phenotype. $^{Allo/15}$BCAR-eNKT cells expressed high levels of T cell memory marker (i.e., CD45RO) and T cell activation marker (i.e., CD69) (Fig.2B). In addition, $^{Allo/15}$BCAR-eNKT cells

were able to produce massive amounts of proinflammatory cytokines (i.e., IFN-γ, IL-2, and TNF-α) and cytotoxic molecules (i.e., granzyme B and perforin) in response to PMA/ionomycin stimulation (Fig. 2B). To test the functionality of the iNKT TCR, we stimulated $^{Allo/15}$BCAR-eNKT cells with the iNKT antigen α-galactosylceramide (αGC) and observed vigorous proliferation (Fig. 2C). In response to αGC, $^{Allo/15}$BCAR-eNKT cells secreted high levels of Th0/Th1 cytokines (i.e., IFN-γ and TNF-α) and a minimal amount of Th2 (i.e., IL-4) and Th17 (i.e., IL-17). (Fig. 2D-G) cytokines. IL-15 engineering did not interfere with the production and development of ^{Allo15}BCAR-eNKT cells (Fig. 2A). IL-15 secretion was confirmed by ELISA (Fig. 2H). While consistent with ^{Allo}BCAR-eNKT cells, ^{Allo15}BCAR-eNKT cells showed similar NKT-like phenotype and functionalities (Fig. 2B-G), they robustly phosphorylated Stat5 and upregulated Bcl-xL expression (Fig. 2I) under a cytokine-deprived serum-free condition.

In vitro anti-tumor efficacy and mechanism of action (MOA) study of $^{Allo/15}$BCAR-eNKT cells.

Due to the NKT nature and CAR engineering, we proposed a CAR/TCR/NK triple-targeting mechanism of $^{Allo/15}$BCAR-eNKT cells for CD1d^{+} tumor and a CAR/NK dual-targeting for CD1d^{-} tumor cells (Fig. 3A). Here we used a human multiple myeloma (MM) cell line, MM, engineered to express the firefly luciferase-enhanced green fluorescence protein (FG) dual-reporters (denoted as MM-FG) and its derivatives to dissect the killing mechanisms. Scanning electron microscopic (SEM) image showed the morphology of an ^{Allo15}BCAR-eNKT cell attacking an MM-FG cell *in vitro* (Fig. 3D). Three MM cell lines (Fig.3B) were used as targets, including MM-FG, MM-FG-CD1d (MM.1S-FG cell line overexpressing human CD1d) and ^{KO}MM-FG (MM.1S-FG cell line with BCMA gene knockout). To dissect the CAR-directed killing, we compared the antitumor efficacy of ^{Allo15}BCAR-eNKT and BCAR-T cells on MM-FG and ^{KO}MM-

FG cells (Fig.3E). PBMC-derived conventional T cells were included as a control. Both ^{Allo15}BCAR-eNKT and BCAR-T cells exhibited significant tumor killing efficacy on BCMA^{+} MM-FG cells, with increased expression of IFN-γ, IL-2 and CD69 (Fig.3E-G &Fig.S5B). Notably, ^{Allo15}BCAR-eNKT cells exhibited slightly higher tumor killing efficacy than BCAR-T cells on BCMA^{-} ^{KO}MM-FG cells at high Effector-to-Target (E-T) ratio (Fig. 3F), suggesting additional tumor-targeting mechanism(s) (Fig. 3G&S5B). To access the iNKT TCR-directed anti-tumor capacity, we used *in vitro* MM-FG-(CD1d) tumor cell killing assay; non-CAR-engineered ^{Allo}eNKT cells, as well as PBMC-T cells (Fig 3H). At low E:T ratio, neither ^{Allo}eNKT nor PBMC-T cells were able to kill MM-FG cells, but the addition of αGC significantly enhanced the killing on CD1d^{+} MM-FG-CD1d cells (Fig. 3I). The iNKT TCR-mediated antitumor pathway was confirmed by CD1d blocking assay (Fig. 3J). In addition, ^{Allo}eNKT cells expressed high levels of NK activating receptors (e.g., NKG2D and DNAM1) (Fig. SXXX) and blocking of these receptors partially abrogated tumor-cell killing (Fig. 3K). The CAR/TCR/NK triple killing mechanism was further verified with MM-FG-CD1d tumor cells (Fig. 3M-N). Since MM was known to be not sensitive to NK-mediated killing, we repeated *in vitro* tumor killing on a NK-sensitive leukemia cell line (K562) (Fig. S5E). Without ligands triggering CAR- and TCR-directed killing, $^{Allo/15}$BCAR-eNKT cells still effectively killed K562 tumor cells through NK activating receptors (i.e., NKG2D and DNAM-1), and the killing potency could be significantly blocked by NK activating receptor blockage (Fig. S5E-G).

In vivo anti-tumor efficacy and pharmacokinetics/pharmacodynamics (PK/PD) study of $^{Allo/15}$BCAR-eNKT cells.

Using MM xenograft NSG (NOD/SCID/γc$^{-/-}$) mouse models, we studied the *in vivo* anti-tumor efficacy (Fig. 4A-B) and PK/PD (Fig. 4F-G) of $^{Allo/15}$BCAR-eNKT cells in comparison with BCAR-T cells. In the efficacy study, MM tumor cells were labeled with FG dual reporters (Fig. 4A). With single administration of effector cells, $^{Allo/15}$BCAR-eNKT and BCAR-T cells effectively delayed tumor progression (Fig. 4C) and significantly prolonged the mouse survival (Fig. 4D-E). Nevertheless, both ^{Allo}BCAR-eNKT and BCAR-T cells could not eradicate tumor with this regimen. All BCAR-T treated mice died at round 1–2-month post treatment where 5 out of 8 mice showed obvious tumor relapse and 3 had severe GvHD symptoms. The IL-15 secreting ^{Allo15}BCAR-eNKT cells exhibited enhanced therapeutic effect, leading to complete cure in 7 out of 8 mice (Fig.4D). However, ^{Allo}BCAR-eNKT cells didn't control tumor progression as well as ^{Allo15}BCAR-eNKT cells, which could be related to the IL-15 function of stimulating T cells. To better understand the *in vivo* PK/PD of three therapeutic cells, we performed a mirror study in the same human MM xenograft NSG mouse model, but this time the therapeutic cells, not the tumor cells, were labeled with the FG dual reporters (Fig. 4F&G). The ^{Allo15}BCAR-eNKT cells mounted an antitumor response in a low tumor antigen condition and persisted after tumor clearance, while ^{Allo}BCAR-eNKT cells and BCAR-T cells only lasted approximately 10 days response to antigen stimulation (Fig. 4H&I). We verified that both ^{Allo}BCAR-eNKT cells and BCAR-T cells were capable to mount sufficient response toward antigen stimulation at a heavy tumor load model (Fig. S6A-D) but insufficient when tumor load was low. The ^{Allo15}BCAR-eNKT cells responded to tumor antigen stimulation rapidly and migrated into different tissues but eventually preferentially resided in liver, lung, and bone marrow providing durable protection (Fig. 4J&K). Compared to FG labeled BCAR-T treated group, ^{Allo15}BCAR-eNKT cells demonstrated no evidence of aberrant proliferation and no host toxicity (Fig.4K). Indeed, minimal signal was detected in ^{Allo15}BCAR-

eNKT cell treated mice at around day 65, while BCAR-T cells treated group had a surge of signal at late stage consisting with the development of GvHD from their xenoreactivity (Fig. 4K)

Gene profiling of $^{Allo/15}$BCAR-eNKT cells in a human MM xenograft NSG mouse model.

To better understand the dynamic features of $^{Allo/15}$BCAR-eNKT cells, we performed scRNA-seq on ^{Allo}BCAR-eNKT, ^{Allo15}BCAR-eNKT and BCAR-T cells isolated from the human MM xenograft NSG mouse model (Fig. 5A). Samples were collected and combined from 10 mice each group at four phases respectively: pre-infusion stage, *in vivo* day 14 and day 28 response stage, and post-stimulation stage. After removing low-quality cells, the combined total 46718 cell transcriptomes were profiled. The *in vivo* day 14 results were not represented in the main figure due to the lack of sufficient numbers in the ^{Allo}BCAR-eNKT and BCAR-T treated groups. Four clusters were identified and visualized by uniform manifold approximation and projection (UMAP; Fig. 5B) as previously described[26]; the expression of marker genes indicated clusters of T-like effector/proliferation cells, NK-like effector/proliferation cells, NK-like effector/exhaustion cells and to be T-like effector/exhaustion cells (Fig.5B). Compared to BCAR-T cells, our $^{Allo/15}$BCAR-eNKT products exhibited more NK features, stronger effector and less exhaustion features (Fig. 5C&D). Notably, conventional T cells also gained NK feature response to antigen stimulation which was consistent with previously reports[27]. However, the NK-like phenotype of BCAR-T cells was correlated with upregulation of exhaustion markers while our $^{Allo/15}$BCAR-eNKT products were not (Fig. 5E&F). Besides, we also compared the transcriptomes of tumor cells under different treatment and no significant differences on clusters (Fig. SA-C). Interestingly, tumors under BCAR-T treatment tended

to downregulate *TNFRSF17* gene (encode BCMA expression) that may correlate with tumor evasion by antigen escape while it was not observed in $^{Allo/15}$BCAR-eNKT treated tumors (Fig. SD).

Safety and immunogenicity study of $^{Allo/15}$BCAR-eNKT cells.

Next, we evaluated the safety and immunogenicity of our $^{Allo/15}$BCAR-eNKT cells. For allogeneic immune cell therapy, GvHD is a major safety concern[28-30]. Due to the recognition of glycolipids and the invariant nature of the iNKT TCR, NKT cells are not expected to mount GvH responses[11, 31]. We implemented an *in vitro* mixed lymphocyte reaction (MLR) assay to evaluate the GvHD risk of ^{Allo}BCAR-eNKT cells (Fig. 6A). ^{Allo}BCAR-eNKT cells did not react to donor-mismatched PBMCs, whereas BCAR-T cells produced significant amounts of IFN-γ, a surrogate for alloreactivity (Fig. 6B). This was consistent with the *in vivo* tissue histology analysis, where severe mononuclear cell infiltration in multiple vital organs was only observed in mice treated with BCAR-T cells but not with $^{Allo/15}$BCAR-eNKT cells (Fig. 6C). Mice treated with $^{Allo/15}$BCAR-eNKT cells mounted lower IL-6 expression compared to that of BCAR-T cells (Fig. 6D-E).

Furthermore, host-versus-graft (HvG) response that may lead to the depletion of allogeneic therapeutic cells by host immune cells (i.e., host T and NK cells), is also a key factor determining whether allogeneic cell therapy would be successful or not. We performed an *in vitro* MLR assay to evaluate the HvG risk of $^{Allo/15}$BCAR-eNKT cells (Fig. 6F-G). Compared to BCAR-T cells, ^{Allo}BCAR-eNKT cells triggered significantly reduced IFN-γ production from PBMCs of multiple mismatched donors, which may be caused by the naturally low expression of HLA molecules by $^{Allo/15}$BCAR-eNKT cells (Fig. 6H&I). Importantly, compared to BCAR-T cells, the $^{Allo/15}$BCAR-eNKT cells could maintain low expression of both HLA-I (B2M) and HLA-II (HLA-DR,DP,DQ) under inflammatory conditions, either post interacting with tumor cells from *in vivo*

experiemnt(Fig. 6J-L) or post IFN-γ stimulation from *in vitro* culture(Fig. 6M). To evaluate the host NK cell-mediated HvG response, we performed another MLR assay to study this aspect (Fig. 6O). Currently, since no other optimal assays to investigate the NK-mediated response, we directly cocultured allogeneic PBMC-derived NK cells with $^{Allo/15}$BCAR-eNKT or BCAR-T cells. The ^{Allo}BCAR-eNKT cells persisted better compared to conventional BCAR-T cells (Fig. 6P-Q). The resistance to the NK rejection of ^{Allo}BCAR-eNKT cells may be attributed to their low expression of "stress molecules" like the NK ligands (i.e., MICA/B, and ULBP) of activating receptors (Fig.6R). To further enhance the safety profile of the cell products, we also demonstrated the feasibility of engineering an sr39TK suicide gene into our products with IL-15 enhanced cells as an example (Fig. S8A). The incorporated sr39TK gene did not interfere with eNKT development (Fig. S8B) and would allow *in vivo* monitoring with positron emission tomography (PET) imaging and, most importantly, elimination of sr39TK expressing cells in the case of a severe adverse event[21]. The prodrug ganciclovir (GCV) induced effective depletion of eNKT cells both *in vitro* and *in vivo* (Fig. S8D-G).

Discussion

Since the first CAR-T cell approval in the United States in 2017, the cell therapy field has rapidly evolved, with the FDA approving five additional CAR-T cell therapies. Nevertheless, autologous CAR-T cell therapy faces challenges surrounding cost, time, and patient access[2]. As such, off-the-shelf assets could be the solution to the industry's current pain point. An idea cell therapy requires effective, safe, robust, and scalable cell products, regardless of the application. Currently, a variety of allogeneic CAR cell therapy platforms have been developed, including engineering PBMC-derived immune cells (i.e., conventional αβT, NK, iNKT and γδT cells), as

well as engineering stem cells (i.e., HSCs, and pluripotent stem cells) for off-the-shelf cancer immunotherapy[5-7, 15, 17, 32]. The most widely used allogeneic CAR platform is to use site-specific nucleases to modify conventional αβT cells. Due to HLA incompatibility of conventional αβT cells between the healthy donor and the host, multiplex gene editing is required to disrupt native αβ TCR (i.e., disrupting the *TRAC* or/and *TRBC* loci), ablate both MHC I (i.e., B2M) and MHC II (i.e., CIITA) molecules, to reduce the risk of GvHD and rejection[4]. The greatest concern with this approach is that the exorbitant genetic manipulations could induce frequent aneuploidy and increase the tumorigenicity risk[33]. Alternatively, unconventional T cells, such as iNKT[7, 17], γδ T[32] and NK[6, 34] cells, that are considered as low/no GvHD risk but restricted by their cell number in PBMC or *in vivo* clonal expansion performance, have also been explored as allogeneic cell products. Currently, three major categories of allogeneic cell products, PBMC-derived universal CAR19 conventional αβT cells (UCART19)[4], PBMC-derived GD2.CAR.IL15 iNKT (PBMC-GD2.CAR.IL15-iNKT)[7] cells, and CB-derived CAR19-NK (CB-CAR19-NK)[6] cells, were tested in clinical trials, showing an inspiring step forward for the field of allogeneic cell therapy.

Compared to the outstanding outcomes of autologous CAR-T therapy, allogeneic CAR therapy, particularly allogeneic CAR-T therapy, has demonstrated acceptable efficacy in B cell malignancies (e19530 abstract). Since there is no FDA approved allogeneic cell therapy yet, we compared the antitumor efficacy of ^{Allo15}BCAR-eNKT cells with BCAR-T cells expanded following a protocol for autologous therapy. ^{Allo15}BCAR-eNKT cells performed superior anti-tumor efficacy over BCAR-T cells without inducing any GvHD. This could be attributed to the high CAR-expressing level, the durable *in vivo* persistence, as well as the multiple tumor-killing mechanism of ^{Allo15}BCAR-eNKT cells. CAR-expressing level on engineered cells is crucial to the efficacy of CAR-engineered cells. At present, the average CAR transduction efficacy of current

allogeneic cell products in clinical is around 40%, with 20-70% in UCAR19-T, 20.18-70.4% CAR in PBMC-GD2.CAR.IL15-iNKT cells, and 22.7-66.5% in CB-CAR19-NK cells. The co-expression of CAR and iNKT TCR genes in our culture leads to high CAR expression rates (Fig. S1) accompanied by the positive selection for the TCR-containing transgene, increasing the sensitivity of tumor-recognition. On the other hand, ^{Allo15}BCAR-eNKT cell products exhibited less exhausted phenotype which maintained during interaction with tumor antigen (Fig. 5C&F). The IL-15 enhancement significantly improved the proliferating and memory signature of cell products (Fig. 5E), allowing ^{Allo15}BCAR-eNKT cells providing durable protection. In addition, BCAR-T cell treated MM cells exhibited significant lower level of *TNFRSF17* gene (encoding the tumor antigen BCMA) and higher expression of MHC molecule, indicating a trend of immune escape, while that was not observed in $^{Allo/15}$BCAR-eNKT treated tumor cells. Antigen escape is a common mechanism of tumor resistance to CAR T therapy, that is observed in a notable proportion of patients of hematological malignancies, GBM, or other solid tumors (cite). The intrinsic downregulation of tumor antigen expression and upregulation of MHC molecules protected tumor cells from CAR- and NK-directed killing (PMID.24850305; 33558511). The enhanced anti-tumor efficacy from multiple tumor-killing mechanism of $^{Allo/15}$BCAR-eNKT cells may be sufficient to eliminate tumor cells regardless of tumor heterogenicity, without triggering tumor intrinsic evasion mechanisms. Together, these data suggest that our *ex vivo* eNKT culture may provide a unique platform for generating powerful therapeutic cells.

Safety and immunogenicity have been another valuable factor to evaluate suitability of allogeneic cellular product candidates. iNKT cells, the distinct cell type that is MHC-independent, naturally do not cause GvHD. The ^{Allo}(CAR)-eNKT cells inherited the iNKT property, without inducing GvHD (Fig. 4xxx). More importantly, IL-15 enhancement, the cytokine that has shown

profound effects in regulating T cell and NK cell proliferation and function, is compatible in our HSC differentiation culture, without interfering the development and differentiation of eNKT cells. The ^{Allo15}BCAR-eNKT cells showed remarkable long-term persistence in the absence of aberrant proliferation and host toxicity. It is important to note that there was evidence showing IL-15 might also have a pro-tumorigenic role in malignancies and long-term exposure to IL-15 may promote tumor evasion (Cite). However, no tumorigenic effect reported from the GD2-targeting PBMC-iNKT cell and CD19-tarting CB-NK cell clinical trials. Incorporating a suicide gene, such as sr39TK or inducible caspase-9-based (iC9) genes might be a potential solution to arrest the issue. More studies will be imperative to elucidate the concerns. On the other hand, the allogeneic cell products carry increased risk of immunogenicity that would result in rejecting by the host immune system, thus affecting the therapeutic efficacy. To decrease immunogenicity, two strategies have been explored: to target β-2 microglobulin (B2M) to eliminate HLA class I molecules as well as knockout of class II major histocompatibility complex transactivator (CIITA) to eliminate HLA class II; or depleting host immune cells by lymphodepleting chemotherapy prior to cellular infusion combined with patient administration of alemtuzumab to sustain the immunosuppression condition. The additional gene manipulation increases the complexity of manufacturing with the potential risk of tumorgenicity, while the long-term administration of alemtuzumab in patients is associated with the increased risk of infection (cite). In terms of this, our eNKT products naturally exhibited low immunogenicity with low expression of MHC I, undetectable levels of MHC II molecules, and low level of NK activating ligands (Fig.xxx), reducing the requisite of multiplex gene editing. Previously studies have shown that two mechanisms may be involved in regulating MHC expression; one is the IFN-γ-JAK-STAT1 pathway and the other is the epigenetic regulation. When stimulated with IFN-γ, the ^{Allo}(CAR)-eNKT exhibited an IFN-γ-desensitized phenotypes,

lack of phosphorylated STAT1 increment. The low expression of *NLRC5*, *CIITA*, and *SP-1* proteins may explain the low immunogenicity ^{Allo}(CAR)-eNKT cells, that may be related to the epigenetic mechanisms involved in the regulation of these genes that have been displayed in hESCs and iPSCs (PMID: 20419139).

Recapitulation of T cell differentiation *in vitro* has been appealing but challenging historically. There are protocols to differentiate CAR-engineered conventional αβT or cells from CB or iPSCs with the supportive of feeder cells overexpressing DL1 or DL4, such as OP9-DL1/4, MS5-DLL1/4 cells. Few studies have explored the generation of CAR-engineered iNKT cells from stem cells. It has been demonstrated that using MS5-DLL1/4 dependent ATO culture system can successfully generate allogeneic iNKT cells from HSCs. However, the use of xenogeneic feeder cells will not be favorable for clinical application. In our platform, we substitute feeders with immortalized-DL4 protein and chemically defined cytokines to produce high CAR-expressing eNKT cells, releasing the safety risk of cross-species contaminations. This technology allows us to generate 1,000,000-fold expansion of ^{Allo}(CAR)-eNKT cells that easily produce 1,000-10,000 doses from 1 single unit of CB (Fig. 1A). The novel culture method is compatible with different CAR cargos, including those that target either hematological malignancies (e.g., BCMA CAR, CAR19) or solid tumors (e.g., GD2.CAR, GPC3.CAR, EGFR.CAR) (Fig.Sxxx). More importantly, additional genes, such as IL-15 and sr39TK genes, are also well-tolerate in our culture without interfering the differentiation of eNKT cells. Allogeneic CAR-eNKT therapy targeting BCMA, has both adaptive and innate cytotoxic effector functions to complement CAR targeting, potentially enhancing efficacy and reducing the possibility of tumor escape due to antigen loss. Express MHC independent iNKT receptors, lowering the risk of GvHD without the need for gene-

editing. The convergence of human stem cell engineering and cell therapy technology holds great promise for the development of a new class of cellular therapeutics.

Although our data suggest HSC-engineered eNKT cells to be an outstanding platform for off-the-shelf cell therapy, there are limitations to be further addressed in the future studies. First, similar as conventional αβ T cells, iNKT cells can also be classified as CD4+ and CD4- cells. The functionality differences between the two subtypes of iNKT cells are not well studied. CD4+ population may also play an important role and impact therapeutic outcomes. Deriving CD4+ cells in vitro in general is challenging. More fundamental knowledge on iNKT development is necessary to elucidate the question. Second, the timing for CAR introduction could be further studied. We tested two costimulatory domain, CD28 and 4-1BB, and either of them interfered with eNKT development and differentiation. However, it is well-known that CAR design could facilitate the therapeutic effects of products, especially the tonic signaling identified. Further exploration of ^{Allo}(CAR)-eNKT cells as allogeneic cell carriers for developing off-the-shelf cell therapy for the treatment of cancer, especially solid tumors, will certainly be an interesting direction for future study.

Online content

Any methods, additional references, Nature Research reporting summaries, source data, supplementary information, acknowledgements, peer review information; details of author contributions and competing interests; and statements of data and code availability are available at https://xxxxxxx.

References

1. June, C.H., O'Connor, R.S., Kawalekar, O.U., Ghassemi, S. & Milone, M.C. CAR T cell immunotherapy for human cancer. *Science* **359**, 1361-1365 (2018).
2. Sterner, R.C. & Sterner, R.M. CAR-T cell therapy: current limitations and potential strategies. *Blood Cancer J* **11**, 69 (2021).
3. Finck, A.V., Blanchard, T., Roselle, C.P., Golinelli, G. & June, C.H. Engineered cellular immunotherapies in cancer and beyond. *Nat Med* **28**, 678-689 (2022).
4. Benjamin, R. et al. Genome-edited, donor-derived allogeneic anti-CD19 chimeric antigen receptor T cells in paediatric and adult B-cell acute lymphoblastic leukaemia: results of two phase 1 studies. *Lancet* **396**, 1885-1894 (2020).
5. van der Stegen, S.J.C. et al. Generation of T-cell-receptor-negative CD8αβ-positive CAR T cells from T-cell-derived induced pluripotent stem cells. *Nature Biomedical Engineering* (2022).
6. Liu, E. et al. Use of CAR-Transduced Natural Killer Cells in CD19-Positive Lymphoid Tumors. *N Engl J Med* **382**, 545-553 (2020).
7. Heczey, A. et al. Anti-GD2 CAR-NKT cells in patients with relapsed or refractory neuroblastoma: an interim analysis. *Nat Med* **26**, 1686-1690 (2020).
8. Godfrey, D.I., Le Nours, J., Andrews, D.M., Uldrich, A.P. & Rossjohn, J. Unconventional T cell targets for cancer immunotherapy. *Immunity* **48**, 453-473 (2018).
9. Brennan, P.J., Brigl, M. & Brenner, M.B. Invariant natural killer T cells: an innate activation scheme linked to diverse effector functions. *Nat Rev Immunol* **13**, 101-117 (2013).

10. Chandra, S. & Kronenberg, M. Activation and function of iNKT and MAIT cells. *Advances in immunology* **127**, 145-201 (2015).

11. Bae, E.-A., Seo, H., Kim, I.-K., Jeon, I. & Kang, C.-Y. Roles of NKT cells in cancer immunotherapy. *Archives of pharmacal research* **42**, 543-548 (2019).

12. Chaidos, A. et al. Graft invariant natural killer T-cell dose predicts risk of acute graft-versus-host disease in allogeneic hematopoietic stem cell transplantation. *Blood, The Journal of the American Society of Hematology* **119**, 5030-5036 (2012).

13. Exley, M.A. et al. Adoptive transfer of invariant NKT cells as immunotherapy for advanced melanoma: a phase I clinical trial. *Clinical Cancer Research* **23**, 3510-3519 (2017).

14. Li, Y.R., Zhou, Y., Kramer, A. & Yang, L. Engineering stem cells for cancer immunotherapy. *Trends Cancer* **7**, 1059-1073 (2021).

15. Wang, Z. et al. 3D-organoid culture supports differentiation of human CAR(+) iPSCs into highly functional CAR T cells. *Cell Stem Cell* (2022).

16. Jing, R. et al. EZH1 repression generates mature iPSC-derived CAR T cells with enhanced antitumor activity. *Cell Stem Cell* **29**, 1181-1196 e1186 (2022).

17. Li, Y.R. et al. Development of allogeneic HSC-engineered iNKT cells for off-the-shelf cancer immunotherapy. *Cell Rep Med* **2**, 100449 (2021).

18. Montel-Hagen, A. et al. Organoid-Induced Differentiation of Conventional T Cells from Human Pluripotent Stem Cells. *Cell Stem Cell* **24**, 376-389 e378 (2019).

19. Labanieh, L., Majzner, R.G. & Mackall, C.L. Programming CAR-T cells to kill cancer. *Nat Biomed Eng* **2**, 377-391 (2018).

20. Ni, Z. et al. Human pluripotent stem cells produce natural killer cells that mediate anti-HIV-1 activity by utilizing diverse cellular mechanisms. *J Virol* **85**, 43-50 (2011).

21. Zhu, Y. et al. Development of Hematopoietic Stem Cell-Engineered Invariant Natural Killer T Cell Therapy for Cancer. *Cell Stem Cell* **25**, 542-557 e549 (2019).

22. Smith, D.J. et al. Genetic engineering of hematopoietic stem cells to generate invariant natural killer T cells. *Proceedings of the National Academy of Sciences* **112**, 1523-1528 (2015).

23. Giannoni, F. et al. Allelic exclusion and peripheral reconstitution by TCR transgenic T cells arising from transduced human hematopoietic stem/progenitor cells. *Molecular Therapy* **21**, 1044-1054 (2013).

24. Gordy, L.E. et al. IL-15 regulates homeostasis and terminal maturation of NKT cells. *The Journal of Immunology* **187**, 6335-6345 (2011).

25. Heczey, A. et al. Anti-GD2 CAR-NKT cells in patients with relapsed or refractory neuroblastoma: an interim analysis. *Nature Medicine* **26**, 1686-1690 (2020).

26. Gur, C. et al. LGR5 expressing skin fibroblasts define a major cellular hub perturbed in scleroderma. *Cell* **185**, 1373-1388 e1320 (2022).

27. Good, C.R. et al. An NK-like CAR T cell transition in CAR T cell dysfunction. *Cell* **184**, 6081-6100 e6026 (2021).

28. Perez, C., Gruber, I. & Arber, C. Off-the-Shelf Allogeneic T Cell Therapies for Cancer: Opportunities and Challenges Using Naturally Occurring "Universal" Donor T Cells. *Frontiers in Immunology* **11** (2020).

29. Depil, S., Duchateau, P., Grupp, S., Mufti, G. & Poirot, L. 'Off-the-shelf'allogeneic CAR T cells: development and challenges. *Nature Reviews Drug Discovery* **19**, 185-199 (2020).

30. Aftab, B.T. et al. Toward "off-the-shelf" allogeneic CAR T cells. *Advances in Cell and Gene Therapy* **3**, e86 (2020).

31. Fujii, S.-i. et al. NKT cells as an ideal anti-tumor immunotherapeutic. *Frontiers in immunology* **4**, 409 (2013).

32. Makkouk, A. et al. Off-the-shelf Vdelta1 gamma delta T cells engineered with glypican-3 (GPC-3)-specific chimeric antigen receptor (CAR) and soluble IL-15 display robust antitumor efficacy against hepatocellular carcinoma. *J Immunother Cancer* **9** (2021).

33. Nahmad, A.D. et al. Frequent aneuploidy in primary human T cells after CRISPR-Cas9 cleavage. *Nat Biotechnol* (2022).

34. Cichocki, F. et al. iPSC-derived NK cells maintain high cytotoxicity and enhance in vivo tumor control in concert with T cells and anti-PD-1 therapy. *Sci Transl Med* **12** (2020).

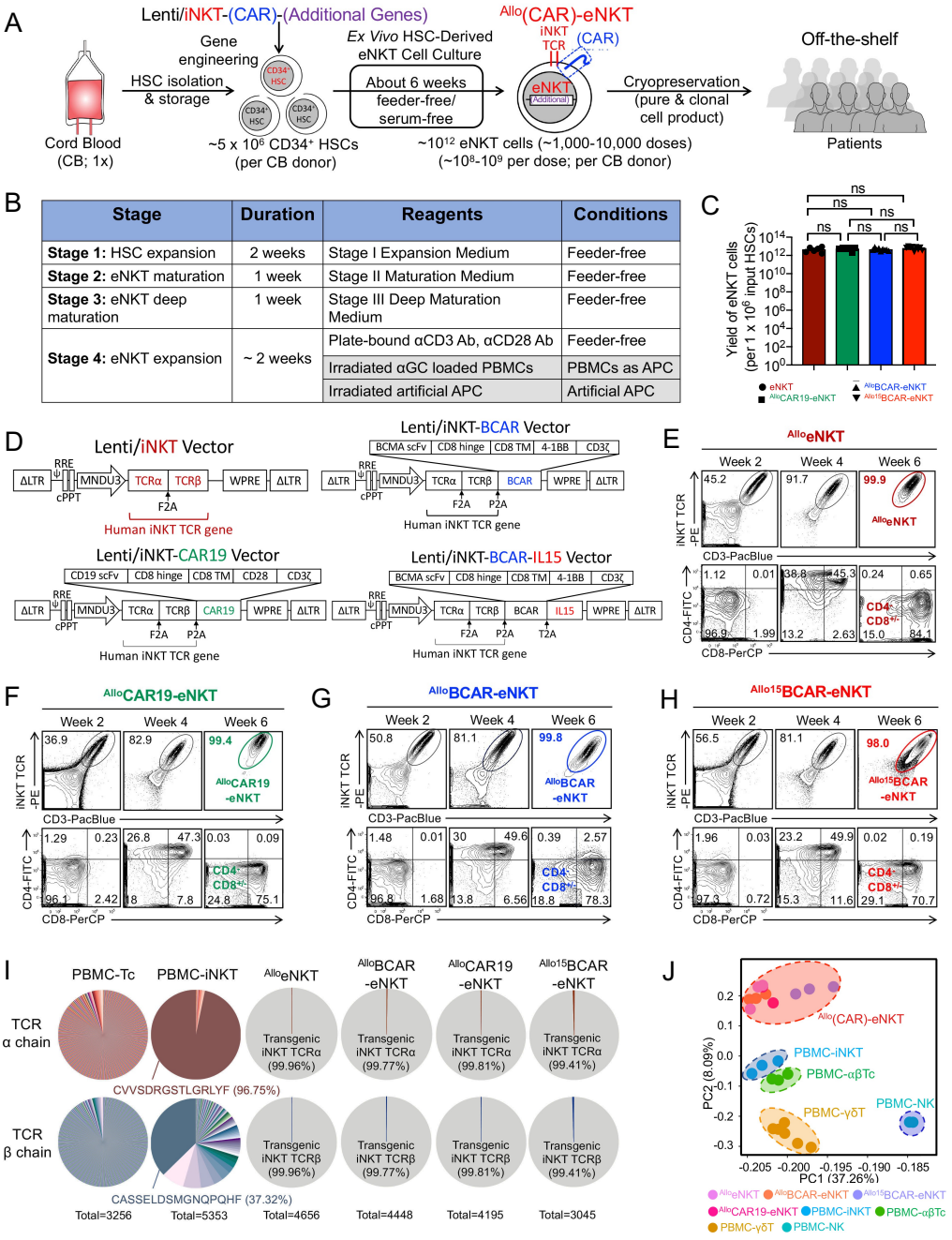

Stage	Duration	Reagents	Conditions
Stage 1: HSC expansion	2 weeks	Stage I Expansion Medium	Feeder-free
Stage 2: eNKT maturation	1 week	Stage II Maturation Medium	Feeder-free
Stage 3: eNKT deep maturation	1 week	Stage III Deep Maturation Medium	Feeder-free
Stage 4: eNKT expansion	~ 2 weeks	Plate-bound αCD3 Ab, αCD28 Ab	Feeder-free
		Irradiated αGC loaded PBMCs	PBMCs as APC
		Irradiated artificial APC	Artificial APC

Figure 1. Generation of allogeneic HSC-engineered NKT (^{Allo}eNKT) cells and their CAR-armed derivatives.

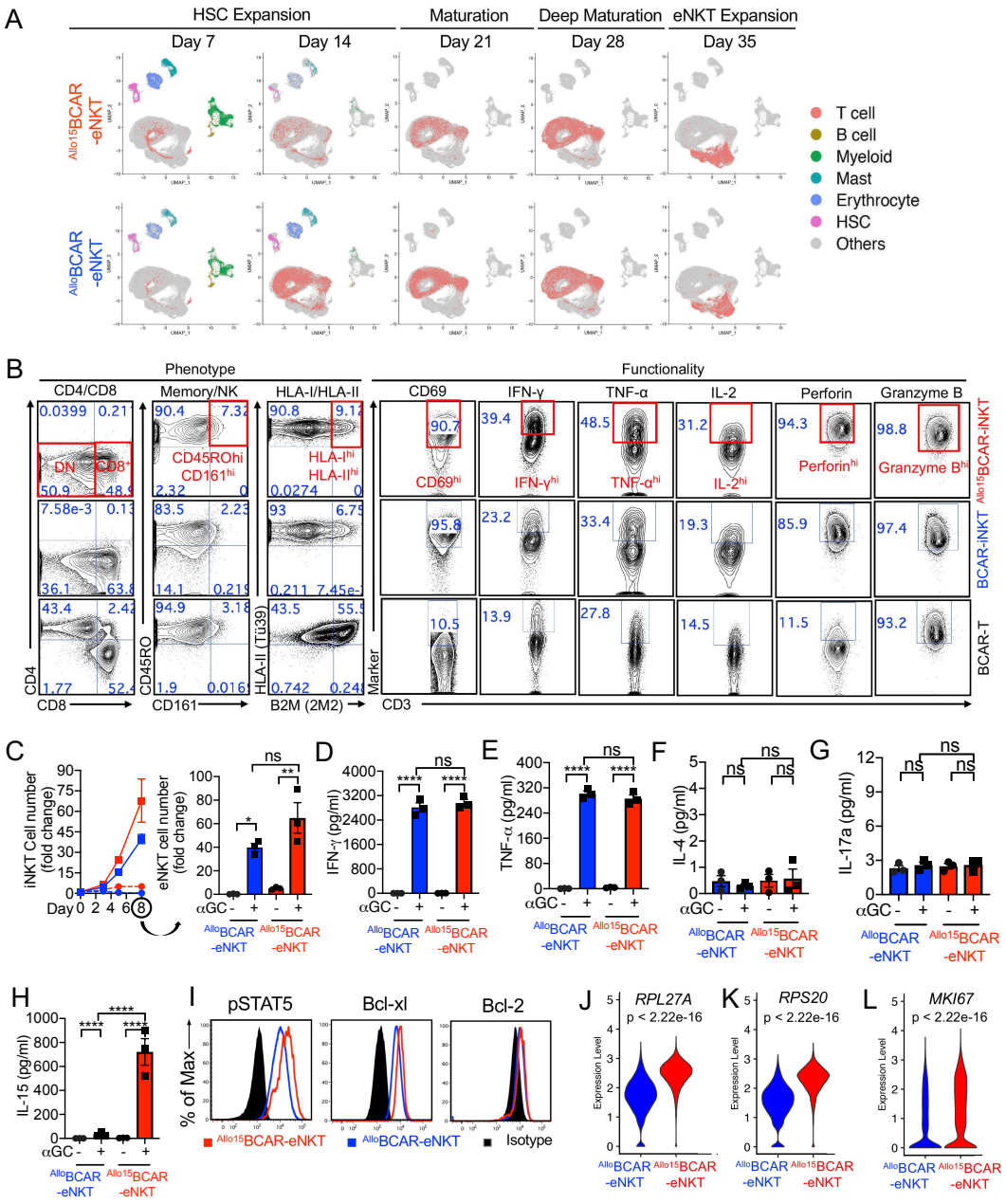

Figure 2. Development, phenotype, and functionality of BCMA-targeting CAR-armed ^{Allo}eNKT cells (^{Allo}BCAR-eNKT) and their IL-15 enhanced derivative(^{Allo15}BCAR-eNKT).

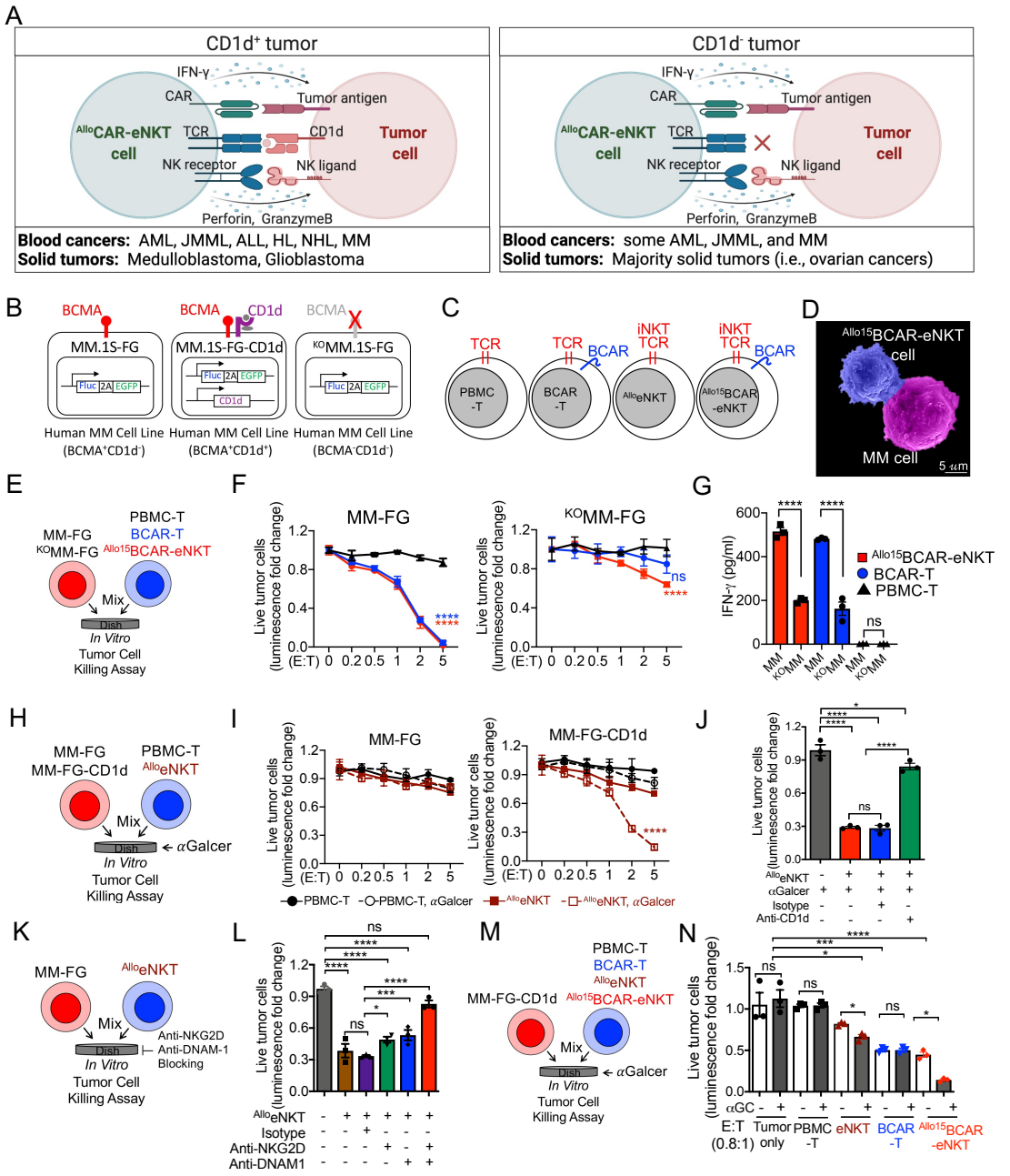

Figure 3. *In vitro* anti-tumor efficacy and mechanism of action (MOA) study of $^{Allo/15}$BCAR-eNKT cells.

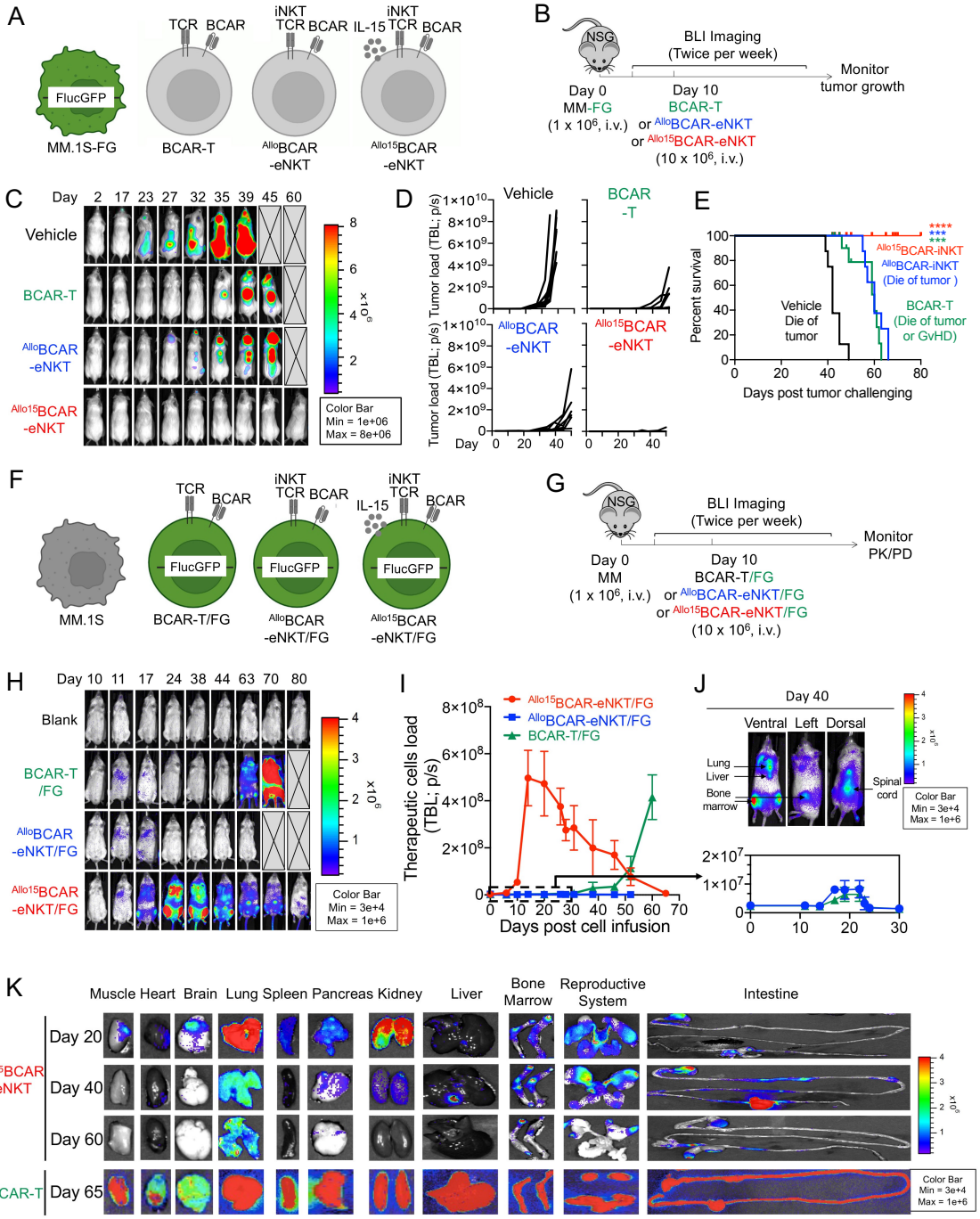

Figure 4. *In vivo* anti-tumor efficacy, pharmacokinetics/pharmacodynamic (PK/PD) study of Allo/^{15}BCAR-eNKT cells.

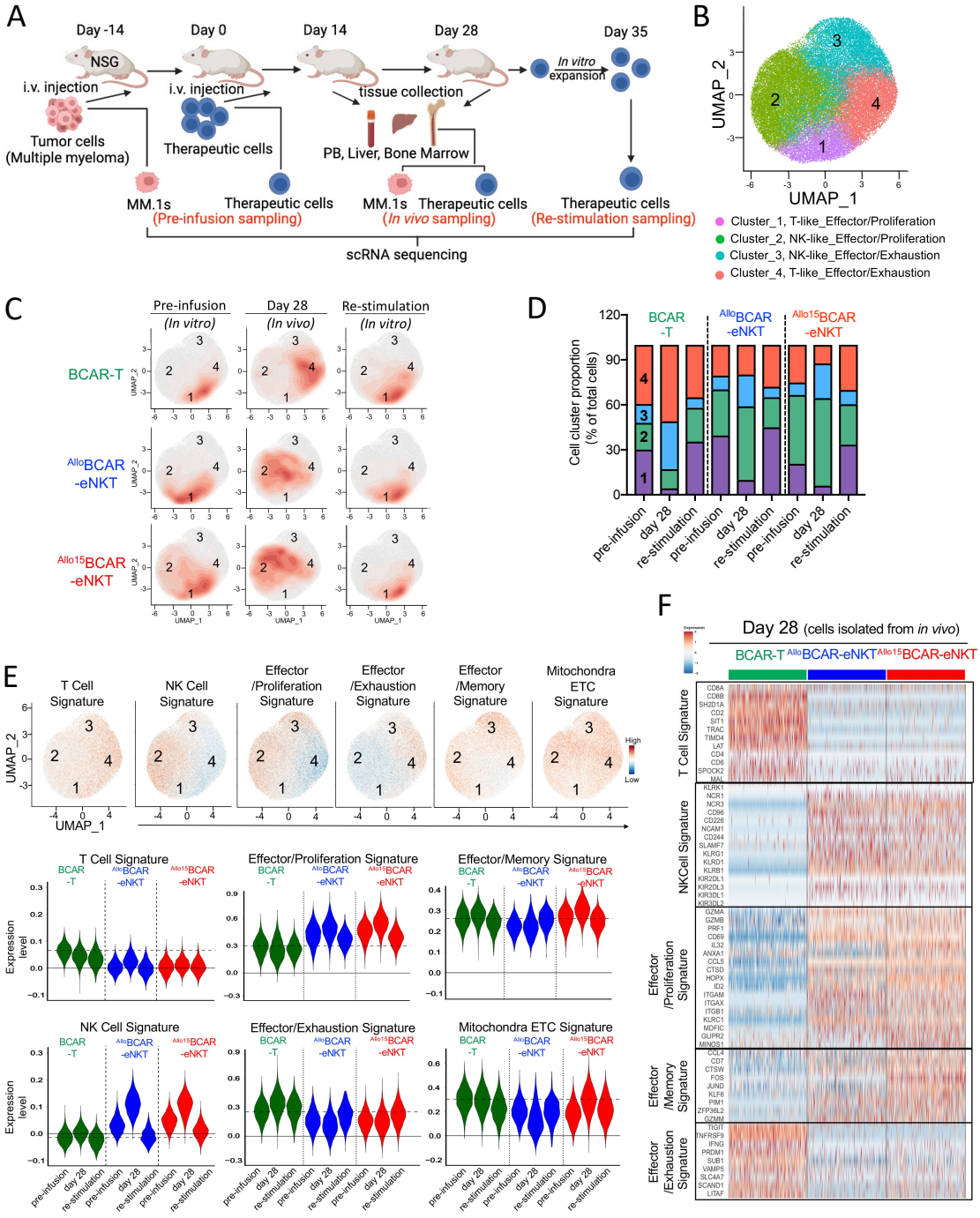

Fig5. *In vivo* phenotype and gene profiling of $^{Allo/15}$BCAR-eNKT cells.

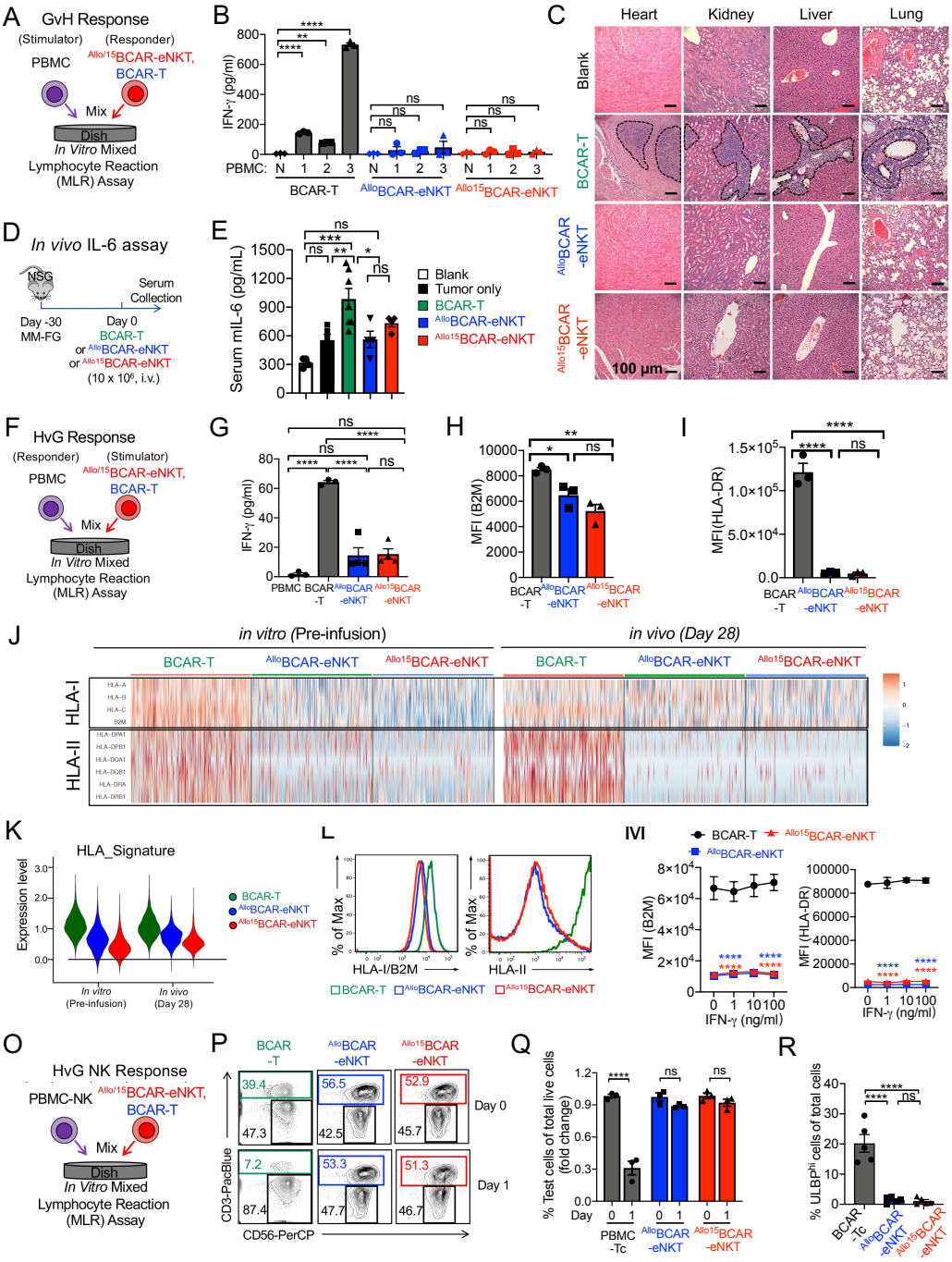

Figure 6. Safety and immunogenicity study of Allo/15BCAR-eNKT cells.

Supplementary Materials for

Scalable HSC-engineered multifunctional and hypoimmunogenic CAR-NKT cells for off-the-shelf cancer immunotherapy

Yang Zhou[1,*], Jiaji Yu[1,*], Yan-Ruide Li[1], Feiyang Ma[2], Miao Li[1], Kuangyi Zhou[1], Zhe Li[1], Yu Jeong Kim[1], Derek Lee[1], Xinjian Cen[1], Tiffany Husman[1], Aarushi Bajhaj[1], Yu-Chen Wang[1], Yuchong Zhang[1], Zoe Hanh[1], Zach Dunn[3], Enbo Zhu[1], Wenbin Guo[4], Pin Wang[3], Matteo Pellegrini[4,5] and Lili Yang[1,5,6,7 §]

Author Affiliation:
[1]Department of Microbiology, Immunology & Molecular Genetics, University of California, Los Angeles, Los Angeles, CA 90095, USA
[2]Division of Rheumatology, Department of Internal Medicine, University of Michigan, Ann Arbor, MI 48109, USA
[3]Department of Pharmacology and Pharmaceutical Sciences, University of Southern California, Los Angeles, CA 90089, USA
[4]Department of Molecular, Cell and Developmental Biology, College of Letters and Sciences, University of California, Los Angeles, Los Angeles, CA 90095, USA
[5]Eli and Edythe Broad Center of Regenerative Medicine and Stem Cell Research, University of California, Los Angeles, Los Angeles, CA 90095, USA
[6]Jonsson Comprehensive Cancer Center, David Geffen School of Medicine, University of California, Los Angeles, Los Angeles, CA 90095, USA
[7]Molecular Biology Institute, University of California, Los Angeles, CA 90095, USA
* These authors contributed equally
[§]Corresponding author. Email: liliyang@ucla.edu.

Address Correspondence to:
Lili Yang, Ph.D.
Department of Microbiology, Immunology & Molecular Genetics
University of California, Los Angeles
Los Angeles, CA 90095, USA.
Phone: 310-825-8609
Email: liliyang@ucla.edu

The SI includes Methods and Supplementary figures 1-10.

Contents

Methods

Mice. NOD.Cg-Prkdc^{SCID}Il2rg^{tm1Wjl}/SzJ (NOD/SCID/IL-2Rγ$^{-/-}$, NSG) mice were maintained in the animal facilities of the University of California, Los Angeles (UCLA). 6-10 weeks old mice were used for all experiments unless otherwise indicated. All animal experiments were approved by the Institutional Animal Care and Use Committee (IACUC) of UCLA. All mice were bred and maintained under specific pathogen-free conditions, and all experiments were conducted in accordance with the animal care and use regulations of the Division of Laboratory Animal Medicine (DLAM) at the UCLA.

Cell lines. Human multiple myeloma cell line MM.1S, chronic myelogenous leukemia cell line K562, Burkitt's lymphoma cell line Raji, acute lymphoblastic leukemia cell line NALM-6, melanoma cell line A375, glioblastoma cell line T98G and U87MG, hepatocellular carcinoma cell line Hep3B, and HEK-293T were purchased from American Type Culture Collection (ATCC).

To make stable tumor cell lines overexpressing human CD1d, and/or firefly luciferase and enhanced green fluorescence protein (FlucEGFP) dual-reporters, the parental tumor cell lines were transduced with lentiviral vectors encoding the intended gene(s). 72h post lentivector transduction, cells were subjected to flow cytometry sorting to isolate gene-engineered cells for making stable cell lines. Nine stable tumor cell lines were generated for this study, including MM-FG, MM-FG-CD1d, K562-FG, Raji-FG, Raji-FG-CD1d, NALM-6-FG, T98G-FG, U87-FG, and Hep3B-FG. ^{KO}MM.1S-FG cell line was engineered from parental MM-FG with BCMA gene disruption by CRISPR/Cas9. HEK-293T cells overexpressing full chains of human CD3 (HEK-293T-hCD3) were engineered by Lili Yang lab.

Artificial antigen presenting cells (aAPCs; human K562 cell line engineered to overexpress human CD83/CD86/4-1BBL co-stimulatory receptors) were obtained from the Dr. Crooks/Seet labs at UCLA. Cells were subjected to flow cytometry sorting to isolate gene-engineered cells for making stable cell lines.

Human CD34$^+$ hematopoietic stem cells (HSCs) and periphery blood mononuclear cells (PBMCs). Purified CD34$^+$ cells from cord blood (CB) were purchased from HemaCare. Healthy donor human PBMCs were obtained from the UCLA/CFAR Virology Core Laboratory without identification information under federal and state regulations.

Medium

α-Galactosylceramide (αGC, KRN7000) was purchased from Avanti Polar Lipids. Recombinant human IL-2, IL-3, IL-7, IL-15, IL-21, Flt3-Ligand (Flt3L), Stem Cell Factor (SCF), and Thrombopoietin (TPO), IFN-γ were purchased from Peprotech. Ganciclovir (GCV) was purchased from Sigma. X-VIVO 15 Serum-Free Hematopoietic Cell Medium was purchased from Lonza.

The HSC Medium used for culturing CD34$^+$ HSCs at the HSC gene-engineering stage was made of X-VIVO 15 supplemented with 50 ng/ml Flt3L, SCF, and TPO, and 20 ng/ml IL-3. The Stage I Expansion Medium was made of StemSpan^{TM} SFEM II Medium supplemented with StemSpan^{TM} Lymphoid Progenitor Expansion Supplement (StemCell Technologies). The Stage II Maturation Medium was made of StemSpan^{TM} SFEM II Medium supplemented with StemSpan^{TM} Lymphoid Progenitor Maturation Supplement (StemCell Technologies). The Stage III Deep Maturation Medium was made of StemSpan^{TM} SFEM II Medium supplemented with StemSpan^{TM}

Lymphoid Progenitor Maturation Supplement, CD3/CD28/CD2 T Cell Activator (StemCell Technologies) and 20 ng/mL human recombinant IL-15. Serum-Free Expansion Medium used for eNKT cell expansion was made of OpTmizer™ CTS™ T-Cell Expansion serum-free medium (Gibco, Thermo Fisher Scientific) with 10ng/ml IL-7, IL-15, and IL-21.

C10 medium was made of RPMI 1640, supplemented with RPMI 1640 supplemented with FBS (10% vol/vol), P/S/G (1% vol/vol), MEM NEAA (1% vol/vol), HEPES (10 mM), Sodium Pyruvate (1 mM), b-ME (50 mM), and Normocin (100 mg/ml). D10 medium was made of DMEM supplemented with FBS (10% vol/vol) and P/S/G (1% vol/vol).

Lentiviral vector construction. Lentiviral vectors used in this study were all constructed from a parental lentivector pMNDW. The 2A sequences derived from foot-and-mouth disease virus (F2A), porcine teschovirus-1 (P2A), and thosea asigna virus 2A (T2A) were used to link the inserted genes to achieve co-expression.

The Lenti/iNKT vector was constructed by inserting into the pMNDW parental vector a synthetic bicistronic gene encoding human iNKT TCRα-F2A-TCRβ; the Lenti/iNKT-sr39TK vector was constructed by inserting into pMNDW vector a synthetic tricistronic gene encoding human iNKT TCRα-F2A-TCRβ-P2A-sr39TK; the Lenti/iNKT-BCAR vector was constructed by inserting into pMNDW vector a synthetic tricistronic gene encoding human iNKT TCRα-F2A-TCRβ-P2A-BCAR (BCAR indicates BCMA-targeting CAR); the Lenti/iNKT-BCAR-IL15 vector was constructed by inserting into pMNDW vector a synthetic tetracistronic gene encoding human iNKT TCRα-F2A-TCRβ-P2A-BCAR-T2A-human IL15; the Lenti/iNKT-CAR19 vector was constructed by inserting into pMNDW vector a synthetic tricistronic gene encoding human iNKT TCRα-F2A-TCRβ-P2A-CD19 CAR (CAR19 indicates CD19-targeting

CAR); the Lenti/FG vector was constructed by inserting into pMNDW a synthetic bicistronic gene encoding Fluc-P2A-EGFP; the Lenti/CD1d vector was constructed by inserting into pMNDW a synthetic gene encoding human CD1d. The synthetic gene fragments were obtained from GenScript and IDT. Lentiviruses were produced using HEK 293T (ATCC) cells, following a standard transfection protocol using the Trans-IT-Lenti Transfection reagent (Mirus Bio), and a centrifugation concentration protocol using the MillipreSigma™Amicon™ Ultra-15 Centrifugal Filter Units, according to the manufactures' instructions. Lentivector titers were measured by transducing HEK-293T-hCD3 cells with serial dilutions and performing flow cytometry following established protocols.

Antibodies and flow cytometry. Fluorochrome-conjugated antibodies specific for human CD45 (Clone H130), TCRαβ (Clone I26), CD3 (Clone HIT3a), CD4 (Clone OKT4), CD8 (Clone SK1), CD45RO (Clone UCHL1), CD45RA (Clone HI100), CD161 (Clone HP-3G10), CD25 (Clone BC96), CD69 (Clone FN50), CD56 (Clone HCD56), CD62L (Clone DREG-56), CTLA-4 (Clone BNI3), PD-1 (clone EH12.2H7), CD1d (Clone 51.1), CCR4 (Clone L291H4), CCR5 (Clone HEK/1/85a), CXCR3 (Clone G025H7), CXCR4 (Clone 12G5), NKG2D (Clone 1D11), DNAM-1 (Clone 11A8), CD158 (KIR2DL1/S1/S3/S5) (Clone HP-MA4), IFN-γ (Clone B27), granzyme B (Clone QA16A02), perforin (Clone dG9), TNF-α (Clone Mab11), IL-2 (Clone MQ1-17H12), HLAE (Clone 3D12), β2-microglobulin (B2M) (Clone 2M2), HLA-DR, DP, DQ (Clone Tü 39), pSTAT-5 (Tyr694, cloneA17016B), and Bcl (Clone BCL/10C4) were purchased from BioLegend. Fluorochrome-conjugated antibody specific for human Bxl-2 (Clone 7B2.5) was purchased from Thermo Fisher Scientific. Fluorochrome-conjugated antibodies specific for human CD34 (Clone 581) and human iNKT TCR Vα24-Jβ18 (Clone 6B11) were purchased from BD Biosciences.

Fluorochrome-conjugated antibody specific for human iNKT TCR Vβ11 was purchased from Beckman-Coulter. Fluorochrome-conjugated antibody specific for human ULBP-2,5,6 (Clone 165903) was purchased from R&D Systems. Fixable Viability Dye eFluor506 (e506) was purchased from Affymetrix eBioscience, mouse Fc Block (anti-mouse CD16/32) was purchased from BD Biosciences, and human Fc Receptor Blocking Solution (TrueStain FcX) was purchased from BioLegend.

All flow cytometry stainings were performed following standard protocols (https://www.bdbiosciences.com/en-us/resources/protocols/flow-cytometry), as well as specific instructions provided by a manufacturer for particular antibodies. Stained cells were analyzed using a MACSQuant Analyzer 10 flow cytometer (Miltenyi Biotech). FlowJo software version 9 (BD Biosciences) was used for data analysis.

Enzyme-Linked Immunosorbent Cytokine Assays (ELISA). The ELISAs for detecting human cytokines were performed following a standard protocol from BD Biosciences. Supernatants from cell culture assays were collected and assayed to quantify human IFN-γ, TNF-α, IL-2, IL-4, and IL-17a. The capture and biotinylated pairs for detecting cytokines were purchased from BD Biosciences. The streptavidin-HRP conjugate was purchased from Invitrogen. Human cytokine standards were purchased from eBioscience. Tetramethylbenzidine (TMB) substrate was purchased from KPL. Human IL-15 was quantified with R&D Systems™ Human IL-15 Quantikine ELISA Kit. Mouse serum IL-6 was quantified with paired Purified anti-mouse IL-6 Antibody and Biotin anti-mouse IL-6 Antibody from Biolegend, following manufactures' instructions. The samples were analyzed for absorbance at 450 nm using an Infinite M1000 microplate reader (Tecan).

Generation of allogeneic HSC-derived CAR-engineered eNKT (^{Allo}CAR-eNKT) cells and derivatives. At Stage 0, frozen-thawed human $CD34^+$ HSCs were revived in serum-free HSC Medium for 24 hours, then transduced with Lenti/iNKT-(CAR)-(Additional Genes) viruses for another 24 hours following an established protocol. The transduced HSCs were then collected and put into a 4-stage *ex vivo* HSC-Derived eNKT Cell Culture.

At Stage 1, gene-engineered HSCs were cultured in the Stage I Expansion Medium for about two weeks. CELLSTAR®24-well Cell Culture Nontreated Multiwell Plates (VWR) were used. The plates were coated with 500 ul/well StemSpan™ Lymphoid Differentiation Coating Material (StemCell Technologies) for 2 hours at room temperature or alternatively, overnight at 4°C. Transduced $CD34^+$ HSCs were suspended in the Stage I Expansion Medium at 2 x 10^4 cells/ml and 500ul of cell suspension was added into each pre-coated well. Twice per week, half of the medium from each well was removed and replaced with fresh medium.

At Stage 2, cells collected from the Stage 1 were cultured in the Stage II Maturation Medium for about one week. Non-Treated Falcon™ Polystyrene 6-well Microplates (Thermo Fisher Scientific) were coated with 1ml/well of StemSpan™ Lymphoid Differentiation Coating Material (StemCell Technologies) as previously described. The Stage 1 cells were collected and resuspended in the Stage II Maturation Medium at 1 x 10^5 cells/ml; 2 ml of cell suspension was added into each pre-coated well. Cells were passaged 2-3 times per week to maintain a cell density at 1-2 x 10^6 cells per well; fresh medium was added at every passage.

At Stage 3, cells collected from the Stage 2 were cultured in the Stage III Deep Maturation Medium for about one week. Non-Treated Falcon™ Polystyrene 6-well Microplates (Thermo Fisher Scientific) were coated with 1ml/well of the StemSpan™ Lymphoid Differentiation Coating Material (StemCell Technologies) as previously described. Stage 2 cells were collected and

resuspended in the Stage III Deep Maturation Medium at 5 x 10^5 cells/ml; 2 ml cell suspension was added into each pre-coated well. Cells were passaged 2-3 times per week to maintain a cell density at 1-2 x 10^6 cells per well; fresh medium was added at every passage.

At Stage 4, cells collected from the Stage 3, now mature ^{Allo}(CAR)-eNKT cells or their derivatives, were expanded using various expansion approaches: 1) αCD3/αCD28 expansion approach, 2) αGC/PBMC expansion approach, or 3) aAPC expansion approach. The expansion stage lasted for about 1-2 weeks. The resulting ^{Allo}(CAR)-eNKT or derivative cell products were aliquoted and cryopreserved using a Thermo scientific CryoMed freezer 7450 for future use.

1) αCD3/αCD28 antibody expansion approach. CELLSTAR®24-well Cell Culture Nontreated Multiwell Plates (VWR) were coated with 1 ug/ml and 500 ul/well of Ultra-LEAF™ Purified anti-human CD3 Antibody (Clone OKT3, Biolegend) for 2 hours at room temperature or alternatively, overnight at 4°C. Mature ^{Allo}(CAR)-eNKT cells or their derivatives collected from the Stage 3 culture were resuspended in the Serum-Free Expansion Medium supplemented with 1 ug/ml Ultra-LEAF™ Purified anti-human CD28 Antibody (Clone CD28.2, Biolegend) at 5 x 10^5 cells/ml; 2 ml cell suspension was added into each pre-coated well. After 3 days of culture, cells were collected and resuspended in fresh Serum-Free Expansion Medium (without αCD28 supplement) at 0.5-1 x 10^6 cells/ml; 2 ml cell suspension was added into each well of Corning™ Costar™ Flat Bottom Cell Culture 6-well Plates (Corning; no αCD3 antibody coating). Cells were passaged 2-3 times per week to maintain a cell density at 0.5-1 x 10^6 cells/ml; fresh medium was added at every passage.

2) αGC/PBMC expansion approach. Healthy donor PBMCs were loaded with α-Galactosylceramide (αGC, Avanti Polar Lipids) at 5 μg/ml in C10 medium for 1 hour following a

previously established protocol. The resulting αGC/PBMCs were then irradiated at 6,000 rads using a Rad Source RS-2000 X-ray irradiator (Rad Source Technologies). Mature ^{Allo}CAR-eNKT cells and derivatives collected from the Stage 3 culture were mixed with the irradiated αGC/PBMCs at 1:5 ratio, resuspended in C10 medium supplemented with 10 ng/ml human recombinant IL-7, IL-15 and IL-21 at 0.5-1 x 10^6 cells/ml, and seeded into the Corning™ Costar™ Flat Bottom Cell Culture 6-well Plates at 2 ml per well. Cells were passaged 2-3 times per week to maintain a cell density at 0.5-1 x 10^6 cells/ml; fresh medium was added at every passage.

3) aAPC expansion approach. aAPCs were irradiated at 10,000 rads using a Rad Source RS-2000 X-ray irradiator (Rad Source Technologies). Mature ^{Allo}CAR-eNKT cells and derivatives collected from the Stage 3 culture were mixed with the irradiated aAPCs at 1:1 ratio, resuspended in C10 medium supplemented with 10 ng/ml human recombinant IL-7, IL-15 and IL-21 at 0.5-1 x 10^6 cells/ml, and seeded into the Corning™ Costar™ Flat Bottom Cell Culture 6-well Plates (Corning) at 2 ml per well. Cells were passaged 2-3 times per week to maintain a cell density at 0.5-1 x 10^6 cells/ml; fresh medium was added at every passage.

Generation of PBMC-Derived conventional αβT, iNKT, and NK cells. Healthy donor PBMCs were used to generate the PBMC-derived conventional αβTc, iNKT, and NK cells (denoted as PBMC-Tc, PBMC-iNKT, and PBMC-NK cells respectively).

To generate PBMC-Tc cells, PBMCs were stimulated with Dynabeads™ Human T-Activator CD3/CD28 (Thermo Fisher Scientific) according to the manufactures' instructions, followed by culturing in the C10 medium supplemented with 20 ng/ml human IL-2 for 2-3 weeks.

To generate PBMC-iNKT cells, PBMCs were MACS-sorted via Anti-iNKT Microbeads (Miltenyi Biotech) labeling to enrich iNKT cells. The enriched iNKT cells were mixed with donor-

matched irradiated αGC/PBMCs at a ratio of 1:1, followed by culturing in C10 medium supplemented with human 10 ng/ml IL-7 and IL-15 for 2-3 weeks. If needed, the resulting cultured cells could be further purified using Fluorescence-Activated Cell Sorting (FACS) via human iNKT TCR antibody (Clone 6B11; BD Biosciences) staining.

To generate PBMC-NK cells, PBMCs were FACS-sorted via human CD56 antibody (Clone HCD56; Biolegend) labeling or MACS-sorted using a Human NK Cell Isolation Kit (Miltenyi Biotech).

Generation of CAR-Engineered conventional αβT (CAR-T) cells. Non-treated tissue culture 24-well plates (Corning) were coated with Ultra-LEAF™ Purified anti-human CD3 Antibody (Clone OKT3, Biolegend) at 1 ug/ml and 500 ul/well, at room temperature for 2 hours or at 4ºC overnight. Healthy donor PBMCs were resuspended in the C10 medium supplemented with 1 ug/ml Ultra-LEAF™ Purified anti-human CD28 Antibody (Clone CD28.2, Biolegend) and 30 ng/ml human recombinant IL-2, and seeded in the pre-coated plates at 1 x10^6 cells/ml and 1 ml/well. After 3 days of culture, cells were collected and resuspended in fresh C10 medium (without αCD28 supplement) supplemented with 30 ng/ml IL-2. Cells were passaged 2-3 times per week to maintain a cell density at 0.5-1 x 10^6 cells/ml; fresh medium was added at every passage.

Single cell TCR sequencing. ^{Allo}eNKT (6B11$^+$TCRαβ$^+$), $^{Allo/15}$BCAR-eNKT (6B11$^+$TCRαβ$^+$), ^{Allo}CAR19-eNKT (6B11$^+$TCRαβ$^+$), PBMC-iNKT (6B11$^+$TCRαβ$^+$), and PBMC-T (6B11$^-$TCRαβ$^+$) cells were sorted using a FACSAria II flow cytometer (BD Biosciences). Sorted cells were immediately delivered to the UCLA TCGB (Technology Center for Genomics and Bioinformatics)

Core to perform single cell TCR sequencing using a 10X Genomics ChromiumTM Controller Single Cell Sequencing System (10X Genomics), following the manufacturer's instructions and the TCGB Core's standard protocol. Libraries were constructed using an Illumina TruSeq RNA Sample Prep Kit (Illumina) and sequenced with 150 bp paired-end reads (5,000 reads/cell) on the Illumina NovaSeq 6000 sequencer. The reads were mapped to the human T cell receptor reference genome (hg38) using Cell Ranger VDJ (10xgenomics). The frequencies of the α or β chain recombination were plotted.

Deep RNA sequencing. A total of 24 cell samples were analyzed, including 3 ^{Allo}eNKT ($6B11^{+}TCR\alpha\beta^{+}$), 3 ^{Allo15}BCAR-eNKT ($6B11^{+}TCR\alpha\beta^{+}$), 3 ^{Allo}BCAR-eNKT ($6B11^{+}TCR\alpha\beta^{+}$), 2 ^{Allo}CAR19-eNKT ($6B11^{+}TCR\alpha\beta^{+}$), 3 PBMC-iNKT ($6B11^{+}TCR\alpha\beta^{+}CD4^{-}$), 8 PBMC-T ($6B11^{-}TCR\alpha\beta^{+}CD4^{-}$), and 2 PBMC-NK ($CD56^{+}$ $TCR\alpha\beta^{-}$). In accordance with the $CD8^{+}$ SP/DN phenotype of ^{Allo}(CAR)-eNKT cells, $CD4^{-}$ populations of PBMC-iNKT ($CD8^{+}$ SP/DN) and PBMC-αβTc ($CD8^{+}$ SP) were used for the sequencing experiment.

Cell samples were sorted using a FACSAria II flow cytometer (BD Biosciences). Total RNAs were isolated from each cell sample using a miRNeasy Mini Kit (QIAGEN) and delivered to the UCLA TCGB Core to perform Deep RNA sequencing using an Illumina HiSeq3000, following the manufacturer's instructions and the TCGB Core's standard protocol. cDNAs were synthesized using an iScript cDNA Synthesis Kit (BioRad). Libraries were constructed using an Illumina TruSeq Stranded Total RNA Sample Prep kit and sequenced with 50 bp single-end reads (targeting 20 x 10^6 reads per sample) on an Illumina HiSeq3000. The reads were mapped with STAR 2.5.3a to the human genome (hg38). The counts for each gene were obtained using quantMode GeneCounts in STAR commands, and the other parameters during alignment were set

to default. Data quality was checked using Illumina's proprietary software. Differential expression analyses were carried out using DESeq2. Sequencing depth normalized counts were obtained using the estimateSizeFactors function from DESeq2, and the log10 values were used for principal component analysis.

***In vitro* ^{Allo}(CAR)-eNKT cell phenotype and functionality study.** ^{Allo}BCAR-eNKT, ^{Allo15}BCAR-eNKT cells were analyzed in comparison BCAR-T cells. Phenotype of these cells was studied using flow cytometry, by analyzing cell surface markers including co-receptors (i.e., CD4 and CD8), NK cell receptors (i.e., CD161), memory T cell markers (i.e., CD45RO). The capacity of these cells to produce cytokines (i.e., IFN-γ, TNF-α, and IL-2) and cytotoxic molecules (i.e., perforin and granzyme B) were studied using flow cytometry via intracellular staining.

Response of $^{Allo/15}$BCAR-eNKT cells to antigen stimulation was studied by culturing $^{Allo/15}$BCAR-eNKT cells *in vitro* in C10 medium for 7 days, in the presence or absence of αGC (100 ng/ml). The proliferation of $^{Allo/15}$BCAR-eNKT cells was measured by cell counting and flow cytometry (identified as $6B11^{+}TCR\alpha\beta^{+}$) over time. Cytokine production was assessed by ELISA analysis of cell culture supernatants collected on day 3 (for human IFN-γ, TNF-α, IL-2, IL-4, and IL-17a).

Cell imaging by scanning electron microscope (SEM). The SEM buffer with pH 7.4 was made by 0.1 M Na-phosphate buffer containing 0.1M Sucrose. The cells were rinsed with warm HBSS. Then they were fixed with warm 3% glutaraldehyde in the SEM buffer, moved to 4 degrees, and stored overnight. The next day the cells were washed with SEM buffer 2 times with 5 minutes each time. Next, they were fixed with 2% osmium tetroxide in SEM buffer on ice for 1 hour and then

washed with SEM buffer 2 times with 5 minutes each time. The cells were dehydrated with 50%, 70%, 95%, 100%, 100% ethanol successively, 15 minutes each time: The final 100% ethanol was replaced with hexamethyldisilazane and then evaporated in the hood. The processed cells were then ready for Low-vacuum Scanning Electron Microscopy (LV-SEM) which was conducted on a FEI Nova Nano 230 SEM.

***In vitro* tumor killing assay.** Tumor cells (1 x 10^4 cells per well) were co-cultured with effector cells (at ratios indicated in figure legends) in Corning 96-well clear bottom black plates for 8-24 hours, in C10 medium with or without the addition of αGC (100 ng/ml). At the end of culture, live tumor cells were quantified by adding D-luciferin (150 μg/ml; Caliper Life Science) to cell cultures and reading out luciferase activities using an Infinite M1000 microplate reader (Tecan).

In tumor killing assays involving blocking CD1d, 10 ug/ml LEAF^{TM} purified anti-human CD1d antibody (Clone 51.1, Biolegend) or LEAF^{TM} purified mouse lgG2bk isotype control antibody (Clone MG2B-57, Biolegend) was added to tumor cell cultures one hour prior to adding ^{Allo}(CAR)-eNKT cells. In some experiments, 10 mg/ml LEAF^{TM} purified anti-human NKG2D (Clone 1D11, Biolegend), anti-human DNAM-1 antibody (Clone 11A8, Biolegend), or LEAF^{TM} purified mouse lgG2bk isotype control antibody (Clone MG2B-57, Biolegend) was added to co-cultures, to study NK activating receptor-mediated tumor cell killing mechanism.

***In vitro* Mixed Lymphocyte Reaction (MLR) assay: studying Graft-versus-Host (GvH) response.** PBMCs of multiple healthy donors were irradiated at 2,500 rads and used as stimulators to study the GvH response of $^{Allo/15}$BCAR-eNKT as responders. PBMC derived BCAR-T cells were included as responder controls. Stimulators (5 x 10^5 cells/well) and responders (2 x 10^4

cells/well) were co-cultured in 96-well round-bottom plates in C10 medium for 4 days; the cell culture supernatants were then collected to measure IFN-γ production using ELISA.

In vitro **MLR Assay: studying Host-Versus-Graft (HvG) response.** PBMCs of multiple healthy donors were used as responders to study the HvG response of $^{Allo/15}$BCAR-eNKT cells as stimulators (irradiated at 2,500 rads). PBMC derived BCAR-T cells were included as stimulator controls. Stimulators (5 x 10^5 cells/well) and responders (2 x 10^4 cells/well) were co-cultured in 96-well round-bottom plates in C10 medium for 4 days; the cell culture supernatants were then collected to measure IFN-γ production using ELISA.

In vitro **MLR assay: studying NK cell-mediated allorejection.** PBMC-NK cells isolated from PBMCs of multiple healthy donors were used to study the NK cell-mediated allorejection of $^{Allo/15}$BCAR-eNKT cells. Allogeneic BCAR-T were included as controls. PBMC-NK cells (2 x 10^4 cells/well) and the corresponding allogeneic cells (2 x 10^4 cells/well) were co-cultured in 96-well round-bottom plates in C10 medium for 24 hours; the cell cultures were then collected to quantify live cells using flow cytometry.

In vivo **Bioluminescence Live Animal Imaging (BLI).** BLI was performed using a Spectral Advanced Molecular Imaging (AMI) HTX imaging system (Spectral instrument Imaging). Live animal imaging was acquired 5 minutes after intraperitoneal (i.p.) injection of D-Luciferin (1 mg/mouse) for total body bioluminescence, and 15 minutes after i.p. injection of D-luciferin (3 mg/mouse) for tissue bioluminescence. Imaging results were analyzed using an AURA im- aging software (Spectral Instrument Imaging).

***In vivo* antitumor efficacy study of $^{Allo/15}$BCAR-eNKT cells: human MM xenograft NSG mouse model.** Experimental design is shown in the main Figure 3B. Briefly, on day 0, NSG mice received intravenously (i.v.) inoculation of MM-FG cells (1 x 10^6 cells per mouse). On day 10, the experimental mice received i.v. injection of vehicle (100 ul PBS per mouse), $^{Allo/15}$BCAR-eNKT cells (10 x 10^6 CAR^+ cells in 100 ul PBS per mouse), or control BCAR-T cells (10 x 10^6 CAR^+ cells in 100 ul PBS per mouse). Over the experiment, mice were monitored for survival and their tumor loads were measured twice per week using BLI. Note in this study, tumor cells, but not the therapeutic immune cells were labeled with the firefly luciferase and enhanced green fluorescence protein (FG) dual-reporters.

***In vivo* PK/PD study of $^{Allo/15}$BCAR-eNKT/FG cells: human MM xenograft NSG mouse model.** Experimental design is shown in the main Figure 3G. Briefly, on day 0, NSG mice received intravenously (i.v.) inoculation of MM cells (1 x 10^6 cells/mouse). On day 10, the experimental mice received i.v. injection of vehicle (100 ul PBS per mouse), $^{Allo/15}$BCAR-eNKT/FG cells (10 x 10^6 CAR^+ cells in 100 ul PBS per mouse), or control BCAR-T/FG cells (10 x 10^6 CAR^+ cells in 100 ul PBS per mouse). Over the experiment, mice were monitored for survival and their tumor loads were measured twice per week using BLI. At certain timepoints, organs were collected from experimental mice to study the tissue biodistribution of the therapeutic cells. Note in this study, therapeutic immune cells, but not the tumor cells, were labeled with the firefly luciferase and enhanced green fluorescence protein (FG) dual-reporters.

***In vivo* gene profiling study using single cell RNA sequencing (scRNA-seq)(cite).** scRNA-seq was used to analyze the gene expression profiling of therapeutic cells (i.e., $^{Allo/15}$BCAR-eNKT and

BCAR-T cells) as well as tumor cells (i.e., MM-FG cells) in an *in vivo* study using an MM-FG human multiple myeloma xenograft NSG mouse model. Bone marrow cells harvested from experimental animals at selected timepoints were subjected to FACS sorting for isolating $^{Allo/15}$BCAR-eNKT cells (hCD45^{+}6B11^{+}hTCRαβ^{+}), BCAR-T cells (hCD45^{+}6B11^{-}hTCRαβ^{+}), and MM-FG cells (GFP^{+}). Cells isolated from 10 experimental mice were combined for each group. Sorted cells were immediately delivered to the UCLA TCGB (Technology Center for Genomics and Bioinformatics) Core for library construction and single cell RNA sequencing.

Sorted cells were quantified using a Cell Countess II automated cell counter (Invitrogen/Thermo Fisher Scientific). A total of 10,000 cells from each experimental group were loaded on the Chromium platform (10X Genomics), and libraries were constructed using the Chromium Next GEM Single Cell 3' Kit v3.1 and the Chromium Next GEM Chip G Single Cell Kit (10X Genomics), according to the manufacturer's instructions. Library quality was assessed using the D1000 ScreenTape on a 4200 TapeStation System (Agilent Technologies). Libraries were sequenced on an Illumina NovaSeq using the NovaSeq S4 Reagent Kit (100 cycles; Illumina).

Data analysis was performed using a Cell Ranger Software Suite (10x Genomics). Binary base call (BCL) files were extracted from the sequencer and used as inputs for the Cell Ranger pipeline to generate the digital expression matrix for each sample. Then, cellranger aggr command was used to aggregate all samples into one digital expression matrix. The matrix was analyzed using Seurat, an R package designed for scRNA-seq.

Specifically, for the therapeutic immune cell analysis, cells were first filtered to have at least 100 genes, at most 20,000 unique molecular identifiers (UMIs), and at most 25% mitochondrial gene expression, with 46,718 cells passed this filter. For the tumor cell analysis, cells were first filtered to have at least 100 genes, at most 30,000 unique molecular identifiers

(UMIs), and at most 40% mitochondrial gene expression, with 59,065 passed this filter. The filtered matrix was normalized using the Seurat function NormalizeData. Variable genes were found using the Seurat function FindVariableGenes. The matrix was scaled to regress out the sequencing depth for each cell. Variable genes that had been previously identified were used in principal components analysis (PCA) to reduce the dimensions of the data. After this, 30 principal components (PCs) were used in the RunHarmony function to correct potential batch effect. The first 20 harmony dimensions were used for Uniform Manifold Approximation and Projection (UMAP) to further reduce the dimensions to two. The same 20 harmony dimensions were also used to group the cells into different clusters by the Seurat function FindClusters. Next, marker genes were found for each cluster and used to define the cell types. Subsequently, four clusters of therapeutic immune cells and two cluster of tumor cells were compared between the different treatment groups.

For GSEA, signal-to-noise ratio was used to rank the genes in correlation with indicated gene signatures. For each cluster, the average expression of each gene in this cluster and in all other clusters was calculated. Fold changes were calculated by comparing the average expressions. The genes were then ranked by fold changes from high to low. To compare our data to pre-annotated datasets, we used the marker genes published on Human Protein Atlas (proteinatlas.org) and by Miller et al.. GSEA was performed on these marker genes against the ranked genes in our dataset.

***In vitro* and *in vivo* ganciclovir (GCV) killing assay.** For GCV *in vitro* killing assay, ^{Allo15}eNKT-TK cells were cultured in C10 medium in the presence of the titrated amount of GCV (0-50 μM) for 4 days; live ^{Allo15}eNKT-TK cells were then counted using flow cytometry with viability staining.

To evaluate the functionality of the suicide gene *in vivo*, mice received i.v. injection of 10 x 10^6 of ^{Allo15}eNKT-TK/FG cells. On day 10, mice were treated with GCV (20mg/kg) i.p. daily for continuous 3 days. Over time, experimental mice were monitored for survival, and their total body luminescence was measured twice per week using BLI.

Histopathologic analysis. Tissues (i.e., heart, liver, kidney, and lung) were collected from the experimental mice and fixed in 10% Neutral Buffered Formalin for up to 36 hours and embedded in paraffin for sectioning (5 μm thickness). Tissue sections were prepared and stained with Hematoxylin and Eosin (H&E) by the UCLA Translational Pathology Core Laboratory, following the Core's standard protocols. Stained sections were imaged using an Olympus BX51 upright microscope equipped with an Optronics Macrofire CCD camera (AU Optronics) at 20 x and 40 x magnifications. The images were analyzed using Optronics PictureFrame software (AU Optronics).

Western blot. Quiescent T cells were freshly sorted using anti-human CD4 (Miltenyi Biotec) and anti-human CD8 magnetic beads (Miltenyi Biotec) from random donor PBMCs. BCAR-T, and $^{Allo/15}$BCAR-eNKT cells were generated as previously described.

Frozen-thawed cells were stimulated with human recombinant IFN-γ (10 ng/ml) for 2 minutes (p-JAK1/p-JAK2/JAK1/JAK2), 15 minutes (p-STAT1/STAT1), 18 hour (IRF-1), or 48 hours (CIITA/SP1). Total protein was extracted using a RIPA lysis buffer (Thermo Fisher Scientific) containing 20 mM HEPES (pH 7.6), 150 mM NaCl, 1mM EDTA, 1% Tritonx-100, and protease/phosphatase inhibitor cocktail (Cell Signaling Technology). Protein concentration was measured using a Bicinchoninic Acid (BCA) Assay Kit (Thermo

Fisher Scientific). Equal amounts of total protein were resolved on a 4–15% Mini-PROTEAN® TGX™ Precast Protein Gel (Bio-rad) and then transferred to a polyvinylidene difluoride (PVDF) membrane by electrophoresis. Polyclonal anti-human CIITA antibody was purchased from Invitrogen. The following monoclonal antibodies were purchased from the Cell Signaling Technology (CST) and used to blot for various proteins of interest: anti-human p-JAK1(Y1034/1035) (clone D7N4Z), anti-human p-JAK2(Y1007/1008) (clone C80C3), anti-human JAK1 (clone 6G4), anti-human JAK2 (clone D2E12), anti-human p-STAT1(Y701) (clone 58D6), anti-human STAT1 (clone D1K9Y), anti-human IRF-1 (clone D5E4), anti-human SP1 (clone D4C3), and secondary anti-rabbit IgG. β-Actin (clone D6A8, CST) and GAPDH (clone D16H11, CST) were used as internal controls for total protein extracts. Signals were visualized with autoradiography using an enhanced chemiluminescence (ECL) system (Cytiva). The data were analyzed using ImageJ (Version 1.53s).

Statistics. Graphpad Prism 8 software (Graphpad) was used for statistical data analysis. Student's two-tailed t test was used for pairwise com- parisons. Ordinary 1-way ANOVA followed by Tukey's or Dunnett's multiple comparisons test was used for multiple comparisons. Log rank (Mantel-Cox) test adjusted for multiple comparisons was used for Meier survival curves analysis. Data are presented as the mean ± SEM, unless otherwise indicated. In all figures and figure legends, ''n'' represents the number of samples or animals uti- lized in the indicated experiments. A P value of less than 0.05 was considered significant. ns, not significant; *$p < 0.05$; **$p < 0.01$; ***$p < 0.001$; ****$p < 0.0001$.

Data availability

All data associated with this study are present in the paper or Supplemental Information. The genomics data generated during this study will be available from the public repository Gene Expression Omnibus Database when the manuscript is published. The authors declare that all data of this study are available within the paper and its supplementary information files.

Acknowledgements

This work was supported by a Partnering Opportunity for Discovery Stage Research Projects Award and a Partnering Opportunity for Translational Research Projects Award from the California Institute for Regenerative Medicine (DISC2-11157 and TRAN1-12250, to L.Y.), a Department of Defense/CDMRP/PRCRP Impact Award (CA200456 to L.Y.), a UCLA BSCRC Innovation Award (to L.Y.), and an Ablon Scholars Award (to L.Y.). Y.Z. is a predoctoral fellow supported by the UCLA Dissertation Year Fellowship. J.Y. is a predoctoral fellow supported by the UCLA Broad Stem Cell Research Center (BSCRC) predoctoral fellowship. Y.-R.L. is a predoctoral fellow supported by the UCLA Whitcome predoctoral fellowship in molecular biology. D.L. is a predoctoral fellow supported by T32 Microbial Pathogenesis Training Grant (Ruth L. Kirschstein National Research Service Award, T32-AI007323). Z.L. is a postdoctoral fellow supported by the UCLA Tumor Immunology Training Grant (USHHS Ruth L. Kirschstein Institutional National Research Service Award, T32-CA009120). We thank the University of California, Los Angeles (UCLA) animal facility for providing animal support; the UCLA Translational Pathology Core Laboratory (TPCL) for providing histology support; the UCLA Technology Center for Genomics & Bioinformatics (TCGB) facility for providing RNA-seq services; the UCLA CFAR Virology Core for providing human cells; and the UCLA BSCRC Flow Cytometry Core Facility for cell sorting support.

Author contributions

Y.Z., J.Y., and L.Y. designed the experiments, analyzed the data, and wrote the manuscript. L.Y. conceived and oversaw the study, with assistance from Y.Z. and J. Y.. Y.Z. performed all experiments, with assistance from J.Y., Y.L., K.Z., Z. L., Y.J.K., D.L., X.C., A.B., T.H., Y.W., Y.Z., Z.H., and E. Z.. F.M., M.L., and W.G. helped with RNA-seq data analysis.

Competing interests

Y.-R.L., Y.J.K., J.Y., P.W., and L.Y. are inventors on patents relating to this study filed by UCLA. J.Y. and X.W. are currently employees of Appia Bio. Z.L. is currently an employee of Allogene. L.Y. is a scientific advisor to AlzChem and Amberstone Biosciensec, and a co-founder, stockholder, and advisory board member of Appia Bio. P.W. is a co-founder, stockholder, and advisory board member of Appia Bio. None of the declared companies contributed to or directed any of the research reported in this article. The remaining authors declare no competing interests.

Additional information

Extended data is available for this paper at https:// xxxxxx.

Supplementary information The online version contains supplementary materials available at https://xxxxxx.

Correspondence and requests for materials should be addressed to Lili Yang.

Peer review information Nature Biotechnology thanks xxx, xxx, for their contributions to the peer review of this work.

Reprints and permissions information is available at www.xxxxx.

A

Viral titer on HEK-293T-hCD3 cells	
Vector	Titer (IFU/mL)
Lenti/iNKT	$1.734 \times 10^8 \pm 7.47 \times 10^7$
Lenti/iNKT-BCAR	$1.628 \times 10^8 \pm 1.86 \times 10^7$
Lenti/iNKT-BCAR-IL15	$1.784 \times 10^8 \pm 5.61 \times 10^7$
Lenti/iNKT-CAR19	$1.592 \times 10^8 \pm 4.29 \times 10^7$

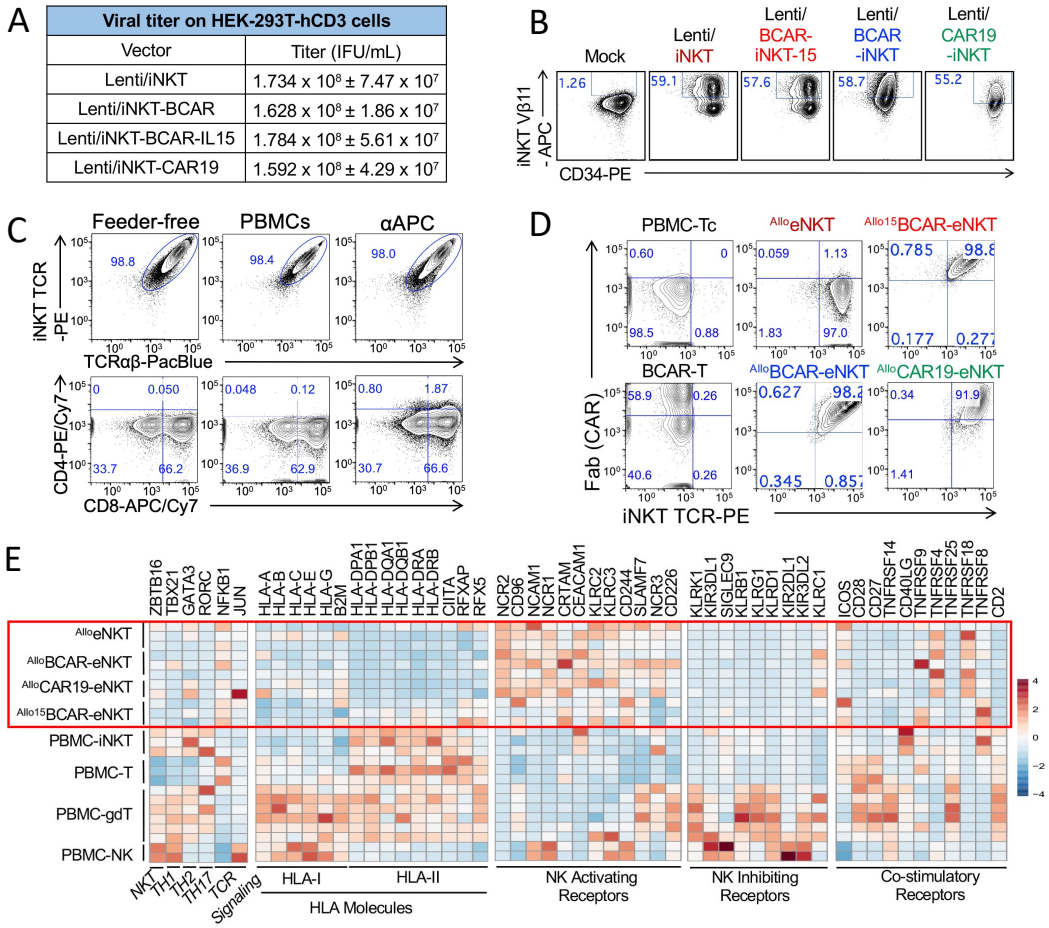

Figure S1. Generation of allogeneic HSC-engineered NKT (^{Allo}eNKT) cells and their CAR-armed derivatives, related to Figure 1.

(A) Representative titers of lentivirus packaged with indicated vectors. The Lentiviruses were produced using a HEK293T virus packaging cell line. Vector titers were measured by transducing HEK-293T-hCD3 cells. HEK-293T-hCD3 cell: parental HEK293T cells overexpressed with human CD3 genes.

(B) FACS detection of intracellular expression of iNKT-TCR (identified as $CD34^+v\beta11^+$) in $CD34^+$ CB HSCs 72 hours post lentivector transduction with untransduced $CD34^+$ CB HSC as a mock control.

(C) FACS detection of expression of iNKT TCR and CD4/CD8 on cells expanded with different expansion approaches.

(D) FACS analyses showing the co-expression of iNKT TCR and CAR on ^{Allo}(CAR)-eNKT cells. PBMC-T and BCAR-T cells were included as controls.

(E) Heat map of selected gene expression profiles related to transcription factors, HLA molecules, NK activating receptors, NK inhibitory receptors and co-stimulatory receptors of eight cell groups. Each row represents one biological repeat. Levels of mRNA expression were determined using RNA sequencing.

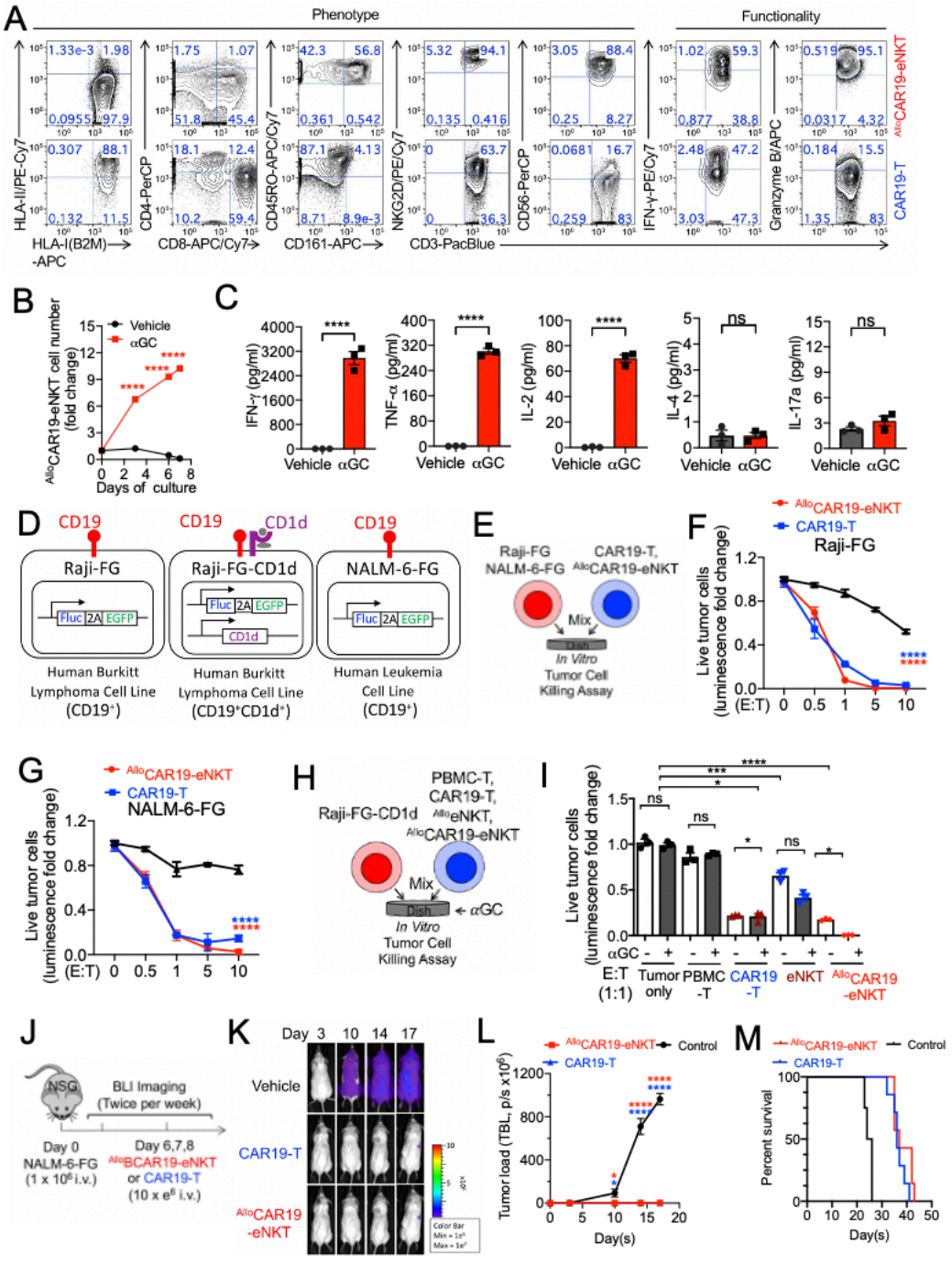

Figure S2. *In vitro* and *in vivo* characterization of CD19-targeting CAR-armed NKT (AlloCAR19-eNKT) cells.

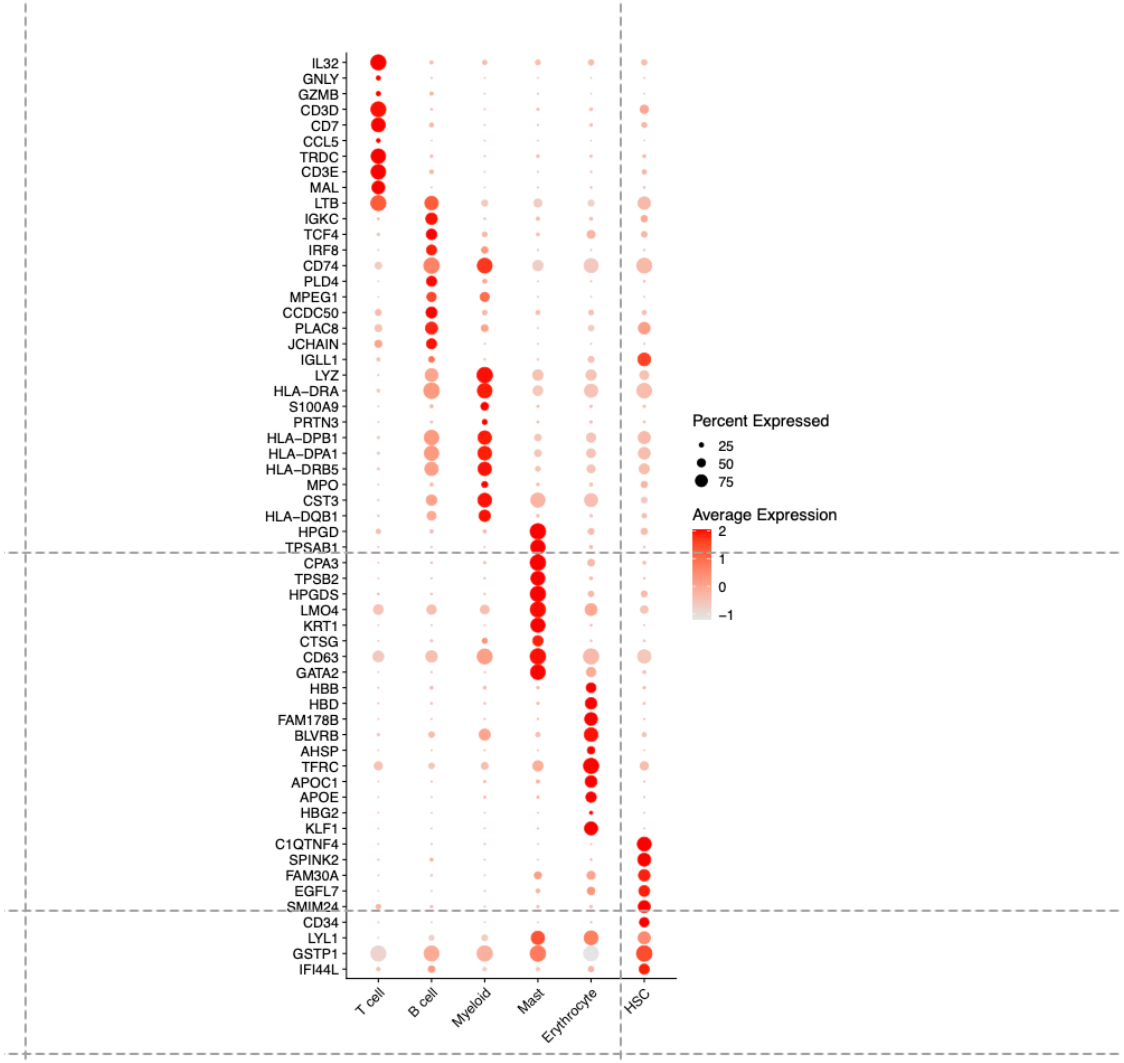

Figure S3. Development of BCMA-targeting CAR-armed ^{Allo}eNKT cells (^{Allo}BCAR-eNKT) and their IL-15 enhanced derivative(^{Allo15}BCAR-eNKT), related to Figure 2.

The development of $^{Allo/15}$BCAR-eNKT cells was analyzed using scRNA-seq. Dot plot is presented, showing gene expression levels. The color scale indicates the expression score of each gene. Circle size indicates the percentage of cells that express the gene. Cell lineages are defined based on their expression of lineage-specific genes.

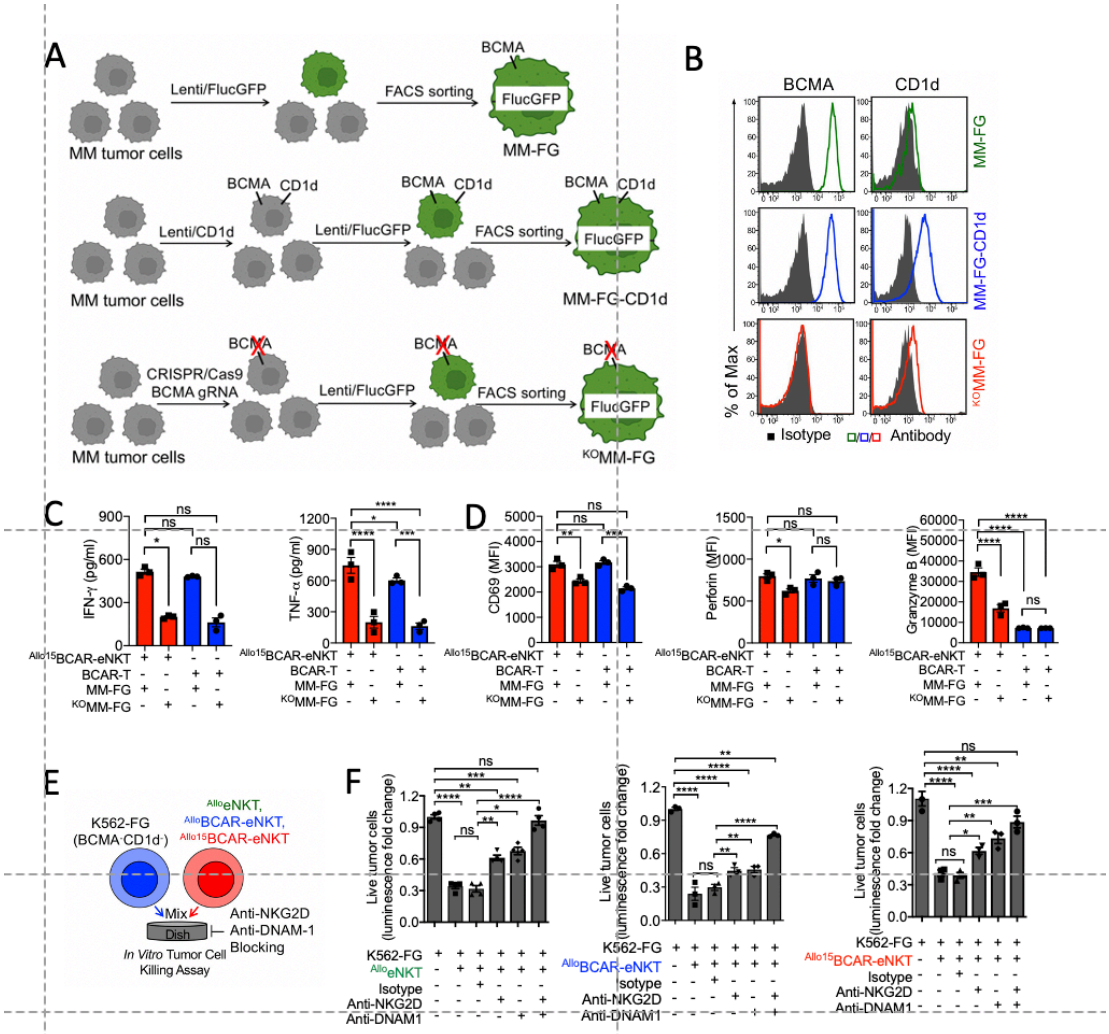

Figure S4. *In vitro* anti-tumor efficacy and mechanism of action (MOA) study of $^{Allo/15}$BCAR-eNKT cells, related to Figure 3.

(A) Schematics showing the generation of indicated tumor cells, related to Figure 3B.

(B) FACS plots showing the expression of BCMA and CD1d on the indicated cells, related to Figure3B.

(C) Elisa detection of cytokines (n = 3), related to Figure 3E & 3F.

(D)Flow cytometry measurements of intracellular Perforin, intracellular Granzme B, and surface CD69 from the indicated experimental cells (n = 3), related to Figure 3E & 3F.

(E and F) Studying the NK killing mechanism, related to Figure 3K & 3L. (E) Experimental design. ^{Allo}(CAR)-eNKT cells killing mechanism were studied using K562-FG, a BCMA$^-$/CD1d$^-$ K562 human leukemia cell line engineered with FG. (F) Tumor killing data of C at 12-hour (n = 3-4).

Representative of 3 experiments. Data are presented as the mean ± SEM. ns, not significant, *p < 0.05, **p < 0.01, ***p < 0.001, ****p < 0.0001, by 1-way ANOVA (B, E, F, G)

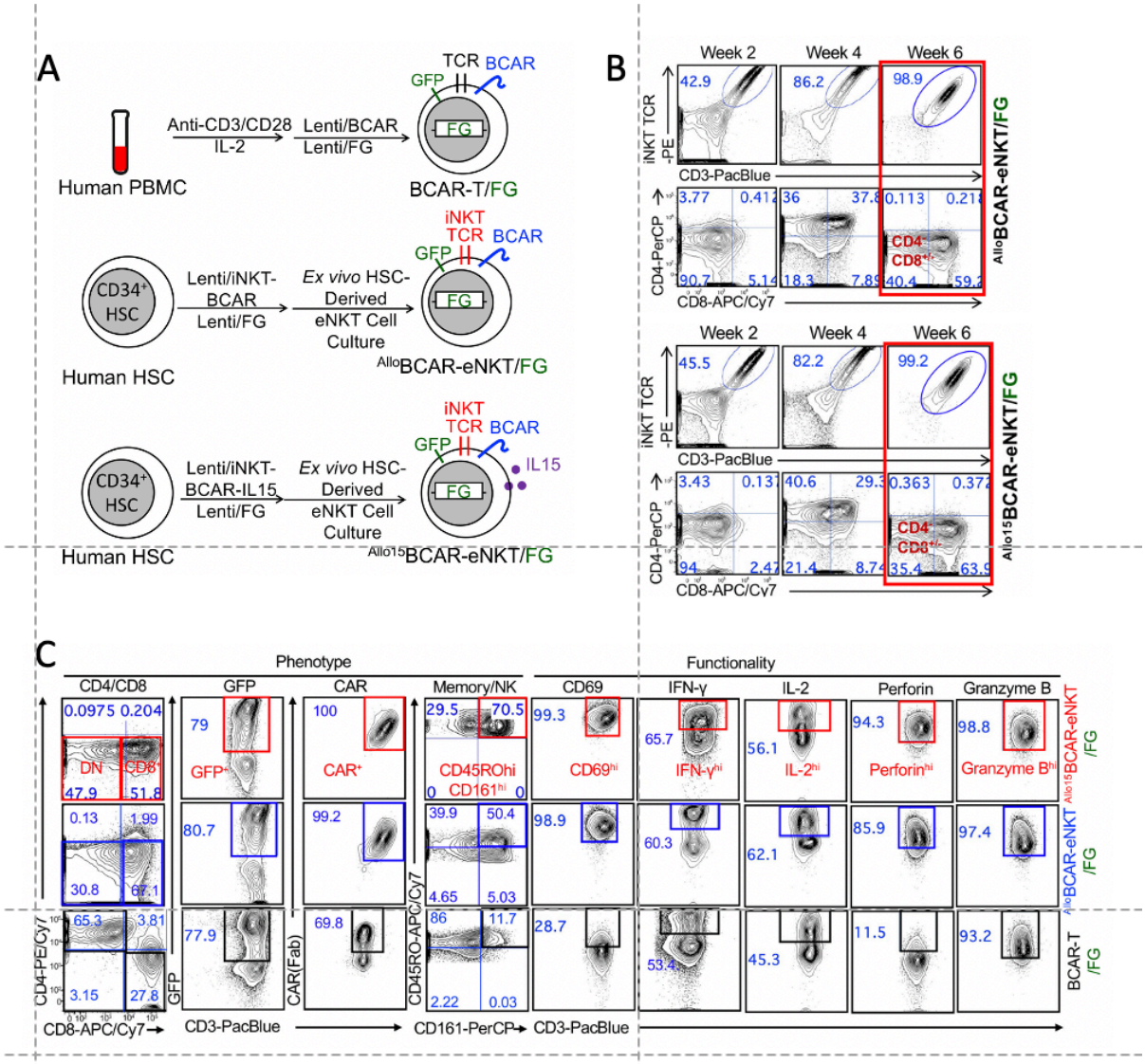

Figure S5. *In vivo* pharmacokinetics/pharmacodynamic (PK/PD) study of Allo/15BCAR-eNKT cells, related to Figure 4.

(A) Schematics showing the generation of indicated firefly luciferase and green fluorescence protein dual reporters (FG) labeled cells.

(B) FACS plots showing the development of AlloBCAR-eNKT/FG and Allo15BCAR-eNKT/FG cells.

(C) FACS measurements comparing the phenotype and functionality of indicated cells.

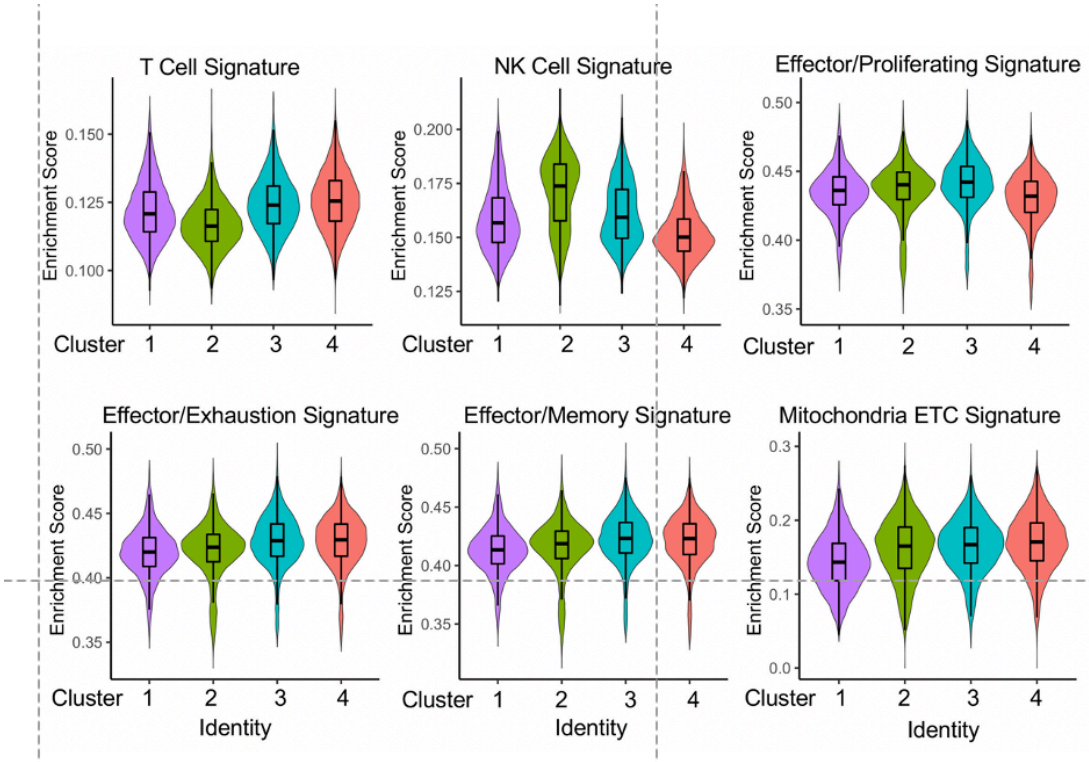

Figure S6. *In vivo* phenotype and gene profiling of $^{Allo/15}$BCAR-eNKT cells, related to Figure 5B.
Gene Set Enrichment Analysis (GSEA) plots showing the enrichment of gene signatures of T cell (Human Protein Atlas proteinatlas.org; 461 genes), NK cell (Human Protein Atlas proteinatlas.org; 343 genes), effector /proliferating T cell (GSE9650, 1002 genes), effector/exhaustion T cell (GSE9650, 1158 genes), effector/memory T cell (GSE9650, 1152 genes), and mitochondria electron transport chain (ETC) (GSE9650, 84 genes) in the indicated cell clusters.

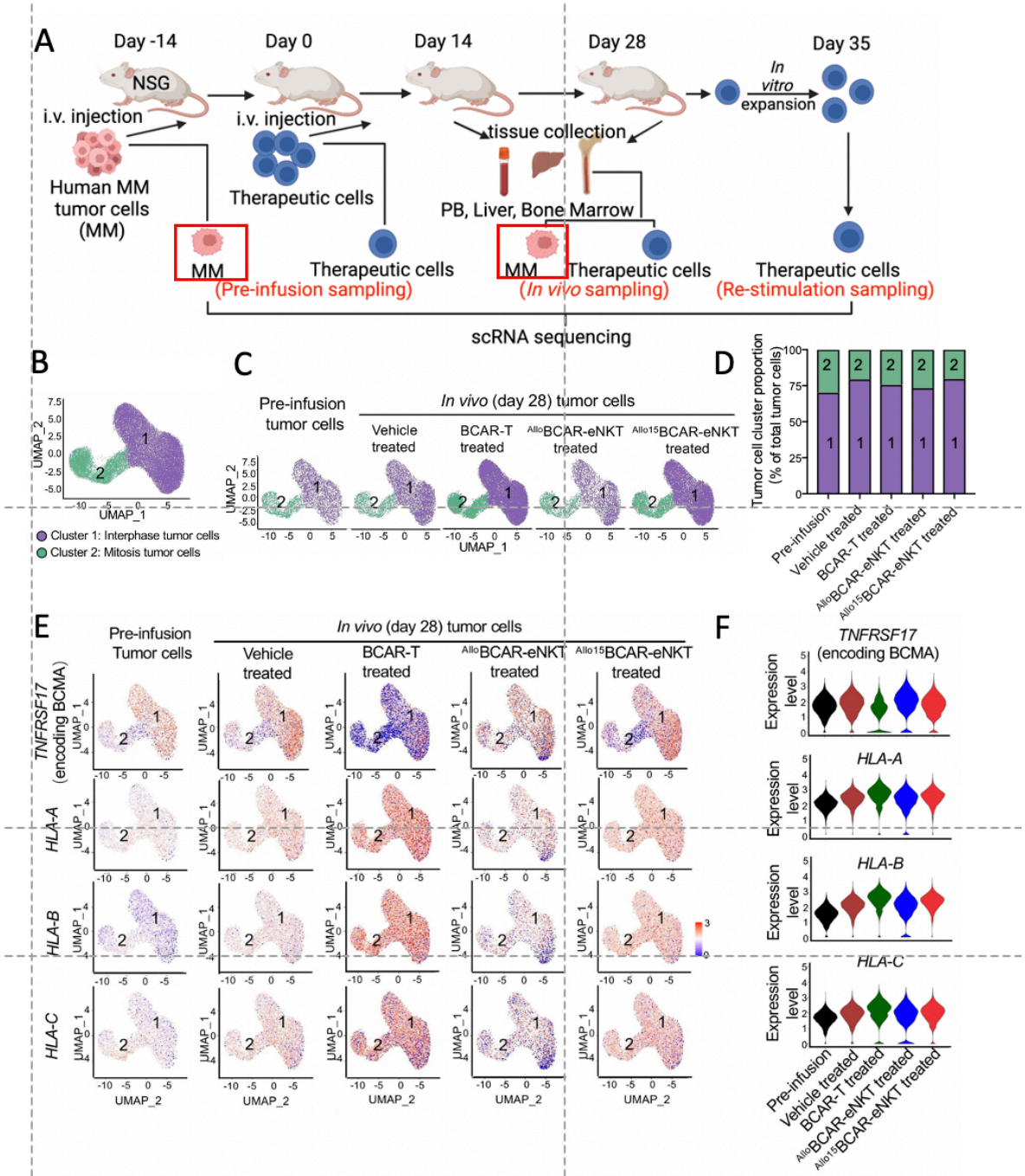

Figure S7. Gene profiling of tumor cells under different therapeutic cell treatments, related to Figure 5.

(A) Schematic of the experimental design to study the gene profiling of MM cells using scRNA-seq. Samples were collected at pre-infusion stages and *in vivo* stages.

(B) UMAP plot showing the formation of two cell clusters.

(C) UMAP plot showing the cluster distribution of MM tumor cells collected at the indicated experimental conditions.

(D) Bar graphs showing the quantification of C.

(E and F) UMAP plots showing the expression of indicated genes in MM.1S tumor cells collected at the indicated experimental conditions. (F) Violin plots showing the quantification of E.

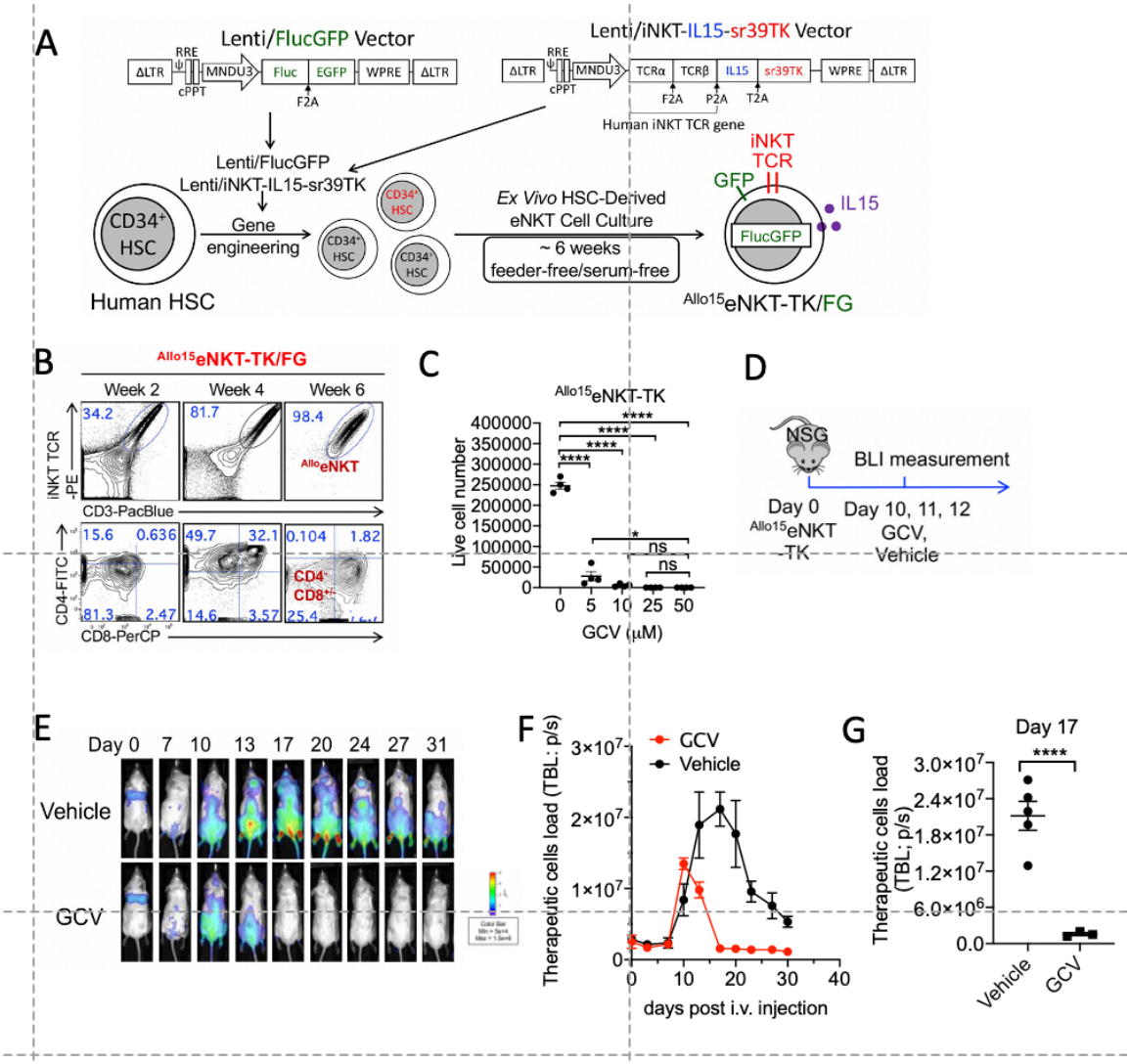

Figure S8. Incorporating of a suicide gene switch in eNKT cells, related to Figure 6.

(A) Schematic showing the experimental design to generate allogeneic HSC-engineered NKT cells equipped with a TK suicide gene (denoted as ^{Allo15}eNKT-TK cells). Lenti/iNKT-IL15-sr39TK vector is constructed to co-deliver genes encoding an iNKT TCR, an IL-15, and an sr39TK suicide/PET imaging dual-reporter.

(B) FACS monitoring of ^{Allo15}eNKT-TK/FG cell development.

(C) In vitro depletion of ^{Allo15}eNKT-TK/FG cells via GCV treatment. GCV, ganciclovir, that specifically depleting cell expressing sr39TK gene. ^{Allo15}eNKT-TK/FG cells were cultured *in vitro* in the presence of gradient concentrations of GCV for 3 days, followed by quantification of live cells via FACS analysis (n = 4).

(D-G) *In vivo* depletion of ^{Allo15}eNKT-TK/FG cells via GCV administration. ^{Allo15}eNKT-TK cells were labeled with FG. (D) Experimental design. (E) BLI images showing the presence and dynamics of ^{Allo15}eNKT-TK/FG cells in experimental animals over time. (F) Quantification of E. (G) Quantification of ^{Allo15}eNKT-TK/FG cell number at day 17.

Representative of 3 experiments. Data are presented as the mean ± SEM. ns, not significant, *p < 0.05, **p < 0.01, ***p < 0.001, ****p < 0.0001, by 1-way ANOVA (C), or by Student's t test (G).

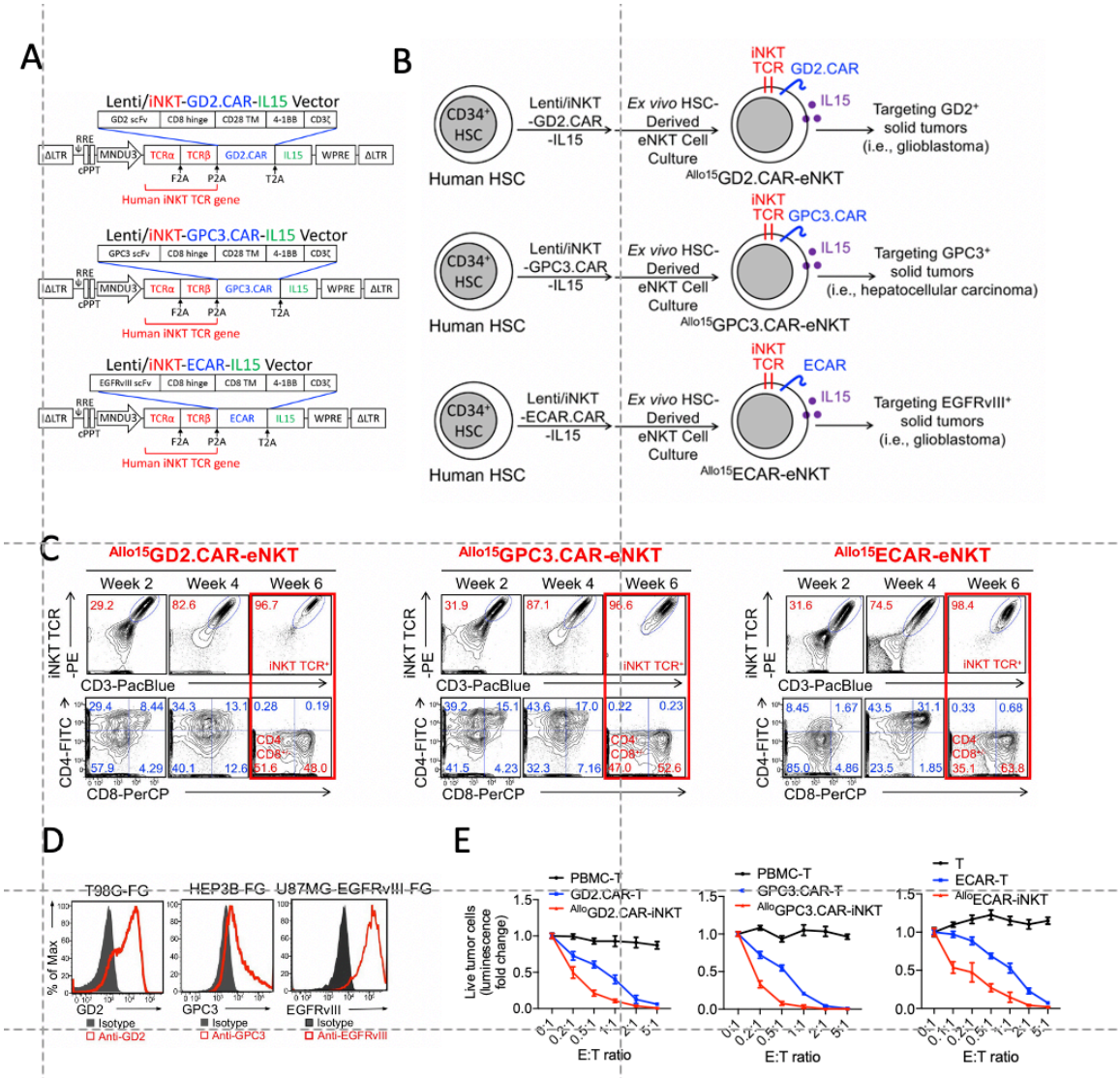

Figure S9. Generation of ^{Allo}(CAR)-eNKT cells for targeting solid tumors.

(A) Schematics showing the design of indicated lentivectors. GD2.CAR, disialoganglioside-targeting CAR. GPC3.CAR, glypican-targeting CAR. EGFRvIII.CAR, epidermal growth factor receptor variant III (EGFRvIII)-targeting CAR.

(B) Schematics showing the generation of ^{Allo15}GD2.CAR-eNKT, ^{Allo15}GPC3.CAR-eNKT, and ^{Allo15}EGFRvIII3.CAR-eNKT cells.

(C) FACS detection showing the development of indicated cell products.

(D) FACS measurements of antigen expression on the indicated solid tumor cell lines. T98G-FG: a human T98G glioblastoma cell line engineered to express firefly luciferase and green fluorescence protein dual reporters (FG). Hep3B-FG, a Hep3B human hepatocellular carcinoma cell line engineered with FG. U87MG-FG, human U87MG glioblastoma cell line engineered with FG.

(E) Tumor killing data measured using an *in vitro* tumor cell killing assay (as shown in Figure 3E) at 24-hour (n = 4). PBMC-T, and PBMC-derived conventional T cells engineered with GD2.CAR, GPC3.CAR, or EGFRvIII.CAR (denoted as GD2.CAR-T, GPC3.CAR-T, or EGFRvIII.CAR-T cells) respectively, were included as a control.

Representative of 3 experiments. Data are presented as the mean ± SEM.

CHAPTER 4:

Pluripotent stem cell-engineered immune cells for off-the-shelf cell therapy

4.1 Engineering induced pluripotent stem cells for cancer immunotherapy

(This project is published on *Cancers* in 2022)

Review

Engineering Induced Pluripotent Stem Cells for Cancer Immunotherapy

Yang Zhou [1,†], Miao Li [1,†], Kuangyi Zhou [1,†], James Brown [1], Tasha Tsao [1], Xinjian Cen [1], Tiffany Husman [1], Aarushi Bajpai [1], Zachary Spencer Dunn [1,2] and Lili Yang [1,3,4,*]

[1] Department of Microbiology, Immunology & Molecular Genetics, University of California, Los Angeles, CA 90095, USA; zzydcat@g.ucla.edu (Y.Z.); ericmli0507@g.ucla.edu (M.L.); kuangyizhou@g.ucla.edu (K.Z.); brownjimw0@gmail.com (J.B.); tytsao@g.ucla.edu (T.T.); xicen@g.ucla.edu (X.C.); tiffanyhusman@g.ucla.edu (T.H.); abajpai2023@g.ucla.edu (A.B.); zacharsd@usc.edu (Z.S.D.)
[2] Mork Family Department of Chemical Engineering and Materials Science, University of Southern California, Los Angeles, CA 90089, USA
[3] Eli and Edythe Broad Center of Regenerative Medicine and Stem Cell Research, University of California, Los Angeles, CA 90095, USA
[4] Jonsson Comprehensive Cancer Center, David Geffen School of Medicine, University of California, Los Angeles, CA 90095, USA
* Correspondence: liliyang@ucla.edu; Tel.: +1-310-825-7885
† These authors contributed equally to this work.

Simple Summary: Induced pluripotent stem cells (iPSCs) that can be genetically engineered and differentiated into different types of immune cells, providing an unlimited resource for developing off-the-shelf cell therapies. Here, we present a comprehensive review that describes the current stages of iPSC-based cell therapies, including iPSC-derived T, nature killer (NK), invariant natural killer T (iNKT), gamma delta T (γδ T), mucosal-associated invariant T (MAIT) cells, and macrophages (Mφs).

Abstract: Cell-based immunotherapy, such as chimeric antigen receptor (CAR) T cell therapy, has revolutionized the treatment of hematological malignancies, especially in patients who are refractory to other therapies. However, there are critical obstacles that hinder the widespread clinical applications of current autologous therapies, such as high cost, challenging large-scale manufacturing, and inaccessibility to the therapy for lymphopenia patients. Therefore, it is in great demand to generate the universal off-the-shelf cell products with significant scalability. Human induced pluripotent stem cells (iPSCs) provide an "unlimited supply" for cell therapy because of their unique self-renewal properties and the capacity to be genetically engineered. iPSCs can be differentiated into different immune cells, such as T cells, natural killer (NK) cells, invariant natural killer T (iNKT) cells, gamma delta T (γδ T), mucosal-associated invariant T (MAIT) cells, and macrophages (Mφs). In this review, we describe iPSC-based allogeneic cell therapy, the different culture methods of generating iPSC-derived immune cells (e.g., iPSC-T, iPSC-NK, iPSC-iNKT, iPSC-γδT, iPSC-MAIT and iPSC-Mφ), as well as the recent advances in iPSC-T and iPSC-NK cell therapies, particularly in combinations with CAR-engineering. We also discuss the current challenges and the future perspectives in this field towards the foreseeable applications of iPSC-based immune therapy.

Keywords: induced pluripotent stem cell (iPSC); immunotherapy; cancer; allogeneic; off-the-shelf; reprogramming; chimeric antigen receptor (CAR); T; natural killer (NK); invariant natural killer T (iNKT); gamma delta T (γδ T); mucosal-associated invariant T (MAIT); macrophages (Mφs)

check for updates

Citation: Zhou, Y.; Li, M.; Zhou, K.; Brown, J.; Tsao, T.; Cen, X.; Husman, T.; Bajpai, A.; Dunn, Z.S.; Yang, L. Engineering Induced Pluripotent Stem Cells for Cancer Immunotherapy. *Cancers* **2022**, *14*, 2266. https://doi.org/10.3390/cancers14092266

Academic Editor: Véronique Décot

Received: 30 March 2022
Accepted: 29 April 2022
Published: 1 May 2022

Publisher's Note: MDPI stays neutral with regard to jurisdictional claims in published maps and institutional affiliations.

1. Introduction

During the past decade, the field of oncology has experienced a remarkable therapeutic overhaul with the advent of cancer immunotherapy, broadening the scope of

what cancer therapy can entail. Anti-CTLA-4 monoclonal antibody (mAb) and anti-PD-1 mAb are examples of immune checkpoint blockade (ICB) medications that have shown striking therapeutic efficacy [1–6]. Alternatively, adoptive cell therapy, where patients receive autologous immune cells, has also shown promising effects on treating persistent viral infections [7–10] and malignancies [11–13]. In currently ongoing trials of adoptive T-cells therapies, T cells are obtained through leukapheresis from the patient and reinjected back to the patient following ex vivo cell engineering or expansion (Figure 1A). Transferring ex vivo-expanded tumor-infiltrating lymphocytes (TILs) [14–17] and transferring antigen-specific TCR genes [18–20], such as the NY-ESO1 TCR gene [21,22], into engineered peripheral T cells yielded positive results in controlling melanoma [15,21] and other types of tumors [11,16], upon infusion back into the patient. Arming T cells with the expression of a chimeric antigen receptor (CAR) that can specifically target tumor associated antigens (TAAs) has been demonstrated to be extremely effective in the treatment of B-cell leukemia/lymphoma [23–25]. The synthetic CAR composes of an extracellular antigen-recognition domain, mostly a single chain variable fragment (scFv), a transmembrane domain and intracellular signaling domains. The extracellular domain was rationally designed to broaden the spectrum of targeted TAAs, including CD19, BCMA, CD22, CD20, EGFR, mesothelin, and many more, and modifications to the intracellular domains resulted in new generations of CAR T cells [26–29]. Currently, the US Food and Drug Administration (FDA) has already approved six CAR T-cell therapies, axicabtagene ciloleucel (Yescarta, Kite Pharma, 2017), tisagenlecleucel (Kymriah, Novartis, 2017), brexucabtagene autoleucel (Tecartus, Kite Pharma, 2020), lisocabtagene maraleucel (Breyanzi, Bristol Myers Squibb, 2021), idecabtagene vicleucel (Abecma, Bristol Myers Squibb, 2021), and ciltacabtagene autoleucel (Carvykti, Legend, 2022) for treating B cell lymphoma or multiple myeloma patients. However, there are challenges that need to be resolved within the autologous treatment settings: (1) time; (2) cost; (3) heterogeneous quality of therapeutic cells. Therefore, new methods for rapidly producing unlimited antigen-specific T cells with optimized therapeutic features are in high demand and would greatly advance the delivery and efficacy of T cell therapy.

Different strategies have been explored for developing allogeneic cell therapy (Table 1).

One approach is to develop allogenic T cell products, where functional T cells are collected from healthy volunteers rather than from cancer patients who have had exposure to chemotherapy (Figure 1B). The biggest challenge of allogenic T cell therapy is the graft versus host disease (GvHD) risk [30,31]. To avoid immunological rejection and minimize GvHD in patients, allogeneic T cells have to be engineered to remove their human leukocyte antigen (HLA) class I and II molecules as well as disrupt TCR expression [32,33]. These additional genetic modifications increase the tumorigenicity risk and largely decrease the yield of final products. Alternatively, natural killer (NK) cells, which are essential effector cells in the innate immune system, possess features that can circumvent certain challenges in T cell therapies [34,35]. NK cells have shown powerful anti-tumor efficacy in both mice and humans. Unlike T cells that recognize antigens presented by major histocompatibility complex (MHC) molecules, NK cells do not require HLA matching so they are significantly less likely cause GvHD and thus can be utilized as an appropriate cell type for allogeneic cell therapy [36,37]. Because of these potential benefits, NK cells obtained from diverse sources, such as the NK-92 cell line, peripheral blood, and umbilical cord blood, have been evaluated to treat cancer patients in clinical studies [38,39]. Alternatively, unconventional T cells, such as invariant natural killer T (iNKT), gamma delta T ($\gamma\delta$T), and mucosal-associated invariant T (MAIT) cells, that naturally do not cause GvHD, have also been investigated as carriers for allogeneic cell therapy [40–42]. However, these innate or innate-like immune cells are difficult to be massively expanded, especially after CAR-engineering or other genetic modifications (Table 2).

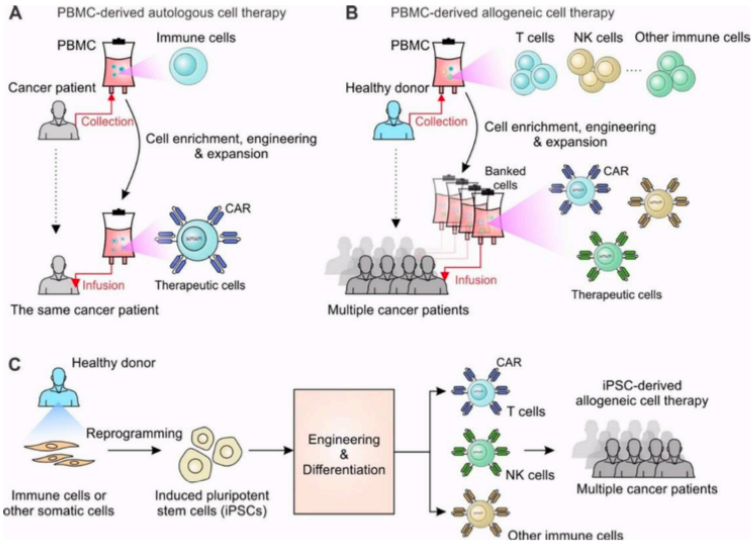

Figure 1. Development of cell therapy from autologous to allogeneic cell therapy. (**A**) PBMC-derived autologous cell therapy. Immune cells collected from cancer patients through leukapheresis are expanded and engineered ex vivo. The engineered cells are infused back to the same patients to fight against cancer. (**B**) PBMC-derived allogeneic cell therapy. Immune cells such as T cells, NK cells and other immune cells are collected from healthy volunteers and stored as banked cells after cell engineering and expansion. The banked cells are ready-to-use and can be utilized to treat multiple cancer patients. (**C**) iPSC-derived allogeneic cell therapy. Immune cells or other somatic cells are collected from healthy donors and reprogrammed to be stable iPSC lines. The reprogrammed iPSCs can be engineered and differentiated into different immune cells for treating multiple cancer patients.

Table 1. Current allogeneic cell therapies in clinical trials.

Clinical Trial	Description	Cell Product	Malignancies	Company
NCT03841110	FT500 in combination with checkpoint inhibitors against solid tumors	iPSC-NK	Solid tumor	Fate Pharmaceutics
NCT04630769, NCT04023071	FT516 and IL2 with Enoblituzumab for ovarian cancer; FT516 combination with CD20-directed monoclonal antibodies	iPSC-NK (non-cleavable CD16 Fc receptor)	Ovarian cancer; Advanced B-cell lymphoma	Fate Pharmaceutics
NCT04555811; NCT04245722	FT596 with Rituximab as relapse prevention after autologous HSCT for NHL; FT596 as a monotherapy and in combination with anti-CD20 monoclonal antibodies	iPSC-NK(hnCD16, IL15RF, CAR-19)	B cell lymphoma (BCL); Chronic lymphocytic leukemia (CLL)	Fate Pharmaceutics

Table 1. *Cont.*

Clinical Trial	Description	Cell Product	Malignancies	Company
NCT04714372; NCT05069935; NCT04614636	FT538 in combination with Daratumumab in acute myeloid leukemia (AML); FT538 in combination with monoclonal antibodies in advance solid tumors; FT538 in subjects with advanced hematologic malignancies	iPSC-NK (hnCD16, IL15RF + CD38KO)	AML, MM, solid tumors	Fate Pharmaceutics
NCT05182073	FT576 in subjects with multiple myeloma (MM)	iPSC-NK (hnCD16, IL15RF + CD38KO, CAR-BCMA)	MM	Fate Pharmaceutics
NCT04629729	FT819 in subjects with B-cell malignancies	iPSC-T (CAR-19, TCR-KO)	BCL, CLL, ALL	Fate Pharmaceutics
NCT03190278	Study evaluating safety and efficacy of UCART123	Allogeneic T-cells expressing anti-CD123 CAR	Relapsed/refractory acute myeloid leukemia (AML)	Cellectis
NCAT041500497	Phase 1 study of UCART22 in patients with R/R CD22+ BALL	Allogeneic T cells expressing anti-CD22 CAR	Relapsed or refractory CD22 + B-cell acute lymphoblastic leukemia	Cellectis
NCT04142619	Study evaluating safety of and efficacy of UCART targeting CS1 in patients with R/R MM	Allogeneic T cells expressing anti-CS1 CAR	Relapsed/refractory MM	Cellectis
NCT02735083; NCT02808442; NCT02746952	Study of UCART19 in patients with R/R BALL	Allogeneic T cells expressing anti-CD19 CAR	R/R BALL	Cellectis
NCT04416984	Safety and efficacy of ALLO-501A anti-CD19 allogeneic CAR T cels in adults with R/R LBCL	Allogeneic T cells expressing anti-CD19 CAR, CD52 KO, TCR KO	R/R LBCL, R/R NHL	Cellectis/Allogene
NCT04093596	Safety and efficacy of ALLO-715 BCMA allogeneic T cells in adults with R/R MM	Allogeneic T cells expressing anti-BCMA CAR, CD52 KO, TCR KO	R/R MM	Cellectis/Allogene
NCT04696731	Safety and efficacy of ALLO-316 in subjects with advanced or metastatic clear cell RCC	Allogeneic T cells targeting CD70	RCC	Allogene
NCT04991948; NCT03692429	Study of Pembrolizumab treatment after CYAD-101 with FOLFOX reconditioning in mCRC	Allogeneic T cells targeting NKG2DL	mCRC	Celyad

Table 1. *Cont.*

Clinical Trial	Description	Cell Product	Malignancies	Company
NCT04613557	Safety, activity and cell kinetics of CYAD-211 in patients with R/R MM	Allogeneic T cells targeting BCMA	r/r MM	Celyad
NCT03769467; NCT04554914; NCT03394365; NCT02822495; NCT03131934; NCT01192464	Therapeutic effects of Tebelecleucel in subjects with diseases	EBV-CTL (Tabelecleucel, or tab-cel)	EBV-induced lymphomas and other diseases	Atara
NCT03283826	Phase 1/2 study to evaluate the safety and efficacy of ATA188 in subjects with progressive MS	EBV-CTL	Progressive MS	Atara
NCT05252403; NCT03389035	Residual disease driven strategy for CARCIK-CD19 (CMN-005) in adults/pediatric BCP-ALL	Allogeneic CARCIK-CD19	ALL	Coimmune
NCT04735471; NCT04911478	A study of ADI-001 in B cell malignancies	Allogeneic CD20-targeted gd T cells	B cell maliganacy	Adicet Bio

R/R: relapsed or refractory; BALL: B-cell acute lymphoblastic leukemia; LBCL: large B cell lymphoma; NHL: non-Hodgkin lymphoma; KO: knock-out; RCC: renal cell carcinoma; mCRC: metastatic colorectal cancer; EBV: Epstein-Barr virus; NPC: Nasopharyngeal carcinoma; MS: multiple sclerosis; ALL: acute lymphoblastic leukemia.

Table 2. Pros and cons of using different types of cells in cancer immunotherapy.

Cell Therapy	Pros	Cons
Conventional T cell	Abundant source Easy to expand in vitro Scalable and standardized quality controls for manufacturing	Time-consuming and costly MHC dependent T cell exhaustion GVHD Low ability of trafficking and infiltrating into solid tumors
NK cell	No need for previous antigen priming Multiple innate activating receptors that can mediate killing MHC independent No GVHD	Low persistence in the absence of cytokine Low number in patients Low ability of trafficking and infiltrating into solid tumors
iNKT cell	Innate and adaptive features Invariant TCR recognizes lipid antigens presented by CD1d No GVHD Low toxicities	Low number in patients May have immunosuppressive properties (Th2, Th17) Limited clinical data with CAR-iNKT cells
γδT cell	Innate and adaptive features MHC independent No GVHD Low toxicities	Extremely low number in patients May have immunosuppressive properties (γδ T17, Vδ1 γδ T cells, γδ Treg) Limited clinical data with CAR- γδT cells
MAIT cell	Solid tumor-infiltrating capacity Direct anti-tumor cytotoxicity both in vitro and in vivo Resistant to tumor antigen escape	Unclear mechanisms in suppressing tumor Lack of clinical data with CAR-MAIT cells
Macrophage cell	Penetration into solid tumors Phagocytosis of tumor cells and innate immune response No GVHD Cross present antigens to αβ T cells	Poor proliferation both in vitro and in vivo May have immunosuppressive properties (M2) Limited clinical data with CAR-macrophage cells

Induced pluripotent stem cells (iPSCs) have been recognized as an ideal source of engineered off-the-shelf allogeneic cell therapies due to their unlimited expansion capabilities, relative ease of genetic engineering, capacity for clonal selection after genetic modification, and the elimination of the need to collect cells from a donor at any point in time, are recognized as an ideal source for generating off-the-shelf allogeneic cell therapy [43,44]

(Figure 1C). Since the discovery that a simple cocktail of transcription factors could restore the pluripotency of adult somatic cells by the Yamanaka group in 2006, enormous progress has been made in the fields of stem cell biology and regenerative medicine [45,46]. iPSCs share similar characteristics with human embryonic stem cells (hESCs) in terms of gene expression and pluripotency, but lack the ethical and regulatory roadblocks to collection that slow progress in hESC research [43,47]. With the introduction of iPSC technology, laboratories all over the world have generated protocols to differentiate various cells of interest. The application of iPSC technology to generate antigen-specific T cell therapy first took hold in Japan during the early 2010s [48,49]. By transducing iPSCs with a CAR or transgenic TCR gene, iPSCs can be converted into antigen-specific T cells with impressive on-target killing efficacies both in vitro and in vivo [48–50]. This process can be further optimized for efficacy and safety with the implementation of CRISPR-Cas9 technology for the insertion of CAR genes into endogenous TCRα constant (TRAC) locus chain position, which would reduce the risk of allo-reaction in response to the host [51]. iPSCs innovators, such as the Kaufman group, have also seen substantial success in the derivation of homogeneous, functional NK cells that can be produced at a clinical scale [52–54]. In particular, the 'spin embryoid body (EB)' protocol together with defined culture conditions makes it feasible to eliminate the use of serum-containing media and stromal cells, producing iPSC-derived immune cells that are better suited for clinical applications. Additionally, unconventional T cells [55,56] and macrophages [57,58] that can also be differentiated from iPSCs are alternative cell carriers for cancer therapy. In this review, we describe the different culture methods of generating iPSC-derived immune cell-based allogeneic therapy, including iPSC-T, iPSC-NK, iPSC-derived unconventional T cells and macrophages, as well as the recent significant breakthroughs, limitations, and future steps towards iPSC cell-based off-the-shelf cell immunotherapy.

2. iPSC Technology: Advances and Opportunities

In 2006, the discovery of induced pluripotent stem cells (iPSCs) was heralded as a significant breakthrough in science and medicine. Pioneered by Shinya Yamanaka's lab in Kyoto, scientists deemed a cocktail of four transcription factors with the ability to induce a shift in somatic cells back to a pluripotent state (OCT4, SOC2, KLF4 and MYC) 'Yamanaka factors' [59,60]. The unique cells generated from somatic cells exhibit similar characteristics to embryonic stem cells (ESCs) with equivalent gene expression, indefinite self-renewal capacity, and potential to differentiate into specialized cell types derived from any primary germ layer: ectoderm, endoderm, and mesoderm [45–47]. Since the advent of iPSC technology, enormous progress has been made to produce therapeutic cells in the fields of stem cell biology and regenerative medicine. In particular, human iPSC technology, which has rapidly progressed since 2007, was quickly employed to generate human 'disease in a dish', implicated in medication screening for drug efficacy and possible toxicity [45,46]. Their human origin, ease of access, expandability, ability to give rise to different cell types, avoidance of ethical concerns related to hESCs, and the possibility to generate personalized medicine utilizing patient-specific iPSCs make them outstanding resources for drug development and understanding disease progression.

There are four major approaches to deliver reprogramming factors: integrating viral systems (e.g., retrovirus, lentivirus), non-integrating vectors (e.g., sendai virus, adenovirus), self-excising vectors (e.g., PiggyBac transposon) and non-integrating non-viral vectors (e.g., CHIR99021, siRNA, and protein delivery) [45,46]. Among them, sendai virus has been widely used as the most efficient and convenient tool. There is a significant effort to establish iPSC banks across the world; however, several requirements need to be fulfilled before banking an iPSC line. According to the International Stem Cell Banking initiative's recommendations [10,13], most biobanks incorporate the following assessments for establishing iPSC lines: (1) morphology evaluation, (v2) pluripotency assessment, (3) in vitro and in vivo differentiation potential test, (4) transgene silencing examination, (5) karyotype analysis for chromosomal abnormalities, (6) identity confirmation, and (7) microbiological

assays avoidance of contamination. To date, several iPSC banks have been established, such as California Institute for Regenerative Medicine (CIRM) in the United States, Center for iPS Cell Research and Application (CiRA) in Japan, and European Bank for induced pluripotent Stem Cells (EBiSC) in Europe [10,13]. These non-profit biobanks obtain samples, generate, and bank clinical-grade iPSC lines to establish a source of standardized, accessible iPSCs across the scientific community. The discovery of iPSC technology not only revolutionized our understanding of cell development, but also opened the door to human-specific drug screening [43–46]. The rapid advance of iPSC banks opens opportunities for researchers to access these vital cells for both foundational and clinical research.

3. Engineering iPSCs for T Cell-Based Therapy

One key component of the adaptive immune system are cytotoxic T lymphocytes (CTLs), which can recognize and kill infected cells and malignant host cells. The innovation of CAR-engineered T cells has resulted in groundbreaking new therapies that can exploit this natural aspect of the body's immune system for targeted therapies against an array of diseases. CARs are genetically modified synthetic receptors with a single chain variable fragment (scFv) joined to the heavy and light chain variable regions of a specialized monoclonal antibody (mAb) linked by a transmembrane domain directly connected to the intracellular signaling domains [61,62]. CARs drive lymphocytes, primarily T cells, to recognize and kill cells that express the specific antigen. The transduced T cell is endowed with an antibody-like specificity capable of effectively transmitting the intracellular signals needed for T-cell activation. CAR attachment to cell surface antigens occurs independently of the MHC molecules, leading to robust T cell activation and potent anti-tumor responses without any need for co-stimulation. Currently, there are more than 1000 CAR-T cell related clinical trials.

However, autologous CAR-T cell therapy necessitates a bespoke manufacturing method for each patient. Despite the excellent clinical results yielded to date, it has a few well-known drawbacks. The high processing cost, risk of manufacturing failure in some patients, and weeks-long manufacturing processes all result in a delay in treatment availability and make it an infusible treatment option for some patients [12,25,30,61,62]. Patients with highly proliferative diseases, such as acute leukemia, may experience disease progression before their CAR-T product is ready for use, or may lose eligibility due to the disease or other treatments [40,41]. Moreover, patients with T cell dysfunctions, which are characterized in many malignancies due to the immunosuppressive tumor microenvironments, may not have the necessary immunological infracture for an effective autologous T cell response. The preceding lines of treatment also have a deleterious impact on the biological features of autologous T cells. On top of this, the high expense of this sophisticated therapeutic strategy remains a huge burden for the health care system. Thus, generating 'off-the-shelf' allogeneic CAR-T cells that allows patients to get treatments right away is in great demand [12,40,41]. This would simplify the process into a single cell product as well as standardizes the CAR-T cell production, allowing redosing if necessary.

3.1. Engineering T-iPSCs

One approach to massively producing cytotoxic cells is using iPSCs derived from T cells (Figure 2). The rationale behind this method posits that since T cell-derived iPSCs should have inherited the rearranged TCR genes, all regenerated T cells should express the same TCR as the original [63,64]. Since iPSCs can be expanded infinitely, it will be feasible to manufacture as many 'fresh' T cells of a given type as needed. Generation of T cells from iPSCs involves a complicated process, requiring first the induction of mesoderm specification and hematopoietic commitment, followed by T cell differentiation [48,50,64,65]. The initial stages of specification to generate hematopoietic lineages were similar among reports. The mesoderm induction is initiated by generating embryoid bodies and/or co-culture iPSCs on murine bone marrow derived stroma cell lines (typically OP9) with morphogens, such as bone morphogenetic protein 4 (BMP4), vascular endothelial growth factor (VEGF), and fibroblast growth factor (FGF), that

support mesoderm specification [48–50] (Figure 2A). Subsequently, cells are transferred to cytokine cocktails that specifically support hemato-endothelial specification; the resulting $CD34^+$ hematopoietic stem cells are collected and replated on a bone marrow-derived stromal cell line OP9 ectopically expressing the Notch ligand Delta-like 1 (DLL1) or DLL4 (OP9-DLL1 and OP9-DLL4) for T cell development [48,50].

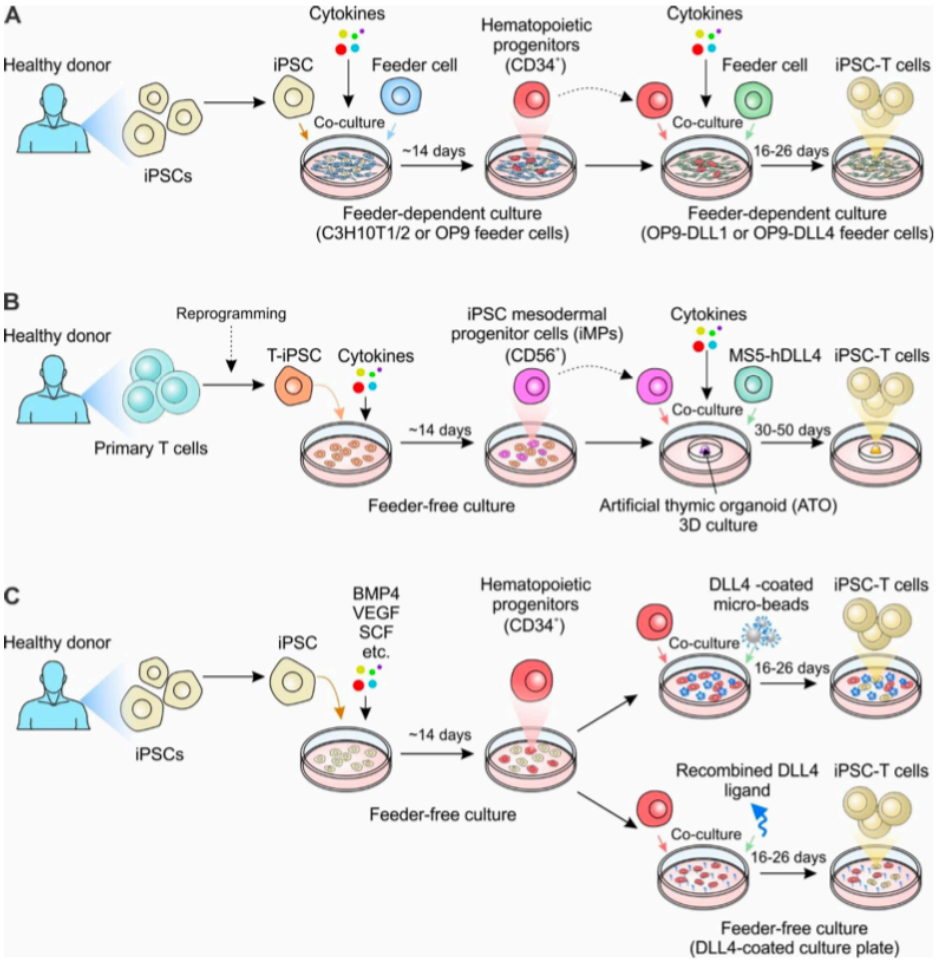

Figure 2. Generation of iPSC-derived T cell-based cell therapy. (**A**) The classic approach to generate iPSC-derived T cells. iPSCs derived from healthy donors are co-cultured with the murine bone marrow stromal cell line C3H10T1/2 or OP9 to allow for the generation of $CD34^+$ hematopoietic progenitors. $CD34^+$ hematopoietic progenitors are then enriched and co-cultured with OP9 overexpressing DLL1 or DLL4 (OP9-DLL1 or OP9-DLL4) with defined cytokines, driving the differentiation of T cells. (**B**) 3D-organoid culture to generate iPSC-derived T cells. The human primary T cells derived from healthy donors are reprogrammed to iPSCs. The T cell-derived iPSCs (T-iPSCs) are cultured in the defined cytokine cocktail to induce iPSC mesodermal progenitor cells (iMPs). The iMPs are then aggregated with mouse stromal cell line MS5 overexpressing human DLL4 (MS5-DLL4) in the air-liquid interface of the artificial thymic organoid (ATO). (**C**) Feeder-free culture systems to generate iPSC-derived T cells. iPSCs are cultured in the medium with defined cytokines for two weeks to generate hematopoietic progenitors. The $CD34^+$ progenitors are selected and reseeded either in the plate containing DLL4-coated micro-beads or plate coated with recombined DLL4 ligand. Notably, for the generation of gene-engineered iPSC-T cells, the healthy donor-derived iPSCs can be replated with genetically-engineered iPSCs, such as CAR-engineered iPSCs.

The RIKEN and CiRA group in Japan were the first to explore the idea of reprogramming antigen-specific T cells to regenerate clonal cytotoxic T cells [48–50] (Table 3). A study by the Kawamoto group generated iPSCs from a MART-1-specific T cell line, the JKF6 cell line, which were long-term cultured tumor infiltrating cytotoxic T cells originally derived from a melanoma patient [48]. JKF6 cells recognize the melanoma epitope MART-1 presented by HLA-A*02:01. MART1-T-iPSCs (iPSCs derived from MART1-specific T cells) were generated by transducing JKF6 with Yamanaka factors [48]. The clones were verified to carry the rearrangement status of the original TCRβ chain, exhibiting hESC-like morphology, as well as expressing pluripotent markers [48]. The MART-1-iPSCs were then cultured with OP9 and subsequently with OP9-DLL1 stromal cells for T cell differentiation. MART-1-iPSCs were successfully developed following DN to DP differentiation. At the DP stage, cells were stimulated with anti-CD3 antibodies for SP differentiation. The MART-1-iPSC-derived $CD8^+$ SP T cells largely bear the TCRα chain gene as the original MART-1-iPSCs and are functionally mature with a substantial amount of IFN-γ production responding to peptide stimulation, but lacked the same cytotoxicity as primary T cells [48]. In the same issue of *Cell: Stem Cell*, Nakauchi et al. published their success in growing viral antigen-specific cytotoxic T lymphocytes (CTLs) by adding to the RIKEN's approach [49]. An HIV type 1 (HIV-1) epitope-specific T cell was selected and induced into iPSC cells. These HIV-1-T-iPSCs (iPSCs from HIV-1-specific T cells) were then re-differented into rejuvenated T cells that showed the same pattern of TCR gene arrangement as the original T cells [49]. Similarly, the in vitro differentiation included two steps: iPSCs giving rise to mesoderm-derived hematopoietic stem cells and/or progenitor cells, and T cell differentiation from hematopoietic stem cells. Instead of using OP9 cells at the beginning, as in Kawamoto's paper, the T-iPSCs generated by Nakauchi et al. were cocultured on C3H10T1/2 feeder cells in the medium supplemented with VEGF, stem cell factor (SCF), and FMS-like tyrosine kinase 3 ligand (FLT-3L) and then on day 14, cells were transferred to OP9-DL1 co-culture in the presence of FLT-3L and interleukin-7 (IL-7) [48,49]. These too, had reduced efficacy, and lacked the antigen-specific cytotoxicity that was expected of adaptive immune cells.

Using T-iPSCs (T cell-derived iPSCs) as base cells, the reprogrammed iPSC clones can inherit the original TCR and drive the re-differentiation into iPSC-T (T cells re-differentiated from iPSCs) cells. However, this method requires time-consuming cloning of antigen-specific T cells and is limited to antigens that can be identified from patient-specific T cells. Moreover, the therapeutic application of iPSC-T cells is restricted in that the recipient patients need to match the HLA of their donors, greatly limiting the 'universality' of any off-the-shelf applications [64,66]. CAR-engineering, however, redirects T-cell specificity in an HLA-independent manner, expelling the need of HLA restriction and enhancing anti-tumor properties. In a 2013 paper by Themeli et al., researchers generated T-iPSC clones by reprogramming peripheral T cells from a healthy donor, then transduced a second-generation CAR specific for CD19 into the selected T-iPSC clone [50]. The CAR-expressing iPSC-T cells exhibited potent anti-tumor efficacy in a xenograft model but were phenotypically similar to innate γδT cells [50]. This method generated an innate type T cell with the expression of a CD8αα homodimer, impacting the re-differentiated T cels' antigen-specific cytotoxic capacity in a similar manner to MART-1-specific T cells. The conventional method was then modified with Maeda et al.'s purification DP cells, which were then stimulated them with monoclonal anti-CD3 antibodies (Abs) to generate CD8αβ T cells that exhibited comparable antigen-specific cytotoxicity to the original CTLs [65].

Table 3. Representative in vitro differentiation methods of generating iPSC-derived T cells for cancer cell therapy.

Publications	Final Products (Immune Cell Types)	Start Material	iPSC Genetic Modification	Feeder or Feeder-Free	Overall Procedure Time	Major Components in Culture Medium
Nishimura et al., 2013 [49]	Conventional αβ T cells	$CD3^+$ PBMC T cells for a healthy donor; HIV-1-specific $CD8^+$ T cells	NA	Feeder: C3H10T1/2, OP9-DL1	33–40 days	VEGF, SCF, FLT-3L, IL-7, IL-15
Themeli et al., 2013 [50]	Conventional αβ T cells	Peripheral blood T lymphocytes (PBL) from a healthy donor	19CAR-engineering	Half feeder-free; Half feeder: OP9-DLL1	~30 days	BMP-4, FGF, VEGF, SCF, FLT-3L, IL-3, IL-7
Vizcardo et al., 2013 [48]	Conventional αβ T cells	JKF6 cells (MART-1 specific TILs)	NA	Feeder: OP9, OP9-DLL1	~40 days	SCF, FLT-3L, IL-7, IL-2
Maeda et al., 2016 [65]	Conventional αβ T cells	LMP2-specific CTLs from a healthy donor	NA	Feeder: OP9, OP9-DLL1	~6–8 weeks	IL-7, FLT-3L, SCF, IL-2, IL-21
Minagawa et al., 2018 [66]	Conventional αβ T cells	GPC3-specific CTLs from GPC3 peptide-vaccinated patients; Monocyte-derived HLA-typed iPSCs	*RAG2* knockout; WT1-TCR transduction	Feeder: C3H10T1/2, OP9-DLL1	NA	FGF, VEGF, SCF, IL-7, FLT-3L, IL-15,
Maeda et al., 2020 [63]	Conventional αβ T cells	Monocytes derived iPSCs from the HLA-homo donor	WT1-TCR transduction	Feeder: OP9, OP9-DLL1	~36 days	FGF, IL-7, FLT-3L, SCF, IL-7, IL-21
Iriguchi et al., 2021 [67]	Conventional αβ T cells	Peripheral blood T cells; HIV-1-specific CTLs; RAG2-deleted GPC3 T-iPSCs	NA	Feeder-free	~42 days	CHIR99021, BMP4, FGF, VEGF, SCF, TPO, FLT-3L, SDF1α
Trotman-Grant et al., 2021 [68]	Conventional αβ T cells	Human IPS11- and STIPS cell lines	NA	Feeder-free	~42 days	BMP4, FGF, VEGF, FLT-3L, SCF, IL-7
Wang et al., 2021 [51]	Conventional αβ T cells	Human iPSC line: GPC3-16-1 (generated from CTLs)	*PVR* knockout; HLA-E transduction; *B2M* knockout; *CIITA* knockout	Feeder: OP9-DLL1	NA	CHIR99201, FGF, VEGF, BMP4, SCF, FLT-3L, TPO, IL-7, IL-15
Wang et al., 2022 [69]	Conventional αβ T cells	iPSC clones from $CD62L^+$ T cells	19CAR-engineering	Feeder: MS5-DLL4	~51–64 days	BMP4, VEGF, FGF, EGM-2, SB-431542, SCF, FLT3, IL-7, TPO, IL-2, IL-7

LMP2: Latent membrane protein 2; CTLs: cytotoxic T lymphocytes; GPC3: Glypican 3; RAG2: recombinase-activating-gene-2; NA: not available.

More recently, a 3D organoid culture system was reported to successfully generate CAR T cells for 'off-the-shelf' manufacturing strategies [69] (Figure 2B). In Wang et al., iPSC clones were reprogrammed from primary $CD62L^+$ T cells, the naïve and memory T cell population which was recognized to have exceptional persistence and enhanced clinical outcomes in CAR-T cell therapy [69]. T-iPSC clones were transduced with lentivirus encoding a CD19-targeting CAR (19CAR). Instead of utilizing the OP9 system, the $19CAR^+$ T-iPSC clones were sorted and cultured under feeder-free conditions to simulate mesodermal development [69]. Then $CD56^+CD326^-$ iPSC mesodermal progenitor cells (iMPs) were sorted and mixed with a mouse stromal cell line overexpressing DLL4 (MS5-hDLL4) feeder cells to differentiate to hematopoietic progenitors, followed by T cell differentiation for additional 5–7 weeks [69]. Unlike iPSC-T cells generated from the monolayer coculture systems displaying an innate-like phenotype, the regenerated 19CAR iPSC T cells from the 3D organoid culture system showed comparable phenotypes to conventional T cells and exhibited similarly potent antitumor function [69].

The classic approaches to generate iPSC-derived T cells requiring feeder cells in each stage, such as OP9 and MS5 cells, have paved the way to allogeneic therapy (Table 1). However, using murine-derived stroma feeder layers increases the risk of cross-species contamination [67,68]. Feeder cell maintenance relies on different serum and basal media, making it challenging for quality control. Developing feeder-free and serum-free culture systems is important for broadening the application of iPSC-T-based 'off-the-shelf' therapy (Figure 2C). In Iriguchi et al. 2021, researchers provided notch signaling for T cell differentiation by incorporating immobilized delta-like 4 (DL4) protein together with retronectin in place of feeder cells [67] (Table 1). The results demonstrated the feasibility of generating progenitor T cells in a feeder-cell-free condition. Alternatively, DL4-μbeads, along with cytokine cocktails, can also induce an ordered sequence of T cell differentiation [68]. All these approaches provide a simple and robust platform for producing clinically applicable T cells, as well as for studying human T- cell differentiation [67,68].

3.2. Engineering iPSCs in Combination with TCR Transgene Overexpression

Despite promising results from using T-cell-derived iPSCs (T-iPSCs) to generate CTLs, certain issues remain limiting the establishment of highly potent T-iPSCs, such as low reprogramming efficiency of T cells into iPSCs and heterogeneity among T-iPSC clones. To overcome these challenges, researchers developed an alternative method where iPSCs were transduced with exogenous TCR genes and then re-differentiated the TCR-engineered iPSCs into CTLs [63,65,66]. With this approach, it was much easier to establish high-quality TCR-iPSCs clones with guaranteed specificity and quality using TCR and iPSCs genes. This method has been verified on different non-T-cell-derived iPSCs, such as myeloid cell-, monocyte- and fibroblast-derived iPSCs, to successfully generate T cells through the transduction of exogenous TCR genes [64,70]. In particular, the cells regenerated from the HLA-homo iPSCs could be transplanted into HLA-hetero patients with minimal rejection. Additionally, this approach has been utilized for treating viral infectious diseases (e.g., COVID-19) [64]. The model has also been tested in the feeder-free culture system to generate WT1-T cells that were specific to the Wilms tumor 1 (WT1) as well as CD19 CAR T cells [67,68].

The combined power of somatic cell reprogramming, CAR-engineering, and gene-editing technology can be used to produce cytotoxic T cells with antigen specificity mimicking that of the human adaptive immune system (Figure 2 and Table 1). Additional modifications such as genetic ablation of HLA expression could be utilized to reduce allogeneic response against these cells and prevent GvHD [51]. Overexpressing minimally polymorphic HLA-E molecules in HLA-deletion T cells can resolve NK lysis of HLA absent cells [51]. Moreover, additional modifications such as the deletion of inhibitory receptors (e.g., PD-1) can further improve anti-tumor activity [51]. With these advances, we should eventually reach the goal of using human iPSC-derived T cells as a novel, stan-

dardized anti-cancer therapy that can utilize the evolved potency of the human adaptive immune system.

4. Engineering iPSCs for NK Cell-Based Therapy

4.1. NK Cells as a Promising Alternative to T Cells for Cellular Therapy

Natural killer (NK) cells are innate cytotoxic lymphocytes that target malignant cells through degranulation. NK cells can also orchestrate an immune response through the release of cytokines. Unlike T cells, which need to be primed against a specific antigen, NK cells can directly kill damaged cells based on the summation of inhibitory and activating signals received from their germline-coded surface receptors. Killer-cell immunoglobulin-like receptors (KIRs) are a class of inhibitory NK receptors that will bind to the major histocompatibility complex class I (MHC I) on adjacent cells and pass on an inhibitory signal. Cells that don't have the correct MHC I expression will lack the inhibitory KIR-MHC I ligation signal, allowing NK cells to recognize non-self-cells. Conversely, NK cell-activating receptors bind to stress-induced ligands that are expressed during conditions such as DNA damage or hypoxia [71]. The binding of those ligands allows for recognition of cells that are in altered states, allowing NK cells to kill them through degranulation. NK cells are also able to kill opsonized cells through CD16 recognition of the IgG Fc region through a process called antibody-dependent cellular cytotoxicity (ADCC) [72–74]. Altogether, these characteristics allow NK cells to respond to a variety of diseased cell states, including cancerous cells.

NK cells have been proven to be safe and effective against certain cancers in various adoptive cell therapy studies without causing GvHD, and engineering only adds to their virulence [71,75–79]. NK cells are a prime candidate for genetically engineered CAR therapies because they are significantly less likely to cause complications such as cytokine release syndrome (CRS), neurotoxicity, or GvHD; they do not require HLA matching, which increases their potential for off-the-shelf allogeneic therapies; and they have multiple mechanisms by which they are able to activate cytotoxic effects independent of the CAR [72,74,75,80–82]. For these reasons, many are shifting their focus from CAR-T therapies to CAR-NK therapies. Currently, there are many ongoing CAR-NK phase I/II clinical trials targeting both hematological malignancies such as acute lymphocytic leukemia (ALL) and non-Hodgkin's lymphoma (NHL), and solid tumor cancers such as colorectal and pancreatic cancer. One such hematological malignancy study from Liu et al. demonstrated the effects of anti-CD19 CAR NK cells in patients with relapsed or refracted $CD19^+$ B cell malignancies. NK cells were isolated and expanded from cord blood then transduced using a retroviral vector containing genes for anti-CD19 CAR, membrane-bound IL-15, and inducible caspase 9. Of the 11 patients treated, 8 responded to treatment, 7 of which patients were able to achieve a complete remission with no reports of serious or irreversible toxicities. The caspase 9 kill switch was not activated at any point during the study because no patients exhibited severe adverse side effects [83] (Clinicaltrials.gov Identifier NCT03056339). CAR-NK therapies have been less effective in certain cancers due to poor trafficking, infiltration, and persistence in vivo, so additional gene engineering has been employed to create "armored" CAR-NK cells that have increased fitness [74,84]. Adding a transgene for membrane-bound IL-15 allows for longer persistence of CAR-NKs in vivo and alleviates the risk of CRS that comes with repeated cytokine injections needed for stimulation [85]. Knocking out the CISH gene deletes the cytokine-inducible Src homology 2-containing (CIS) protein, a negative regulator of IL-15 signaling, which increases the cell's metabolic activity and subsequent anti-tumor activity [84,86]. These and many other studies show that allogeneic CAR-NK cells are both safe to use in clinical applications and can be effective in cancer treatments.

4.2. Generation of iPSC-NK Cells

Like iPSC-Ts, iPSCs are a renewable source that can be used to generate homogenous NK cell populations for off-the-shelf allogeneic therapies [74,80,85] (Figure 3). Methods for generating NK cells from iPSCs were first adapted from the human embryonic stem cell NK (hESC-NK) differentiation protocols, since hESCs were the main source of stem cells before the discovery of iPSCs [71,87]. The original two-step feeder-dependent culture method initially

outlined by the Kaufman group entailed coculturing iPSCs with mouse stromal cell line M210-B4 for 19-21 days to induce hematopoietic stem cell (HSC) differentiation [88,89] (Figure 3A). The $CD34^+$ $CD45^+$ hematopoietic progenitors were isolated and then cultured on a second murine stromal line AFT024 or EL08-1D2 with a cocktail of cytokines including IL-3, IL-7, IL-15, SCF, and Flt-3L for 4–5 weeks to generate mature NK cells [80,88,89] (Figure 3A). This method produced functional, mature NK cells that demonstrated the ability to potently kill multiple types of tumor cells. However, from a large-scale manufacturing perspective, maintaining murine-derived feeder cells requires additional cost and increases the risk of cross-species contamination [53,71,74,90].

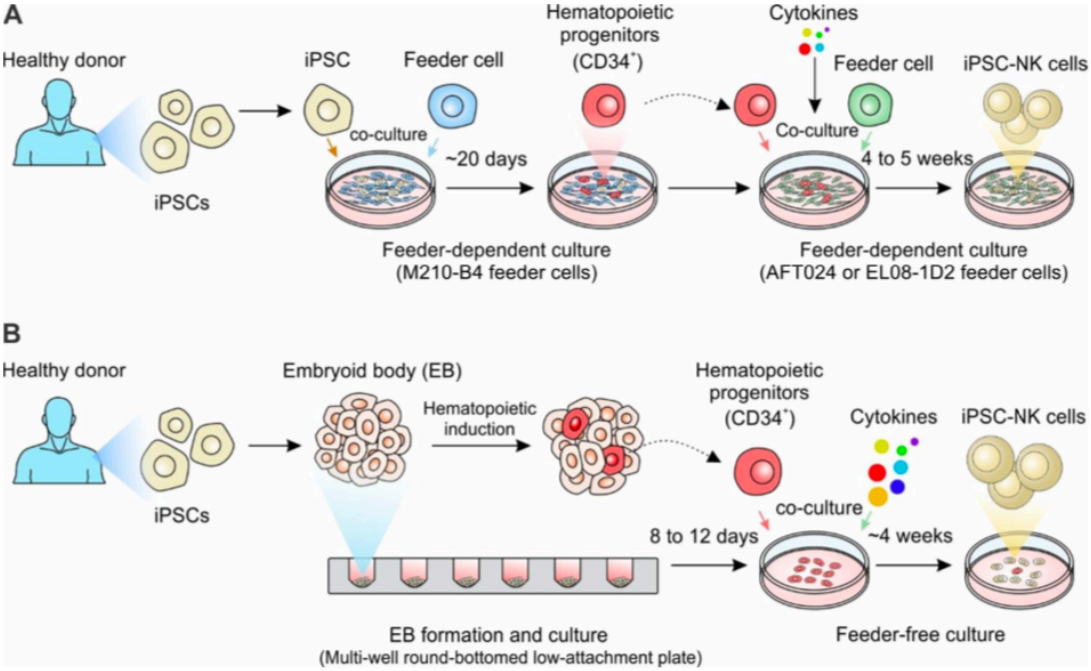

Figure 3. Generation of iPSC-derived NK cell-based cell therapy. (**A**) The iPSCs derived from healthy donors are co-cultured with the murine bone marrow stromal cell line M210-B4 for ~20 days to allow for the generation of CD34 + hematopoietic progenitors. CD34 + hematopoietic progenitors are then enriched and co-cultured with a monolayer of murine AFT024 (a fetal liver-derived stromal cell line) or EL08-1D2 stroma cells with defined cytokines for 4 to 5 weeks, eventually generating mature NK cells. (**B**) The iPSC derived from healthy donors are spun to aggregate in a multi-well round-bottomed low-attachment plate, forming the embryoid bodies (EBs) of uniform size in each well. After 8 to12 days of culture, the hematopoietic progenitor cells containing EBs were transferred to feeder-free plates in NK differentiation media containing cytokine combinations for 4 weeks to generate iPSC-derived NK cells. Notably, for the generation of gene-engineered iPSC-NK cells, the healthy donor-derived iPSCs can be replaced with genetically-engineered iPSCs, such as CAR-engineered iPSCs.

Subsequently, the Kaufman group developed an embryoid body (EB)-derived feeder-free 3D culture method (Figure 3B). iPSCs were initially grown under feeder-free conditions for a week, then aggregated into ultra-low attachment 96-well plates to form EBs [91]. Cells within EBs form self-stromal cells to help support the growth of lymphocytes, which eliminates the need for other stromal cell lines. EBs were cultured in the feeder-free media supplemented with SCF, BMP4, VEGF to induce the formation of HSC progenitors. After 8-12 days of culture, the hematopoietic progenitor cells containing EBs were transferred to feeder-free media containing IL-3, IL-7, IL-15, SCF, and Flt3L for 4 weeks to generate

$CD45^+CD56^+$ NK cells [53,92]. The iPSC-derived NK cells can be further expanded using different NK culture methods and share similar growth rate, phenotypes, and activity compared to PB-NK cells and UCB-NK cells [53,71,73,74,89].

4.3. iPSC-NK Cells in Cell Therapy

iPSCs provide an ideal platform for NK-based allogeneic therapy. Once the stable engineered iPSC lines are established, they can be indefinitely expanded and used to produce a standardized population of appropriately engineered iPSC-derived NK cells. Preclinically, many studies are highlighting the efficacy of engineered iPS-NK cells against cancers. In a representative study, iPSCs have been genetically engineered to express 3rd generation CARs, which express a single-chain antibody fragment recognizing either CD19 or mesothelin, a CD8α hinge region, the transmembrane protein CD28, a co-stimulatory protein 4-1BB, and the activating domain CD3ζ. NK cells derived from this dual CAR-engineered iPSC exhibited higher killing abilities towards $CD19^+$ or $mesothelin^+$ tumor cells [93]. This can further be improved by the knockout of the IL-15 signaling regulatory protein CISH, creating iPS-NK cells with improved metabolic profile, increased expansion and persistence, and enhanced cytotoxicity in human AML xenograft tumor models. Additionally, the deletion of CISH does not affect the pluripotency or stability of iPSCs. A separate study from the Kaufman group showed that CARs generated against the NK-activating domain NKG2D greatly improves the anti-tumor activity in iPS-NKs by activating PLC-gamma, the Syk-vav1-Erk pathway, and the NK-κB pathway. As a result, these iPS-NKG2D-CAR-NK cells show improved granulation, cytokine production, and cytotoxicity towards antigen-expressing tumor cells [94].

Clinically, there are several universal off-the-shelf iPSC-derived NK cell products currently undergoing Phase I trials: FT500, FT516, FT576, and FT596, all of which are products of Fate Therapeutics (Clinicaltrials.gov Identifier NCT03841110, NCT04023071, NCT05182073, NCT04245722). To date, these are the only iPSC-derived NK therapy products cleared for use in clinical investigations within the United States. The most modified of these four trial therapies is FT576, which is an iPS-NK therapy engineered with a B cell maturation antigen (BCMA) CAR for use in patients with multiple myeloma (MM; Clinicatrials.gov Identifier NCT05182073). BCMA-CAR recognizes BCMA, an antigen highly expressed on malignant plasma cells, which allows for tumor recognition. This antigen-directed killing is further improved by the addition of hnCD16 Fc receptors, which help augment the effect of ADCC, and an IL-15 fusion receptor (IL-15RF), which enhances NK activity, as well as supplementation with daratumumab, which is an anti-CD38 monoclonal antibody that prevents the possibility of NK cell fratricide [95]. In their preclinical studies, FT576 NK cells outperformed peripheral blood NK (PB NK) cells in vitro during fratricide and cytotoxicity assays and were found to have greater persistence than PB NK cells. When using FT576 alongside daratumumab in MM mice models, FT576 was able to achieve complete clearance [96]. FT576 is a promising cell therapy candidate with the possibility to become the first curative MM therapeutic, but clinical results have yet to be seen.

Overall, iPSC-NK cells have shown to be a promising alternative to T cells for cell immunotherapy due to their ability to be genetically engineered, cultured at a large scale, and their adaptation to treating various cancers. However, the in vivo persistence and the durability of iPSC-NK cells, as well as their efficacy in combination with other immune checkpoint inhibitors are still unclear and remain to be clarified in order to move the iPSC-derived NK cells to clinical applications for the treatment of hematologic and solid tumors.

5. Engineering iPSCs for Other Immune Cell-Based Therapy

5.1. iPSC-Engineered Macrophage Cell Therapy

Macrophages (Mφs) constitute heterogeneous populations of immune cells that play plastic and vital roles in embryonic development, tissue homeostasis and innate immunity [97]. In the context of host immune response, 'classically activated' M1 Mφs, typically induced by lipopolysaccharide (LPS), interferon (IFN)-γ, or tumor necrosis factor (TNF),

and serve as professional APCs [144], which may in turn recruit and regulate activation of tumor-specific αβ T cells, acting synergistically towards effective anti-tumor immunity. Moreover, unlike αβ T cells, γδ T cells are less frequently found in secondary lymphoid organs and preferentially migrate to peripheral tissues (most commonly barrier surfaces like the skin, intestine, lung, etc.) [145]. This potentially renders γδ T cells a crucial role in tumor immunosurveillance and may be the basis for their capacity to infiltrate solid tumors. Due to their potent anti-tumor cytotoxicity, immune-regulatory functions, homing and infiltration capacity towards peripheral tissues, as well as safe immunogenicity profiles, γδ T cells have attracted increasing interest in the development of allogeneic cell-based cancer immunotherapy [134,136,138]. In September 2021, GammaDelta Therapeutics announced the initiation of a first-in-human phase 1 trial (GDX012) of allogeneic, non-engineered γδ T cells for treating acute myeloid leukemia (Clinicatrials.gov Identifier NCT05001451). As the current clinical trials start to unveil the anti-tumor potential of "off-the-shelf" allogeneic γδ T cell therapy in clinical patients, further genetic modifications with tumor-targeting CARs or administration in combination with immune checkpoint blockades may further benefit the therapeutic outcomes of γδ T cells in the context of human cancer.

During the past decade, established evidence has shown that a majority of γδ T cells in the peripheral blood express Vγ9Vδ2 TCRs [146], and functional studies suggest Vγ9Vδ2 T cells are the most potent effector γδ T populations [136]. Vγ9Vδ2 T cells target and kill a variety of solid tumors and lymphoma/leukemia cells in vitro and in vivo [136,138,146], and thus, further discussion will mainly focus on Vγ9Vδ2 T cells, unless otherwise noted. Building upon that, several groups have reported successful generation and evaluation of CAR-engineered γδ T cells in suppressing tumor growth both in vitro and in vivo [147–149]. Deniger et al. were among the first to generate engineered γδ T cells with bispecific tumor targeting, namely through Vγ9Vδ2 TCR and anti-CD19 CAR [147]. Anti-CD19-CAR-γδ T cells were ex vivo expanded with CD19-expressing artificial APC and showed enhanced killing against CD19-positive tumor cells lines both in vitro and in vivo, in comparison to γδ T cells without CAR engineering [147,150]. More recently, a group led by Herrman M. from Adicet Therapeutics developed anti-Glypican-3 (GPC-3) CAR-γδ T cells, equipped with constitutively secreted IL-15. In vitro and in vivo killing assays demonstrated that these cell products effectively target and kill hepatocellular carcinoma (HCC) cell lines with prolonged persistence [148] (note, Adicet Therapeutics uses δ1T cells). Furthermore, Nishimoto et al. from Adicet Therapeutics isolated, expanded, and engineered PBMC-derived γδ T cells with anti-CD20 CAR [149]. These CD20-CAR-γδ T cells exhibited both innate (rapid secretion of pro-inflammatory cytokines) and adaptive (TCR-dependent tumor cell killing) anti-tumor response against B cell lymphoma both in vitro and in xenograft immunodeficient mice [149]. These remarkable advances in proof-of-concept investigation have led to the clinical trial of ADI-001 from Adicet Therapeutics in treating B cell non-Hodgkin's lymphoma with anti-CD20-CAR-γδ T cells, which is currently recruiting patients (Clinicatrials.gov Identifier NCT04735471).

Although there has been a great number of encouraging results in recent years, there are some drawbacks to utilizing γδ T cells as CAR-T therapy carriers. Due to the fact that γδ T cells only constitute a small proportion (1–5%) of PB T lymphocytes, current protocols actively used to generate autologous and/or allogeneic γδ T cell therapy rely heavily on ex vivo expansion with ZOL and pro-inflammatory cytokines such as IL-2 and IL-15 [137,148,149]. However, ex vivo expanded T cells gradually lose their anti-tumor potential due to T-cell exhaustion brought on by long-term stimulation, which is also known as T cell exhaustion [151]. Thus, there is an unmet need to manufacture homogeneous and functional CAR-engineered γδ T cells with standardized quality controls on a large scale. To circumvent this roadblock, several groups have investigated whether iPSCs can serve as an unlimited source of γδ T cells. Watanabe et al. reported the generation of γδ T cells from human γδ T cell-derived iPSCs [152]. The researchers first activated PBMC-derived γδ T cells with ZOL and IL-2, and subsequently transduced them with Sendai viral vector to re-program γδ T cell-derived iPSC clones [152]. Around 70% of the resultant iPSC clones expressed TCRs rearranged from TCRG and TCRD gene locus [152], indicating

retention of the original TCR genes. Next, γδ T cell-derived iPSCs were cultured in Stem Fit medium on laminin-511 E8 fragments, as previously described [153], and two iPSC cell lines were able to differentiate. Whether they were able to generate promising results, such as hematovascular precursor markers and $CD34^+CD43^+$ expression in the majority of cells, however, the group did not investigate whether it is feasible to generate functional and phenotypically defined γδ T-like cells from these HSPC populations. Functional studies are required to further evaluate the anti-tumor capacity of γδ T cells generated from these iPSC clones. More recently, Zeng et al. showed that mimetic γδ T cells can be generated from γδ T cell-derived iPSCs and skewed towards more NK-like effector cells (designated as γδ natural killer T cells, γδ NKT cells) [154]. These γδ NKT cells express an array of NK-activating receptors such as NKG2D, NKp30, NKp44, NKp46 and DNAM-1, with low to no expression of inhibitory killer immunoglobulin-like receptors (KIRs) [154]. Similar to previous reports, the group isolated Vγ9Vδ2 T cells from PBMC and transduced them with Sendai viruses carrying the Yamanaka reprogramming factors. However, this did not result in viable iPSC clones that can be seeded onto feeder fibroblasts [154]. As alternatives, they tried using episomal vectors derived through nucleofection, which resulted in iPSC cell lines derived from γδ T cells [154]. Interestingly, to obtain iPSC-derived γδ T-like cells with increased NK functions, the group co-cultured the γδ T-iPSC clones with OP9-DLL1 feeder cells under NK cell "promoting" differentiation conditions previously developed in their lab [154]. Through in vitro tumor-killing assays with antibody blockage of different surface receptors, γδ NKT cells were shown to exhibit effective tumor cell cytotoxicity via NK activating receptors as well as CD16-dependent ADCC [154].

5.4. iPSC-Engineered iNKT Cell Therapy

Invariant natural killer T (iNKT) cells, also known as type I or classical NKT cells, are a subpopulation of unconventional T cells. They express an invariant TCR chain V14-J18 that is paired with V8/7/2 in mice or V24-J18 with V11 in humans [155,156]. Unlike conventional T cells that recognize peptides presented by MHC molecules, iNKT cells recognize glycolipids such as alpha-galactosylceramide (α-GalCer) presented by the MHC-I-like molecule CD1d [157]. iNKT cells are at the forefront of a variety of immunological responses by secreting a wide range of cytokines in response to lipid antigen stimulation and serving as a bridge between innate and adaptive immune systems [158]. More importantly, iNKT cells do not recognize mismatched MHC molecules, freeing them from causing GvHD. Multiple clinical trials have reported that the adoptive transfer of iNKT cells was associated with reduced GvHD [159]. However, the extremely low number of iNKT cells in peripheral blood (0.01–1% of PBMCs) restricts iNKT cell-based immunotherapy. We have recently developed different approaches to generate iNKT cells from engineered hematopoietic stem cells (HSCs) using either the bone marrow-liver-thymus (BLT) mouse model or artificial thymic organoid (ATO) culture system [160–163]. The HSC-derived iNKT cells represented similar characteristics compared to PBMC-derived iNKT cells with enhanced NK functions against cancers [160,161]. The unique innate feature of iNKT cells and their capability to bridge innate and adaptive immunity have cultivated an increasing interest in generating iNKT-based cell therapy. Using a combination of iPSC technology, iNKT cells may play a significant role as an ideal allogeneic cell carrier for next-generation medicine.

The first step in the generation of effective iNKT-based cell therapy was the in vitro differentiation of fibroblasts into iNKT cells by Watarai et al. [164]. The differentiation was achieved using the OP9/DLL1 culture system with the addition of cytokine combinations such as IL-15 and IL-7. The generated iPSC-iNKT cells expanded in response to α-GalCer stimulation and produced abundant Th1 cytokine INF-γ, induced dendritic cell maturation, and activated both CTL and NK cells [164]. Using the same culture system, Kitayama et. al. reported that human iNKT cell-derived iPSCs can re-differentiate into functional iNKT in vitro [56]. The generated human iPSC-iNKT cells not only recapitulated the adjuvant effect of natural iNKT cells, but also exhibited NK cell-like cytotoxicity against cancer cell

lines [56]. These preclinical studies provide foundations for studying human iNKT cell biology and the clinical translation of allogeneic iPSC-iNKT cell therapy.

In October 2020, Professor Motohashi at Chiba University Hospital led the World's first clinical trial of iPSC-derived NKT cells for head and neck cancer [165]. This study was done in an allogeneic situation, where NKT cells, isolated from a healthy donor, were reprogrammed to iPSCs and further differentiated into iPS-NKT cells in vitro. The expanded NKTs are administered 3 times every 2 weeks to the blood vessels of cancer patients and are intended to activate the patient's immunity in an antigen-agnostic manner, similar to how an adjuvant works. This study may provide supporting information to translate allogeneic iPSC-iNKT cell immunotherapy to clinical applications.

6. Outlook

While autologous CAR-T cells have shown promising therapeutic results in patients with relapsed or refractory B-cell malignancies and multiple myeloma, the current technology has several safety and logistical flaws, emphasizing the need to explore alternative populations for cellular treatment, particularly allogeneic cell therapy (Figure 1A,B). iPSCs are promising cell sources for generating off-the-shelf therapy (Figure 1C). However, despite the breakthrough in differentiating iPSCs into T, NK or other immune cells, there are still challenges to be overcome and necessary concerns to address.

Cell therapy, especially off-the-shelf therapy, requires high yield of final products for transplantation. Current iPSC differentiation culture approach can already generate approximately 600 $\times$ 10^6 of iPSC-T cells and 10^5-fold of iPS-NK cells from 1 $\times$ 10^6 of iPSCs for example, which are applicable for iPSC-based cell therapy [67–69]. The current classic culture approaches to iPSCs re-differentiation are largely dependent on murine-derived feeder cells, which can increase the risk of cross-species contamination. The utilization of serum for maintaining feeder cells may also increase the variation of final cell products, presenting major issues for large-scale industrial standardization and real-patient applications and clinical trials. A few studies have started to develop xeno-free and feeder-free culture systems that are more suitable for industrialized applications [67,68]. However, before these can be brought to large-scale production it must be determined: (1) How these approaches can be applied to a wide array of products? (2) Whether they hold up under the scrutiny of quality control standards at a large scale? (3) Whether the yield large enough for multiple patients?

In addition to the evaluation of these xeon-free culture techniques, the extent to which the T, NK, macrophages, and other cells derived from iPSCs truly resemble the original immune cells must be determined before they can safely be introduced into patients at a large scale. Papers like that of Kawamoto et al. found that a small portion of T cells aberrantly expressing TCRαβ was found during the DP stage [44–46]. It was explained that during the TCRA-encoded a chain assembly stage, the negative-feedback regulation for a could be loosely compared to that for b chain, resulting in a small portion of T cells expressing rearranged TCRα. Although the number was low, such rearranged TCRα was exceedingly undesirable that could potentially convert the tropism of TCR, making re-differentiated T cells incapable of attacking targeted antigens, and, more importantly, might cause GvHD in patients. By mimicking TCR signaling using anti-CD3 antibodies during the DN-to-DP transition stage or alternatively, CRISPR knockout of a recombinase gene in the T-iPSCs, could end the expression of RAG genes or prevent undesired additional TCR assembly [65,66]. The aberrantly early expression of TCRαβ from pre-assembled TCRα and TCRβ in murine thymocytes could lead to subsequent lymphomagenesis, which raises concerns about the safety of T-iPSCs [166]. As a result, the redifferentiation approach needs to be further refined and clinically validated before being used in real-world treatments, and the employment of an inducible suicide-gene system to eliminate undesired malignancies might be necessary.

The heterogenicity of final products may be important for the therapeutic outcome. One of the benefits of using iPSCs is the flexibility to select a specific phenotype of immune

cells before reprograming them into a stable iPSC line. The progeny cells, for example, the T-iPSC derived T cells, can inherit certain epigenetic modifications from their original immune cells and recapitulate the heterogeneity in the final product. However, the iPSC-derived CAR T cells were found to be predominantly CD8-expressing with low levels of MHC [69]. While low MHC expression is desirable to improve iPSC-T persistency by reducing host versus graft (HvG) response, the imbalance between $CD4^+$ and $CD8^+$ populations may be a bottleneck for the application [69]. It is still challenging to generated $CD4^+$ T cells with current in vitro culture methods, which could potentially be resolved by manipulating the culture conditions or additional gene editing.

Moreover, iPSCs represent the "primed" state, and are heterogeneous in both cell population and differentiation potential. iPSC clones show large variations in differentiation efficiency. The tumorigenicity and toxicity of iPSCs pose a significant safety risk of iPSC-derived immune cell therapy [167]. Instead of using reto/lenti-virus to reprogram iPSCs, using episomal vectors, Sendai virus vectors or modified RNAs that do not result in chromosomal integration provides a safer way to mitigate the tumorigenicity and toxicity [167]. Removing undifferentiated cells or optimizing culture methods to generate pure final cell product is also necessary. Regardless, the redifferentiation approach needs to be further refined and clinically validated before being used in real-world treatments, and the employment of an inducible suicide-gene system to eliminate undesired malignancies might be necessary. However, what type of cells should be considered as good starting materials for iPSC-based therapy? How robust are the current differentiation approaches for generating clinically scalable numbers of cell products? CRISPR/CAS9-based genome-wide genetic modification and CAR-engineering could open a new avenue for utilizing human iPSCs, but will these modifications impact the quality or quantity of final products? What is the most efficient way to better manage the off-target risk of gene modifications? All these questions remain to be better clarified. It is important that final products be carefully selected and thoroughly characterized prior to clinical application in order to protect the safety of patients and maximize the efficacy of the medicines being developed.

Besides, the iPSC-generated cell therapeutics may still encounter obstacles in treating solid tumors, which is mainly due to the intrinsic barriers imposed by the hostile immunosuppressive tumor microenvironment (TME), including the formation of extracellular matrix (ECM) derived from cancer-associated fibroblasts (CAFs), anti-inflammatory cytokines secreted by suppressive immune cells (Tregs, tumor-associated macrophages, as well as myeloid-derived suppressive cells), and competition for metabolic fuels which limits long-term immune cell persistence [168–170]. The TME impedes therapeutical cells trafficking, infiltration, persistence, or function in the immunosuppressive milieu by producing suppressive soluble factors and by overexpressing negative immune checkpoints [171]. To overcome these hurdles, a series of genetical engineering approaches have been used to manipulate the chemotaxis and tissue homing of therapeutical cells for improving trafficking and infiltration, or to design new CARs such as tumor stroma targeting for depletion of immunosuppressive cells or depletion of stromal cells at TME. To counteract immune cell dysfunction in solid tumors, checkpoint (CTLA-4, PD-1 and TIM-3) blockades have also been tested in combination of cell therapies [172]. Alternatively, pro-inflammatory cytokine-armored immune cells, such as IL-12-, IL-18- or IL-23-armored T cells were tested to re-shape TME to favor T cell anti-tumor immunity [168,173,174]. Likewise, similar gene-engineering strategies can be applied to modify the iPSCs before differentiating into final products, which could pave the way towards the generation of "off-the-shelf" iPSC-derived cells for an adoptive cell therapy (ACT) with a broader therapeutical spectrum.

The advent and adoption of iPSC technology represent a paradigm shift in CAR-based call therapy, revolutionizing the potential for universal 'off-the-shelf' therapy from unlimited cell supplies. While there is a significant amount of research that must be done to address the questions and concerns regarding the safety and efficacy of iPSC-generated cell therapies, we already foresee its irreplaceable role in developing next-generation medicines. We look forward to more studies and clinical trial results coming out in the next

few decades that will push the field forward and improve the life-saving capabilities of cell-based immunotherapy.

Author Contributions: Conceptualization, Y.Z.; writing—original draft preparation, Y.Z., M.L., K.Z., T.T. and X.C.; writing—review and editing, J.B., Z.S.D., T.H. and A.B.; visualization, M.L. and Y.Z.; validation, Y.Z. and L.Y. supervision, L.Y. All authors have read and agreed to the published version of the manuscript.

Funding: Ablon Scholars Award (to L.Y.). UCLA BSCRC Innovation Award (to L.Y.). A Partnering Opportunity for Translational Research Projects Award from the California Institute for Regenerative Medicine (CIRM TRAN1-12250, to L.Y.).

Acknowledgments: We thank the University of California, Los Angeles (UCLA) for providing supports. We thank all members in Lili Yang's lab for insightful discussion. We thank Xiang Gao for proofreading.

Conflicts of Interest: Y.Z. and L.Y. are listed on the IP-related documents filed by UCLA.

References

1. Ji, H.H.; Tang, X.W.; Dong, Z.; Song, L.; Jia, Y.T. Adverse Event Profiles of Anti-CTLA-4 and Anti-PD-1 Monoclonal Antibodies Alone or in Combination: Analysis of Spontaneous Reports Submitted to FAERS. *Clin. Drug Investig.* **2019**, *39*, 319–330. [CrossRef] [PubMed]
2. Lisi, L.; Lacal, P.M.; Martire, M.; Navarra, P.; Graziani, G. Clinical experience with CTLA-4 blockade for cancer immunotherapy: From the monospecific monoclonal antibody ipilimumab to probodies and bispecific molecules targeting the tumor microenvironment. *Pharmacol. Res.* **2022**, *175*, 105997. [CrossRef] [PubMed]
3. Liu, Y.; Zheng, P. How Does an Anti-CTLA-4 Antibody Promote Cancer Immunity? *Trends Immunol.* **2018**, *39*, 953–956. [CrossRef] [PubMed]
4. Lei, Q.; Wang, D.; Sun, K.; Wang, L.; Zhang, Y. Resistance Mechanisms of Anti-PD1/PDL1 Therapy in Solid Tumors. *Front. Cell Dev. Biol.* **2020**, *8*, 672. [CrossRef] [PubMed]
5. Sun, L.; Zhang, L.; Yu, J.; Zhang, Y.; Pang, X.; Ma, C.; Shen, M.; Ruan, S.; Wasan, H.S.; Qiu, S. Clinical efficacy and safety of anti-PD-1/PD-L1 inhibitors for the treatment of advanced or metastatic cancer: A systematic review and meta-analysis. *Sci. Rep.* **2020**, *10*, 2083. [CrossRef]
6. Botticelli, A.; Cirillo, A.; Strigari, L.; Valentini, F.; Cerbelli, B.; Scagnoli, S.; Cerbelli, E.; Zizzari, I.G.; Rocca, C.D.; D'Amati, G.; et al. Anti-PD-1 and Anti-PD-L1 in Head and Neck Cancer: A Network Meta-Analysis. *Front. Immunol.* **2021**, *12*, 705096. [CrossRef]
7. Ottaviano, G.; Chiesa, R.; Feuchtinger, T.; Vickers, M.A.; Dickinson, A.; Gennery, A.R.; Veys, P.; Todryk, S. Adoptive T Cell Therapy Strategies for Viral Infections in Patients Receiving Haematopoietic Stem Cell Transplantation. *Cells* **2019**, *8*, 47. [CrossRef]
8. Kaeuferle, T.; Krauss, R.; Blaeschke, F.; Willier, S.; Feuchtinger, T. Strategies of adoptive T -cell transfer to treat refractory viral infections post allogeneic stem cell transplantation. *J. Hematol. Oncol.* **2019**, *12*, 13. [CrossRef]
9. Parajuli, S.; Jorgenson, M.; Meyers, R.O.; Djamali, A.; Galipeau, J. Role of Virus-Specific T Cell Therapy for Cytomegalovirus and BK Infections in Kidney Transplant Recipients. *Kidney360* **2021**, *2*, 905–915. [CrossRef]
10. O'Reilly, R.J.; Prockop, S.; Hasan, A.N.; Koehne, G.; Doubrovina, E. Virus-specific T-cell banks for 'off the shelf' adoptive therapy of refractory infections. *Bone Marrow Transplant.* **2016**, *51*, 1163–1172. [CrossRef]
11. Morotti, M.; Albukhari, A.; Alsaadi, A.; Artibani, M.; Brenton, J.D.; Curbishley, S.M.; Dong, T.; Dustin, M.L.; Hu, Z.; McGranahan, N.; et al. Promises and challenges of adoptive T-cell therapies for solid tumours. *Br. J. Cancer* **2021**, *124*, 1759–1776. [CrossRef] [PubMed]
12. Rohaan, M.W.; Wilgenhof, S.; Haanen, J. Adoptive cellular therapies: The current landscape. *Virchows Arch.* **2019**, *474*, 449–461. [CrossRef] [PubMed]
13. Mehta, R.S.; Rezvani, K. Chimeric Antigen Receptor Expressing Natural Killer Cells for the Immunotherapy of Cancer. *Front. Immunol.* **2018**, *9*, 283. [CrossRef] [PubMed]
14. Lee, S.; Margolin, K. Tumor-infiltrating lymphocytes in melanoma. *Curr. Oncol. Rep.* **2012**, *14*, 468–474. [CrossRef] [PubMed]
15. van den Berg, J.H.; Heemskerk, B.; van Rooij, N.; Gomez-Eerland, R.; Michels, S.; van Zon, M.; de Boer, R.; Bakker, N.A.M.; Jorritsma-Smit, A.; van Buuren, M.M.; et al. Tumor infiltrating lymphocytes (TIL) therapy in metastatic melanoma: Boosting of neoantigen-specific T cell reactivity and long-term follow-up. *J. Immunother. Cancer* **2020**, *8*, e000848. [CrossRef] [PubMed]
16. Wang, S.; Sun, J.; Chen, K.; Ma, P.; Lei, Q.; Xing, S.; Cao, Z.; Sun, S.; Yu, Z.; Liu, Y.; et al. Perspectives of tumor-infiltrating lymphocyte treatment in solid tumors. *BMC Med.* **2021**, *19*, 140. [CrossRef] [PubMed]
17. Kumar, A.; Watkins, R.; Vilgelm, A.E. Cell Therapy With TILs: Training and Taming T Cells to Fight Cancer. *Front. Immunol.* **2021**, *12*, 690499. [CrossRef]
18. Tsimberidou, A.M.; Van Morris, K.; Vo, H.H.; Eck, S.; Lin, Y.F.; Rivas, J.M.; Andersson, B.S. T-cell receptor-based therapy: An innovative therapeutic approach for solid tumors. *J. Hematol. Oncol.* **2021**, *14*, 102. [CrossRef]

19. Manfredi, F.; Cianciotti, B.C.; Potenza, A.; Tassi, E.; Noviello, M.; Biondi, A.; Ciceri, F.; Bonini, C.; Ruggiero, E. TCR Redirected T Cells for Cancer Treatment: Achievements, Hurdles, and Goals. *Front. Immunol.* **2020**, *11*, 1689. [CrossRef]
20. Zhao, Q.; Jiang, Y.; Xiang, S.; Kaboli, P.J.; Shen, J.; Zhao, Y.; Wu, X.; Du, F.; Li, M.; Cho, C.H.; et al. Engineered TCR-T Cell Immunotherapy in Anticancer Precision Medicine: Pros and Cons. *Front. Immunol.* **2021**, *12*, 658753. [CrossRef]
21. Poncette, L.; Chen, X.; Lorenz, F.K.; Blankenstein, T. Effective NY-ESO-1-specific MHC II-restricted T cell receptors from antigen-negative hosts enhance tumor regression. *J. Clin. Investig.* **2019**, *129*, 324–335. [CrossRef] [PubMed]
22. Bethune, M.T.; Li, X.H.; Yu, J.; McLaughlin, J.; Cheng, D.; Mathis, C.; Moreno, B.H.; Woods, K.; Knights, A.J.; Garcia-Diaz, A.; et al. Isolation and characterization of NY-ESO-1-specific T cell receptors restricted on various MHC molecules. *Proc. Natl. Acad. Sci. USA* **2018**, *115*, E10702–E10711. [CrossRef] [PubMed]
23. Leahy, A.B.; Newman, H.; Li, Y.; Liu, H.; Myers, R.; DiNofia, A.; Dolan, J.G.; Callahan, C.; Baniewicz, D.; Devine, K.; et al. CD19-targeted chimeric antigen receptor T-cell therapy for CNS relapsed or refractory acute lymphocytic leukaemia: A post-hoc analysis of pooled data from five clinical trials. *Lancet Haematol.* **2021**, *8*, e711–e722. [CrossRef]
24. Spiegel, J.Y.; Patel, S.; Muffly, L.; Hossain, N.M.; Oak, J.; Baird, J.H.; Frank, M.J.; Shiraz, P.; Sahaf, B.; Craig, J.; et al. CAR T cells with dual targeting of CD19 and CD22 in adult patients with recurrent or refractory B cell malignancies: A phase 1 trial. *Nat. Med.* **2021**, *27*, 1419–1431. [CrossRef] [PubMed]
25. Halim, L.; Maher, J. CAR T-cell immunotherapy of B-cell malignancy: The story so far. *Ther. Adv. Vaccines Immunother.* **2020**, *8*, 2515135520927164. [CrossRef]
26. Guedan, S.; Calderon, H.; Posey, A.D., Jr.; Maus, M.V. Engineering and Design of Chimeric Antigen Receptors. *Mol. Ther. Methods Clin. Dev.* **2019**, *12*, 145–156. [CrossRef] [PubMed]
27. Lindner, S.E.; Johnson, S.M.; Brown, C.E.; Wang, L.D. Chimeric antigen receptor signaling: Functional consequences and design implications. *Sci. Adv.* **2020**, *6*, eaaz3223. [CrossRef]
28. Jayaraman, J.; Mellody, M.P.; Hou, A.J.; Desai, R.P.; Fung, A.W.; Pham, A.H.T.; Chen, Y.Y.; Zhao, W. CAR-T design: Elements and their synergistic function. *EBioMedicine* **2020**, *58*, 102931. [CrossRef]
29. Ponterio, E.; De Maria, R.; Haas, T.L. Identification of Targets to Redirect CAR T Cells in Glioblastoma and Colorectal Cancer: An Arduous Venture. *Front. Immunol.* **2020**, *11*, 565631. [CrossRef]
30. Sanber, K.; Savani, B.; Jain, T. Graft-versus-host disease risk after chimeric antigen receptor T-cell therapy: The diametric opposition of T cells. *Br. J. Haematol.* **2021**, *195*, 660–668. [CrossRef]
31. Liu, P.; Liu, M.; Lyu, C.; Lu, W.; Cui, R.; Wang, J.; Li, Q.; Mou, N.; Deng, Q.; Yang, D. Acute Graft-Versus-Host Disease After Humanized Anti-CD19-CAR T Therapy in Relapsed B-ALL Patients After Allogeneic Hematopoietic Stem Cell Transplant. *Front. Oncol.* **2020**, *10*, 573822. [CrossRef] [PubMed]
32. Eyquem, J.; Mansilla-Soto, J.; Giavridis, T.; van der Stegen, S.J.; Hamieh, M.; Cunanan, K.M.; Odak, A.; Gonen, M.; Sadelain, M. Targeting a CAR to the TRAC locus with CRISPR/Cas9 enhances tumour rejection. *Nature* **2017**, *543*, 113–117. [CrossRef] [PubMed]
33. Liu, X.; Zhang, Y.; Cheng, C.; Cheng, A.W.; Zhang, X.; Li, N.; Xia, C.; Wei, X.; Liu, X.; Wang, H. CRISPR-Cas9-mediated multiplex gene editing in CAR-T cells. *Cell Res.* **2017**, *27*, 154–157. [CrossRef] [PubMed]
34. Albinger, N.; Hartmann, J.; Ullrich, E. Current status and perspective of CAR-T and CAR-NK cell therapy trials in Germany. *Gene Ther.* **2021**, *28*, 513–527. [CrossRef] [PubMed]
35. Myers, J.A.; Miller, J.S. Exploring the NK cell platform for cancer immunotherapy. *Nat. Rev. Clin. Oncol.* **2021**, *18*, 85–100. [CrossRef]
36. Liu, S.; Galat, V.; Galat, Y.; Lee, Y.K.A.; Wainwright, D.; Wu, J. NK cell-based cancer immunotherapy: From basic biology to clinical development. *J. Hematol. Oncol.* **2021**, *14*, 7. [CrossRef]
37. Minetto, P.; Guolo, F.; Pesce, S.; Greppi, M.; Obino, V.; Ferretti, E.; Sivori, S.; Genova, C.; Lemoli, R.M.; Marcenaro, E. Harnessing NK Cells for Cancer Treatment. *Front. Immunol.* **2019**, *10*, 2836. [CrossRef]
38. Islam, R.; Pupovac, A.; Evtimov, V.; Boyd, N.; Shu, R.; Boyd, R.; Trounson, A. Enhancing a Natural Killer: Modification of NK Cells for Cancer Immunotherapy. *Cells* **2021**, *10*, 1058. [CrossRef]
39. Kim, H.S.; Kim, J.Y.; Seol, B.; Song, C.L.; Jeong, J.E.; Cho, Y.S. Directly reprogrammed natural killer cells for cancer immunotherapy. *Nat. Biomed. Eng.* **2021**, *5*, 1360–1376. [CrossRef]
40. Caldwell, K.J.; Gottschalk, S.; Talleur, A.C. Allogeneic CAR Cell Therapy-More Than a Pipe Dream. *Front. Immunol.* **2020**, *11*, 618427. [CrossRef]
41. Depil, S.; Duchateau, P.; Grupp, S.A.; Mufti, G.; Poirot, L. 'Off-the-shelf' allogeneic CAR T cells: Development and challenges. *Nat. Rev. Drug Discov.* **2020**, *19*, 185–199. [CrossRef] [PubMed]
42. Godfrey, D.I.; Le Nours, J.; Andrews, D.M.; Uldrich, A.P.; Rossjohn, J. Unconventional T Cell Targets for Cancer Immunotherapy. *Immunity* **2018**, *48*, 453–473. [CrossRef] [PubMed]
43. Zhu, H.; Lai, Y.S.; Li, Y.; Blum, R.H.; Kaufman, D.S. Concise Review: Human Pluripotent Stem Cells to Produce Cell-Based Cancer Immunotherapy. *Stem Cells* **2018**, *36*, 134–145. [CrossRef]
44. Yamanaka, S. Pluripotent Stem Cell-Based Cell Therapy-Promise and Challenges. *Cell Stem Cell* **2020**, *27*, 523–531. [CrossRef] [PubMed]
45. Shi, Y.; Inoue, H.; Wu, J.C.; Yamanaka, S. Induced pluripotent stem cell technology: A decade of progress. *Nat. Rev. Drug Discov.* **2017**, *16*, 115–130. [CrossRef]

46. Huang, C.Y.; Liu, C.L.; Ting, C.Y.; Chiu, Y.T.; Cheng, Y.C.; Nicholson, M.W.; Hsieh, P.C.H. Human iPSC banking: Barriers and opportunities. *J. Biomed. Sci.* **2019**, *26*, 87. [CrossRef] [PubMed]
47. Liang, G.; Zhang, Y. Embryonic stem cell and induced pluripotent stem cell: An epigenetic perspective. *Cell Res.* **2013**, *23*, 49–69. [CrossRef]
48. Vizcardo, R.; Masuda, K.; Yamada, D.; Ikawa, T.; Shimizu, K.; Fujii, S.; Koseki, H.; Kawamoto, H. Regeneration of human tumor antigen-specific T cells from iPSCs derived from mature CD8(+) T cells. *Cell Stem Cell* **2013**, *12*, 31–36. [CrossRef] [PubMed]
49. Nishimura, T.; Kaneko, S.; Kawana-Tachikawa, A.; Tajima, Y.; Goto, H.; Zhu, D.; Nakayama-Hosoya, K.; Iriguchi, S.; Uemura, Y.; Shimizu, T.; et al. Generation of rejuvenated antigen-specific T cells by reprogramming to pluripotency and redifferentiation. *Cell Stem Cell* **2013**, *12*, 114–126. [CrossRef]
50. Themeli, M.; Kloss, C.C.; Ciriello, G.; Fedorov, V.D.; Perna, F.; Gonen, M.; Sadelain, M. Generation of tumor-targeted human T lymphocytes from induced pluripotent stem cells for cancer therapy. *Nat. Biotechnol.* **2013**, *31*, 928–933. [CrossRef]
51. Wang, B.; Iriguchi, S.; Waseda, M.; Ueda, N.; Ueda, T.; Xu, H.; Minagawa, A.; Ishikawa, A.; Yano, H.; Ishi, T.; et al. Generation of hypoimmunogenic T cells from genetically engineered allogeneic human induced pluripotent stem cells. *Nat. Biomed. Eng.* **2021**, *5*, 429–440. [CrossRef] [PubMed]
52. Zhu, H.; Blum, R.H.; Bjordahl, R.; Gaidarova, S.; Rogers, P.; Lee, T.T.; Abujarour, R.; Bonello, G.B.; Wu, J.; Tsai, P.F.; et al. Pluripotent stem cell-derived NK cells with high-affinity noncleavable CD16a mediate improved antitumor activity. *Blood* **2020**, *135*, 399–410. [CrossRef] [PubMed]
53. Zhu, H.; Kaufman, D.S. An Improved Method to Produce Clinical-Scale Natural Killer Cells from Human Pluripotent Stem Cells. *Methods Mol. Biol.* **2019**, *2048*, 107–119. [CrossRef] [PubMed]
54. Ni, Z.; Knorr, D.A.; Kaufman, D.S. Hematopoietic and nature killer cell development from human pluripotent stem cells. *Methods Mol. Biol.* **2013**, *1029*, 33–41. [CrossRef]
55. Capsomidis, A.; Benthall, G.; Van Acker, H.H.; Fisher, J.; Kramer, A.M.; Abeln, Z.; Majani, Y.; Gileadi, T.; Wallace, R.; Gustafsson, K.; et al. Chimeric Antigen Receptor-Engineered Human Gamma Delta T Cells: Enhanced Cytotoxicity with Retention of Cross Presentation. *Mol. Ther.* **2018**, *26*, 354–365. [CrossRef]
56. Kitayama, S.; Zhang, R.; Liu, T.Y.; Ueda, N.; Iriguchi, S.; Yasui, Y.; Kawai, Y.; Tatsumi, M.; Hirai, N.; Mizoro, Y.; et al. Cellular Adjuvant Properties, Direct Cytotoxicity of Re-differentiated Valpha24 Invariant NKT-like Cells from Human Induced Pluripotent Stem Cells. *Stem Cell Rep.* **2016**, *6*, 213–227. [CrossRef]
57. Zhang, L.; Tian, L.; Dai, X.; Yu, H.; Wang, J.; Lei, A.; Zhu, M.; Xu, J.; Zhao, W.; Zhu, Y.; et al. Pluripotent stem cell-derived CAR-macrophage cells with antigen-dependent anti-cancer cell functions. *J. Hematol. Oncol.* **2020**, *13*, 153. [CrossRef]
58. Ackermann, M.; Rafiei Hashtchin, A.; Manstein, F.; Carvalho Oliveira, M.; Kempf, H.; Zweigerdt, R.; Lachmann, N. Continuous human iPSC-macrophage mass production by suspension culture in stirred tank bioreactors. *Nat. Protoc.* **2022**, *17*, 513–539. [CrossRef]
59. Takahashi, K.; Yamanaka, S. Induction of pluripotent stem cells from mouse embryonic and adult fibroblast cultures by defined factors. *Cell* **2006**, *126*, 663–676. [CrossRef]
60. Takahashi, K.; Tanabe, K.; Ohnuki, M.; Narita, M.; Ichisaka, T.; Tomoda, K.; Yamanaka, S. Induction of pluripotent stem cells from adult human fibroblasts by defined factors. *Cell* **2007**, *131*, 861–872. [CrossRef]
61. Sterner, R.C.; Sterner, R.M. CAR-T cell therapy: Current limitations and potential strategies. *Blood Cancer J.* **2021**, *11*, 69. [CrossRef] [PubMed]
62. Fischer, J.W.; Bhattarai, N. CAR-T Cell Therapy: Mechanism, Management, and Mitigation of Inflammatory Toxicities. *Front. Immunol.* **2021**, *12*, 693016. [CrossRef] [PubMed]
63. Maeda, T.; Nagano, S.; Kashima, S.; Terada, K.; Agata, Y.; Ichise, H.; Ohtaka, M.; Nakanishi, M.; Fujiki, F.; Sugiyama, H.; et al. Regeneration of Tumor-Antigen-Specific Cytotoxic T Lymphocytes from iPSCs Transduced with Exogenous TCR Genes. *Mol. Ther. Methods Clin. Dev.* **2020**, *19*, 250–260. [CrossRef] [PubMed]
64. Kawamoto, H.; Masuda, K.; Nagano, S. Regeneration of antigen-specific T cells by using induced pluripotent stem cell (iPSC) technology. *Int. Immunol.* **2021**, *33*, 827–833. [CrossRef]
65. Maeda, T.; Nagano, S.; Ichise, H.; Kataoka, K.; Yamada, D.; Ogawa, S.; Koseki, H.; Kitawaki, T.; Kadowaki, N.; Takaori-Kondo, A.; et al. Regeneration of CD8alphabeta T Cells from T-cell-Derived iPSC Imparts Potent Tumor Antigen-Specific Cytotoxicity. *Cancer Res.* **2016**, *76*, 6839–6850. [CrossRef]
66. Minagawa, A.; Yoshikawa, T.; Yasukawa, M.; Hotta, A.; Kunitomo, M.; Iriguchi, S.; Takiguchi, M.; Kassai, Y.; Imai, E.; Yasui, Y.; et al. Enhancing T Cell Receptor Stability in Rejuvenated iPSC-Derived T Cells Improves Their Use in Cancer Immunotherapy. *Cell Stem Cell* **2018**, *23*, 850–858.e4. [CrossRef]
67. Iriguchi, S.; Yasui, Y.; Kawai, Y.; Arima, S.; Kunitomo, M.; Sato, T.; Ueda, T.; Minagawa, A.; Mishima, Y.; Yanagawa, N.; et al. A clinically applicable and scalable method to regenerate T-cells from iPSCs for off-the-shelf T-cell immunotherapy. *Nat. Commun.* **2021**, *12*, 430. [CrossRef]
68. Trotman-Grant, A.C.; Mohtashami, M.; De Sousa Casal, J.; Martinez, E.C.; Lee, D.; Teichman, S.; Brauer, P.M.; Han, J.; Anderson, M.K.; Zuniga-Pflucker, J.C. DL4-mubeads induce T cell lineage differentiation from stem cells in a stromal cell-free system. *Nat. Commun.* **2021**, *12*, 5023. [CrossRef]

69. Wang, Z.; McWilliams-Koeppen, H.P.; Reza, H.; Ostberg, J.R.; Chen, W.; Wang, X.; Huynh, C.; Vyas, V.; Chang, W.C.; Starr, R.; et al. 3D-organoid culture supports differentiation of human CAR(+) iPSCs into highly functional CAR T cells. *Cell Stem Cell* **2022**, *29*, 515–527.e8. [CrossRef]
70. Sadeqi Nezhad, M.; Abdollahpour-Alitappeh, M.; Rezaei, B.; Yazdanifar, M.; Seifalian, A.M. Induced Pluripotent Stem Cells (iPSCs) Provide a Potentially Unlimited T Cell Source for CAR-T Cell Development and Off-the-Shelf Products. *Pharm. Res.* **2021**, *38*, 931–945. [CrossRef]
71. Karagiannis, P.; Kim, S.I. iPSC-Derived Natural Killer Cells for Cancer Immunotherapy. *Mol. Cells* **2021**, *44*, 541–548. [CrossRef] [PubMed]
72. Bagheri, Y.; Barati, A.; Aghebati-Maleki, A.; Aghebati-Maleki, L.; Yousefi, M. Current progress in cancer immunotherapy based on natural killer cells. *Cell Biol. Int.* **2021**, *45*, 2–17. [CrossRef] [PubMed]
73. Goldenson, B.H.; Zhu, H.; Wang, Y.M.; Heragu, N.; Bernareggi, D.; Ruiz-Cisneros, A.; Bahena, A.; Ask, E.H.; Hoel, H.J.; Malmberg, K.J.; et al. Umbilical Cord Blood and iPSC-Derived Natural Killer Cells Demonstrate Key Differences in Cytotoxic Activity and KIR Profiles. *Front. Immunol.* **2020**, 2435. [CrossRef] [PubMed]
74. Hsu, L.J.; Liu, C.L.; Kuo, M.L.; Shen, C.N.; Shen, C.R. An Alternative Cell Therapy for Cancers: Induced Pluripotent Stem Cell (iPSC)-Derived Natural Killer Cells. *Biomedicines* **2021**, *9*, 1323. [CrossRef]
75. Ruggeri, L.; Capanni, M.; Urbani, E.; Perruccio, K.; Shlomchik, W.D.; Tosti, A.; Posati, S.; Rogaia, D.; Frassoni, F.; Aversa, F.; et al. Effectiveness of donor natural killer cell alloreactivity in mismatched hematopoietic transplants. *Science* **2002**, *295*, 2097–2100. [CrossRef]
76. Lupo, K.B.; Matosevic, S. Natural Killer Cells as Allogeneic Effectors in Adoptive Cancer Immunotherapy. *Cancers* **2019**, *11*, 769. [CrossRef]
77. Dolstra, H.; Roeven, M.W.H.; Spanholtz, J.; Hangalapura, B.N.; Tordoir, M.; Maas, F.; Leenders, M.; Bohme, F.; Kok, N.; Trilsbeek, C.; et al. Successful Transfer of Umbilical Cord Blood CD34(+) Hematopoietic Stem and Progenitor-derived NK Cells in Older Acute Myeloid Leukemia Patients. *Clin. Cancer Res.* **2017**, *23*, 4107–4118. [CrossRef]
78. Romee, R.; Rosario, M.; Berrien-Elliott, M.M.; Wagner, J.A.; Jewell, B.A.; Schappe, T.; Leong, J.W.; Abdel-Latif, S.; Schneider, S.E.; Willey, S.; et al. Cytokine-induced memory-like natural killer cells exhibit enhanced responses against myeloid leukemia. *Sci. Transl. Med.* **2016**, *8*, 357ra123. [CrossRef]
79. Michel, T.; Ollert, M.; Zimmer, J. A Hot Topic: Cancer Immunotherapy and Natural Killer Cells. *Int. J. Mol. Sci.* **2022**, *23*, 797. [CrossRef]
80. Heipertz, E.L.; Zynda, E.R.; Stav-Noraas, T.E.; Hungler, A.D.; Boucher, S.E.; Kaur, N.; Vemuri, M.C. Current Perspectives on "Off-The-Shelf" Allogeneic NK and CAR-NK Cell Therapies. *Front. Immunol.* **2021**, *12*, 732135. [CrossRef]
81. Lu, H.; Zhao, X.Y.; Li, Z.Y.; Hu, Y.; Wang, H.F. From CAR-T Cells to CAR-NK Cells: A Developing Immunotherapy Method for Hematological Malignancies. *Front. Oncol.* **2021**, *11*, 720501. [CrossRef] [PubMed]
82. Xie, G.Z.; Dong, H.; Liang, Y.; Ham, J.D.; Rizwan, R.; Chen, J.Z. CAR-NK cells: A promising cellular immunotherapy for cancer. *Ebiomedicine* **2020**, *59*, 102975. [CrossRef] [PubMed]
83. Liu, E.L.; Marin, D.; Banerjee, P.; Macapinlac, H.A.; Thompson, P.; Basar, R.; Kerbauy, L.N.; Overman, B.; Thall, P.; Kaplan, M.; et al. Use of CAR-Transduced Natural Killer Cells in CD19-Positive Lymphoid Tumors. *N. Engl. J. Med.* **2020**, *382*, 545–553. [CrossRef] [PubMed]
84. Daher, M.; Basar, R.; Gokdemir, E.; Baran, N.; Uprety, N.; Cortes, A.K.N.; Mendt, M.; Kerbauy, L.N.; Banerjee, P.P.; Shanley, M.; et al. Targeting a cytokine checkpoint enhances the fitness of armored cord blood CAR-NK cells. *Blood* **2021**, *137*, 624–636. [CrossRef]
85. Wrona, E.; Borowiec, M.; Potemski, P. CAR-NK Cells in the Treatment of Solid Tumors. *Int. J. Mol. Sci.* **2021**, *22*, 5899. [CrossRef]
86. Marofi, F.; Saleh, M.M.; Rahman, H.S.; Suksatan, W.; Al-Gazally, M.E.; Abdelbasset, W.K.; Thangavelu, L.; Yumashev, A.V.; Hassanzadeh, A.; Yazdanifar, M.; et al. CAR-engineered NK cells; a promising therapeutic option for treatment of hematological malignancies. *Stem Cell Res. Ther.* **2021**, *12*, 374. [CrossRef]
87. Woll, P.S.; Grzywacz, B.; Tian, X.H.; Marcus, R.K.; Knorr, D.A.; Verneris, M.R.; Kaufman, D.S. Human embryonic stem cells differentiate into a homogeneous population of natural killer cells with potent in vivo antitumor activity. *Blood* **2009**, *113*, 6094–6101. [CrossRef]
88. Ni, Z.Y.; Knorr, D.A.; Clouser, C.L.; Hexum, M.K.; Southern, P.; Mansky, L.M.; Park, I.H.; Kaufman, D.S. Human Pluripotent Stem Cells Produce Natural Killer Cells That Mediate Anti-HIV-1 Activity by Utilizing Diverse Cellular Mechanisms. *J. Virol.* **2011**, *85*, 43–50. [CrossRef]
89. Knorr, D.A.; Ni, Z.; Hermanson, D.; Hexum, M.K.; Bendzick, L.; Cooper, L.J.; Lee, D.A.; Kaufman, D.S. Clinical-scale derivation of natural killer cells from human pluripotent stem cells for cancer therapy. *Stem Cells Transl. Med.* **2013**, *2*, 274–283. [CrossRef]
90. Euchner, J.; Sprissler, J.; Cathomen, T.; Furst, D.; Schrezenmeier, H.; Debatin, K.M.; Schwarz, K.; Felgentreff, K. Natural Killer Cells Generated From Human Induced Pluripotent Stem Cells Mature to CD56(bright)CD16(+)NKp80(+/−) In-Vitro and Express KIR2DL2/DL3 and KIR3DL1. *Front. Immunol.* **2021**, *12*, 640672. [CrossRef]
91. Ng, E.S.; Davis, R.; Stanley, E.G.; Elefanty, A.G. A protocol describing the use of a recombinant protein-based, animal product-free medium (APEL) for human embryonic stem cell differentiation as spin embryoid bodies. *Nat. Protoc.* **2008**, *3*, 768–776. [CrossRef] [PubMed]

92. Bock, A.M.; Knorr, D.; Kaufman, D.S. Development, expansion, and in vivo monitoring of human NK cells from human embryonic stem cells (hESCs) and and induced pluripotent stem cells (iPSCs). *J. Vis. Exp.* **2013**, *74*, e50337. [CrossRef] [PubMed]
93. Hermanson, D.L.; Ni, Z.Y.; Knorr, D.A.; Bendzick, L.; Pribyl, L.J.; Geller, M.; Kaufman, D.S. Functional Chimeric Antigen Receptor-Expressing Natural Killer Cells Derived From Human Pluripotent Stem Cells. *Blood* **2013**, *122*, 896. [CrossRef]
94. Li, Y.; Hermanson, D.L.; Moriarity, B.S.; Kaufman, D.S. Human iPSC-Derived Natural Killer Cells Engineered with Chimeric Antigen Receptors Enhance Anti-tumor Activity. *Cell Stem Cell* **2018**, *23*, 181–192.e185. [CrossRef]
95. Bjordahl, R.; Gaidarova, S.; Goodridge, J.P.; Mahmood, S.; Bonello, G.; Robinson, M.; Ruller, C.; Pribadi, M.; Lee, T.; Abujarour, R.; et al. FT576: A Novel Multiplexed Engineered Off-the-Shelf Natural Killer Cell Immunotherapy for the Dual-Targeting of CD38 and Bcma for the Treatment of Multiple Myeloma. *Blood* **2019**, *134*, 3214. [CrossRef]
96. Goodridge, J.P.; Bjordahl, R.; Mahmood, S.; Reiser, J.; Gaidarova, S.; Blum, R.; Cichocki, F.; Chu, H.Y.; Bonello, G.; Lee, T.; et al. FT576: Multi-Specific Off-the-Shelf CAR-NK Cell Therapy Engineered for Enhanced Persistence, Avoidance of Self-Fratricide and Optimized Mab Combination Therapy to Prevent Antigenic Escape and Elicit a Deep and Durable Response in Multiple Myeloma. *Blood* **2020**, *136*, 4–5. [CrossRef]
97. Wynn, T.A.; Chawla, A.; Pollard, J.W. Macrophage biology in development, homeostasis and disease. *Nature* **2013**, *496*, 445–455. [CrossRef]
98. Weiss, G.; Schaible, U.E. Macrophage defense mechanisms against intracellular bacteria. *Immunol. Rev.* **2015**, *264*, 182–203. [CrossRef]
99. Takiguchi, H.; Yang, C.X.; Yang, C.W.T.; Sahin, B.; Whalen, B.A.; Milne, S.; Akata, K.; Yamasaki, K.; Yang, J.S.W.; Cheung, C.Y.; et al. Macrophages with reduced expressions of classical M1 and M2 surface markers in human bronchoalveolar lavage fluid exhibit pro-inflammatory gene signatures. *Sci. Rep.* **2021**, *11*, 8282. [CrossRef]
100. Arango Duque, G.; Descoteaux, A. Macrophage cytokines: Involvement in immunity and infectious diseases. *Front. Immunol.* **2014**, *5*, 491. [CrossRef]
101. Mantovani, A.; Biswas, S.K.; Galdiero, M.R.; Sica, A.; Locati, M. Macrophage plasticity and polarization in tissue repair and remodelling. *J. Pathol.* **2013**, *229*, 176–185. [CrossRef] [PubMed]
102. Trapnell, B.C.; Nakata, K.; Bonella, F.; Campo, I.; Griese, M.; Hamilton, J.; Wang, T.; Morgan, C.; Cottin, V.; McCarthy, C. Pulmonary alveolar proteinosis. *Nat. Rev. Dis. Primers* **2019**, *5*, 16. [CrossRef] [PubMed]
103. Ma, Y.; Mouton, A.J.; Lindsey, M.L. Cardiac macrophage biology in the steady-state heart, the aging heart, and following myocardial infarction. *Transl. Res.* **2018**, *191*, 15–28. [CrossRef] [PubMed]
104. Galloway, D.A.; Phillips, A.E.M.; Owen, D.R.J.; Moore, C.S. Phagocytosis in the Brain: Homeostasis and Disease. *Front. Immunol.* **2019**, *10*, 790. [CrossRef] [PubMed]
105. Cassetta, L.; Pollard, J.W. Targeting macrophages: Therapeutic approaches in cancer. *Nat. Rev. Drug Discov.* **2018**, *17*, 887–904. [CrossRef]
106. Gajewski, T.F.; Schreiber, H.; Fu, Y.X. Innate and adaptive immune cells in the tumor microenvironment. *Nat. Immunol.* **2013**, *14*, 1014–1022. [CrossRef]
107. Noy, R.; Pollard, J.W. Tumor-associated macrophages: From mechanisms to therapy. *Immunity* **2014**, *41*, 49–61. [CrossRef]
108. Klichinsky, M.; Ruella, M.; Shestova, O.; Lu, X.M.; Best, A.; Zeeman, M.; Schmierer, M.; Gabrusiewicz, K.; Anderson, N.R.; Petty, N.E.; et al. Human chimeric antigen receptor macrophages for cancer immunotherapy. *Nat. Biotechnol.* **2020**, *38*, 947–953. [CrossRef]
109. Chen, Y.; Yu, Z.; Tan, X.; Jiang, H.; Xu, Z.; Fang, Y.; Han, D.; Hong, W.; Wei, W.; Tu, J. CAR-macrophage: A new immunotherapy candidate against solid tumors. *Biomed. Pharmacother.* **2021**, *139*, 111605. [CrossRef]
110. Lyadova, I.; Gerasimova, T.; Nenasheva, T. Macrophages Derived From Human Induced Pluripotent Stem Cells: The Diversity of Protocols, Future Prospects, and Outstanding Questions. *Front. Cell Dev. Biol.* **2021**, *9*, 640703. [CrossRef]
111. Bosshart, H.; Heinzelmann, M. THP-1 cells as a model for human monocytes. *Ann. Transl. Med.* **2016**, *4*, 438. [CrossRef]
112. Carpenedo, R.L.; Sargent, C.Y.; McDevitt, T.C. Rotary suspension culture enhances the efficiency, yield, and homogeneity of embryoid body differentiation. *Stem Cells* **2007**, *25*, 2224–2234. [CrossRef] [PubMed]
113. Spelke, D.P.; Ortmann, D.; Khademhosseini, A.; Ferreira, L.; Karp, J.M. Methods for embryoid body formation: The microwell approach. *Methods Mol. Biol.* **2011**, *690*, 151–162. [CrossRef] [PubMed]
114. Wu, H.W.; Hsiao, Y.H.; Chen, C.C.; Yet, S.F.; Hsu, C.H. A PDMS-Based Microfluidic Hanging Drop Chip for Embryoid Body Formation. *Molecules* **2016**, *21*, 882. [CrossRef]
115. Mukherjee, C.; Hale, C.; Mukhopadhyay, S. A Simple Multistep Protocol for Differentiating Human Induced Pluripotent Stem Cells into Functional Macrophages. *Methods Mol. Biol.* **2018**, *1784*, 13–28. [CrossRef]
116. Cao, X.; Yakala, G.K.; van den Hil, F.E.; Cochrane, A.; Mummery, C.L.; Orlova, V.V. Differentiation and Functional Comparison of Monocytes and Macrophages from hiPSCs with Peripheral Blood Derivatives. *Stem Cell Rep.* **2019**, *12*, 1282–1297. [CrossRef]
117. Ackermann, M.; Kempf, H.; Hetzel, M.; Hesse, C.; Hashtchin, A.R.; Brinkert, K.; Schott, J.W.; Haake, K.; Kuhnel, M.P.; Glage, S.; et al. Bioreactor-based mass production of human iPSC-derived macrophages enables immunotherapies against bacterial airway infections. *Nat. Commun.* **2018**, *9*, 5088. [CrossRef]
118. Toubal, A.; Nel, I.; Lotersztajn, S.; Lehuen, A. Mucosal-associated invariant T cells and disease. *Nat. Rev. Immunol.* **2019**, *19*, 643–657. [CrossRef] [PubMed]

119. Dias, J.; Boulouis, C.; Gorin, J.B.; van den Biggelaar, R.; Lal, K.G.; Gibbs, A.; Loh, L.; Gulam, M.Y.; Sia, W.R.; Bari, S.; et al. The CD4(−)CD8(−) MAIT cell subpopulation is a functionally distinct subset developmentally related to the main CD8(+) MAIT cell pool. *Proc. Natl. Acad. Sci. USA* **2018**, *115*, E11513–E11522. [CrossRef]
120. Vacchini, A.; Chancellor, A.; Spagnuolo, J.; Mori, L.; De Libero, G. MR1-Restricted T Cells Are Unprecedented Cancer Fighters. *Front. Immunol.* **2020**, *11*, 751. [CrossRef]
121. Won, E.J.; Ju, J.K.; Cho, Y.N.; Jin, H.M.; Park, K.J.; Kim, T.J.; Kwon, Y.S.; Kee, H.J.; Kim, J.C.; Kee, S.J.; et al. Clinical relevance of circulating mucosal-associated invariant T cell levels and their anti-cancer activity in patients with mucosal-associated cancer. *Oncotarget* **2016**, *7*, 76274–76290. [CrossRef] [PubMed]
122. Ling, L.; Lin, Y.; Zheng, W.; Hong, S.; Tang, X.; Zhao, P.; Li, M.; Ni, J.; Li, C.; Wang, L.; et al. Circulating and tumor-infiltrating mucosal associated invariant T (MAIT) cells in colorectal cancer patients. *Sci. Rep.* **2016**, *6*, 20358. [CrossRef] [PubMed]
123. Shaler, C.R.; Tun-Abraham, M.E.; Skaro, A.I.; Khazaie, K.; Corbett, A.J.; Mele, T.; Hernandez-Alejandro, R.; Haeryfar, S.M.M. Mucosa-associated invariant T cells infiltrate hepatic metastases in patients with colorectal carcinoma but are rendered dysfunctional within and adjacent to tumor microenvironment. *Cancer Immunol. Immunother.* **2017**, *66*, 1563–1575. [CrossRef] [PubMed]
124. Duan, M.; Goswami, S.; Shi, J.Y.; Wu, L.J.; Wang, X.Y.; Ma, J.Q.; Zhang, Z.; Shi, Y.; Ma, L.J.; Zhang, S.; et al. Activated and Exhausted MAIT Cells Foster Disease Progression and Indicate Poor Outcome in Hepatocellular Carcinoma. *Clin. Cancer Res.* **2019**, *25*, 3304–3316. [CrossRef]
125. Tourret, M.; Talvard-Balland, N.; Lambert, M.; Ben Youssef, G.; Chevalier, M.F.; Bohineust, A.; Yvorra, T.; Morin, F.; Azarnoush, S.; Lantz, O.; et al. Human MAIT cells are devoid of alloreactive potential: Prompting their use as universal cells for adoptive immune therapy. *J. Immunother. Cancer* **2021**, *9*, e003123. [CrossRef]
126. Petley, E.V.; Koay, H.F.; Henderson, M.A.; Sek, K.; Todd, K.L.; Keam, S.P.; Lai, J.; House, I.G.; Li, J.; Zethoven, M.; et al. MAIT cells regulate NK cell-mediated tumor immunity. *Nat. Commun.* **2021**, *12*, 4746. [CrossRef]
127. Dusseaux, M.; Martin, E.; Serriari, N.; Peguillet, I.; Premel, V.; Louis, D.; Milder, M.; Le Bourhis, L.; Soudais, C.; Treiner, E.; et al. Human MAIT cells are xenobiotic-resistant, tissue-targeted, CD161hi IL-17-secreting T cells. *Blood* **2011**, *117*, 1250–1259. [CrossRef]
128. Kawaguchi, K.; Umeda, K.; Hiejima, E.; Iwai, A.; Mikami, M.; Nodomi, S.; Saida, S.; Kato, I.; Hiramatsu, H.; Yasumi, T.; et al. Influence of post-transplant mucosal-associated invariant T cell recovery on the development of acute graft-versus-host disease in allogeneic bone marrow transplantation. *Int. J. Hematol.* **2018**, *108*, 66–75. [CrossRef]
129. Bhattacharyya, A.; Hanafi, L.A.; Sheih, A.; Golob, J.L.; Srinivasan, S.; Boeckh, M.J.; Pergam, S.A.; Mahmood, S.; Baker, K.K.; Gooley, T.A.; et al. Graft-Derived Reconstitution of Mucosal-Associated Invariant T Cells after Allogeneic Hematopoietic Cell Transplantation. *Biol. Blood Marrow Transplant.* **2018**, *24*, 242–251. [CrossRef]
130. Reantragoon, R.; Corbett, A.J.; Sakala, I.G.; Gherardin, N.A.; Furness, J.B.; Chen, Z.; Eckle, S.B.; Uldrich, A.P.; Birkinshaw, R.W.; Patel, O.; et al. Antigen-loaded MR1 tetramers define T cell receptor heterogeneity in mucosal-associated invariant T cells. *J. Exp. Med.* **2013**, *210*, 2305–2320. [CrossRef]
131. Wakao, H.; Yoshikiyo, K.; Koshimizu, U.; Furukawa, T.; Enomoto, K.; Matsunaga, T.; Tanaka, T.; Yasutomi, Y.; Yamada, T.; Minakami, H.; et al. Expansion of functional human mucosal-associated invariant T cells via reprogramming to pluripotency and redifferentiation. *Cell Stem Cell* **2013**, *12*, 546–558. [CrossRef] [PubMed]
132. Hayday, A.C.; Saito, H.; Gillies, S.D.; Kranz, D.M.; Tanigawa, G.; Eisen, H.N.; Tonegawa, S. Structure, organization, and somatic rearrangement of T cell gamma genes. *Cell* **1985**, *40*, 259–269. [CrossRef]
133. Born, W.; Miles, C.; White, J.; O'Brien, R.; Freed, J.H.; Marrack, P.; Kappler, J.; Kubo, R.T. Peptide sequences of T-cell receptor delta and gamma chains are identical to predicted X and gamma proteins. *Nature* **1987**, *330*, 572–574. [CrossRef] [PubMed]
134. Carding, S.R.; Egan, P.J. Gammadelta T cells: Functional plasticity and heterogeneity. *Nat. Rev. Immunol.* **2002**, *2*, 336–345. [CrossRef] [PubMed]
135. Pistoia, V.; Tumino, N.; Vacca, P.; Veneziani, I.; Moretta, A.; Locatelli, F.; Moretta, L. Human gammadelta T-Cells: From Surface Receptors to the Therapy of High-Risk Leukemias. *Front. Immunol.* **2018**, *9*, 984. [CrossRef]
136. Kunkele, K.P.; Wesch, D.; Oberg, H.H.; Aichinger, M.; Supper, V.; Baumann, C. Vgamma9Vdelta2 T Cells: Can We Re-Purpose a Potent Anti-Infection Mechanism for Cancer Therapy? *Cells* **2020**, *9*, 829. [CrossRef]
137. Kunzmann, V.; Bauer, E.; Wilhelm, M. Gamma/delta T-cell stimulation by pamidronate. *N. Engl. J. Med.* **1999**, *340*, 737–738. [CrossRef]
138. Kabelitz, D.; Serrano, R.; Kouakanou, L.; Peters, C.; Kalyan, S. Cancer immunotherapy with gammadelta T cells: Many paths ahead of us. *Cell. Mol. Immunol.* **2020**, *17*, 925–939. [CrossRef]
139. Handgretinger, R.; Schilbach, K. The potential role of gammadelta T cells after allogeneic HCT for leukemia. *Blood* **2018**, *131*, 1063–1072. [CrossRef] [PubMed]
140. Yazdanifar, M.; Barbarito, G.; Bertaina, A.; Airoldi, I. gammadelta T Cells: The Ideal Tool for Cancer Immunotherapy. *Cells* **2020**, *9*, 1305. [CrossRef]
141. Simoes, A.E.; Di Lorenzo, B.; Silva-Santos, B. Molecular Determinants of Target Cell Recognition by Human gammadelta T Cells. *Front. Immunol.* **2018**, *9*, 929. [CrossRef]
142. Correia, D.V.; Lopes, A.; Silva-Santos, B. Tumor cell recognition by gammadelta T lymphocytes: T-cell receptor vs. NK-cell receptors. *Oncoimmunology* **2013**, *2*, e22892. [CrossRef] [PubMed]

143. Gao, Y.; Yang, W.; Pan, M.; Scully, E.; Girardi, M.; Augenlicht, L.H.; Craft, J.; Yin, Z. Gamma delta T cells provide an early source of interferon gamma in tumor immunity. *J. Exp. Med.* **2003**, *198*, 433–442. [CrossRef]
144. Moser, B.; Brandes, M. Gammadelta T cells: An alternative type of professional APC. *Trends Immunol.* **2006**, *27*, 112–118. [CrossRef] [PubMed]
145. Fischer, M.A.; Golovchenko, N.B.; Edelblum, K.L. gammadelta T cell migration: Separating trafficking from surveillance behaviors at barrier surfaces. *Immunol. Rev.* **2020**, *298*, 165–180. [CrossRef] [PubMed]
146. Braza, M.S.; Klein, B.; Fiol, G.; Rossi, J.F. gammadelta T-cell killing of primary follicular lymphoma cells is dramatically potentiated by GA101, a type II glycoengineered anti-CD20 monoclonal antibody. *Haematologica* **2011**, *96*, 400–407. [CrossRef] [PubMed]
147. Deniger, D.C.; Switzer, K.; Mi, T.; Maiti, S.; Hurton, L.; Singh, H.; Huls, H.; Olivares, S.; Lee, D.A.; Champlin, R.E.; et al. Bispecific T-cells expressing polyclonal repertoire of endogenous gammadelta T-cell receptors and introduced CD19-specific chimeric antigen receptor. *Mol. Ther.* **2013**, *21*, 638–647. [CrossRef] [PubMed]
148. Makkouk, A.; Yang, X.C.; Barca, T.; Lucas, A.; Turkoz, M.; Wong, J.T.S.; Nishimoto, K.P.; Brodey, M.M.; Tabrizizad, M.; Gundurao, S.R.Y.; et al. Off-the-shelf Vdelta1 gamma delta T cells engineered with glypican-3 (GPC-3)-specific chimeric antigen receptor (CAR) and soluble IL-15 display robust antitumor efficacy against hepatocellular carcinoma. *J. Immunother. Cancer* **2021**, *9*, e003441. [CrossRef] [PubMed]
149. Nishimoto, K.P.; Barca, T.; Azameera, A.; Makkouk, A.; Romero, J.M.; Bai, L.; Brodey, M.M.; Kennedy-Wilde, J.; Shao, H.; Papaioannou, S.; et al. Allogeneic CD20-targeted gammadelta T cells exhibit innate and adaptive antitumor activities in preclinical B-cell lymphoma models. *Clin. Transl. Immunol.* **2022**, *11*, e1373. [CrossRef]
150. Rozenbaum, M.; Meir, A.; Aharony, Y.; Itzhaki, O.; Schachter, J.; Bank, I.; Jacoby, E.; Besser, M.J. Gamma-Delta CAR-T Cells Show CAR-Directed and Independent Activity Against Leukemia. *Front. Immunol.* **2020**, *11*, 1347. [CrossRef]
151. Schietinger, A.; Greenberg, P.D. Tolerance and exhaustion: Defining mechanisms of T cell dysfunction. *Trends Immunol.* **2014**, *35*, 51–60. [CrossRef] [PubMed]
152. Watanabe, D.; Koyanagi-Aoi, M.; Taniguchi-Ikeda, M.; Yoshida, Y.; Azuma, T.; Aoi, T. The Generation of Human gammadeltaT Cell-Derived Induced Pluripotent Stem Cells from Whole Peripheral Blood Mononuclear Cell Culture. *Stem Cells Transl. Med.* **2018**, *7*, 34–44. [CrossRef] [PubMed]
153. Ohta, R.; Niwa, A.; Taniguchi, Y.; Suzuki, N.M.; Toga, J.; Yagi, E.; Saiki, N.; Nishinaka-Arai, Y.; Okada, C.; Watanabe, A.; et al. Laminin-guided highly efficient endothelial commitment from human pluripotent stem cells. *Sci. Rep.* **2016**, *6*, 35680. [CrossRef] [PubMed]
154. Zeng, J.; Tang, S.Y.; Wang, S. Derivation of mimetic gammadelta T cells endowed with cancer recognition receptors from reprogrammed gammadelta T cell. *PLoS ONE* **2019**, *14*, e0216815. [CrossRef]
155. Berzins, S.P.; Smyth, M.J.; Baxter, A.G. Presumed guilty: Natural killer T cell defects and human disease. *Nat. Rev. Immunol.* **2011**, *11*, 131–142. [CrossRef]
156. Brennan, P.J.; Brigl, M.; Brenner, M.B. Invariant natural killer T cells: An innate activation scheme linked to diverse effector functions. *Nat. Rev. Immunol.* **2013**, *13*, 101–117. [CrossRef]
157. Beekman, E.M.; Porcelli, S.A.; Morita, C.T.; Behar, S.M.; Furlong, S.T.; Brenner, M.B. Recognition of a Lipid Antigen by Cd1-Restricted Alpha-Beta(+) T-Cells. *Nature* **1994**, *372*, 691–694. [CrossRef]
158. Fujii, S.I.; Hemmi, H.; Steinman, R.M. Innate V alpha 14(+) natural killer T cells mature dendritic cells, leading to strong adaptive immunity. *Immunol. Rev.* **2007**, *220*, 183–198. [CrossRef]
159. Mavers, M.; Maas-Bauer, K.; Negrin, R.S. Invariant Natural Killer T Cells As Suppressors of Graft-versus-Host Disease in Allogeneic Hematopoietic Stem Cell Transplantation. *Front. Immunol.* **2017**, *8*, 900. [CrossRef]
160. Li, Y.R.; Zhou, Y.; Kim, Y.J.; Zhu, Y.N.; Ma, F.Y.; Yu, J.J.; Wang, Y.C.; Chen, X.H.; Li, Z.; Zeng, S.; et al. Development of allogeneic HSC-engineered iNKT cells for off-the-shelf cancer immunotherapy. *Cell Rep. Med.* **2021**, *2*, 100449. [CrossRef]
161. Zhu, Y.N.; Smith, D.J.; Zhou, Y.; Li, Y.R.; Yu, J.J.; Lee, D.; Wang, Y.C.; Di Biase, S.; Wang, X.; Hardoy, C.; et al. Development of Hematopoietic Stem Cell-Engineered Invariant Natural Killer T Cell Therapy for Cancer. *Cell Stem Cell* **2019**, *25*, 542–557.e9. [CrossRef] [PubMed]
162. Li, Y.R.; Zhou, Y.; Kramer, A.; Yang, L. Engineering stem cells for cancer immunotherapy. *Trends Cancer* **2021**, *7*, 1059–1073. [CrossRef] [PubMed]
163. Zhou, Y.; Li, Y.R.; Zeng, S.; Yang, L. Methods for Studying Mouse and Human Invariant Natural Killer T Cells. *Methods Mol. Biol.* **2021**, *2388*, 35–57. [CrossRef] [PubMed]
164. Watarai, H.; Fujii, S.; Koseki, H.; Taniguchi, M. Murine induced pluripotent stem cells can be derived from and differentiate into natural killer T cells. *Differentiation* **2010**, *80*, S45. [CrossRef]
165. Motohashi, S.; Iinuma, T.; Kurokawa, T.; Koseki, H. Application of iPS Cell-Derived NKT Cells to Cancer Immunotherapy. *Gan Kagaku Ryoho* **2020**, *47*, 1411–1414.
166. Serwold, T.; Hochedlinger, K.; Inlay, M.A.; Jaenisch, R.; Weissman, I.L. Early TCR expression and aberrant T cell development in mice with endogenous prerearranged T cell receptor genes. *J. Immunol.* **2007**, *179*, 928–938. [CrossRef]
167. Ando, M.; Kinoshita, S.; Furukawa, Y.; Ando, J.; Nakauchi, H.; Brenner, M.K. Improving the safety of iPSC-derived T cell therapy. In *Molecular Players in iPSC Technology*; Academic Press: Cambridge, MA, USA, 2022; pp. 95–115. [CrossRef]
168. Hou, A.J.; Chen, L.C.; Chen, Y.Y. Navigating CAR-T cells through the solid-tumour microenvironment. *Nat. Rev. Drug Discov.* **2021**, *20*, 531–550. [CrossRef]

169. Kankeu Fonkoua, L.A.; Sirpilla, O.; Sakemura, R.; Siegler, E.L.; Kenderian, S.S. CAR T cell therapy and the tumor microenvironment: Current challenges and opportunities. *Mol. Ther.-Oncolytics* **2022**, *25*, 69–77. [CrossRef]
170. Parihar, R.; Rivas, C.; Huynh, M.; Omer, B.; Lapteva, N.; Metelitsa, L.S.; Gottschalk, S.M.; Rooney, C.M. NK Cells Expressing a Chimeric Activating Receptor Eliminate MDSCs and Rescue Impaired CAR-T Cell Activity against Solid Tumors. *Cancer Immunol. Res.* **2019**, *7*, 363–375. [CrossRef]
171. Giraldo, N.A.; Sanchez-Salas, R.; Peske, J.D.; Vano, Y.; Becht, E.; Petitprez, F.; Validire, P.; Ingels, A.; Cathelineau, X.; Fridman, W.H.; et al. The clinical role of the TME in solid cancer. *Br. J. Cancer* **2019**, *120*, 45–53. [CrossRef]
172. Wang, H.; Kaur, G.; Sankin, A.I.; Chen, F.; Guan, F.; Zang, X. Immune checkpoint blockade and CAR-T cell therapy in hematologic malignancies. *J. Hematol. Oncol.* **2019**, *12*, 59. [CrossRef] [PubMed]
173. Narayan, V.; Barber-Rotenberg, J.S.; Jung, I.Y.; Lacey, S.F.; Rech, A.J.; Davis, M.M.; Hwang, W.T.; Lal, P.; Carpenter, E.L.; Maude, S.L.; et al. PSMA-targeting TGFbeta-insensitive armored CAR T cells in metastatic castration-resistant prostate cancer: A phase 1 trial. *Nat. Med.* **2022**, *28*, 724–734. [CrossRef] [PubMed]
174. Yin, Y.; Boesteanu, A.C.; Binder, Z.A.; Xu, C.; Reid, R.A.; Rodriguez, J.L.; Cook, D.R.; Thokala, R.; Blouch, K.; McGettigan-Croce, B.; et al. Checkpoint Blockade Reverses Anergy in IL-13Ralpha2 Humanized scFv-Based CAR T Cells to Treat Murine and Canine Gliomas. *Mol. Ther.-Oncolytics* **2018**, *11*, 20–38. [CrossRef] [PubMed]

4.2 Pluripotent stem cell-engineered immune cells for off-the-shelf cell therapy

(This project leads to a on filing US Patent: *UCLA-30435.430-US-P1*)

Significance

Progress in adoptive iNKT cell therapy for cancer is hampered by the lack of readily available human iNKT cells. Having rapid access to unlimited iNKT cells, particularly antigen-specific iNKT cells, with optimized therapeutic features would greatly advance the scope and delivery of iNKT cell therapies. The unique combination of pluripotentiality and unlimited capacity for proliferation of human embryonic stem cell (hESC)/ induced pluripotent stem cell (iPSC) provide speculation that they can be good resources as "unlimited supply" of human iNKT cells. Previous studies have showed that genetic engineering of iPSCs with CAR can efficiently generate phenotypically defined and functional antigen-specific T[31–36] and NK cells[4,37–39], that concomitantly harness the unlimited availability of iPSCs. However, limited studies have been working on to produce iPSC- derived human iNKT cells[8], in particular CAR-iNKT cells. And no study has been done to regeneration human iNKT or CAR-iNKT cells from iPSCs independent of OP9/DLL1culture system[8]. **Here, we propose to generate human iNKT and/or CAR-iNKT cells from gene- engineered hESC/iPSC cells using an *ex vivo* feeder free culture system.** This work offers a potential new source of off-the-shelf iNKT cells. **In the combination of genetic modification and CAR technologies, it opens a new direction of iNKT cell-based cancer immunotherapy suitable for a range of therapeutic indications.**

Approach

Lentiviral vector construction, lentiviral production and lentivector transduction of hESCs. The tricistronic vector including BCMACAR, iNKT TCRa and iNKT TCRb coding sequences, was

sub-cloned into the third generation pCCL lentiviral vector downstream of a ubiquitin C (UBC) promoter. A 2A-linked GFP coding sequence was added downstream of TCRb gene. Lentivirus particles packaging and concentration were performed in 293T(ATCC) cells by co-transfected with a lentiviral vector plasmid, pCMV-DR8.9, and pCAGGS-VSVG using TransIT 293T (Mirus Bio, Madison, WI) for 16-18 hours followed by treatment with 20mM sodium butyrate for 8hours, followed by generation of cell supernatants in serum-free UltraCulture for 48 hours. Supernantants were concentrated by ultrafiltration using Amicon Ultra-15 100K filters (EMD Millpore, Billerica, MA) at 4000g for 40 minutes at 4°C and stored as aliquots at -80°C. hESCs were seeded in 6-well plate in the ES culture media followed by the addition of concentrated viral particles. ES cells and viral particles will be incubated at 37°C overnight. FACS detection of GFP expression at 3 days post virus transduction to detect the transduction rate.

Establish stable engineered BCAR-iNKT-hESC cell line(s)

The successfully transduced hESCs will express GFP. Single clone of hESC-GFP cells will be sorted out by FACS sorting. We will verify the “stemness” markers on engineered hESCs. mRNA levels expression of Oct-4, Nanog, REX-1, Sox-2, GCTM-2 and FGF-4 will be quantified by RT PCR. The pluripotent markers, SSEA-3, SSEA-4, TRA-1-60, TRA-1-81, NANOG, OCT4 can be measured by immunohistochemistry.

***Ex vivo* differentiate BCAR-iNKT-hESCs into functional human iNKT cells**

iNKT-hESCs will be cultured either in artificial organoid thymus[16,20] or StemSpan T differentiation medium to induce iNKT differentiation from engineered BCAR-iNKT-hESCs. hESC-BCAR-iNKT cells will be characterized by their expression of surface markers, such as 6B11 (TCRa chain maker), CD3, CD4, CD8, CD45RO, CD161, and the expression level of cytotoxic molecules, including INFg, TNF α , perforin and granzyme B.

***In vitro* and *in vivo* Tumor Killing Efficacy of hESC-BCAR-iNKT Cells**

The efficacy of iNKT killing in response to tumor antigen stimulation will also be evaluated by *in vitro* mixed killing assay and in vivo human multiple myeloma (MM.1S) xenograft mouse model[19].

Figures:

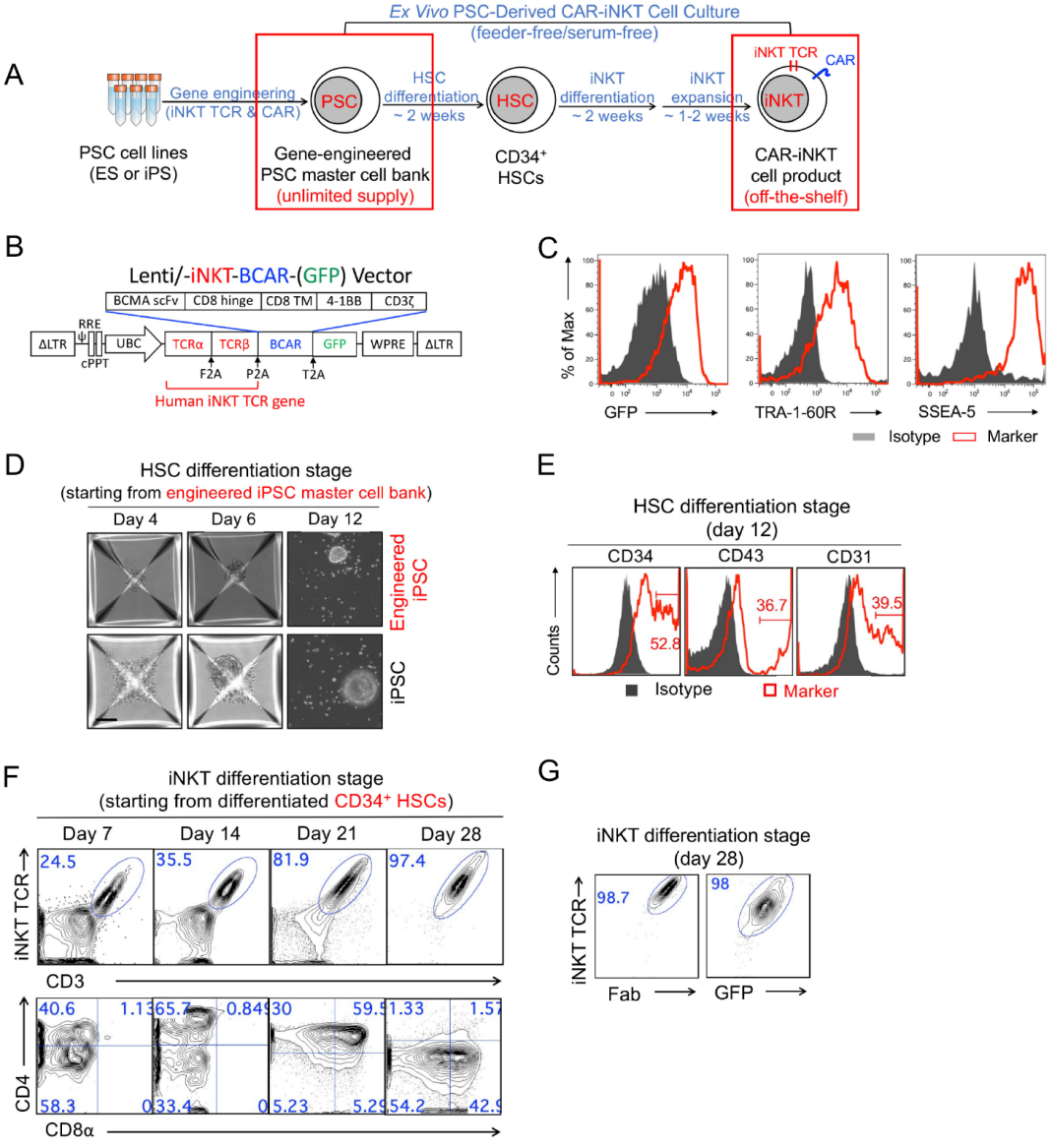

Figure 1. CMC study- Generation of ^{PSC}BCAR-iNKT cells from iPSCs. (A) Experimental design to generate the ^{PSC}BCAR-iNKT cell product. BCMA, B-cell maturation

antigen; CAR, chimeric antigen receptor; BCAR, BCMA-targeting CAR. (B) Schematics of Lenti/iNKT-BCAR-(GFP) lentivector encoding a human iNKT TCR gene, a BCAR gene, and an optional GFP reporter gene. (C) FACS plots showing the retention of pluripotency markers (i.e., TRA-1-60R and SSEA-5) on gene-engineered DMD iPSC master cell line. Note the co-expression of the GFP reporter. (D-E) Differentiation of gene-engineered iPSC master cell line into HSCs at the HSC Differentiation Stage. (D) Microscope images showing the cell cultures over time. (E) FACS plots showing the detection of HSC markers (i.e., CD34, CD43, and CD31) on cells from day 12 culture. (F-G) Differentiation of iPSC-derived HSCs into ^{PSC}BCAR-iNKT cells at the iNKT Differentiation Stage. (F) FACS plots showing the generation of human iNKT cells (identified as CD3+iNKT TCR+) over time. (G) FACS plots showing the co-expression of iNKT TCR, BCAR, and the GFP reporter on mature ^{PSC}BCAR-iNKT cells collected at day 28 of the iNKT Differentiation Stage culture.

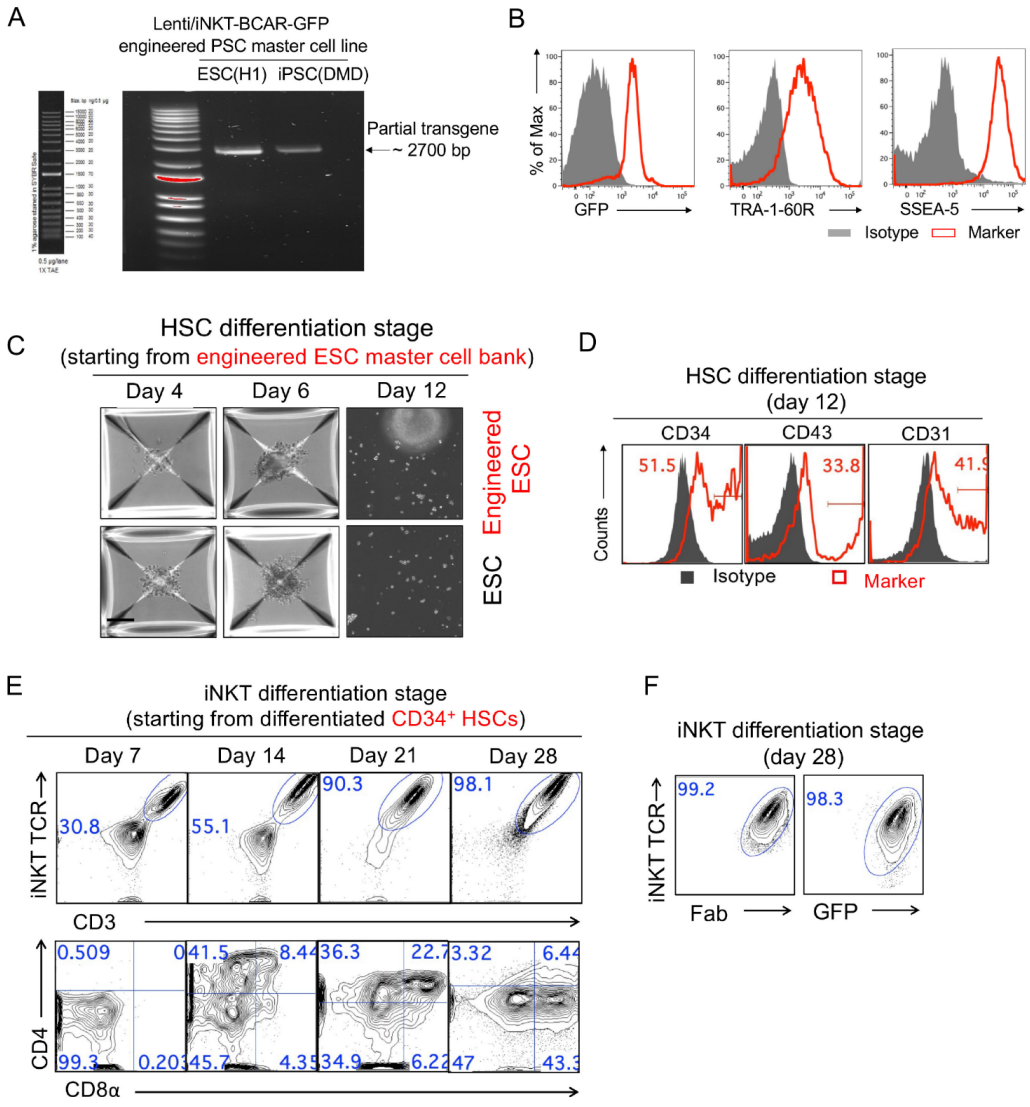

Figure 2. CMC study- Generation of ^{PSC}BCAR-iNKT cells from ESCs. (A) DNA gel image showing the detection of transgene in Lenti/iNKT-BCAR-GFP vector-transduced PSC master cell lines (H1 ESC line and DMD iPSC line). Genomic DNA was extracted from the indicated PSC master cell line and subjected to polymerase chain reaction (PCR) to amplify a ~2,700bp partial transgene fragment. (B) FACS plots showing the retention of pluripotency markers (i.e., TRA-1-60R and SSEA-5) on gene-engineered H1 ESC master cell line. Note the co-expression of the GFP reporter. (C-D) Differentiation of gene-engineered ESC master cell line into HSCs at the HSC Differentiation Stage. (D)

Microscope images showing the cell cultures over time. (E) FACS plots showing the detection of HSC markers (i.e., CD34, CD43, and CD31) on cells from day 12 culture. (E-F) Differentiation of ESC-derived HSCs into PSCBCAR-iNKT cells at the iNKT Differentiation Stage. (E) FACS plots showing the generation of human iNKT cells (identified as CD3+iNKT TCR+) over time. (F) FACS plots showing the co-expression of iNKT TCR, BCAR, and the GFP reporter on mature PSCBCAR-iNKT cells collected at day 28 of the iNKT Differentiation Stage culture.

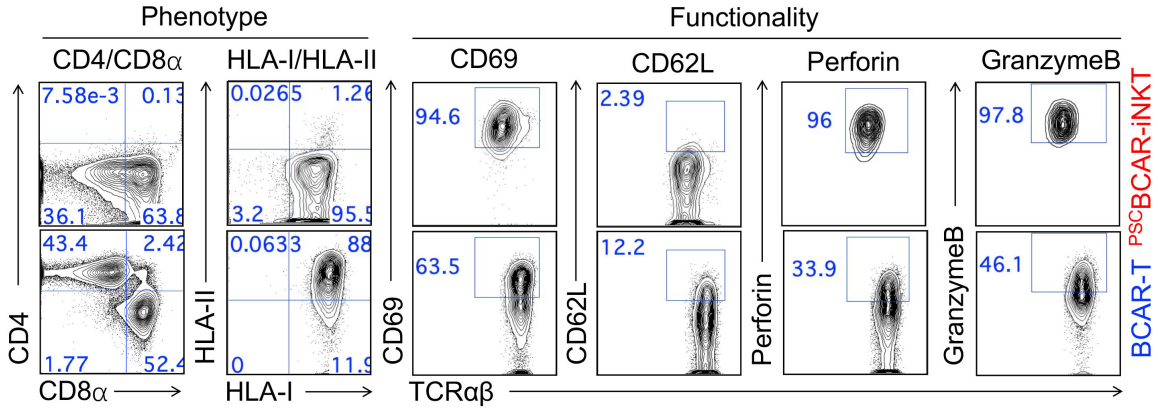

Figures 3. Pharmacology Studies – ^{PSC}BCAR-iNKT Cells. In Figure 3, representative FACS plots are presented, showing the analysis of phenotype (surface markers) and functionality (intracellular production of effector molecules) of ^{PSC}BCAR-iNKT cells. Healthy donor PBMC-derived conventional αβ T cells engineered to express the same BCAR (denoted as BCAR-T cells) were included as a benchmark control.

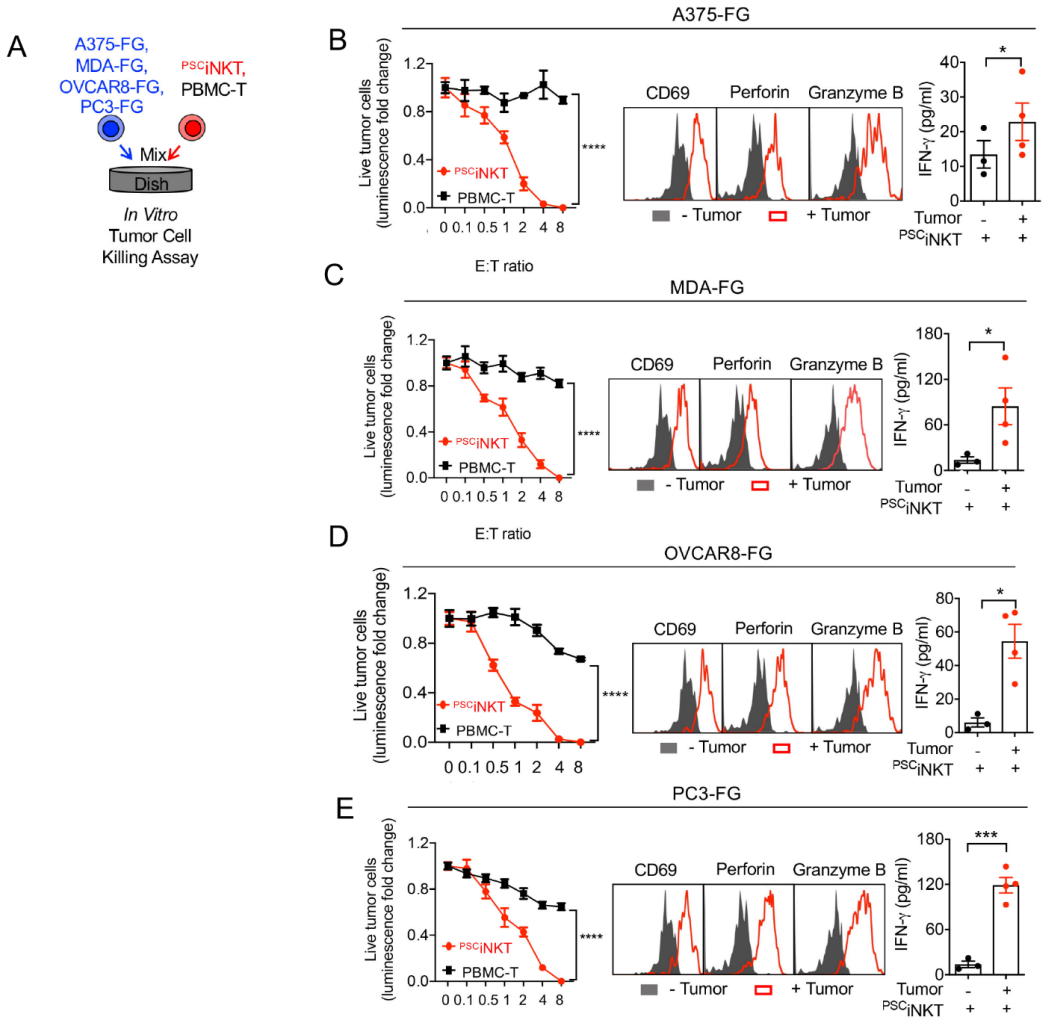

Figure 4. *In Vitro* Efficacy Study - ^{PSC}iNKT Cells. *In vitro* direct killing of human tumor cells by ^{PSC}iNKT cells were studied. Healthy donor PBMC-derived conventional αβ T (PBMC-T) cells were included as a control. Four human tumor cell lines were studied: A375 (melanoma), MDA (breast cancer), OVCAR8 (ovarian cancer), and PC3 (prostate cancer). All four tumor cell lines were engineered to express firefly luciferase and green fluorescence protein (FG) dual-reporters. N = 4. (A) Experimental design. (B-E) Tumor cell killing data at 24-hours. Also presented are FACS plots showing the upregulation of surface activation markers (i.e., CD69) and intracellular cytotoxic molecules (i.e., Perforin and Granzyme B) in ^{PSC}iNKT cells post co-culturing with tumor cells, as well as the ELISA

analyses of cell culture supernatants showing increased IFN-γ secretion by ^{PSC}iNKT cells post co-culturing with tumor cells. Data are presented as the mean ± SEM. ns, not significant, *P < 0.05, **P < 0.01, ***P < 0.001, ****P < 0.0001, by Student's t test.

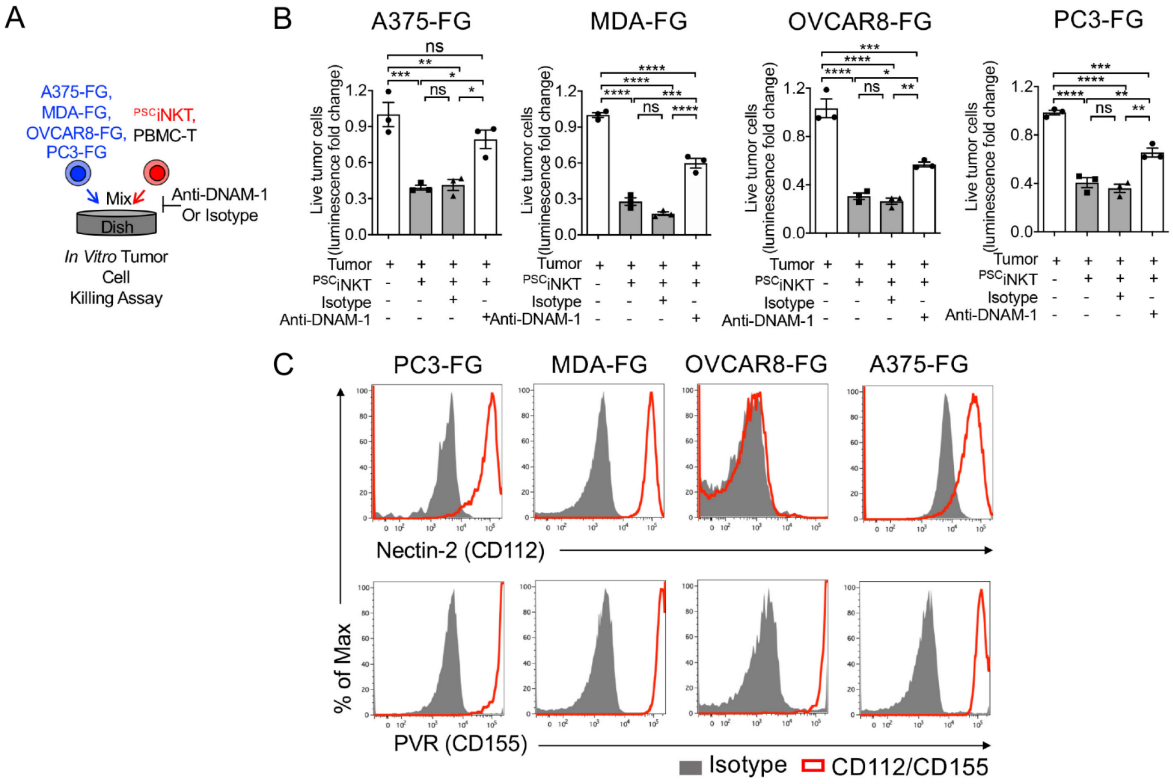

Figure 5. MOA Study - ^{PSC}iNKT Cells. Direct killing of human tumor cells by ^{PSC}iNKT cells via NK pathway was studied. Healthy donor PBMC-derived conventional αβ T (PBMC-T) cells were included as a control. Four human tumor cell lines were studied: A375 (melanoma), MDA (breast cancer), OVCAR8 (ovarian cancer), and PC3 (prostate cancer). All four tumor cell lines were engineered to express firefly luciferase and green fluorescence protein (FG) dual-reporters. (A) Experimental design. The NK activating receptor DNAM-1 mediated pathway was studied. (B) Tumor cell killing data at 24-hours (tumor:effector cell ratio 1:2; n = 3). Data are presented as the mean ± SEM. ns, not significant, *P < 0.05, **P < 0.01, ***P < 0.001, ****P < 0.0001, by 1-way ANOVA. (C)

FACS plots showing the detection of DNAM-1 ligands stress molecules (i.e., Nectin-2/CD112 and PVR/CD155) on the indicated human tumor cell lines.

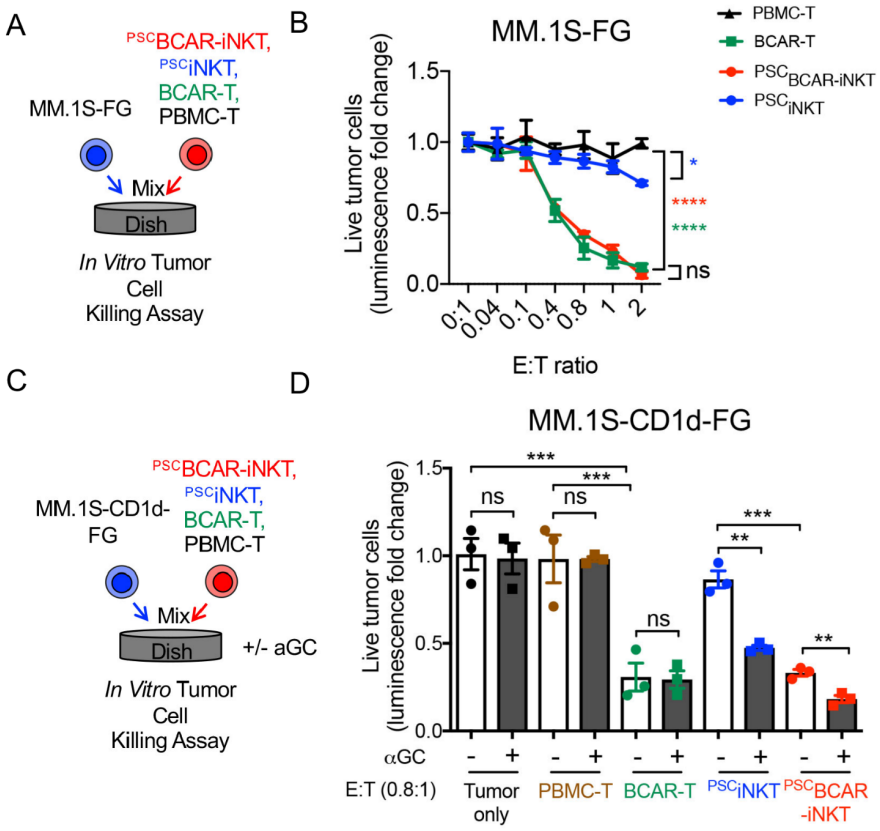

Figure 6. *In Vitro* Efficacy and MOA Study- ^{PSC}BCAR-iNKT Cells. (A-B) *In vitro* direct killing of MM.1S-FG tumor cells. (A) Experimental design. (B) Tumor killing data at 24-hours (n = 3). (C-D) *In vitro* direct killing of MM.1S-CD1d-FG tumor cells. (A) Experimental design. (B) Tumor killing data at 24-hours (n = 3). MM.1S, human multiple myeloma cell line; MM.1S-FG, MM.1S cell line engineered to express firefly luciferase and green fluorescence protein dual-reporters; MM.1S-CD1d-FG, MM.1S cell line engineered to express human CD1d as well as the firefly luciferase and green fluorescence protein dual-reporters. Four effector cells were studied: healthy donor PBMC-derived conventional αβ T (PBMC-T) cells, BCMA-targeting CAR-engineered PBMC-T (BCAR-T) cells, PSC-derived iNKT (^{PSC}iNKT) cells, and PSC-derived BCMA-targeting CAR-armed iNKT

(PSCBCAR-iNKT) cells. Data are presented as the mean ± SEM. ns, not significant, *P < 0.05, **P < 0.01, ***P < 0.001, ****P < 0.0001, by 1-way ANOVA.

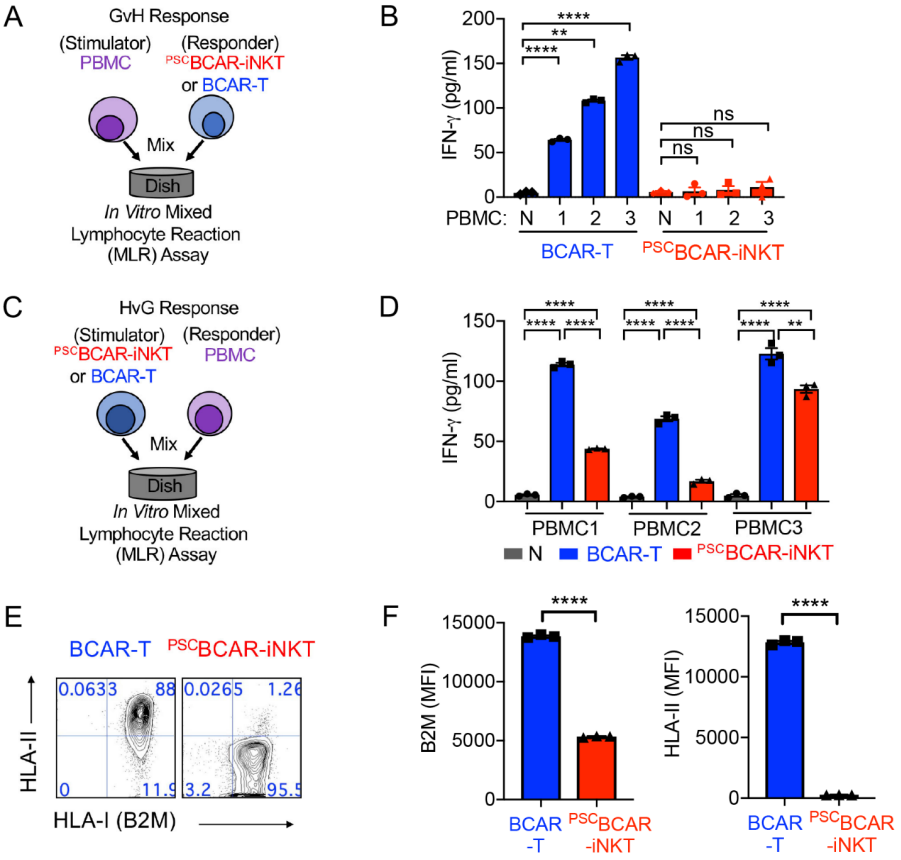

Figure 7. Safety & Immunogenicity Study- PSCBCAR-iNKT Cells. (A-B) In Vitro Mixed Lymphocyte Reaction (MLR) Assay studying graft-versus-host (GvH) response. PSCBCAR-iNKT cells were studied as responder cells; healthy donor PBMC-derived conventional BCAR-T cells were included as a responder control; irradiated donor-mismatched PBMCs from 3 random healthy donors were used as stimulator cells. (A) Experimental design. (B) ELISA analyses of IFN-γ production at day 4 (n = 3). N, no stimulator cells. (C-D) In Vitro Mixed Lymphocyte Reaction (MLR) Assay studying t-versus-host (GvH) response. Irradiated PSCBCAR-iNKT were studied as stimulator cells; irradiated healthy donor PBMC-derived conventional BCAR-T cells were included as a stimulator control; donor-mismatched PBMCs from 3 random healthy donors were used

as responder cells. (C) Experimental design. (D) ELISA analyses of IFN-γ production at day 4 (n = 3). (E) FACS plots showing the detection of surface HLA-I(B2M) and HLA-II molecules on PSCBCAR-iNKT cells. Healthy donor PBMC-derived conventional BCAR-T cells were included as a control. (F) Quantification of E (n = 3). Data are presented as the mean ±SEM. ns, not significant, *P < 0.05, **P < 0.01, ****P < 0.0001, by 1-way ANOVA (B and D) or Student's t test (F).

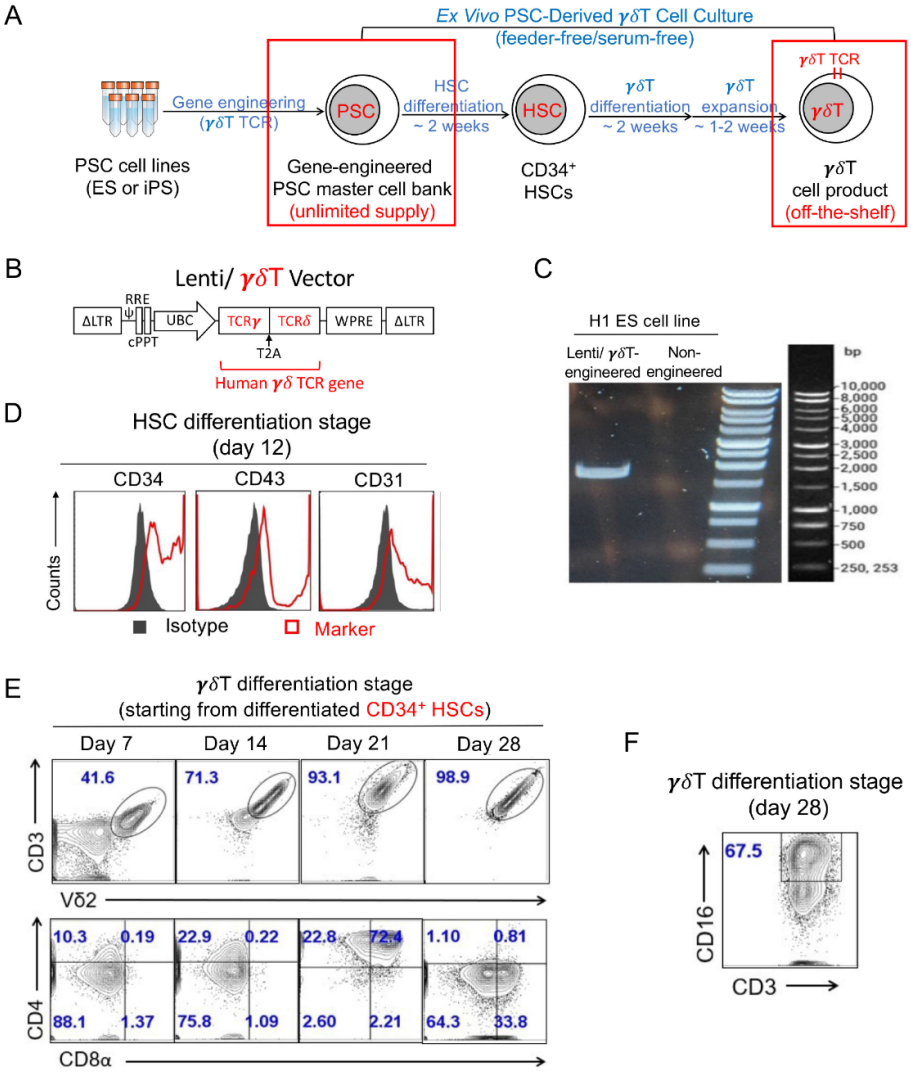

Figure 8. CMC study- Generation of PSCγδT cells. (A) Experimental design to generate the PSCγδT cell product. (B) Schematics of Lenti/γδT lentivector encoding a pair of human γ9 and δ2 TCR genes. (C) DNA gel image showing the detection of transgene in Lenti/γδT vector-transduced H1 ESC master cell line. Genomic DNA was extracted from the γδ TCR gene-engineered H1 ESC master cell line and subjected to polymerase chain reaction (PCR) to amplify a partial transgene fragment. Non-engineered H1 ESC line was included

as a control. Detection of HSC markers (i.e., CD34, CD43, and CD31) on cells from day 12 culture. (D) Differentiation of γδ TCR gene-engineered ESC master cell line into HSCs at the HSC Differentiation Stage. FACS plots are presented showing the detection of HSC markers (i.e., CD34, CD43, and CD31) on cells from day 12 culture. (E-F) Differentiation of ESC-derived HSCs into PSCγδT cells at the γδT Differentiation Stage. (E) FACS plots showing the generation of human γδT cells (identified as CD3+Vδ2 TCR+) over time. (F) FACS plots showing the detection of CD16 expression on mature PSCγδT cells collected at day 28 of the γδT Differentiation Stage culture.

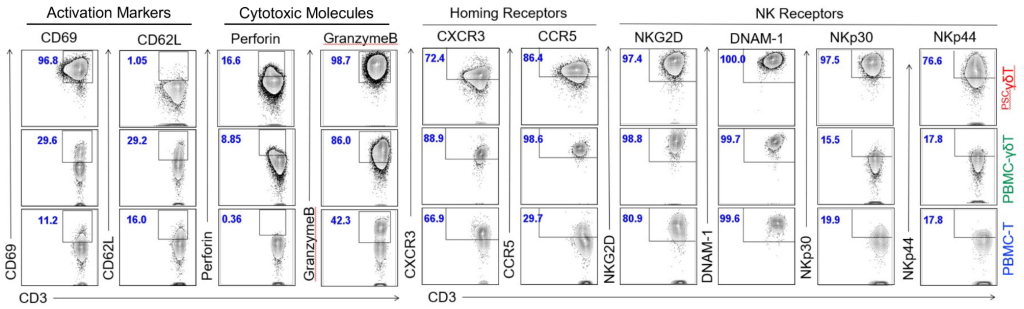

Figure 9. Pharmacology Study – PSCγδT Cells. In Figure 9, representative FACS plots are presented, showing the analysis of phenotype (surface markers) and functionality (intracellular production of effector molecules) of PSCγδT cells. Healthy donor PBMC-derived conventional γδT (PBMC-T) and γδT (PBMC-γδT) cells were included as staining controls.

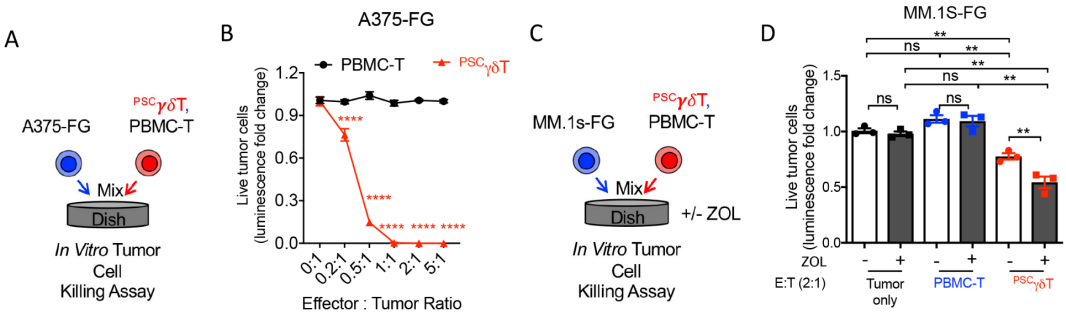

Figure 10. In Vitro Efficacy and MOA Study- PSCγδT Cells. (A-B) In vitro direct killing of A375-FG tumor cells. (A) Experimental design. (B) Tumor killing data at 24-hours (n = 3). (C-D) In vitro direct killing of MM.1S-FG tumor cells. (A) Experimental design. (B) Tumor killing data at 24-hours (n = 3). ZOL: zoledronate, a γ9γ=δ2 TCR stimulator. A375-FG, a human melanoma cell line A375 engineered to express the firefly luciferase and green fluorescence protein dual-reporters; MM.1S-FG, a human multiple myeloma cell line MM.1S engineered to express the firefly luciferase and green fluorescence protein dual-reporters. PSC-derived human γδT (PSCγδT) cells were studied; healthy donor PBMC-derived conventional γδT (PBMC-T) cells were included as a control. Data are presented as the mean ± SEM. ns, not significant, *P < 0.05, **P < 0.01, ***P < 0.001, ****P < 0.0001, by Student's t test (B) or by 1-way ANOVA (D).

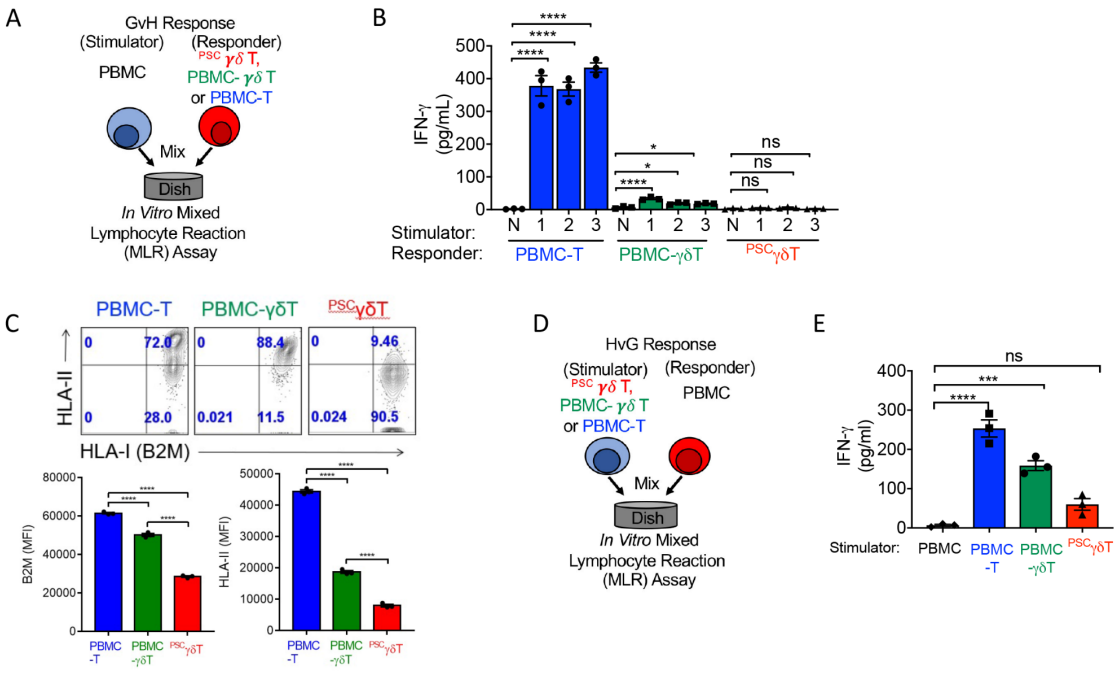

Figure 11. Safety & Immunogenicity Study- PSCγδT Cells. (A-B) In Vitro Mixed Lymphocyte Reaction (MLR) Assay studying graft-versus-host (GvH) response. PSCγδT cells were studied as responder cells; healthy donor PBMC-derived conventional γδT (PBMC-T) and γδT (PBMC-γδT) cells were included as responder controls; irradiated donor-mismatched PBMCs from 3 random healthy donors were used as stimulator cells. (A) Experimental design. (B) ELISA analyses of IFN-γ production at day 4 (n = 3). N, no stimulator cells. (C) FACS measurements of surface HLA-I/II molecules on the indicated cells (n = 3). (D-E) In Vitro Mixed Lymphocyte Reaction (MLR) Assay studying host-versus-graft (HvG) response. Irradiated PSCγδT were studied as stimulator cells; irradiated healthy donor PBMC-T and PBMC-γδT cells were included as stimulator controls; donor-mismatched PBMCs from a random healthy donor were used as responder cells. (D) Experimental design. (E) ELISA analyses of IFN-γ production at day 4 (n = 3). Data are presented as the mean ± SEM. ns, not significant, *P < 0.05, **P < 0.01, ****P < 0.0001, by 1-way ANOVA.

References

1. Labanieh, L., Majzner, R. G. & Mackall, C. L. Programming CAR-T cells to kill cancer. *Nat. Biomed. Eng.* **2**, 377–391 (2018).
2. Lim, W. A. & June, C. H. The Principles of Engineering Immune Cells to Treat Cancer. *Cell* **168**, 724–740 (2017).
3. Iriguchi, S. & Kaneko, S. Toward the development of true “off-the-shelf” synthetic T-cell immunotherapy. *Cancer Sci.* **110**, 16–22 (2019).
4. Saetersmoen, M. L., Hammer, Q., Valamehr, B., Kaufman, D. S. & Malmberg, K. J. Off- the-shelf cell therapy with induced pluripotent stem cell-derived natural killer cells. *Semin. Immunopathol.* **41**, 59–68 (2019).
5. Exley, M. A. *et al.* Adoptive transfer of invariant NKT cells as immunotherapy for advanced melanoma: A phase I clinical trial. *Clin. Cancer Res.* **23**, (2017).
6. de Lalla, C. *et al.* Invariant NKT Cell Reconstitution in Pediatric Leukemia Patients Given HLA-Haploidentical Stem Cell Transplantation Defines Distinct CD4 + and CD4 − Subset Dynamics and Correlates with Remission State . *J. Immunol.* **186**, 4490–4499 (2011).
7. iNKT review-2-annurev-immunol.pdf.
8. *Insti-, N. Efficient Regeneration of Human V a 24 1 Invariant Natural Killer T Cells and*
9. *Their Anti-Tumor Activity In Vivo.*
10. *Krijgsman, D., Hokland, M. & Kuppen, P. J. K. The role of natural killer T cells in cancer-A*

11. *phenotypical and functional approach. Front. Immunol. 9, (2018).*
12. *Vivier, E., Ugolini, S., Blaise, D., Chabannon, C. & Brossay, L. Targeting natural killer*
13. *cells and natural killer T cells in cancer. Nat. Rev. Immunol. 12, 239–252 (2012).*
14. *Giaccone, G. et al. A phase I study of the natural killer T-cell ligand α-galactosylceramide*
15. *(KRN7000) in patients with solid tumors. Clin. Cancer Res. 8, 3702–3709 (2002).*
16. *Yamasaki, K. et al. Induction of NKT cell-specific immune responses in cancer tissues* after NKT cell-targeted adoptive immunotherapy. *Clin. Immunol.* **138**, 255–265 (2011).
17. Fujii, S. ichiro *et al.* NKT cells as an ideal anti-tumor immunotherapeutic. *Front. Immunol.* **4**, 1–7 (2013).
18. Watarai, H. *et al.* Generation of functional NKT cells in vitro from embryonic stem cells bearing rearranged invariant Vα14-Jα18 TCRα gene. *Blood* **115**, 230–237 (2010).
19. Amsen, D., Helbig, C. & Backer, R. A. Notch in T Cell Differentiation: All Things Considered. *Trends Immunol.* **36**, 802–814 (2015).
20. Seet, C. S. *et al.* Generation of mature T cells from human hematopoietic stem and progenitor cells in artificial thymic organoids. *Nat. Methods* **14**, 521–530 (2017).
21. Bennstein, S. B. Unraveling natural killer T-cells development. *Front. Immunol.* **8**, (2018).

22. Gapin, L. Development of invariant natural killer T cells. Physiol. Behav. 176, 139–148
23. (2018).
24. Zhu, Y. et al. Development of Hematopoietic Stem Cell-Engineered Invariant Natural
25. Killer T Cell Therapy for Cancer. Cell Stem Cell 25, 542-557.e9 (2019).
26. Montel-Hagen, A. et al. Organoid-Induced Differentiation of Conventional T Cells from
27. Human Pluripotent Stem Cells. Cell Stem Cell 24, 376-389.e8 (2019).
28. Godfrey, D. I. & Berzins, S. P. Control points in NKT-cell development. Nat. Rev.
29. Immunol. 7, 505–518 (2007).
30. Timmers, M. et al. Chimeric antigen receptor-modified T cell therapy in multiple myeloma:
31. Beyond B cell maturation antigen. Front. Immunol. 10, 1–12 (2019).
32. Ren, J. et al. Multiplex genome editing to generate universal CAR T cells resistant to PD1
33. inhibition. Clin. Cancer Res. 23, 2255–2266 (2017).
34. Steimle, V., Siegrist, C. A., Mottet, A., Lisowska-Grospierre, B. & Mach, B. Regulation of
35. MHC class II expression by interferon-γ mediated by the transactivator gene CIITA. Science (80-.). 265, 106–109 (1994).
36. Abrahimi, P. et al. Efficient gene disruption in cultured primary human endothelial cells by CRISPR/Cas9. Circ. Res. 117, 121–128 (2015).

37. Anderson, G. & Jenkinson, E. J. Thymus organ cultures and T-cell receptor repertoire development. Immunology 100, 405–410 (2000).
38. Schmitt, T. M. et al. Induction of T cell development and establishment of T cell competence from embryonic stem cells differentiated in vitro. Nat. Immunol. 5, 410–417 (2004).
39. Roh, K. H. & Roy, K. Engineering approaches for regeneration of T lymphopoiesis. Biomater. Res. 20, 1–10 (2016).
40. Dolens, A. C. & Taghon, T. Human T cell development notched up a level. Nat. Methods 14, 477–478 (2017).
41. Nature Methods_Progenitor T-cell differentiation from hematopoietic stem cells using Delta-like-4 and VCAM-1.pdf.
42. Rowe, R. G. & Daley, G. Q. Induced pluripotent stem cells in disease modelling and drug discovery. Nat. Rev. Genet. 20, 377–388 (2019).
43. Themeli, M. et al. Generation of tumor-targeted human T lymphocytes from induced pluripotent stem cells for cancer therapy. Nat. Biotechnol. 31, 928–933 (2013).
44. Nianias, A. & Themeli, M. Induced Pluripotent Stem Cell (iPSC)–Derived Lymphocytes for Adoptive Cell Immunotherapy: Recent Advances and Challenges. Current Hematologic Malignancy Reports vol. 14 (2019).
45. Ando, M. & Nakauchi, H. 'Off-the-shelf' immunotherapy with iPSC-derived rejuvenated cytotoxic T lymphocytes. Experimental Hematology vol. 47 2–12 (2017).

46. Depil, S., Duchateau, P., Grupp, S. A., Mufti, G. & Poirot, L. ‘Off-the-shelf’ allogeneic CAR T cells: development and challenges. Nat. Rev. Drug Discov. 19, 185–199 (2020).
47. Kimbrel, E. A. & Lanza, R. Next-generation stem cells — ushering in a new era of cell- based therapies. Nat. Rev. Drug Discov. 19, 463–479 (2020).
48. Knorr, D. A. & Kaufman, D. S. Pluripotent stem cell-derived natural killer cells for cancer therapy. Transl. Res. 156, 147–154 (2010).
49. Li, Y., Hermanson, D. L., Moriarity, B. S. & Kaufman, D. S. Human iPSC-Derived Natural Killer Cells Engineered with Chimeric Antigen Receptors Enhance Anti-tumor Activity. Cell Stem Cell 23, 181-192.e5 (2018).
50. Shimasaki, N., Jain, A. & Campana, D. NK cells for cancer immunotherapy. Nat. Rev. Drug Discov. 19, 200–218 (2020).

CHAPTER 5

Concluding Remarks and Future Outlooks

The combination of stem cell engineering and adoptive cell transfer has shown its unique advantages for developing the next-generation off-the-shelf cancer immunotherapy. Studies have shown that stem cell-derived cell products have its unique NK-like properties, indicating that such a platform may be more compatible for generating natural innate-like unconventional T cells, including iNKT, gdT and MAIT cells. More studies are required to elucidate the feasibility. Meanwhile, the efficacy of current stem cell products is less potent compared to their autologous counterparts. The *in vitro* differentiated cellular products may still be not fully mature to reach their maximum capacity. The persistency of stem cell-derived products needs to be further improved. In combination of cytokine engineering, such as co-expressing IL-15 or IL-15 receptor, could be a potential solution. However, the safety and immunogenicity of cytokine co-engineered products need to be further elucidated.

In summary, stem cell engineering has brought numerous potentials for developing off-the-shelf products. While there are still limitations and bottlenecks for improving the quality and quantity of cellular products, by incorporating big data analysis (e.g., RNA sequencing, single cell RNA sequencing, epigenetic analysis, and proteomics) to compare stem cell derived cells with their endogenous counterparts, we believe that more and more key genes will be identified, allowing us better understand their intrinsic regulatory pathway; thus, products with better efficacy and safety will be developed in the near future can be utilized for all patients as needed.